Inhibition of Nucleotide and One-Carbon Metabolism for the Treatment of Cancer

by

Christine Cuthbertson

A dissertation submitted in partial fulfillment
of the requirements for the degree of
Doctor of Philosophy
(Medicinal Chemistry)
in the University of Michigan
2021

Doctoral Committee:

Professor Nouri Neamati, Chair
Associate Professor Amanda L. Garner
Associate Professor Jolanta Grembecka
Professor Shaomeng Wang

Christine R. Cuthbertson

ccuthbe@med.umich.edu

ORCID 0000-0003-0430-985X

DEDICATION

For my mother, Tami Cuthbertson.

She is my hero in every way and has been my biggest cheerleader through it all.

I'm also pretty sure she is prouder of this accomplishment than I am.

ACKNOWLEDGEMENTS

I honestly could write another dissertation just thanking everyone who has been a part of this journey with me. First, I would like to thank my advisor Dr. Nouri Neamati for his support, time, and patience. He instilled in me a rigorous work ethic and provided many opportunities for me to grow as a scientist, a professional, and a person – I will never forget this invaluable experience. I also would like to thank my committee members Drs. Amanda Garner, Jolanta Grembecka, and Shaomeng Wang for their time, advice, and guidance throughout the years. I also want to acknowledge the Pharmacological Sciences Training Program (PSTP, T32-GM007767) for both funding and the innumerable opportunities afforded from being a trainee. Other College of Pharmacy faculty and staff that have been instrumental in my success include Drs. Mustapha Beleh and Cherie Dotson.

The Neamati lab has always been a big family so there are many people (*easily* upwards of 50) that have contributed to my success in one way or another whether it was through a smile, a conversation, technical advice, or experimental contributions. The first person I want to thank is Joe Madak - a previous graduate student and collaborator on the DHODH project. He is a phenomenal person to work with (and just in general) and an important role model for me. Tiangong Lu and I joined the lab around the same time, she as a post-doc and me as a baby graduate student, and an amazing friendship blossomed between us and I am so grateful for that and the scientific knowledge she shared over time. Wenmin Chen was her successor as my desk mate and she was very patient with all my chemistry questions and is now a dear friend. Zahra Arabzada was assigned to work with me in the end of 2019, and her work is sprinkled all throughout this

dissertation. She was so instrumental to my finishing through her technical contributions and friendship. Last but not least, I want to thank my fellow graduate students and friends Andrea Shergalis, Shuai Hu and Maha Hanafi. Words cannot express enough how **much** the three of you mean to me. Everything from listening to practice talks, to late nights at the lab, to weddings, this experience has solidified a bond that will last a lifetime!

Next, I want to thank my family. Everyone in my immediate and extended family has been supportive throughout these past 6+ years and I couldn't have done this without their love, patience, understanding, and generosity. I'd like to especially thank my Mom for always listening to me when I would call with happy news, or to complain about things not working (lots of the latter… God bless her soul). I'd like to thank my Dad for teaching me how to troubleshoot from a young age, encouraging me along the way, and being the best role model on how to not give up in a difficult situation. Finally, I want to thank my sister and brother. Though they are younger than me, I really look up to them and they have inspired me to grow in ways that only siblings can.

My chosen family that I have gained throughout life and especially graduate school have been my rock; and pillow when I needed it. In addition to my friends mentioned above, there are a few more special ones I want to acknowledge. My best friend Katlyn from my hometown who has been so supportive and encouraging. My long-time roommate Amy Fraley who I could count on for anything – I also cherished our date nights! Nick Ragazzone for being an amazing listener and helping me through all the hard times and being eager to celebrate the good. I've learned that it's really important to have people in your life that celebrate both the little and the big victories. Sarah Burris-Hiday for being the first one to volunteer to help whenever and wherever there's a need. I also want to thank my cohort of 15 and other UM graduate students for enriching my life through tailgates/football games, camping trips, holiday parties, and other events. Lastly, the

University of Michigan Ballroom Dance Team and especially Alex Vidinas and Lizzie Nabney. Dancing was an immensely joyful stress outlet and dancing with Alex helped me forget about all my troubles, even if it was just for a couple hours.

Finally, and most importantly, I need to thank my Lord and Savior Jesus Christ. Without God this work would not have been possible. Even before I had my personal encounter with Him, He was providing for me all along the way and I only wish I had surrendered to Him sooner. I want to thank all the prayer warriors who held me in their intentions throughout this time. I especially want to thank Our Lady for keeping me under her protection and to the members of the Michigan Rosary Group for keeping me grounded in the last year of my studies.

One more thing. I feel like I needed to mention COVID-19 somewhere in here. While it has been such a struggle to finish this dissertation in the midst of a pandemic with the "Stay Home, Stay Safe" order and reduced lab hours among other things, this period of time has been a blessing in disguise. I didn't take the time to write consistently throughout my Ph.D. (do not follow my example) so a lot of this was written during the pandemic following labs closing. So, thanks 'Rona.

TABLE OF CONTENTS

LIST OF FIGURES

LIST OF TABLES

LIST OF ABBREVIATIONS

1CM – One-carbon metabolism

5FU – 5-Fluorouracil

BREQ – Brequinar

CETSA – Cellular thermal shift assay

CFA – Colony formation assay

CMAP – Connectivity Map

CNT – Concentrative nucleoside transporter

DAVID – Database for annotation, visualization and integrated discovery

DEG – Differentially expressed gene

DHFR – Dihydrofolate reductase

DHODH – Dihydroorotate dehydrogenase

DOX – Doxycycline

DPM – Dipyridamole

ECM – Extracellular matrix

ENT – Equilibrative nucleoside transporter

FC – Fold change

FDA – Food and Drug Administration

GFP – Green fluorescence protein

GO – Gene ontology

GSEA – Gene set enrichment analysis

GSH – Glutathione

HDAC – Histone deacetylase

IC_{50} – Half maximal inhibitory concentration

KDC – Knockdown control

KDS – Knockdown SHMT2

KDS-Rec – Recovery of knockdown SHMT2

KO - Knockout

LEF - Leflunomide

$\log D^{7.4}$ – Distribution coefficient at pH 7.4

miR - microRNA

MTHFD1 – Methylenetetrahydrofolate dehydrogenase 1, cytosolic (trifunctional)

MTHFD1L – Methylenetetrahydrofolate dehydrogenase 1-like, mitochondrial (monofunctional)

MTHFD2 – Methylenetetrahydrofolate dehydrogenase 2, mitochondrial (bifunctional)

MTHFD2L – Methylenetetrahydrofolate dehydrogenase 2-like, mitochondrial (bifunctional)

MTX – Methotrexate

NAC – N-acetylcysteine

NAD(H) – Nicotinamide dinucleotide (reduced)

ncRNA – Non-coding RNA

NSCLC – Non-small cell lung cancer

OEC – Overexpression control

OES – Overexpression SHMT2

OES-Rec – Recovery of overexpression SHMT2

PAINS – Pan-assay interference compounds

PHZ – Phlorizin

PTM – Post-translational modification

RPKM - Reads Per Kilobase per Million mapped reads

SAR – Structure-activity relationships

SHMT1 – Serine hydroxymethyltransferase 1, cytosolic

SHMT2 – Serine hydroxymethyltransferase 2, mitochondrial

TCGA – The Cancer Genome Atlas

TERF – Teriflunomide

TGF-β – Transforming growth factor beta

THF – Tetrahydrofolate

TYMS – Thymidylate synthase

WT – Wildtype

ABSTRACT

Metabolic reprogramming in cancer was first described in the early to mid-1900s and later labeled as a hallmark. Rapidly proliferating cells require sufficient concentrations of nucleotides and other biomass precursor molecules to sustain growth. Nucleotide biosynthesis and one-carbon metabolism (1CM) inhibitors were among the first targeted cancer chemotherapies and remain as some of the most successful (e.g. 5-fluorouracil and methotrexate). Despite mounting evidence, the mitochondrial enzymes dihydroorotate dehydrogenase (DHODH), serine hydroxymethyltransferase (SHMT2), and methylenetetrahydrofolate dehydrogenase (MTHFD2) have yet to be successfully clinically targeted for the treatment of cancer.

DHODH is a vital enzyme in the *de novo* pyrimidine biosynthesis pathway. However, the DHODH inhibitor brequinar (BREQ) failed all cancer clinical trials in solid tumors. Therefore, we sought to address a potential avenue to improve the efficacy of BREQ by employing a combination strategy to simultaneously inhibit nucleotide salvage. BREQ was synergistic with the equilibrative nucleoside transporter (ENT) inhibitor dipyridamole, but not the concentrative nucleoside transporter inhibitor phlorizin. This synergy carried over to ENT1/2 inhibition, but not ENT4. Our previously described brequinar analog **41** was also synergistic with dipyridamole as were the FDA-approved DHODH inhibitors leflunomide and teriflunomide but the latter required much higher concentrations than BREQ. Therefore, combination of BREQ with ENT inhibitors presents a potential anticancer strategy in select tumors.

SHMT2 and MTHFD2 participate in the folate metabolism arm of 1CM and are emerging anticancer targets. Both are overexpressed in several cancer types and correlate with poor

prognosis and other clinicopathological parameters. Significant progress towards the development of inhibitors against these enzymes has been made in a relatively short amount of time, but there is still much to be understood about their involvement in cancer progression. Thus, we performed extensive characterization of genetically engineered cell lines via transcriptomic profiling and bioinformatics. The data show changes in genes and gene sets related to hypoxia, MYC, and mTOR, all of which are well-established 1CM-related pathways. Prior research connected SHMT2 and MTHFD2 to RNA metabolism, and we built upon that work by identifying links to alternative splicing and non-coding RNA processing. Glycosylation was also a strong theme for SHMT2. Additionally, we observed changes in expression of Ephrin-related genes supporting previous work that connected 1CM to Ephrin signaling and differentiation. Moreover, we disclosed inhibitors that showed correlations to gene expression changes in response to modulation of SHMT2 and MTHFD2 expression which may pose as synthetically lethal agents.

Finally, we developed a pharmacophore model that led to the discovery of a novel class of MTHFD2 inhibitors. Virtual screening of our in-house database identified **CBN-1** which significantly stabilizes MTHFD2 to thermal denaturation and inhibits its enzymatic activity. Mechanistic studies revealed that **CBN-1** covalently binds MTHFD2 but does not react with general antioxidants. **CBN-1** analogs possess antiproliferative and antimigratory activity with **CBN-1** being the most potent in the series. **CBN-1** showed significant selectivity to cells cultured in galactose medium indicating impaired mitochondrial function and potential inhibition of OXPHOS. Structure-activity relationship studies with other analogs did not produce a superior compound to **CBN-1**, thus further optimization is required to improve the potency of our hit compound. Our hit **CBN-1** is the first covalent MTHFD2 inhibitor reported.

Collectively, this dissertation provides further evidence to pursue SHMT2 and MTHFD2 inhibitors for the treatment of cancer and a potential strategy to improve the efficacy of DHODH inhibitors in the clinic.

CHAPTER I Introduction

Background[1]

One carbon metabolism (1CM) is commonly dysregulated in cancer due to its contribution to core cellular building blocks (e.g. purine and pyrimidine nucleotides), epigenetics, post-translational modifications (PTMs), and redox homeostasis and is comprised of a complex network of enzymes.[1-2] Targeting of one carbon metabolism was one of the original chemotherapeutic strategies with the discovery of aminopterin by Sidney Farber in 1948 and has led to some of the most successful approaches to halt cell growth.[3-5] Methotrexate (MTX) and 5-fluorouracil (5FU) were pioneering drugs in this field and are still widely used today. Dihydrofolate reductase (DHFR) and thymidylate synthase (TYMS) are the targets of these drugs, respectively, and have been successfully targeted for other proliferative diseases such as arthritis.[6] Two other enzymes complete the folate cycle arm of 1CM but have not been targeted clinically at this point: serine hydroxymethyltransferase (SHMT) and methylenetetrahydrofolate dehydrogenase (MTHFD). Literature continues to suggest that the mitochondrial isoforms of these enzymes are clinically relevant in the context of cancer.[7-9]

The 1CM Pathway

Preliminary metabolism before folate cycle entry

---

[1] **Author contributions:** Zahra Arabzada assisted in generating figures I-2 and I-3, tables I-1, I-2, I-3, and I-4 and Appendix tables I-1, I-2, I-3, I-4, I-5, and I-6. Armand Bankhead III generated figures I-4 and I-5. Armita Kyani assisted with writing of the manuscript.

1CM begins with the folate cycle and provides the 1C unit to the methionine cycle. The one-carbon metabolism pathway is illustrated in Figure I-1. The 1C unit largely is supplied by serine, either from the extracellular environment or *de novo* synthesis, but can be donated by other amino acids as well.[4] *De novo* serine biosynthesis is carried out by a series of three enzymes from a glycolytic intermediate: phosphoglycerate dehydrogenase (PHGDH), phosphoserine aminotransferase 1 (PSAT1), and phosphoserine phosphatase (PSPH) which extends off of glycolysis. Folate is not able to diffuse through the plasma membrane due to its high polarity (cLogP = -2.37), therefore it must be transported. Folate and its derivatives enter cells through three mechanisms: internalization of the folate receptors (FRα/FOLR1 and FRβ/FOLR2), passive transport by the reduced folate carrier (RFC, encoded by *SLC19A1*), and active transport by the proton-coupled folate transporter (PCFT, encoded by *SLC46A1*). In the context of cancer, the α isoform seems to be more relevant.[10] Polyglutamylation of folate and its derivatives are regulated by the extracellular folate hydrolase 1, FOLH1 (also known as PSMA and GCPII), and intracellular folylpolyglutamate synthase, FPGS. Only monoglutamate forms of folate are able to be transported.[11] Notably, polyglutamylated folate derivatives are usually better substrates for folate-dependent enzymes. Folate is subsequently reduced to dihydrofolate (DHF) and further to tetrahydrofolate (THF) by DHFR to yield the bioactive form.

Cytosolic folate metabolism

After DHFR reduces folate to THF, SHMT1 transfers a 1C unit from serine to produce 5,10-methylene-THF ($5,10\text{-}CH_2\text{-}THF$). This can be recycled back to DHF by TYMS, which transfers the 1C unit to dUMP to form dTMP.[2] This is the first contribution to nucleotide biosynthesis (pyrimidines). Alternatively, $5,10\text{-}CH_2\text{-}THF$ can go through a series of oxidation reactions catalyzed by MTHFD1. MTHFD1 has three functions: dehydrogenase, cyclohydrolase,

and synthetase. The first intermediate, 5,10-methenyl-THF (5,10-CH$^+$-THF) is short-lived due to

its instability and is subsequently reduced to 10-formyl-THF (10-CHO-THF). 10-CHO-THF can

go on to participate in purine biosynthesis (GAR transformylase, GART and AICAR

formyltransferase, AICARFT) or be converted back to THF by MTHFD1 or aldehyde

dehydrogenase 1 family member L1 (ALDH1L1) releasing formate or CO_2, respectively.

Methenyltetrahydrofolate synthetase can contribute to this pathway by converting 5-CHO-THF

into 5,10-CH$^+$-THF. 5,10-CH$_2$-THF can also be further reduced to 5-methyl-THF (5-CH$_3$-THF)

by methylenetetrahydrofolate reductase (MTHFR), acting as the methyl donor to the methionine

cycle.
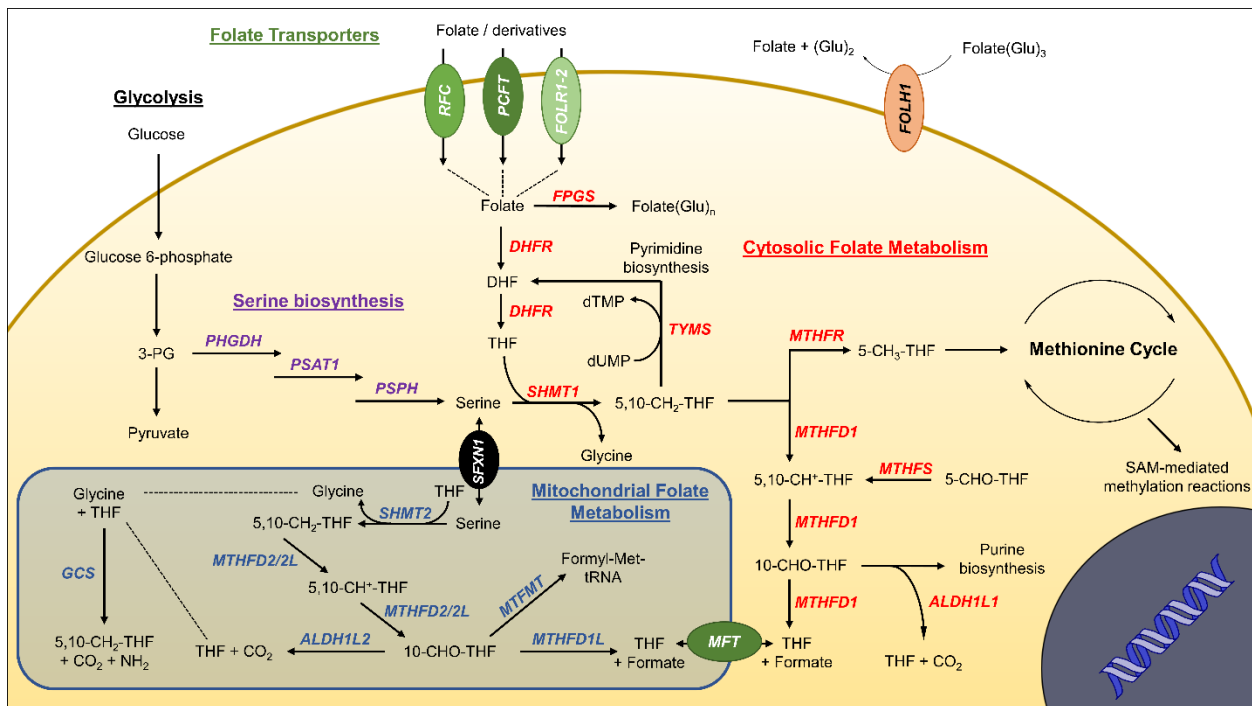
Figure I-1. Key enzymes involved in one-carbon metabolism.

Mitochondrial folate metabolism

In order for mitochondrial folate metabolism to function, serine and THF must first be

transported into the organelle by sideroflexin 1 (SFXN1) and the mitochondrial folate transporter

(MFT), respectively. SHMT2 is the mitochondrial isoform of SHMT1 and performs the same

enzymatic reaction to donate a 1C unit from serine to THF.[2] In addition to serine, glycine is another amino acid that can donate a 1C unit and this is facilitated by the glycine cleavage system (GCS). Both SHMT2 and the GCS generate 5,10-CH_2-THF, which is a substrate for MTHFD2/2L. MTHFD2 and MTHFD2L catalyze the oxidation of 5,10-CH_2-THF to 10-CHO-THF. MTHFD1L completes what the trifunctional MTHFD1 is able to catalyze in the cytosol, regeneration of THF and production of formate. 10-CHO-THF is also a substrate for ALDH1L2 and MTFMT. ALDH1L2 has the same function as the cytosolic ALDH1L1; production of THF and carbon dioxide. MTFMT, or mitochondrial methionyl-tRNA formyltransferase, transfers the formyl group from 10-CHO-THF to methionine-tRNAs to produce formyl-methionine-tRNA which is required for the initiation of translation of mitochondrial proteins.

Select inhibitors of 1CM

Inhibitors have been discovered for most enzymes and transporters involved in 1CM (Figure I-2), also recently succinctly summarized by Robinson et al.[12] Those that remain to be targeted are PSAT1, MFT (SLC25A32), PCFT (SLC46A1), SFXN1, ALDH1L1/2, MTFMT, MTRR, and DMGDH. A list of inhibitors of 1CM proteins and their structures, activities, and status can be found in the Appendix Tables I-1-6. Inhibitors of subsections of 1CM are discussed briefly below. It should be noted that only experimentally validated compounds with activity levels ≤ 50 μM are included, and structures likely to be pan-assay inhibitors (PAINS) are excluded.
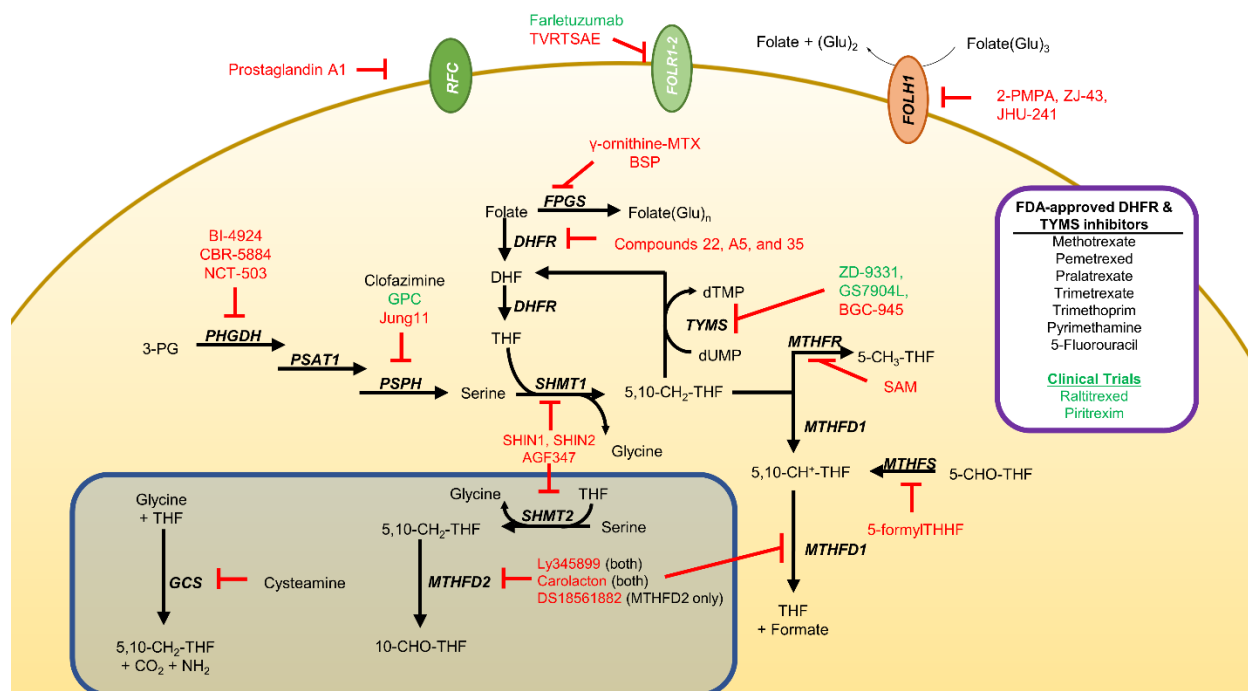
Figure I-2. Summary of select preclinical and clinically used compounds targeting 1CM. Coloring: black indicates FDA-approved, green indicates clinical trials, red indicates preclinical. BSP, bromosulfophthalein; GPC, glycerylphosphorylcholine.

Serine biosynthesis inhibitors

Two out of the three enzymes that make up the serine biosynthesis pathway have inhibitors discovered for them (Figure I-2, Appendix Table I-1). A good portion of the reported serine biosynthesis inhibitors have antibacterial activity and have been recently reviewed.[13] PHGDH is an emerging anticancer target and there has been extensive effort to develop compounds that inhibit this enzyme.[14] BI-4924 is the most potent among them with an IC_{50} of 2 nM.[15]

Folate glutamylation-modifying enzyme inhibitors

Glutamylation-states of folates or derivatives are important for activity against their targets and also determine cell-permeability/uptake by transporters.[16] Inhibitors have been discovered for both FOLH1 and FPGS although none are FDA-approved (Figure I-2, Appendix Table I-2). FOLH1 inhibitors have suffered from poor oral bioavailability (due to their acidic nature in mimicking the glutamate substrate) or toxicity which prevented progress in clinical trials.[17] However, there is still interest in pursuing pro-drug strategies for the inhibitors in which there was

5

not dose-limiting toxicity because of promising preclinical data.[17] Folate analogs are reported to inhibit FPGS, albeit only modestly in the mid-micromolar range.[18]

Folate and serine transporter inhibitors

Folate transporters play an important role in the efficacy of antifolate chemotherapies.[10, 19] The small molecule inhibitors of these cell surface transporters require high concentrations in order to be effective (>100 μM). In pursuit of delivering oncolytic virotherapy to ovarian cancer cells, Hulin-Curtis and colleagues identified a peptide that competes with folic acid for binding to FOLR1 (Appendix Table I-3).[20] There are many antibody-drug conjugates and folic acid-conjugates built on the same premise of delivering chemotherapy selectively to the cancer cells.[10] The unconjugated monoclonal antibody farletuzumab specifically targets FOLR1 but interestingly, inhibition of folic acid uptake is not part of its mechanism of action.[10] Despite encouraging preclinical data, farletuzumab did not meet its primary endpoint in a Phase III trial.[10]

Cytosolic and mitochondrial folate metabolism inhibitors

DHFR and TYMS were the first 1CM proteins to be clinically validated as targets for cancer therapy and remain the most successful in this context to date (Figure I-2, Appendix Table I-4). All FDA-approved DHFR and TYMS inhibitors are classical or non-classical folate derivatives, with the obvious exception of 5FU. There are also several compounds targeting these two enzymes in the clinical trial pipeline: raltitrexed, piritrexim, ZD-9331, and GS7904L (Figure I-2, green text; Appendix Table I-4). Detailed reviews are available for these classical inhibitors.[21-22] The only known inhibitor for MTHFR is S-adenosylmethionine (SAM), which is a product feedback inhibitor.[23-24] There are no reported inhibitors for human MTHFS, but 5-formyltetrahydrohomofolate (5-formylTHHF) inhibits the murine homolog with a K_i of 0.7 μM.[25] The GCS is a multi-enzyme complex composed of four proteins which all work to convert glycine

and THF to 5,10-CH$_2$-THF, carbon dioxide, and ammonia. To our knowledge, cysteamine is the only described inhibitor for the GCS with a K$_i$ of 5 μM.[26] Cysteamine is FDA-approved for nephropathic cystinosis and is undergoing clinical trials for multiple indications (Appendix Table I-4).

Inhibitors of the methionine cycle arm of 1CM

The methionine cycle has great implications because through it the 1C unit is transferred to S-adenosylhomocysteine (SAH) to form SAM, a cofactor used by many methyltransferases.[27] MTRR (methionine synthase reductase) and DMGDH (dimethylglycine dehydrogenase, mitochondrial) are the two enzymes yet to be targeted of the methionine cycle. Most of the established inhibitors are folate, adenosine, or amino acid analogs, however there are some exceptions (Appendix Table I-5). Methionine synthase (MS) inhibitors contain interesting electrophilic folate analogs such as compound **6** and **6c** which take advantage of MS's mechanism of action and possess anticancer activity.[28-29] Inhibitors of GNMT (glycine N-methyltransferase) include one of its products, SAH, and 5-CH$_3$-THF, which acts as a regulator of pathway flux,[30] but no inhibitors outside of these downstream molecules have been discovered. A clinical trial with a compound targeting the 2A isoform of methionine adenosyltransferase (MAT2A), AG-270, is currently underway (NCT03435250). Biochemical or preclinical data from Agios Pharmaceuticals is not available at this time. The first non-substrate or product-based allosteric MAT2A inhibitor with nanomolar activity came from Pfizer in 2017.[31] The natural product AKBA was recently identified as a potent and selective allosteric inhibitor of MAT2A with a K$_d$ of 130 nM.[32] There are many potent inhibitors discovered for SAHH (S-adenosyl-L-homocysteine hydrolase) (Appendix Table I-5). Many are, unsurprisingly, adenine analogs.[33-35] However, several compounds with new scaffolds for SAHH were recently identified using a novel high-throughput

screening technique.[36] The physiological roles of BHMT1/2 (betaine-homocysteine methyltransferases 1 or 2) are still incompletely understood, especially in the context of cancer. Potent inhibitors of both isoforms have been discovered and could be important tools in elucidating BHMT/2's function.[37-38]

Inhibitors of folate-dependent enzymes in purine biosynthesis

Purine biosynthesis is carried out by the purinosome, a multienzyme complex, where two of the enzymes (GART and AICARFT) are folate-dependent, both requiring 10-CHO-THF.[39] Nearly all discovered inhibitors for these enzymes mimic the folate substrate except for the peptidomimetic identified (compound **14**) for AICARFT (Appendix Table I-6).[40] The FDA-approved inhibitor pemetrexed does possess inhibitory activity against GART and AICARFT, but only in the low micromolar range.[41] Lometrexol is much more potent with a K_i of 60 nM for GART,[42] but was discontinued from clinical trials. The most potent inhibitor of GART to date is AG2034 with a K_i of 28 nM, but unfortunately did not advance past Phase I clinical trials due to toxicity.[43-44] The discovery of the AICARFT inhibitor LSN3213128 by Eli Lilly and Company is exciting as it is orally bioavailable, efficacious in murine xenografts, and selective against other 1CM enzymes.[45] Given the success of other anti-purinic antimetabolites (e.g. gemcitabine), the field awaits data on the further development of this potential anticancer therapeutic.

SHMT2

Function and regulation

SHMT2 simultaneously converts serine and THF to glycine and 5,10-CH_2-THF (Figure I-1). SHMT2 seems to promote chemosensitivity or resistance in a context-specific manner.[46-47] Outside of nutrient contributions, SHMT2 knockout caused mitochondrial translation to stall at specific methylated tRNAs, and this was dependent on its enzymatic activity.[48] Protein translation

initiation requires formylmethionyl-tRNAs and when SHMT2 is knocked out 10-CHO-THF, a downstream product, is no longer available for conjugation by MTFMT.[49] SHMT2 also plays a role in redox balance. Expression of SHMT2 was shown to be associated with changes in the level of expression of mitochondrial respiration complex proteins.[50] Hypoxia induces SHMT2 expression and was found to be necessary for redox homeostasis and cell survival under hypoxic conditions.[51-52] Additionally, expression of SHMT2 promotes survival in the ischemic tumor microenvironment in glioma.[53] Recent structural studies have identified a novel function of SHMT2 that contributes to immune regulation through the BRISC-complex.[54-56] This function was in turn regulated by a PTM modulated by HDAC11.[57] Other PTMs such as acetylation and succinylation determine enzymatic activity and are modulated by SIRT3 and SIRT5, respectively.[58-59] Besides canonical regulation by known metabolic master regulators (Figure I-3, black text),[1] novel epigenetic mechanisms, transcriptional programs and non-coding RNAs have been reported to modulate SHMT2 expression (Figure I-3, red text). Knockdown of the histone methyltransferase G9A resulted in a decrease in expression of SHMT2 as well as reduced H3K9Me1 levels for serine synthesis pathway genes.[60] Novel transcription factors and signaling pathways that regulate SHMT2 include TGF-β, STAT3, and EWS-FLI1.[61-63] Interestingly, SHMT1 was shown to bind to the 5'-untranslated region of the SHMT2 transcript thereby preventing its expression.[64] SHMT2 expression has also been reported to be under the control of several micro-RNAs (miRs) and long intergenic non-coding RNAs (lincRNAs).[65-68] A summary of regulation of SHMT2 is summarized in Figure I-3. Despite encouraging evidence that SHMT2

is a viable anti-cancer target, only a handful of inhibitors have been published to date (discussed below).[69-72] However, none are specific to SHMT2.
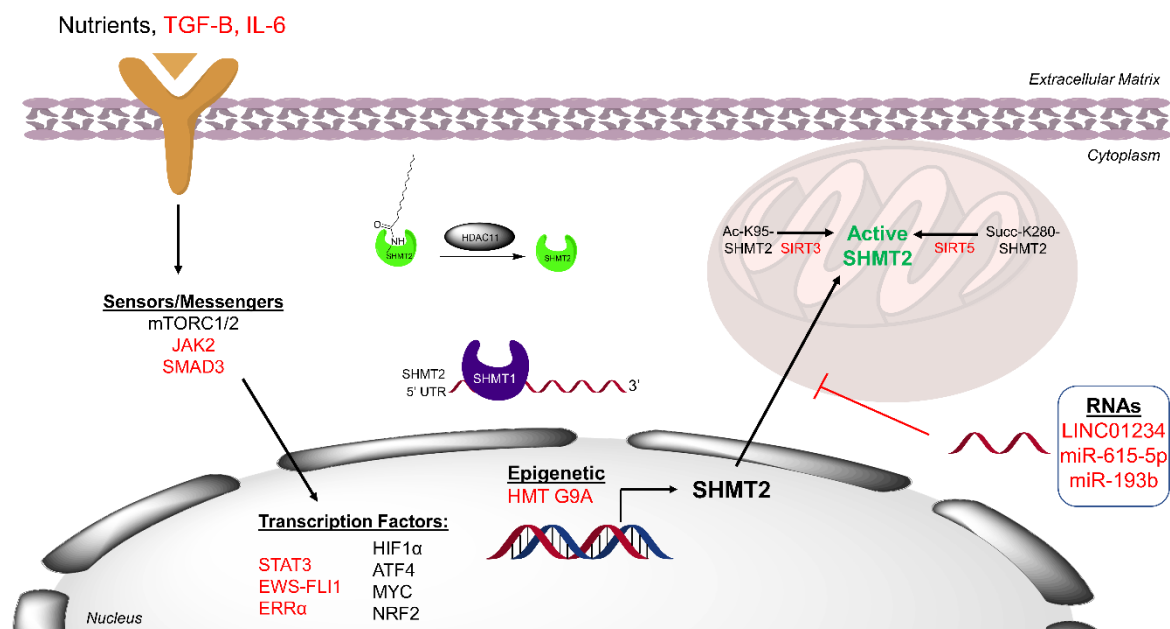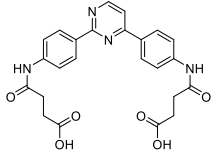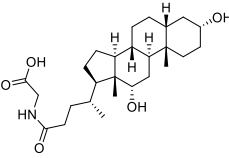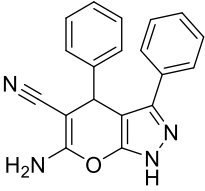
Figure I-3. Summary of the regulation of SHMT2 expression in cancer. Canonical mechanisms are in black text, and non-canonical in red.

SHMT Inhibitors

The pyrazolopyran scaffold is the predominant series of compounds that make up the SHMT1/2 inhibitor space (Table I-1 summarizes select inhibitors for the human isoforms). This class of compounds was originally disclosed as plant SHMT inhibitors in a patent application by BASF (WO 2013182472 A1). This scaffold was then evaluated for activity against *Plasmodium* SHMT and showed nanomolar enantioselective activity against the enzyme and the parasites.[73] That same year, Marani and colleagues published the first data on the human isoforms.[74] In addition to having selective activity against SHMT1, compound **2.12** (Table I-1) also displayed anticancer activity in the mid-micromolar range[74] Further optimization of this scaffold led to potent inhibitors of both SHMT1 and SHMT2.[69] However, as was also shown in the anti-malarial studies,[73] this scaffold suffered from poor pharmacokinetic properties that prevented *in vivo* efficacy studies.[69] A breakthrough came this year with the disclosure of (+)SHIN2 which showed

10

in vivo target engagement of SHMT2 in addition to anticancer activity in models of T-ALL.[71] The first *in vivo*-active SHMT inhibitor, AGF347, is a folate mimetic.[70] Despite being much less potent than the pyrazolopyran compounds, AGF347 showed *in vivo* activity in colon cancer models;[70] notably, the least-sensitive cell line *in vitro* was used for the xenograft model. FDA-approved antifolates do inhibit SHMTs, but higher concentrations are required ($\geq$ 100 μM).[75-77]

Table I-1. Inhibitors of human SHMTs.

Compound	Structure	Isoform activity	Anticancer activity	Refs.
2.12		SHMT1 IC_{50} = 0.65 μM SHMT2 IC_{50} = 1.4 μM	H1299 IC_{50} = ~30 μM	74, 78
($\pm$)SHIN1		SHMT1 IC_{50} = 5 nM SHMT2 IC_{50} = 13 nM	HCT 116 IC_{50} = 870 nM ((+)- isomer)	69
(+)SHIN2		Biochemical data not available	MOLT-4 IC_{50} = 89 nM *In vivo* efficacy in primary mouse T-ALL and human patient-derived xenograft model of T-ALL	71
AGF347		SHMT1 K_i = 2.91 $\pm$ 0.59 μM SHMT2 K_i = 2.19 $\pm$ 0.23 μM	MIA PaCa-2 IC_{50} = 0.64 μM *In vivo* efficacy in MIA PaCa-2 xenograft	70, 79

"Hit 1"		SHMT2 IC$_{50}$ = 0.53 μM	To be determined	[80]
"Hit 2"		SHMT2 IC$_{50}$ = 0.72 μM	To be determined	[80]
AM-807/42004633	Derivatives of:	SHMT2 IC$_{50}$ = 9.43 μM	To be determined	[72]
AM-807/40675298		SHMT2 IC$_{50}$ = 12.7 μM		
AM-807/42004511		SHMT2 IC$_{50}$ = 14.5 μM		

Generally, only marginal selectivity between the two SHMT isoforms has been achieved, with the inhibitors being selective for SHMT1 by 2-3-fold.[69, 78] The cysteine-reactive inhibitor 3-bromopyruvate is selective for SHMT1 due to the absence of a cysteine residue in SHMT2's active site.[81] Crystal structures are available for both isoforms (summarized in Table I-2), but there are currently no co-crystal structures of SHMT1 with any of the published inhibitors. If selectivity is ultimately desired, it will be critical to experimentally determine differences in the binding pockets. However, one could pose the question: is SHMT2 selectivity ideal? *In vivo* studies of the dual SHMT1/2 inhibitors show that co-inhibition is efficacious with minimal systemic toxicities,[70-71] suggesting that selectivity may not be required.

Table I-2. Crystal structures of the human SHMTs.

Protein	Variant	Ligands	Macromolecule	Method	Resolution	PDB ID	Refs.
SHMT1	WT	PLP	NA^a	X-ray	2.65 Å	1BJ4	[82]

H135N, R137A, E168N	PLP	NA	X-ray	3.60 Å	6FL5	[83]
SHMT2	WT	NA	NA	X-ray	2.04 Å	6DK3	TBP[b]
	A264T	NA	BRISC-complex	Cryo-EM	3.90 Å	6H3C	[54]
	WT	NA	BRISC-complex	Cryo-EM	3.80 Å	6R8F	[55]
	WT	PLP, pemetrexed	NA	X-ray	2.28 Å	6QVL	[75]
	WT	PLP, lometrexol	NA	X-ray	2.32 Å	6QVG	
	WT	PLP	NA	X-ray	2.60 Å	4PVF	[84]
	WT	PLP, Compound **2**	NA	X-ray	2.47 Å	5V7I	[69]
	K74R, A264T	NA	NA	X-ray	2.85 Å	5X3V	TBP

[a]NA, not applicable; [b]TBP, to be published

Impact on cancer patient survival

The mitochondrial isoform of SHMT is selectively overexpressed compared to its cytosolic counterpart and is associated with poor patient prognosis, staging, and metastasis in several cancers including kidney, gastric, liver, breast, lung, colorectal, esophageal and intrahepatic cholangiocarcinoma, oral squamous carcinoma, and glioma.[85-95] Across the NCI-60 panel of cell lines, SHMT2 expression held a stronger correlation with proliferation rate than SHMT1.[8] TCGA disease patient samples were evaluated for reduced survival by comparing survival outcomes for patients with high SHMT1/2 expression to those with low SHMT1/2 expression. Patients were stratified based on median gene expression and a log-rank statistic was used to quantify differences

in survival with p-values FDR adjusted across 33 cancer types and FDR adjusted p-values < 0.05 considered significant (Figure 4). Gene expression thresholding and Kaplan-Meier (KM) plots were generated using patient sample RNA-Seq RSEM-normalized gene expression values and survival metadata sourced from the TCGA GDAC Firehose.[96] Survival test statistics and KM plots were generated using the R statistical programming language.[97] We observed higher expression of SHMT2 in adrenocortical carcinoma (ACC), which was significantly associated with reduced survival; SHMT1 was also marginally associated with reduced survival (p-value not significant after multiple testing). This result is novel based on our search of the literature. Not much is known about the metabolic landscape of ACC, but gemcitabine and capecitabine are part of second-line therapy regimens.[98] Additionally, some mTOR inhibitors are currently undergoing clinical trials.[98] We identified three TCGA diseases for which higher levels of SHMT1 was associated with improved survival and would not recommend targeting SHMT1 in these diseases. Interestingly, in LGG, patients with higher expression of SHMT1 were significantly associated with reduced survival and patients with higher expression of SHMT1 were moderately associated with improved survival (p-value not significant after FDR correction).
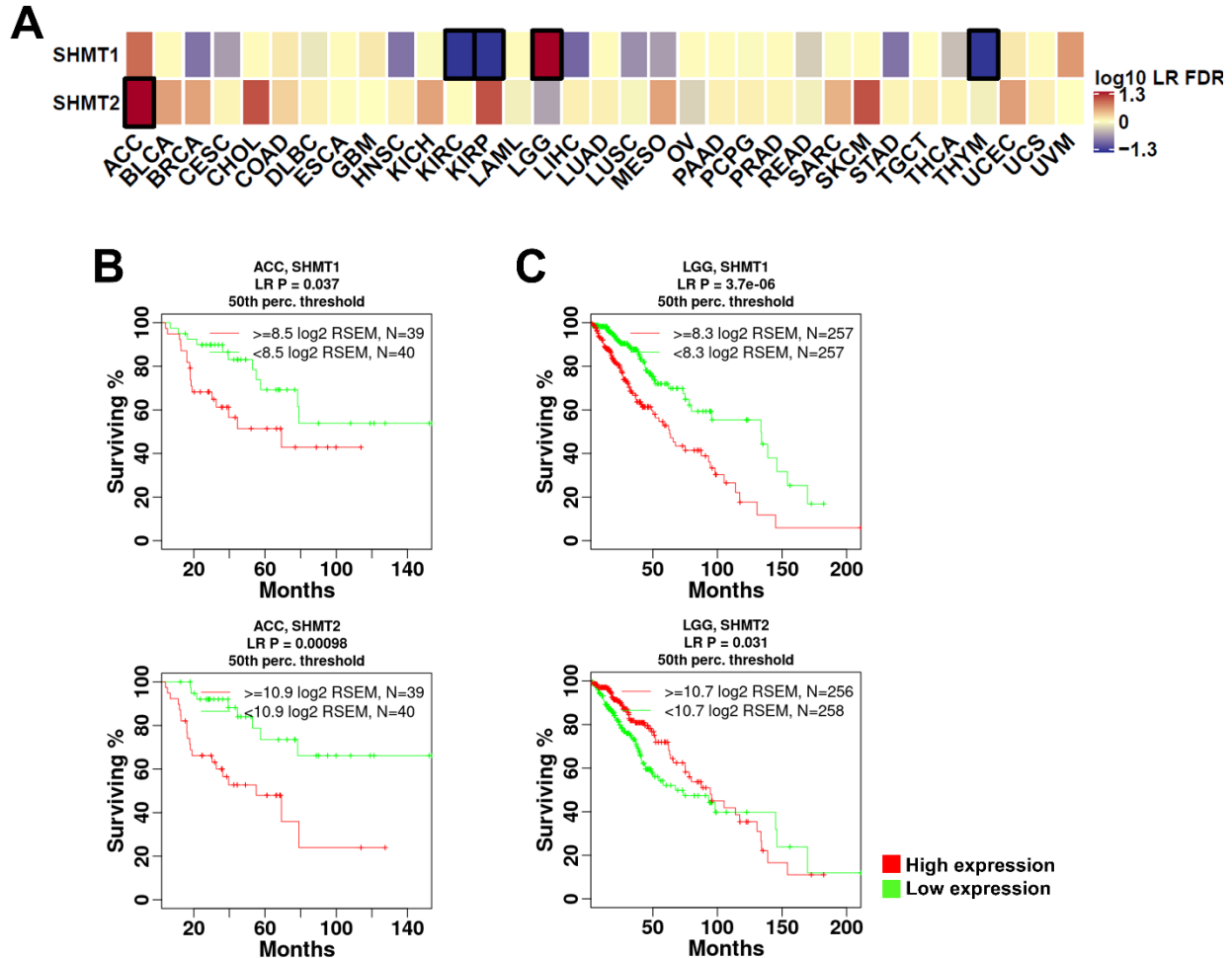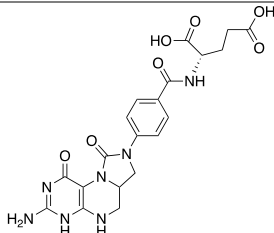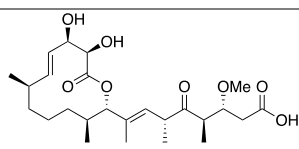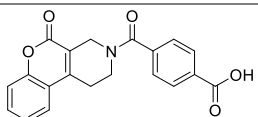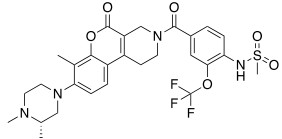
Figure I-4. Pan-cancer SHMT1 and SHMT2 patient survival association survey. (A) *SHMT1* and *SHMT2* expression are associated with overall survival (OS) in several cancers. Patients from each disease were stratified by median expression of SHMT1 and SHMT2. Heatmap color indicates directionality and significance of association (red = reduced survival, blue = increased survival) with increased gene expression. Heatmap cells with black borders indicate FDR p-value < 0.05. (B) *SHMT1* and *SHMT2* expression associate with reduced survival in ACC. (C) LGG patients with high expression of SHMT1 had significantly reduced survival while patients with high levels of SHMT2 marginally associated with improved survival. Log-rank (LR) statistic p-values used to quantify association with survival were FDR adjusted across cancers per gene. ACC SHMT1 and LGG SHMT2 LR p-values not significant after FDR correction. **MTHFD2**

Function and regulation

MTHFD2 possesses two enzymatic activities, a dehydrogenase and cyclohydrolase (Figure I-1). The role of MTHFD2 in cancer was recently reviewed.[7] Both through genetic and small molecule approaches, inhibition of MTHFD2 reduces proliferation, migration, invasion, tumor growth, stem cell-like properties and promotes cell death, differentiation, and chemosensitivity in several cancer types.[7, 99-102] In addition to its involvement in nutrient regulation, MTHFD2 plays a role in redox homeostasis through the use of its co-factor NAD^+, as well as involvement with

expression of hypoxia-related proteins such as HIF-2α.[103-107] Other secondary functions of MTHFD2 have also been discovered such as non-enzymatic driven proliferation, potential physical interaction with nuclear RNA-related proteins, and localization to DNA replication sites.[108-109] The mechanism how the non-enzymatic function drives proliferation is not well understood. Overexpression of MTHFD2 with an active site residue mutated that's required for catalysis still had a proliferative advantage compared to overexpression of the vector.[108] Similar to SHMT2, regulation of MTHFD2 expression extends beyond canonical metabolism-related transcription factors such as c-MYC, mTOR, ATF4, HIF-1α, AMPK, and NRF2.[1] For example, several microRNAs and transcription factors like the chimeric oncogene EWS-FLI1 have been shown to impact MTHFD2 expression.[7, 63] Non-coding RNAs reported to regulate MTHFD2 expression include miR-9 (along with lncRNA *TUG1*), miR-92a, miR-940, miR-33a-5p, miR-22, and *LIN28B*.[110-116] MTHFD2 is a predicted target gene of miR-99a-3p, miR-186-5p, and hsa-miR-202.[117-119] Similar to SHMT2, acetylation of an active site residue (Lys88) was reported to be removed by SIRT3 thereby activating MTHFD2's enzymatic activity.[120] Five sites of phosphorylation on MTHFD2 have been identified through phosphoproteomics (S149, T187, T191, T306, and T324).[121] However, it is unknown what kinases catalyze these phosphorylations or what purpose they serve. PTMs in general can act as a switch for metabolic enzymes to take on their moonlighting functions.[122] For example, phosphorylation of superoxide dismutase 1 (SOD1) causes its translocation to the nucleus where it is able to transcriptionally upregulate antioxidant-related genes.[123] As MTHFD2 has been shown to be present at DNA replication sites,[108] it would be interesting to see if PTMs regulated this function.

Table I-3. Inhibitors of human MTHFDs.

Compound	Structure	Isoform activity	Anticancer activity	Refs.
LY345899		MTHFD1 IC_{50} = 96 nM MTHFD2 IC_{50} = 663 nM	SW620 IC_{50} = ~10 μM *In vivo* efficacy in SW620-based xenograft and patient-derived xenograft	103, 124
Carolacton		MTHFD1 (dehydrogenase function) IC_{50} = 38 nM MTHFD1 (cyclohydrolase function) IC_{50} = 19 nM MTHFD2 (dehydrogenase function) IC_{50} = 6.5 nM MTHFD2 (cyclohydrolase function) IC_{50} = 86 nM	HCT 116 IC_{50} = 25 μM	99
DS44960156		MTHFD1 IC_{50} = >30 μM MTHFD2 IC_{50} = 1.6 μM	No data published	125
DS18561882		MTHFD1 IC_{50} = 0.57 μM MTHFD2 IC_{50} = 6.3 nM	MDA-MB-231 IC_{50} = 140 nM *In vivo* efficacy in MDA-MB-231 xenograft	100

MTHFD Inhibitors

The mounting evidence of the clinical relevance of MTHFD2 has led to intense interest in developing MTHFD2-targeting therapeutics. The development of MTHFD2 inhibitors was recently reviewed, so will only be discussed here briefly.[7] There are fewer published inhibitors of MTHFD2 than for SHMT2 (Table I-3), but significant progress in selectivity over the cytosolic MTHFD isoform (MTHFD1) was achieved in a very short amount of time. The first described MTHFD2 inhibitor, LY345899, is a folate analog. While it had activity in the high nanomolar range, it was still ~7-fold selective for MTHFD1.[124] Around the same time, the natural product carolacton was originally discovered as a inhibitor of the *E. coli* isoform, FolD, but also possessed potent activity against MTHFD1 and MTHFD2.[99] Interestingly, carolacton was selective for MTHFD2 with the dehydrogenase function, but for MTHFD1 with the cyclohydrolase function.[99] The first truly MTHFD2-selective inhibitor was reported in 2019, DS44960156, although potency was lacking.[125] Later that year, the same group followed up with an optimized inhibitor, DS18561882, that was not only potent *in vitro* but was also efficacious *in vivo*.[100] MTHFD2L takes the place of MTHFD2's function in normal adult tissues, so an important next step would be to evaluate the activity of these molecules against this mitochondrial isoform. Currently there are no crystal structures available for the other two human mitochondrial isoforms (Table I-4).

Table I-4. X-ray crystal structures of human MTHFDs.

Protein	Ligands	Resolution (Å)	PDB ID	Refs.
MTHFD1	NADP	1.50	1A4I	[126]
	NADP, LY249543	2.20	1DIA	[127]
	NADP, LY345899	2.70	1DIB	
	NADP, LY374571	2.20	1DIG	
	NADP, LY249543	2.20	6ECP	

	NADP, LY345899	2.70	6ECQ	[128]
	NADP	2.20	6ECR	
MTHFD2	NAD, LY345899	1.89	5TC4	[124]
	DS44960156	2.25	6JIB	[125]
	Compound **1**	2.50	6JID	
	DS18561882	2.25	6KG2	[100]
MTHFD1L	NA	NA	NA	NA
MTHFD2L	NA	NA	NA	NA

[a]NA, not applicable

Impact on cancer patient survival

Of the four MTHFD isoforms, MTHFD2 is the only one that it is not expressed in adult human tissues and is primarily expressed during embryonic development or in cancerous cells, making it an attractive anti-cancer target.[9] Overexpression of MTHFD2 associates with poor prognosis and clinicopathological parameters in breast, renal, liver, pancreatic, and colorectal cancers and some brain cancers.[7] A TCGA pan-disease survival association analysis with MTHFD2 expression was performed using the GDAC Firehose-sourced data as described above (Figure 5). Our analysis corroborated previous findings with pancreatic (pancreatic adenocarcinoma, PAAD), kidney renal clear cell carcinoma (KIRC), and kidney renal papillary cell carcinoma (KIRP) malignancies.[129-130] We identified significant reduction in survival with higher expression of *MTHFD2* in bladder urothelial carcinoma (BLCA) and uterine corpus endometrial carcinoma (UCEC) (Figure 5B). These findings have not been published to our knowledge. Significant reduction in survival was seen with lower expression of *MTHFD2* in glioblastoma multiforme (GBM) and low-grade glioma (LGG) (Figure 5C). The role of MTHFD2 in brain cancer seems to be quite complex as other studies have seen similar and contrasting results.[7]
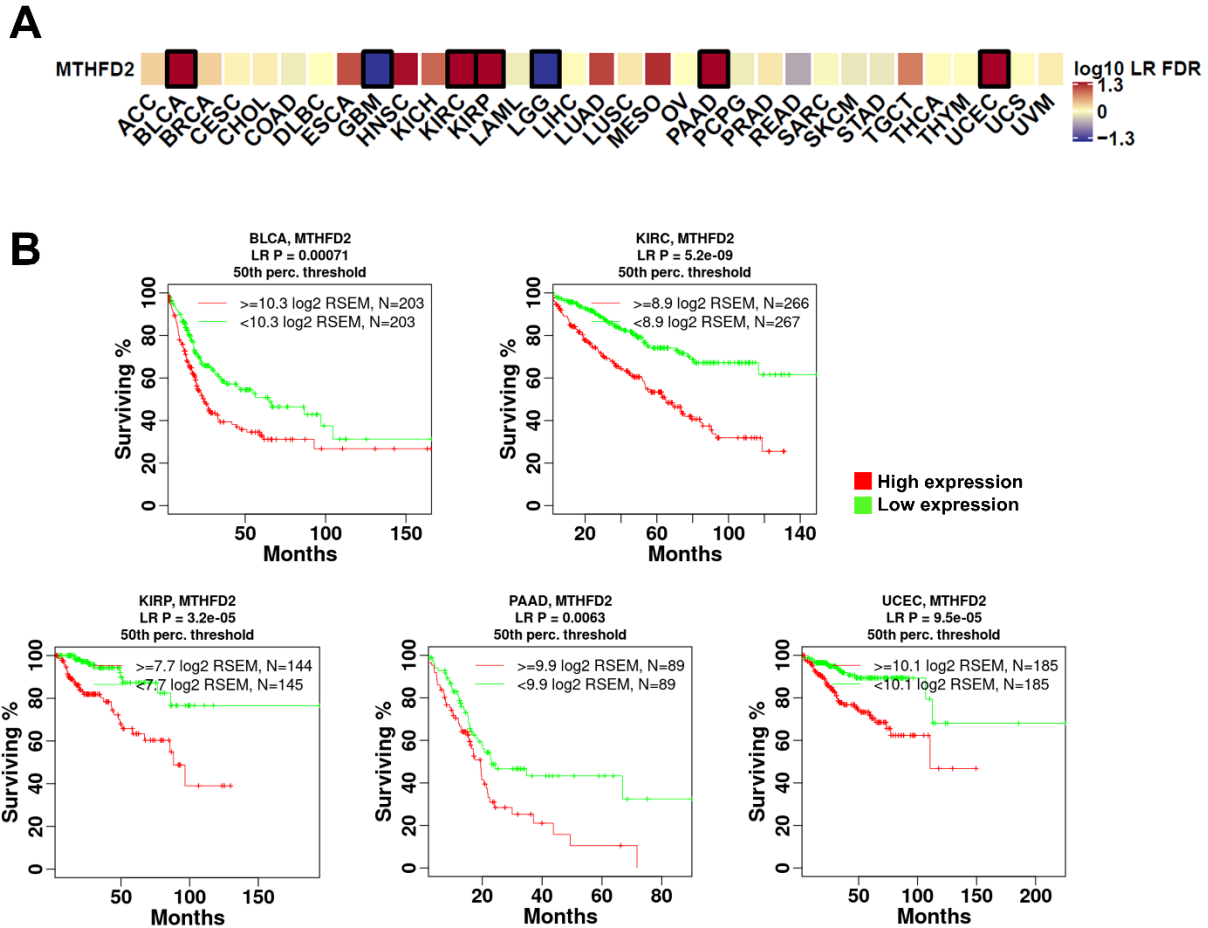
Figure I-5. Pan-cancer MTHFD2 patient survival association survey. (A) *MTHFD2* expression correlates with cancer patient survival in several cancers. Patients from each disease were stratified by median expression of MTHFD2. Heatmap color indicates directionality and significance of association (red = reduced survival, blue = increased survival) with increased gene expression. Heatmap cells with black borders indicate FDR p-value < 0.05. (B) High *MTHFD2* expression associates with reduced survival in BLCA, KIRC, KIRP, PAAD, and UCEC. Log-rank (LR) statistic p-values used to quantify association with survival were FDR adjusted across cancers.

Summary
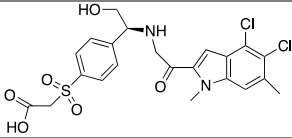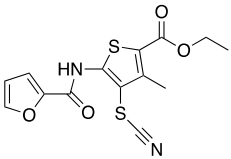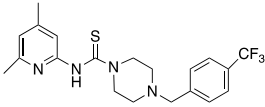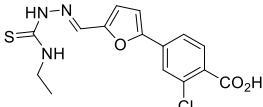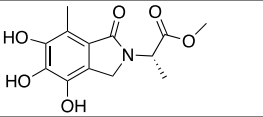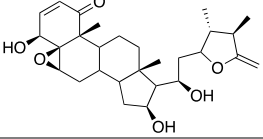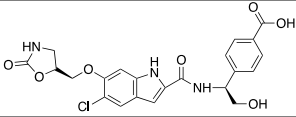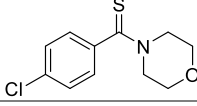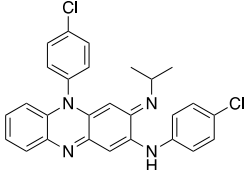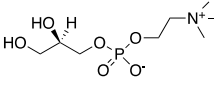
Metabolic reprogramming shifts a cell's metabolism from an energetically efficient process to one which is more biomass production centric. As a result, this allows cancer cells to rapidly proliferate, resist chemotherapies, invade, metastasize, and survive a nutrient-deprived microenvironment. 1CM has its hand in many biosynthetic pathways that fuel growth, regulate redox status, contributes to post-translational modifications, among others. In this review, we focused on the 1CM pathway as a target for cancer therapy, and in particular, SHMT2 and MTHFD2.
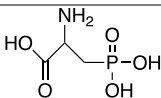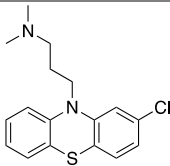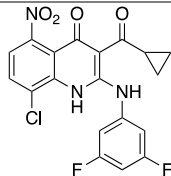
The function, regulation, and clinical relevance of SHMT2 and MTHFD2 were all discussed. These enzymes are critical for their contributions to the synthesis of one carbon donors in different oxidation states ($5,10\text{-}CH_2\text{-}THF$ and $10\text{-}CHO\text{-}THF$) that are donated to biosynthetic pathways such as pyrimidine and purine biosynthesis, respectively. Several post-translational modifications have been discovered that regulate SHMT2's activity. Interestingly, both SHMT2's and MTHFD2's enzymatic activity is regulated by SIRT3.[59, 120] Additionally, the expression of both enzymes are controlled by an increasing number of miRs and other non-coding RNAs. Through our independent analysis of The Cancer Genome Atlas we identified several cancers whose survival was associated with the high expression of SHMT2 (ACC) and MTHFD2 (BLCA, ESCA, HNSC, LUAD, MESO, and UCEC).

We also provided a comprehensive overview of preclinical and clinical inhibitors targeting the 1CM pathway. Most clinically approved drugs for this pathway target DHFR and TYMS, and there are still even new drugs undergoing clinical trials that target these enzymes (raltitrexed, piritrexim, ZD-9331, and GS7904L). However, there are other 1CM enzymes with inhibitors undergoing clinical trials (MAT2A and GART). There is considerable interest in pursuing development of SHMT2 and MTHFD2 inhibitors due to their selective overexpression and association with myriad of clinicopathological parameters. Significant progress has been made in the discovery of potent inhibitors of these enzymes.[70-71, 100] In summary, we believe that targeting 1CM will be a mainstay therapeutic strategy for the treatment of cancer for years to come.
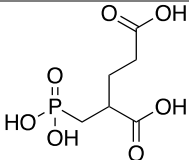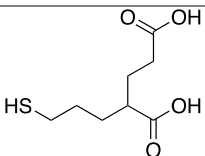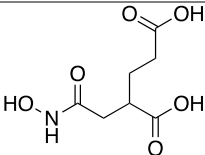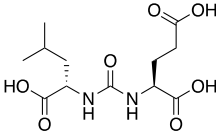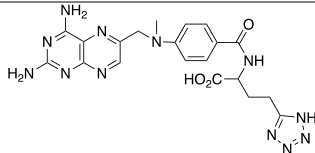
Appendix
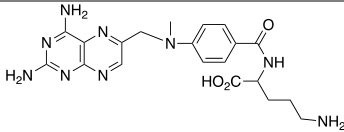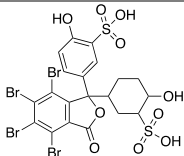
Appendix Table I-1. Serine biosynthesis inhibitors.

Protein	Inhibitor	Structure	Targets/activity	Disease/status
PHGDH	BI-4924		IC_{50} = 2 nM[15]	Preclinical
	CBR-5884		IC_{50} = 33 μM[131]	Preclinical
	NCT-503		IC_{50} = 2.5 μM[132]	Preclinical
	PKUMDL-WQ-2201		IC_{50} = 35.7 μM[133]	Preclinical
	Azacoccone E		IC_{50} = 9.8 μM[134]	Preclinical
	Ixocarpalactone A		IC_{50} = ~1.5 μM[135]	Preclinical
	Compound **1**		IC_{50} = 238 nM[136]	Preclinical
	Compound **38**		IC_{50} = 10.4 μM[137]	Preclinical
PSAT1	None	N/A	N/A	N/A
PSPH	Clofazimine		M. tuberculosis isoform K_i = 2.74 ± 0.016 μM[13]	FDA-approved to treat leprosy and tuberculosis[138]
	Glycerylphosphorylcholine		IC_{50} = 18 μM[139]	Clinical trials Physical and psychomotor performance[140] Dementia disorders[141]

				No trials for cancer
D-2-amino-3-phosphonopropionic acid			$K_i = 48$ μM[142]	Preclinical
Chlorpromazine			MtSerB2 phosphatase domain $IC_{50} = 6.25 \pm 0.3$ μM[143]	Preclinical
Jung11			*P. gingivalis* isoform $K_i = 1.0$ μM[13]	Preclinical
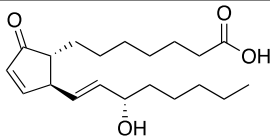
Appendix Table I-2. Folate glutamylation-modifying enzyme inhibitors.

Protein	Inhibitor	Structure	Targets/activity	Disease/status
FOLH1[a]	2-PMPA		$IC_{50} = 0.3$ nM[17]	Preclinical; poor oral bioavailability prevented from advancing to clinic Prodrug: TrisPOC-2PMPA Prodrug: TetraODOL-2PMPA
	2-MPPA (GPI5693)		$IC_{50} = 90$ nM[17]	Preclinical; not advanced to human clinical trials due to toxicity
	JHU 241		$IC_{50} = 220$ nM[17]	Preclinical Prodrug: P-acetoxybenzyl (PAB)
	ZJ-43		$IC_{50} = 2.4$ nM[17]	Preclinical
FPGS	γ-Tetrazolyl-MTX		$K_i = 50$ μM[18]	Preclinical

γ-ornithine-MTX			$IC_{50} = 33\ \mu M$[18]	Preclinical
Bromosulfophthalein			$IC_{50} = 17\ \mu M$[144]	Preclinical

[a]Consult Ref. 17 for details on clinical use of FOLH1 inhibitors
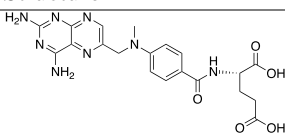
Appendix Table I-3. Folate and serine transporter inhibitors.
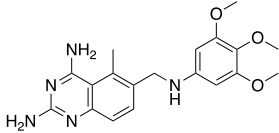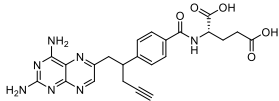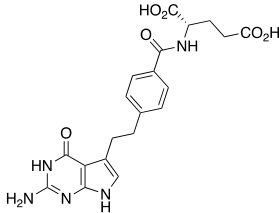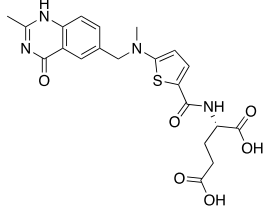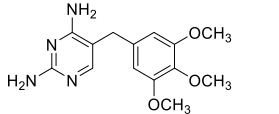
Protein	Inhibitor	Structure	Targets/activity	Disease/status
MFT (SLC25A32)	None	NA	NA	NA
FOLR1	Farletuzumab (MORAb-003)	monoclonal antibody of IgG1κ	human FRα; Does not inhibit folate uptake; elicits antibody-dependent cellular toxicity[10]	Ovarian cancer Phase I[145] Phase II[146] Phase III, Did not meet primary endpoint[147]
	TVRTSAE peptide	Thr-Val-Arg-Thr-Ser-Ala-Glu	Competes with folic acid for binding to FOLR1[20]	Preclinical
SFXN1	None	NA	NA	NA
PCFT (SLC46A1)[a]	None[b]	NA	NA	NA
RFC (SLC19A1)[a]	Prostaglandin A1		$K_i = 21\ \mu M$[148]	Preclinical
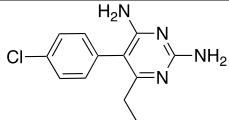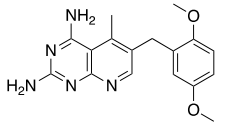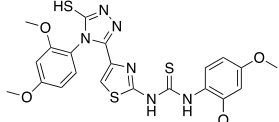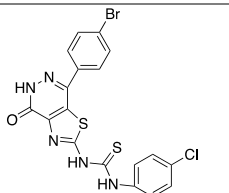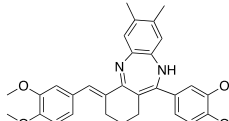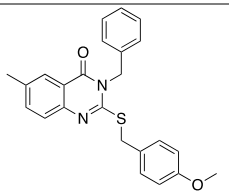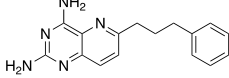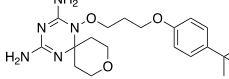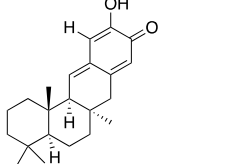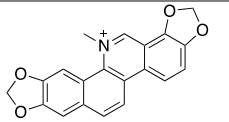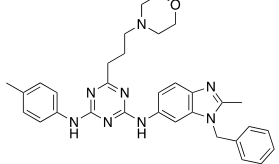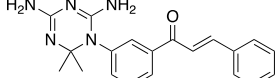
[a]Anti-folates are excluded as they are also substrates
[b]Compounds with K_i or $IC_{50} > 50\ \mu M$ are not included
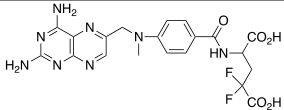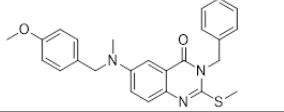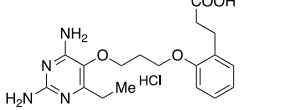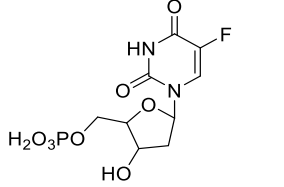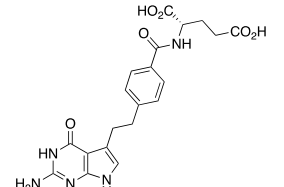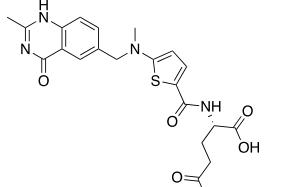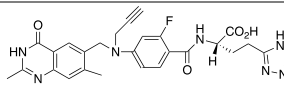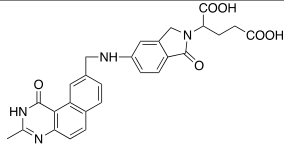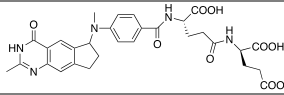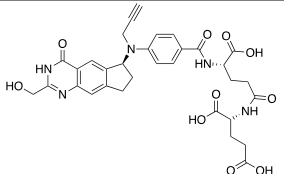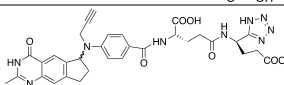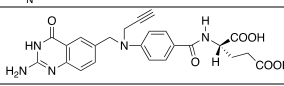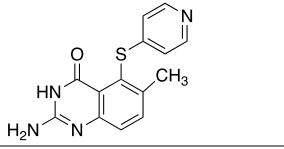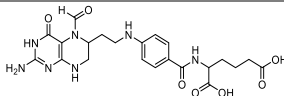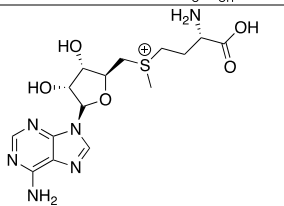
Appendix Table I-4. Cytosolic and mitochondrial folate metabolism inhibitors.
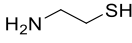
Protein	Inhibitor	Structure	Targets/activity	Disease/status
DHFR	Methotrexate (MTX)[a]		$K_i = 5.5\ pM$[149]	FDA-approved for rheumatoid arthritis, psoriasis, and neoplastic diseases[150] Osteosarcoma Phase III, NCT01176981

Trimetrexate		$IC_{50} = 80.9 \pm 12.5$ nM[151]	FDA approved for treatment of malignant pleural mesothelioma and NSCLC
			Colorectal cancer Phase II, NCT00003446
			Pancreatic cancer Phase II, NCT00002955
			Sarcoma Phase I, NCT00119301 Phase II, NCT00003776
			Leukemia Phase II, NCT00002738
Pralatrexate		$K_i = 13.4$ pM[152]	Approved for recurrent or refractory peripheral T-cell lymphoma[21]
			Multiple trials
Pemetrexed[a]		$K_i = 7.0$ nM[41]	FDA-approved for NSCLC and malignant pleural mesothelioma
			Multiple trials
Raltitrexed		$K_i = 92$ nM[153]	Approved by EMA to treat colorectal cancer (not approved by FDA)
			Esophageal cancer Phase II, NCT03585530
			Mesothelioma Phase II, NCT00004254
			Colorectal cancer Phase IV, NCT02557490, and NCT01959061
			HNSCC Phase IV, NCT03196843
Trimethoprim		*ec*DHFR $IC_{50} = 20$ nM[154]	FDA-approved for urinary tract infections (antibacterial)[155]

Pyrimethamine		IC_{50} = ~15 µM K_i^{app} = 5.41 nM[156-157]	FDA-approved for toxoplasmosis Multiple trials
Piritrexim		IC_{50} = 5 nM[158]	Bladder cancer Phase II, NCT00002914
Compound **34**		IC_{50} = 0.03 µM[159]	Preclinical
Compound **26**		IC_{50} = 0.06 µM[160]	Preclinical
Compound **35**		IC_{50} = 4 nM[161]	Preclinical
Compound **61**		IC_{50} = 0.01 µM[162]	Preclinical
Compound **3.5**		IC_{50} = 0.06 µM[163]	Preclinical
Compound **A5**		IC_{50} = 3.72 nM[164]	Preclinical
Puupehenone		IC_{50} = 5 µg/mL[165]	Preclinical
Sanguinarine		Cellular DHFR IC_{50} < 1.5 µM[166]	Preclinical
Compound **22**		IC_{50} = 0.28 nM[167]	Preclinical
Compound **11b**		IC_{50} = 2.4 µM[168]	Preclinical

	DL-γ,γ-F$_2$MTX (Compound 2)	IC$_{50}$ = 1.53 ± 0.03 μM[169]	Preclinical
	Compound **31**	IC$_{50}$ = 0.4 μM[170]	Preclinical
	P218	K$_i$ = 5.41 ± 0.12 μM[157]	Preclinical
TYMS	5-Fluorodeoxyuridylate (active form of 5-fluorouracil)[b]	K$_i$ = 0.2 nM[171]	5FU is FDA-approved for colorectal, breast, gastric, and pancreatic cancer Actinic Keratosis Phase III, NCT03727074 Phase IV, NCT00696488 Ectropion Phase II, NCT02705352 Cervical dysplasia Phase III, NCT00000758 Glaucoma Phase III, NCT00000122 Bladder cancer Phase II, NCT00003175
	Pemetrexed	K$_i$ = 109 nM[41]	See above for DHFR
	Raltitrexed	K$_i$ = 62 nM[153]	See above for DHFR
	ZD-9331	K$_i$ = 0.44 nM[172]	Ovarian cancer Phase II, NCT00014690

			K_i	
	GS7904L		$K_i = 90$ pM[173]	Colorectal cancer Phase I, NCT00081237
				Head and Neck Phase II, NCT00116909
				Advanced Solid Tumors Phase I, NCT00116896
				Gastric Adenocarcinoma Phase II, NCT00073502
				Locally Advanced or Metastatic Adenoma of the Biliary Tract Phase II, NCT00088270
	Compound **1a**		$K_i^{app} = 14$ nM[174]	Preclinical
	BGC-945		$K_i = 1.2$ nM[175]	Preclinical
	Compound **7j**		$K_i^{app} = 0.2$ nM[176]	Preclinical
	CB-3717		$K_i = 3$ nM[172]	Withdrawn from clinical study due to toxicity
	AG-337 (nolatrexed)		$K_i = 16$ nM[172]	FDA refused approval in 2005 for liver cancer
ALDH1L1/2	None	NA	NA	NA
MTHFS	5-formylTHHF		$K_i = 0.7 \pm 0.3$ μM^{25}	Preclinical
MTHFR	SAM (product feedback inhibitor)		$K_i = 2.7$ μM^{23}	Not approved for medicinal use; available as an herbal supplement

28
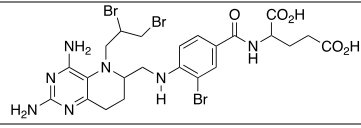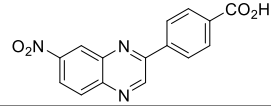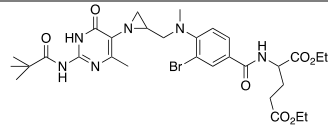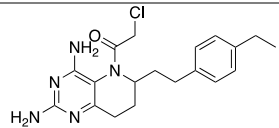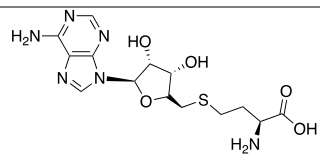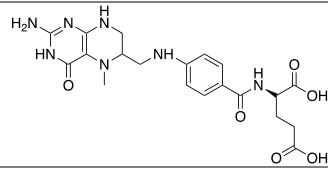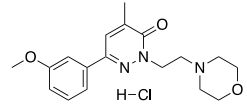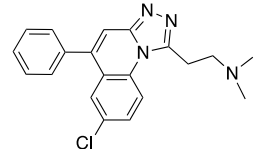
MTFMT	None	NA	NA	NA
GCS	Cysteamine	H_2N⌒SH	$K_i = 5\ \mu M$[26]	FDA-approved for nephropathic cystinosis Multiple trials
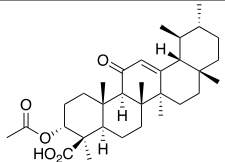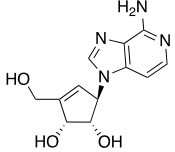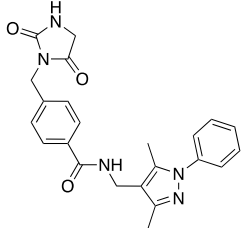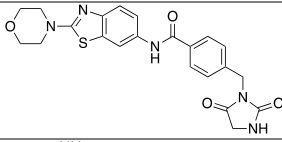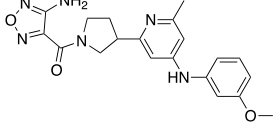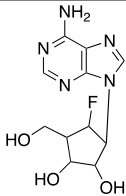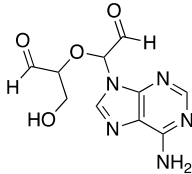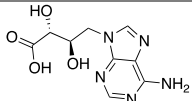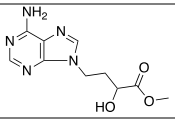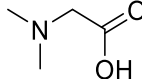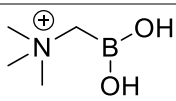
Appendix Table I-5. Inhibitors of the methionine cycle arm of 1CM.

Protein	Inhibitor	Structure	Targets/activity	Disease/status
MS/MTR	Compound 16		$IC_{50} = 1.43 \pm 0.40\ \mu M$[177]	Preclinical
	Compound 5c		$IC_{50} = 9\ \mu M$[178]	Preclinical
	Compound 6		$IC_{50} = 4.15\ \mu M$[28]	Preclinical
	Compound 6c		$IC_{50} = 12.1\ \mu M$[29]	Preclinical
MTRR	None	NA	NA	NA
DMGDH	None	NA	NA	NA
GNMT	Adenosylhomo-cysteine		$K_i = 40\ \mu M$[30]	Preclinical
	5-methyl-THF		$IC_{50} = 2\ \mu M$ $K_d = 95\ nM$[30]	Preclinical
MAT	AG-270		MAT2A inhibitor; no activity data published	Advanced Solid Tumors & Lymphoma Phase I, NCT03435250
	PF-9366		MAT2A $IC_{50} = 420 \pm 50\ nM$ $K_d = 170\ nM$[31]	Preclinical

	AKBA		MAT2A $K_d = 129 \pm 28$ nM[32]	Preclinical
AHCY/ SAHH	DZNep		$IC_{50} =$ 0.23 μM[36]	Preclinical
	Compound **1a**		$IC_{50} =$ 1.0 μM[36]	Preclinical
	Compound **1b**		$IC_{50} =$ 0.8 μM[36]	Preclinical
	Compound **2**		$IC_{50} =$ 1.0 μM[36]	Preclinical
	Compound **10**		$IC_{50} = 8$ nM[33]	Preclinical
	Adenosine dialdehyde		$IC_{50} = 40$ nM[33]	Preclinical
	D-eritadenine		$IC_{50} = 12$ nM[34]	Preclinical
	DZ2002		$K_i = 17.9$ nM[35]	Preclinical
BHMT	N,N-dimethylglycine		$K_i = 10$ μM[179]	Preclinical
	TAMB		$IC_{50} = 45$ μM[180]	Preclinical

Compound **2**		IC$_{50}$ = 87 nM[37]	Preclinical	
Compound **11**		BHMT2 IC$_{50}$ = 3.6 μM K$_i^{app}$ ~77 nM BHMT IC$_{50}$ = 77 μM[38]	Preclinical	

Appendix Table I-6. Inhibitors of folate-dependent enzymes in purine biosynthesis.

Protein	Inhibitor	Structure	Targets/activity	Disease/status
GART	Pemetrexed		K$_i$ = 9.3 μM[41]	See above for DHFR
	Lometrexol		K$_i$ = 60 nM[42]	Cancer Phase I, NCT00024310 and[181] Lung cancer Phase II, NCT00033722 Discontinued in clinical trials
	Compound **12**		K$_i$ = 130 nM[182]	Preclinical
	AG2034		K$_i$ = 28 nM[183]	Did not advance past Phase I due to toxicity[43-44]
ATIC/AICARFT	Pemetrexed		K$_i$ = 3.58 μM[41]	See above for DHFR
	LSN3213128		IC$_{50}$ = 16 nM[45]	Preclinical
	BW2315		K$_i$ = 6 nM[184]	Preclinical

Compound **14**		$K_i = 685$ nM[40]	Preclinical

References

1.   Rosenzweig, A.; Blenis, J.; Gomes, A. P., Beyond the Warburg effect: how do cancer cells regulate one-carbon metabolism? *Front Cell Dev Biol.* **2018,** *6*, 90.

2.   Li, A. M.; Ye, J., Reprogramming of serine, glycine and one-carbon metabolism in cancer. *Biochim Biophys Acta Mol Basis Dis.* **2020,** *1866* (10), 165841.

3.   Farber, S.; Diamond, L. K.; Mercer, R. D.; Sylvester Jr, R. F.; Wolff, J. A., Temporary remissions in acute leukemia in children produced by folic acid antagonist, 4-aminopteroyl-glutamic acid (aminopterin). *N Engl J Med.* **1948,** *238*, 787-793.

4.   Locasale, J. W., Serine, glycine and one-carbon units: cancer metabolism in full circle. *Nat Rev Cancer.* **2013,** *13* (8), 572-583.

5.   Asai, A.; Konno, M.; Koseki, J.; Taniguchi, M.; Vecchione, A.; Ishii, H., One-carbon metabolism for cancer diagnostic and therapeutic approaches. *Cancer Lett.* **2020,** *470*, 141-148.

6.   Cronstein, B. N.; Aune, T. M., Methotrexate and its mechanisms of action in inflammatory arthritis. *Nat Rev Rheumatol.* **2020,** *16* (3), 145-154.

7.   Zhu, Z.; Leung, G. K. K., More than a metabolic enzyme: MTHFD2 as a novel target for anticancer therapy? *Front Oncol.* **2020,** *10*, 658.

8.   Jain, M. N., R.; Sharma, S.; Madhusuhan, N.; Kitami, T.; Souza, A.L.; Kafri, R.; Kirschner, M.W.; Clish, C.B. Mootha, V.K., Metabolite profiling identifies a key role for glycine in rapid cancer cell proliferation. *Science.* **2012,** *336*, 1040-1044.

9.   Nilsson, R.; Jain, M.; Madhusudhan, N.; Sheppard, N. G.; Strittmatter, L.; Kampf, C.; Huang, J.; Asplund, A.; Mootha, V. K., Metabolic enzyme expression highlights a key role for MTHFD2 and the mitochondrial folate pathway in cancer. *Nat Commun.* **2014,** *5*, 3128.

10.   Scaranti, M.; Cojocaru, E.; Banerjee, S.; Banerji, U., Exploiting the folate receptor alpha in oncology. *Nat Rev Clin Oncol.* **2020,** *17* (6), 349-359.

11.   Shane, B., Folylpolyglutamate synthesis and role in the regulation of one-carbon metabolism. 1989; pp 263-335.

12.   Robinson, A. D.; Eich, M. L.; Varambally, S., Dysregulation of de novo nucleotide biosynthetic pathway enzymes in cancer and targeting opportunities. *Cancer Lett.* **2020,** *470*, 134-140.

13.   Haufroid, M.; Wouters, J., Targeting the serine sathway: a promising approach against tuberculosis? *Pharmaceuticals.* **2019,** *12* (2), 66.

14.   Ravez, S.; Spillier, Q.; Marteau, R.; Feron, O.; Frederick, R., Challenges and opportunities in the development of serine synthetic pathway inhibitors for cancer therapy. *J Med Chem.* **2017,** *60* (4), 1227-1237.

15.   Weinstabl, H.; Treu, M.; Rinnenthal, J.; Zahn, S. K.; Ettmayer, P.; Bader, G.; Dahmann, G.; Kessler, D.; Rumpel, K.; Mischerikow, N.; Savarese, F.; Gerstberger, T.; Mayer, M.; Zoephel, A.; Schnitzer, R.; Sommergruber, W.; Martinelli, P.; Arnhof, H.; Peric-Simov, B.; Hofbauer, K. S.; Garavel, G.; Scherbantin, Y.; Mitzner, S.; Fett, T. N.; Scholz, G.; Bruchhaus, J.; Burkard, M.; Kousek, R.; Ciftci, T.; Sharps, B.; Schrenk, A.; Harrer, C.; Haering, D.; Wolkerstorfer, B.; Zhang, X.; Lv, X.; Du, A.; Li, D.; Li, Y.; Quant, J.; Pearson, M.; McConnell, D. B., Intracellular trapping of the selective phosphoglycerate dehydrogenase (PHGDH) inhibitor BI-4924 disrupts serine biosynthesis. *J Med Chem.* **2019,** *62* (17), 7976-7997.

16.   Kim, S. E., Enzymes involved in folate metabolism and its implication for cancer treatment. *Nutr Res Pract.* **2020,** *14* (2), 95-101.

17.   Vornov, J. J.; Peters, D.; Nedelcovych, M.; Hollinger, K.; Rais, R.; Slusher, B. S., Looking for drugs in all the wrong places: use of GCPII inhibitors outside the brain. *Neurochem Res.* **2020,** *45* (6), 1256-1267.

18.   McGuire, J. J.; Tsukamoto, T.; Hart, B. P.; Coward, J. K.; Kalman, T. I.; Galivan, J., Exploitation of folate and antifolate polyglutamylation to achieve selective anticancer chemotherapy. *Invest. New Drugs.* **1996,** *14*, 317-323.

19.   Matherly, L. H.; Hou, Z.; Gangjee, A., The promise and challenges of exploiting the proton-coupled folate transporter for selective therapeutic targeting of cancer. *Cancer Chemother Pharmacol.* **2018,** *81* (1), 1-15.

20.   Hulin-Curtis, S. L.; Davies, J. A.; Nestic, D.; Bates, E. A.; Baker, A. T.; Cunliffe, T. G.; Majhen, D.; Chester, J. D.; Parker, A. L., Identification of folate receptor alpha (FRalpha) binding oligopeptides and their evaluation for targeted virotherapy applications. *Cancer Gene Ther.* **2020.**

21.   Carmona-Martinez, V.; Ruiz-Alcaraz, A. J.; Vera, M.; Guirado, A.; Martinez-Esparza, M.; Garcia-Penarrubia, P., Therapeutic potential of pteridine derivatives: A comprehensive review. *Med Res Rev.* **2019,** *39* (2), 461-516.

22.   Vodenkova, S.; Buchler, T.; Cervena, K.; Veskrnova, V.; Vodicka, P.; Vymetalkova, V., 5-fluorouracil and other fluoropyrimidines in colorectal cancer: Past, present and future. *Pharmacol Ther.* **2020,** *206*, 107447.

23.   Froese, D. S.; Kopec, J.; Rembeza, E.; Bezerra, G. A.; Oberholzer, A. E.; Suormala, T.; Lutz, S.; Chalk, R.; Borkowska, O.; Baumgartner, M. R.; Yue, W. W., Structural basis for the regulation of human 5,10-methylenetetrahydrofolate reductase by phosphorylation and S-adenosylmethionine inhibition. *Nat Commun.* **2018,** *9* (1), 2261.

24.   Bhatia, M.; Thakur, J.; Suyal, S.; Oniel, R.; Chakraborty, R.; Pradhan, S.; Sharma, M.; Sengupta, S.; Laxman, S.; Masakapalli, S. K.; Bachhawat, A. K., Allosteric inhibition of MTHFR prevents futile SAM cycling and maintains nucleotide pools in one carbon metabolism. *J Biol Chem.* **2020**.

25.   Field, M. S.; Szebenyl , D. M. E.; Perry, C. A.; Stover, P. J., Inhibition of 5,10-methenyltetrahydrofolate synthetase. *Arch Biochem Biophys.* **2007,** *2*, 194-201.

26.   Lowry, M.; Hall, M. S.; Brosnan, J. T., Specificity and mechanism of the inhibition by cysteamine of the renal glycine-cleavage complex. *Biochem Soc Trans.* **1986,** *14*, 131-132.

27.   Shen, W.; Gao, C.; Cueto, R.; Liu, L.; Fu, H.; Shao, Y.; Yang, W. Y.; Fang, P.; Choi, E. T.; Wu, Q.; Yang, X.; Wang, H., Homocysteine-methionine cycle is a metabolic sensor system controlling methylation-regulated pathological signaling. *Redox Biol.* **2020,** *28*, 101322.

28.   Deng, X.; Guo, Y.; Tian, C.; Liu, J.; Wang, X.; Zhang, Z., Design, synthesis and activities of aziridine derivatives of N5-methyltetrahydrofolate against methionine synthase. *Chem Res Chinese U.* **2015,** *31* (5), 742-745.

29.   Wang, M.; Tian, C.; Xue, L.; Li, H.; Cong, J.; Fang, F.; Yang, J.; Yuan, M.; Chen, Y.; Guo, Y.; Wang, X.; Liu, J.; Zhang, Z., Design, synthesis and biological activity of N(5)-substituted tetrahydropteroate analogs as non-classical antifolates against cobalamin-dependent methionine synthase and potential anticancer agents. *Eur J Med Chem.* **2020,** *190*, 112113.

30.   Luka, Z., Methyltetrahydrofolate in folate-binding protein glycine N-methyltransferase. In *Folic Acid and Folates*, 2008; pp 325-345.

31.   Quinlan, C. L.; Kaiser, S. E.; Bolanos, B.; Nowlin, D.; Grantner, R.; Karlicek-Bryant, S.; Feng, J. L.; Jenkinson, S.; Freeman-Cook, K.; Dann, S. G.; Wang, X.; Wells, P. A.; Fantin, V. R.; Stewart, A. E.; Grant, S. K., Targeting S-adenosylmethionine biosynthesis with a novel allosteric inhibitor of Mat2A. *Nat Chem Biol.* **2017,** *13* (7), 785-792.

32.   Bai, J.; Gao, Y.; Chen, L.; Yin, Q.; Lou, F.; Wang, Z.; Xu, Z.; Zhou, H.; Li, Q.; Cai, W.; Sun, Y.; Niu, L.; Wang, H.; Wei, Z.; Lu, S.; Zhou, A.; Zhang, J.; Wang, H., Identification of a natural inhibitor of methionine adenosyltransferase 2A regulating one-carbon metabolism in keratinocytes. *EBioMedicine.* **2019,** *39*, 575-590.

33.   Madhavan, B. G. V.; McGee, D. P. C.; Rydzewski, R. M.; Boehme, R.; Martin, J. C.; Prisbe, E. J., Synthesis and antiviral evaluation of 6'-substituted aristeromycin: potential mechanism-based inhibitors of S-adenosylhomocysteine hydrolase 1. *J Med Chem.* **1988,** *31*, 1798-1804.

34.   Votruba, I.; Holy, A., Studies on S-adenosyl-L-homocysteine hydrolase. III. Eritadenines - a novel type of potent inhibitors of S-adenosyl-L-homocysteine hydrolase. *Collect Czech Chem C.* **1982,** *47*, 167-172.

35.   Wu, Q. L.; Fu, Y. F.; Zhou, W. L.; Wang, J. X.; Feng, Y. H.; Liu, J.; Xu, J. Y.; He, P. L.; Zhou, R.; Tang, W.; Wang, G. F.; Zhou, Y.; Yang, Y. F.; Ding, J.; Li, X. Y.; Chen, X. R.; Yuan, C.; Lawson, B. R.; Zuo, J. P., Inhibition of S-adenosyl-L-homocysteine hydrolase induces immunosuppression. *J Pharmacol Exp Ther.* **2005,** *313* (2), 705-711.

36.   Uchiyama, N.; Dougan, D. R.; Lawson, J. D.; Kimura, H.; Matsumoto, S. I.; Tanaka, Y.; Kawamoto, T., Identification of AHCY inhibitors using novel high-throughput mass spectrometry. *Biochem Biophys Res Commun.* **2017,** *491* (1), 1-7.

37.   Jiracek, J.; Collinsova, M.; Rosenberg, I.; Budesinsky, M.; Protivinska, E.; Netusilova, H.; Garrow, T. A., S-alkylated homocysteine derivatives: new inhibitors of human betaine-homocysteine S-methyltransferase. *J Med Chem.* **2006,** *49* (13), 3982-3989.

38.   Mladkova, J.; Vanek, V.; Budesinsky, M.; Elbert, T.; Demianova, Z.; Garrow, T. A.; Jiracek, J., Double-headed sulfur-linked amino acids as first inhibitors for betaine-homocysteine S-methyltransferase 2. *J Med Chem.* **2012,** *55* (15), 6822-6831.

39.   Pedley, A. M.; Benkovic, S. J., A new view into the regulation of purine metabolism: the purinosome. *Trends Biochem Sci.* **2017,** *42* (2), 141-154.

40.   Spurr, I. B.; Birts, C. N.; Cuda, F.; Benkovic, S. J.; Blaydes, J. P.; Tavassoli, A., Small molecule inhibitor of AICAR transformylase homodimerization. *Chembiochem.* **2012,** *13* (11), 1628-1634.

41.   Shih, C.; Chen, V. J.; Gossett, L. S.; Gates, S. B.; MacKellar, W. C.; Habeck, L. L.; Shackelford, K. A.; Mendelsohn, L. G.; Soose, D. J.; Patel, V. F.; Andis, S. L.; Bewley, J. R.; Rayl, E. A.; Moroson, B. A.; Beardsley, G. P.; Kohier, W.; Ratnam, M.; Schultz, R. M., LY231514, a pyrrolo[2,3-d]pyrimidine-based antifolate that inhibits multiple folate-requiring enzymes. *Cancer Res.* **1997,** *57*, 1116-1123.

42.   Zhang, Y.; Desharnais, J.; Marsilje, T. H.; Li, C.; Hedrick, M. P.; Gooljarsingh, L. T.; Tavassoli, A.; Benkovic, S. J.; Olson, A. J.; Boger, D. L.; Wilson, I. A., Rational design, synthesis, evaluation, and crystal structure of a potent inhibitor of human GAR Tfase: 10-(trifluoroacetyl)-5,10-dideazaacyclic-5,6,7,8-tetrahydrofolic acid. *Biochemistry.* **2003,** *42* (20), 6043-6056.

43.   Bissett, D.; McLeod, H. L.; Sheedy, B.; Collier, M.; Pithavala, Y.; Paradiso, L.; Pitsiladis, M.; Cassidy, J., Phase I dose-escalation and pharmacokinetic study of a novel folate analogue AG2034. *Br J Cancer.* **2001,** *84* (3), 308-312.

44.   Roberts, J. D.; Shibata, S.; Spicer, D. V.; McLeod, H. L.; Tombes , M. B.; Carrol, B. K. M.; Sheedy, B.; Colier, M. A.; Pithavala, Y. K.; Paradiso, L. J.; Clendeninn, N. J., Phase I study of AG2034, a targeted GARFT inhibitor, administered once every 3 weeks. *Cancer Chemother Pharmacol.* **1999**, 423-427.

45.   Brooks, H. B.; Meier, T. I.; Geeganage, S.; Fales, K. R.; Thrasher, K. J.; Konicek, S. A.; Spencer, C. D.; Thibodeaux, S.; Foreman, R. T.; Hui, Y. H.; Roth, K. D.; Qian, Y. W.; Wang, T.; Luo, S.; Torrado, A.; Si, C.; Toth, J. L.; Mc Cowan, J. R.; Frimpong, K.; Lee, M. R.; Dally, R. D.; Shepherd, T. A.; Durham, T. B.; Wang, Y.; Wu, Z.; Iversen, P. W.; Njoroge, F. G., Characterization of a novel AICARFT inhibitor which potently elevates ZMP and has anti-tumor activity in murine models. *Sci Rep.* **2018,** *8* (1), 15458.

46.   Min, D. J.; Vural, S.; Krushkal, J., Association of transcriptional levels of folate-mediated one-carbon metabolism-related genes in cancer cell lines with drug treatment response. *Cancer Genet.* **2019,** *237*, 19-38.

47.   Li, X.; Zhang, K.; Hu, Y.; Luo, N., ERRalpha activates SHMT2 transcription to enhance the resistance of breast cancer to lapatinib via modulating the mitochondrial metabolic adaption. *Biosci Rep.* **2020,** *40* (1), BSR20192465.

48.   Morscher, R. J.; Ducker, G. S.; Li, S. H.; Mayer, J. A.; Gitai, Z.; Sperl, W.; Rabinowitz, J. D., Mitochondrial translation requires folate-dependent tRNA methylation. *Nature.* **2018,** *554* (7690), 128-132.

49.   Minton, D. R.; Nam, M.; McLaughlin, D. J.; Shin, J.; Bayraktar, E. C.; Alvarez, S. W.; Sviderskiy, V. O.; Papagiannakopoulos, T.; Sabatini, D. M.; Birsoy, K.; Possemato, R., Serine catabolism by SHMT2 is required for proper mitochondrial translation initiation and maintenance of formylmethionyl-tRNAs. *Mol Cell.* **2018,** *69* (4), 610-621.

50.   Tong, J.; Krieger, J. R.; Taylor, P.; Bagshaw, R.; Kang, J.; Jeedigunta, S.; Wybenga-Groot, L. E.; Zhang, W.; Badr, H.; Mirhadi, S.; Pham, N. A.; Coyaud, E.; Yu, M.; Li, M.; Cabanero, M.; Raught, B.; Maynes, J. T.; Hawkins, C.; Tsao, M. S.; Moran, M. F., Cancer proteome and metabolite changes linked to SHMT2. *PLoS One.* **2020,** *15* (9), e0237981.

51.   Engel, A. L.; Lorenz, N. I.; Klann, K.; Munch, C.; Depner, C.; Steinbach, J. P.; Ronellenfitsch, M. W.; Luger, A. L., Serine-dependent redox homeostasis regulates glioblastoma cell survival. *Br J Cancer.* **2020,** *122* (9), 1391-1398.

52.   Ye, J.; Fan, J.; Venneti, S.; Wan, Y. W.; Pawel, B. R.; Zhang, J.; Finley, L. W.; Lu, C.; Lindsten, T.; Cross, J. R.; Qing, G.; Liu, Z.; Simon, M. C.; Rabinowitz, J. D.; Thompson, C. B., Serine catabolism regulates mitochondrial redox control during hypoxia. *Cancer Discov.* **2014,** *4* (12), 1406-1417.

53.   Kim, D.; Fiske, B. P.; Birsoy, K.; Freinkman, E.; Kami, K.; Possemato, R. L.; Chudnovsky, Y.; Pacold, M. E.; Chen, W. W.; Cantor, J. R.; Shelton, L. M.; Gui, D. Y.; Kwon, M.; Ramkissoon, S. H.; Ligon, K. L.; Kang, S. W.; Snuderl, M.; Vander Heiden, M. G.; Sabatini, D. M., SHMT2 drives glioma cell survival in ischaemia but imposes a dependence on glycine clearance. *Nature.* **2015,** *520* (7547), 363-367.

54.   Rabl, J.; Bunker, R. D.; Schenk, A. D.; Cavadini, S.; Gill, M. E.; Abdulrahman, W.; Andres-Pons, A.; Luijsterburg, M. S.; Ibrahim, A. F. M.; Branigan, E.; Aguirre, J. D.; Marceau,

A. H.; Guerillon, C.; Bouwmeester, T.; Hassiepen, U.; Peters, A.; Renatus, M.; Gelman, L.; Rubin, S. M.; Mailand, N.; van Attikum, H.; Hay, R. T.; Thoma, N. H., Structural basis of BRCC36 function in DNA repair and immune regulation. *Mol Cell.* **2019,** *75* (3), 483-497.

55.   Walden, M.; Tian, L.; Ross, R. L.; Sykora, U. M.; Byrne, D. P.; Hesketh, E. L.; Masandi, S. K.; Cassel, J.; George, R.; Ault, J. R.; El Oualid, F.; Pawlowski, K.; Salvino, J. M.; Eyers, P. A.; Ranson, N. A.; Del Galdo, F.; Greenberg, R. A.; Zeqiraj, E., Metabolic control of BRISC-SHMT2 assembly regulates immune signalling. *Nature.* **2019,** *570* (7760), 194-199.

56.   Rabl, J., BRCA1-A and BRISC: multifunctional molecular machines for ubiquitin signaling. *Biomolecules.* **2020,** *10* (11).

57.   Cao, J.; Sun, L.; Aramsangtienchai, P.; Spiegelman, N. A.; Zhang, X.; Huang, W.; Seto, E.; Lin, H., HDAC11 regulates type I interferon signaling through defatty-acylation of SHMT2. *Proc Natl Acad Sci USA.* **2019,** *116* (12), 5487-5492.

58.   Yang, X.; Wang, Z.; Li, X.; Liu, B.; Liu, M.; Liu, L.; Chen, S.; Ren, M.; Wang, Y.; Yu, M.; Wang, B.; Zou, J.; Zhu, W. G.; Yin, Y.; Gu, W.; Luo, J., SHMT2 desuccinylation by SIRT5 drives cancer cell proliferation. *Cancer Res.* **2018,** *78* (2), 372-386.

59.   Wei, Z.; Song, J.; Wang, G.; Cui, X.; Zheng, J.; Tang, Y.; Chen, X.; Li, J.; Cui, L.; Liu, C. Y.; Yu, W., Deacetylation of serine hydroxymethyl-transferase 2 by SIRT3 promotes colorectal carcinogenesis. *Nat Commun.* **2018,** *9* (1), 4468.

60.   Ding, J.; Li, T.; Wang, X.; Zhao, E.; Choi, J. H.; Yang, L.; Zha, Y.; Dong, Z.; Huang, S.; Asara, J. M.; Cui, H.; Ding, H. F., The histone H3 methyltransferase G9A epigenetically activates the serine-glycine synthesis pathway to sustain cancer cell survival and proliferation. *Cell Metab.* **2013,** *18* (6), 896-907.

61.   Selvarajah, B.; Azuelos, I.; Platé, M.; Guillotin, D.; Forty, E. J.; Contento, G.; Woodcock, H. V.; Redding, M.; Taylor, A.; Brunori, G.; Durrenberger, P. F.; Ronzoni, R.; Blanchard, A. D.; Mercer, P. F.; Anastasiou, D.; Chambers, R. C., mTORC1 amplifies the ATF-dependent de novo serine-glycine pathway to supply glycine during TGF-β-induced collagen biosynthesis. *Sci Signal.* **2019,** *12*, eaav3048.

62.   Marrocco, I.; Altieri, F.; Rubini, E.; Paglia, G.; Chichiarelli, S.; Giamogante, F.; Macone, A.; Perugia, G.; Magliocca, F. M.; Gurtner, A.; Maras, B.; Ragno, R.; Patsilinakos, A.; Manganaro, R.; Eufemi, M., Shmt2: a Stat3 signaling new player in prostate cancer energy metabolism. *Cells.* **2019,** *8* (9), 1048.

63.   Sen, N.; Cross, A. M.; Lorenzi, P. L.; Khan, J.; Gryder, B. E.; Kim, S.; Caplen, N. J., EWS-FLI1 reprograms the metabolism of Ewing sarcoma cells via positive regulation of glutamine import and serine-glycine biosynthesis. *Mol Carcinog.* **2018,** *57* (10), 1342-1357.

64.   Guiducci, G.; Paone, A.; Tramonti, A.; Giardina, G.; Rinaldo, S.; Bouzidi, A.; Magnifico, M. C.; Marani, M.; Menendez, J. A.; Fatica, A.; Macone, A.; Armaos, A.; Tartaglia, G. G.;

Contestabile, R.; Paiardini, A.; Cutruzzola, F., The moonlighting RNA-binding activity of cytosolic serine hydroxymethyltransferase contributes to control compartmentalization of serine metabolism. *Nucleic Acids Res.* **2019,** *47* (8), 4240-4254.

65.   Lin, C.; Zhang, Y.; Chen, Y.; Bai, Y.; Zhang, Y., Long noncoding RNA LINC01234 promotes serine hydroxymethyltransferase 2 expression and proliferation by competitively binding miR-642a-5p in colon cancer. *Cell Death Dis.* **2019,** *10* (2), 137.

66.   Wu, X.; Deng, L.; Tang, D.; Ying, G.; Yao, X.; Liu, F.; Liang, G., miR-615-5p prevents proliferation and migration through negatively regulating serine hydromethyltransferase 2 (SHMT2) in hepatocellular carcinoma. *Tumour Biol.* **2016,** *37* (5), 6813-6821.

67.   Pinweha, P.; Rattanapornsompong, K.; Charoensawan, V.; Jitrapakdee, S., MicroRNAs and oncogenic transcriptional regulatory networks controlling metabolic reprogramming in cancers. *Comput Struct Biotechnol J.* **2016,** *14*, 223-233.

68.   Leivonen, S. K.; Rokka, A.; Ostling, P.; Kohonen, P.; Corthals, G. L.; Kallioniemi, O.; Perala, M., Identification of miR-193b targets in breast cancer cells and systems biological analysis of their functional impact. *Mol Cell Proteomics.* **2011,** *10* (7), M110.005322.

69.   Ducker, G. S.; Ghergurovich, J. M.; Mainolfi, N.; Suri, V.; Jeong, S. K.; Hsin-Jung Li, S.; Friedman, A.; Manfredi, M. G.; Gitai, Z.; Kim, H.; Rabinowitz, J. D., Human SHMT inhibitors reveal defective glycine import as a targetable metabolic vulnerability of diffuse large B-cell lymphoma. *Proc Natl Acad Sci USA.* **2017,** *114* (43), 11404-11409.

70.   Dekhne, A. S.; Shah, K.; Ducker, G. S.; Katinas, J. M.; Wong-Roushar, J.; Nayeen, M. J.; Doshi, A.; Ning, C.; Bao, X.; Fruhauf, J.; Liu, J.; Wallace-Povirk, A.; O'Connor, C.; Dzinic, S. H.; White, K.; Kushner, J.; Kim, S.; Huttemann, M.; Polin, L.; Rabinowitz, J. D.; Li, J.; Hou, Z.; Dann, C. E., 3rd; Gangjee, A.; Matherly, L. H., Novel pyrrolo[3,2-d]pyrimidine compounds target mitochondrial and cytosolic one-carbon metabolism with broad-spectrum antitumor efficacy. *Mol Cancer Ther.* **2019,** *18* (10), 1787-1799.

71.   Garcia-Canaveras, J. C.; Lancho, O.; Ducker, G. S.; Ghergurovich, J. M.; Xu, X.; da Silva-Diz, V.; Minuzzo, S.; Indraccolo, S.; Kim, H.; Herranz, D.; Rabinowitz, J. D., SHMT inhibition is effective and synergizes with methotrexate in T-cell acute lymphoblastic leukemia. *Leukemia.* **2020**.

72.   Han, Y.; He, L.; Qi, Y.; Zhao, Y.; Pan, Y.; Fang, B.; Li, S.; Zhang, J. Z. H.; Zhang, L., Identification of three new compounds that directly target human serine hydroxymethyltransferase SHMT2. *Chem Biol Drug Des.* **2020**.

73.   Witschel, M. C.; Rottmann, M.; Schwab, A.; Leartsakulpanich, U.; Chitnumsub, P.; Seet, M.; Tonazzi, S.; Schwertz, G.; Stelzer, F.; Mietzner, T.; McNamara, C.; Thater, F.; Freymond, C.; Jaruwat, A.; Pinthong, C.; Riangrungroj, P.; Oufir, M.; Hamburger, M.; Maser, P.; Sanz-Alonso, L. M.; Charman, S.; Wittlin, S.; Yuthavong, Y.; Chaiyen, P.; Diederich, F., Inhibitors of

plasmodial serine hydroxymethyltransferase (SHMT): cocrystal structures of pyrazolopyrans with potent blood- and liver-stage activities. *J Med Chem.* **2015,** *58* (7), 3117-3130.

74.   Marani, M.; Paone, A.; Fiascarelli, A.; Macone, A.; Gargano, M.; Rinaldo, S.; Giardina, G.; Pontecorvi, V.; Koes, D.; McDermott, L.; Yang, T.; Paiardini, A.; Contestabile, R.; Cutruzzola, F., A pyrazolopyran derivative preferentially inhibits the activity of human cytosolic serine hydroxymethyltransferase and induces cell death in lung cancer cells. *Oncotarget.* **2015,** *7* (4), 4570-4583.

75.   Scaletti, E.; Jemth, A. S.; Helleday, T.; Stenmark, P., Structural basis of inhibition of the human serine hydroxymethyltransferase SHMT2 by antifolate drugs. *FEBS Lett.* **2019,** *593* (14), 1863-1873.

76.   Paiardini, A.; Fiascarelli, A.; Rinaldo, S.; Daidone, F.; Giardina, G.; Koes, D. R.; Parroni, A.; Montini, G.; Marani, M.; Paone, A.; McDermott, L. A.; Contestabile, R.; Cutruzzola, F., Screening and in vitro testing of antifolate inhibitors of human cytosolic serine hydroxymethyltransferase. *ChemMedChem.* **2015,** *10* (3), 490-497.

77.   Daidone, F.; Florio, R.; Rinaldo, S.; Contestabile, R.; di Salvo, M. L.; Cutruzzola, F.; Bossa, F.; Paiardini, A., In silico and in vitro validation of serine hydroxymethyltransferase as a chemotherapeutic target of the antifolate drug pemetrexed. *Eur J Med Chem.* **2011,** *46* (5), 1616-1621.

78.   Tramonti, A.; Paiardini, A.; Paone, A.; Bouzidi, A.; Giardina, G.; Guiducci, G.; Magnifico, M. C.; Rinaldo, S.; McDermott, L.; Menendez, J. A.; Contestabile, R.; Cutruzzola, F., Differential inhibitory effect of a pyrazolopyran compound on human serine hydroxymethyltransferase-amino acid complexes. *Arch Biochem Biophys.* **2018,** *653*, 71-79.

79.   Dekhne, A. S.; Ning, C.; Nayeen, M. J.; Shah, K.; Kalpage, H.; Fruhauf, J.; Wallace-Povirk, A.; O'Connor, C.; Hou, Z.; Kim, S.; Huttemann, M.; Gangjee, A.; Matherly, L. H., Cellular pharmacodynamics of a novel pyrrolo[3,2-d]pyrimidine inhibitor targeting mitochondrial and cytosolic one-carbon metabolism. *Mol Pharmacol.* **2020,** *97* (1), 9-22.

80.   Nonaka, H.; Nakanishi, Y.; Kuno, S.; Ota, T.; Mochidome, K.; Saito, Y.; Sugihara, F.; Takakusagi, Y.; Aoki, I.; Nagatoishi, S.; Tsumoto, K.; Sando, S., Design strategy for serine hydroxymethyltransferase probes based on retro-aldol-type reaction. *Nat Commun.* **2019,** *10* (1), 876.

81.   Paiardini, A.; Tramonti, A.; Schirch, D.; Guiducci, G.; di Salvo, M. L.; Fiascarelli, A.; Giorgi, A.; Maras, B.; Cutruzzola, F.; Contestabile, R., Differential 3-bromopyruvate inhibition of cytosolic and mitochondrial human serine hydroxymethyltransferase isoforms, key enzymes in cancer metabolic reprogramming. *Biochim Biophys Acta.* **2016,** *1864* (11), 1506-1517.

82.   Renwick, S. B.; Snell, K.; Baumann, U., The crystal structure of human cytosolic serine hydroxymethyltransferase: a target for cancer chemotherapy. *Structure.* **1998,** *6*, 1105-1116.

83.   Giardina, G.; Paone, A.; Tramonti, A.; Lucchi, R.; Marani, M.; Magnifico, M. C.; Bouzidi, A.; Pontecorvi, V.; Guiducci, G.; Zamparelli, C.; Rinaldo, S.; Paiardini, A.; Contestabile, R.; Cutruzzola, F., The catalytic activity of serine hydroxymethyltransferase is essential for de novo nuclear dTMP synthesis in lung cancer cells. *FEBS J.* **2018,** *285* (17), 3238-3253.

84.   Giardina, G.; Brunotti, P.; Fiascarelli, A.; Cicalini, A.; Costa, M. G.; Buckle, A. M.; di Salvo, M. L.; Giorgi, A.; Marani, M.; Paone, A.; Rinaldo, S.; Paiardini, A.; Contestabile, R.; Cutruzzola, F., How pyridoxal 5'-phosphate differentially regulates human cytosolic and mitochondrial serine hydroxymethyltransferase oligomeric state. *FEBS J.* **2015,** *282* (7), 1225-1241.

85.   Shi, H.; Fang, X.; Li, Y.; Zhang, Y., High expression of serine hydroxymethyltransferase 2 indicates poor prognosis of gastric cancer patients. *Med Sci Monit.* **2019,** *25*, 7430-7438.

86.   Liu, Y.; Yin, C.; Deng, M.-M.; Wang, Q.; He, X.-Q.; Li, M.-T.; Li, C.-P.; Wu, H., High expression of SHMT2 is correlated with tumor progression and predicts poor prognosis in gastrointestinal tumors. *Eur Rev Med Pharmacol Sci.* **2019,** *23*, 9379-9392.

87.   Ji, L.; Tang, Y.; Pang, X.; Zhang, Y., Increased expression of serine hydroxymethyltransferase 2 (SHMT2) is a negative prognostic marker in patients with hepatocellular carcinoma and is associated with proliferation of HepG2 cells. *Med Sci Monit.* **2019,** *25*, 5823-5832.

88.   Bernhardt, S.; Bayerlova, M.; Vetter, M.; Wachter, A.; Mitra, D.; Hanf, V.; Lantzsch, T.; Uleer, C.; Peschel, S.; John, J.; Buchmann, J.; Weigert, E.; Burrig, K. F.; Thomssen, C.; Korf, U.; Beissbarth, T.; Wiemann, S.; Kantelhardt, E. J., Proteomic profiling of breast cancer metabolism identifies SHMT2 and ASCT2 as prognostic factors. *Breast Cancer Res.* **2017,** *19* (1), 112.

89.   Zhang, L.; Chen, Z.; Xue, D.; Zhang, Q.; Liu, X.; Luh, F.; Hong, L.; Zhang, H.; Pan, F.; Liu, Y.; Chu, P.; Zheng, S.; Lou, G.; Yun, Y., Prognostic and therapeutic value of mitochondrial serine hydroxyl-methyltransferase 2 as a breast cancer biomarker. *Oncol Rep.* **2016,** *36* (5), 2489-2500.

90.   Lee, G. Y.; Haverty, P. M.; Li, L.; Kljavin, N. M.; Bourgon, R.; Lee, J.; Stern, H.; Modrusan, Z.; Seshagiri, S.; Zhang, Z.; Davis, D.; Stokoe, D.; Settleman, J.; de Sauvage, F. J.; Neve, R. M., Comparative oncogenomics identifies PSMB4 and SHMT2 as potential cancer driver genes. *Cancer Res.* **2014,** *74* (11), 3114-3126.

91.   Ning, S.; Ma, S.; Saleh, A. Q.; Guo, L.; Zhao, Z.; Chen, Y., SHMT2 overexpression predicts poor prognosis in intrahepatic cholangiocarcinoma. *Gastroenterol Res Pract.* **2018,** *2018*, 4369253.

92.   Wu, M.; Wanggou, S.; Li, X.; Liu, Q.; Xie, Y., Overexpression of mitochondrial serine hydroxyl-methyltransferase 2 is associated with poor prognosis and promotes cell proliferation and invasion in gliomas. *Onco Targets Ther.* **2017,** *10*, 3781-3788.

93.   Wang, B.; Wang, W.; Zhu, Z.; Zhang, X.; Tang, F.; Wang, D.; Liu, X.; Yan, X.; Zhuang, H., Mitochondrial serine hydroxymethyltransferase 2 is a potential diagnostic and prognostic biomarker for human glioma. *Clin Neurol Neurosurg.* **2017,** *154*, 28-33.

94.   Wang, H.; Chong, T.; Li, B. Y.; Chen, X. S.; Zhen, W. B., Evaluating the clinical significance of SHMT2 and its co-expressed gene in human kidney cancer. *Biol Res.* **2020,** *53* (1), 46.

95.   Wu, Z. Z.; Wang, S.; Yang, Q. C.; Wang, X. L.; Yang, L. L.; Liu, B.; Sun, Z. J., Increased expression of SHMT2 is associated with poor prognosis and advanced pathological grade in oral squamous cell carcinoma. *Front Oncol.* **2020,** *10*, 588530.

96.   Broad Institute TCGA Genome Data Analysis Center. Firehose stddata__2016_01_28 run. Broad Institute of MIT Harvard: 2016.

97.   Team, R. C. *R: A language and environment for statistical computing. R Foundation for Statistical Computing*, Vienna, Austria, 2018.

98.   Altieri, B.; Ronchi, C. L.; Kroiss, M.; Fassnacht, M., Next-generation therapies for adrenocortical carcinoma. *Best Pract Res Clin Endocrinol Metab.* **2020,** *34* (3), 101434.

99.   Fu, C.; Sikandar, A.; Donner, J.; Zaburannyi, N.; Herrmann, J.; Reck, M.; Wagner-Dobler, I.; Koehnke, J.; Muller, R., The natural product carolacton inhibits folate-dependent C1 metabolism by targeting FolD/MTHFD. *Nat Commun.* **2017,** *8* (1), 1529.

100.   Kawai, J.; Toki, T.; Ota, M.; Inoue, H.; Takata, Y.; Asahi, T.; Suzuki, M.; Shimada, T.; Ono, K.; Suzuki, K.; Takaishi, S.; Ohki, H.; Matsui, S.; Tsutsumi, S.; Hirota, Y.; Nakayama, K., Discovery of a potent, selective, and orally available MTHFD2 inhibitor (DS18561882) with in vivo antitumor activity. *J Med Chem.* **2019,** *62* (22), 10204-10220.

101.   Yu, C.; Yang, L.; Cai, M.; Zhou, F.; Xiao, S.; Li, Y.; Wan, T.; Cheng, D.; Wang, L.; Zhao, C.; Huang, X., Down-regulation of MTHFD2 inhibits NSCLC progression by suppressing cycle-related genes. *J Cell Mol Med.* **2020,** *24* (2), 1568-1577.

102.   Chan, C.-H.; Wu, C.-Y.; Dubey, N. K.; Wei, H.-J.; Lu, J.-H.; Mao, S.; Liang, J.; Liang, Y.-H.; Cheng, H.-C.; Deng, W.-P., Modulating redox homeostasis and cellular reprogramming through inhibited methylenetatrahydrofolate dehydrogenase 2 enzymatic activities in lung cancer. *Aging.* **2020,** *12*, 17930-17947.

103.   Ju, H. Q.; Lu, Y. X.; Chen, D. L.; Zuo, Z. X.; Liu, Z. X.; Wu, Q. N.; Mo, H. Y.; Wang, Z. X.; Wang, D. S.; Pu, H. Y.; Zeng, Z. L.; Li, B.; Xie, D.; Huang, P.; Hung, M. C.; Chiao, P. J.;

Xu, R. H., Modulation of redox homeostasis by inhibition of MTHFD2 in colorectal cancer: mechanisms and therapeutic implications. *J Natl Cancer Inst.* **2018,** *111*, 584-596.

104.   Ducker, G. S.; Chen, L.; Morscher, R. J.; Ghergurovich, J. M.; Esposito, M.; Teng, X.; Kang, Y.; Rabinowitz, J. D., Reversal of cytosolic one-carbon flux compensates for loss of the mitochondrial folate pathway. *Cell Metab.* **2016,** *23* (6), 1140-1153.

105.   Green, N. H.; Galvan, D. L.; Badal, S. S.; Chang, B. H.; LeBleu, V. S.; Long, J.; Jonasch, E.; Danesh, F. R., MTHFD2 links RNA methylation to metabolic reprogramming in renal cell carcinoma. *Oncogene.* **2019,** *38* (34), 6211-6225.

106.   Yang, L.; Garcia Canaveras, J. C.; Chen, Z.; Wang, L.; Liang, L.; Jang, C.; Mayr, J. A.; Zhang, Z.; Ghergurovich, J. M.; Zhan, L.; Joshi, S.; Hu, Z.; McReynolds, M. R.; Su, X.; White, E.; Morscher, R. J.; Rabinowitz, J. D., Serine catabolism feeds NADH when respiration is impaired. *Cell Metab.* **2020,** *31* (4), 809-821.

107.   Fan, J.; Ye, J.; Kamphorst, J. J.; Shlomi, T.; Thompson, C. B.; Rabinowitz, J. D., Quantitative flux analysis reveals folate-dependent NADPH production. *Nature.* **2014,** *510* (7504), 298-302.

108.   Gustafsson Sheppard, N.; Jarl, L.; Mahadessian, D.; Strittmatter, L.; Schmidt, A.; Madhusudan, N.; Tegner, J.; Lundberg, E. K.; Asplund, A.; Jain, M.; Nilsson, R., The folate-coupled enzyme MTHFD2 is a nuclear protein and promotes cell proliferation. *Sci Rep.* **2015,** *5*, 15029.

109.   Koufaris, C.; Nilsson, R., Protein interaction and functional data indicate MTHFD2 involvement in RNA processing and translation. *Cancer Metab.* **2018,** *6*, 12.

110.   Selcuklu, S. D.; Donoghue, M. T.; Rehmet, K.; de Souza Gomes, M.; Fort, A.; Kovvuru, P.; Muniyappa, M. K.; Kerin, M. J.; Enright, A. J.; Spillane, C., MicroRNA-9 inhibition of cell proliferation and identification of novel miR-9 targets by transcriptome profiling in breast cancer cells. *J Biol Chem.* **2012,** *287* (35), 29516-29528.

111.   Gu, Y.; Si, J.; Xiao, X.; Tian, Y.; Yang, S., miR-92a inhibits proliferation and induces apoptosis by regulating methylenetetrahydrofolate dehydrogenase 2 (MTHFD2) expression in acute myeloid leukemia. *Oncol Res.* **2017,** *25* (7), 1069-1079.

112.   Xu, T.; Zhang, K.; Shi, J.; Huang, B.; Wang, X.; Qian, K.; Ma, T.; Qian, T.; Song, Z.; Li, L., MicroRNA-940 inhibits glioma progression by blocking mitochondrial folate metabolism through targeting of MTHFD2. *Am J Cancer Res.* **2019,** *9* (2), 250-269.

113.   Yan, Y.; Zhang, D.; Lei, T.; Zhao, C.; Han, J.; Cui, J.; Wang, Y., MicroRNA-33a-5p suppresses colorectal cancer cell growth by inhibiting MTHFD2. *Clin Exp Pharmacol Physiol.* **2019,** *46* (10), 928-936.

114.   Zhou, J.; Bi, C.; Ching, Y. Q.; Chooi, J. Y.; Lu, X.; Quah, J. Y.; Toh, S. H.; Chan, Z. L.; Tan, T. Z.; Chong, P. S.; Chng, W. J., Inhibition of LIN28B impairs leukemia cell growth and metabolism in acute myeloid leukemia. *J Hematol Oncol.* **2017,** *10* (1), 138.

115.   Zhao, X. B.; Ren, G. S., LncRNA taurine-upregulated gene 1 promotes cell proliferation by inhibiting microRNA-9 in MCF-7 cells. *J Breast Cancer.* **2016,** *19* (4), 349-357.

116.   Tong, D.; Zhang, J.; Wang, X.; Li, Q.; Liu, L.; Lu, A.; Guo, B.; Yang, J.; Ni, L.; Qin, H.; Zhao, L.; Huang, C., MiR-22, regulated by MeCP2, suppresses gastric cancer cell proliferation by inducing a deficiency in endogenous S-adenosylmethionine. *Oncogenesis.* **2020,** *9* (11), 99.

117.   Wei, G. G.; Guo, W. P.; Tang, Z. Y.; Li, S. H.; Wu, H. Y.; Zhang, L. C., Expression level and prospective mechanism of miRNA-99a-3p in head and neck squamous cell carcinoma based on miRNA-chip and miRNA-sequencing data in 1, 167 cases. *Pathol Res Pract.* **2019,** *215* (5), 963-976.

118.   Jones, D. Z.; Schmidt, M. L.; Suman, S.; Hobbing, K. R.; Barve, S. S.; Gobejishvili, L.; Brock, G.; Klinge, C. M.; Rai, S. N.; Park, J.; Clark, G. J.; Agarwal, R.; Kidd, L. R., Micro-RNA-186-5p inhibition attenuates proliferation, anchorage independent growth and invasion in metastatic prostate cancer cells. *BMC Cancer.* **2018,** *18* (1), 421.

119.   Gamazon, E. R.; Trendowski, M. R.; Wen, Y.; Wing, C.; Delaney, S. M.; Huh, W.; Wong, S.; Cox, N. J.; Dolan, M. E., Gene and microRNA perturbations of cellular response to pemetrexed implicate biological networks and enable imputation of response in lung adenocarcinoma. *Sci Rep.* **2018,** *8* (1), 733.

120.   Wan, X.; Wang, C.; Huang, Z.; Zhou, D.; Xiang, S.; Qi, Q.; Chen, X.; Arbely, E.; Liu, C. Y.; Du, P.; Yu, W., Cisplatin inhibits SIRT3-deacetylation MTHFD2 to disturb cellular redox balance in colorectal cancer cell. *Cell Death Dis.* **2020,** *11* (8), 649.

121.   Hornbeck, P. V.; Kornhauser, J. M.; Tkachev, S.; Zhang, B.; Skrzypek, E.; Murray, B.; Latham, V.; Sullivan, M., PhosphoSitePlus: a comprehensive resource for investigating the structure and function of experimentally determined post-translational modifications in man and mouse. *Nucleic Acids Res.* **2012,** *40* (Database issue), D261-270.

122.   Snaebjornsson, M. T.; Schulze, A., Non-canonical functions of enzymes facilitate cross-talk between cell metabolic and regulatory pathways. *Exp Mol Med.* **2018,** *50* (4), 34.

123.   Banks, C. J.; Andersen, J. L., Mechanisms of SOD1 regulation by post-translational modifications. *Redox Biol.* **2019,** *26*, 101270.

124.   Gustafsson, R.; Jemth, A. S.; Gustafsson, N. M. S.; Farnegardh, K.; Loseva, O.; Wiita, E.; Bonagas, N.; Dahllund, L.; Llona-Minguez, S.; Haggblad, M.; Henriksson, M.; Andersson, Y.; Homan, E.; Helleday, T.; Stenmark, P., Crystal structure of the emerging cancer target MTHFD2 in complex with a substrate-based inhibitor. *Cancer Res.* **2017,** *77* (4), 937-948.

125.   Kawai, J.; Ota, M.; Ohki, H.; Toki, T.; Suzuki, M.; Shimada, T.; Matsui, S.; Inoue, H.; Sugihara, C.; Matsuhashi, N.; Matsui, Y.; Takaishi, S.; Nakayama, K., Structure-based design and synthesis of an isozyme-selective MTHFD2 inhibitor with a tricyclic coumarin scaffold. *ACS Med Chem Lett.* **2019,** *10* (6), 893-898.

126.   Allaire, M.; Li, Y.; MacKenzie, R. E.; Cygler, M., The 3-D structure of a folate-dependent dehydrogenase/cyclohydrolase bifunctional enzyme at 1.5 Å resolution. *Structure.* **1998,** *6*, 173-182.

127.   Schmidt, A.; Wu, H.; MacKenzie, R. E.; Chen, V. J.; Bewly, J. R.; Ray, J. E.; Toth, J. E.; Cygler, M., Structures of three inhibitor complexes provide insight into the reaction mechanism of the human methylenetetrahydrofolate dehydrogenase/cyclohydrolase. *Biochemistry.* **2000,** *39*, 6325-6335.

128.   Bueno, R.; Dawson, A.; Hunter, W. N., An assessment of three human methylenetetrahydrofolate dehydrogenase/cyclohydrolase-ligand complexes following further refinement. *Acta Crystallogr F Struct Biol Commun.* **2019,** *75* (Pt 3), 148-152.

129.   Noguchi, K.; Konno, M.; Koseki, J.; Nishida, N.; Kawamoto, K.; Yamada, D.; Asaoka, T.; Noda, T.; Wada, H.; Gotoh, K.; Sakai, D.; Kudo, T.; Satoh, T.; Eguchi, H.; Doki, Y.; Mori, M.; Ishii, H., The mitochondrial one-carbon metabolic pathway is associated with patient survival in pancreatic cancer. *Oncol Lett.* **2018,** *16* (2), 1827-1834.

130.   Lin, H.; Huang, B.; Wang, H.; Liu, X.; Hong, Y.; Qiu, S.; Zheng, J., MTHFD2 overexpression predicts poor prognosis in renal cell carcinoma and is associated with cell proliferation and vimentin-modulated migration and invasion. *Cell Physiol Biochem.* **2018,** *51* (2), 991-1000.

131.   Mullarky, E.; Lucki, N. C.; Zavareh, R. B.; Anglin, J. L.; Gomes, A. P.; Nicolay, B. N.; Wong, J. C. Y.; Christen, S.; Takahashi, H.; Singh, P. K.; Blenis, J.; Warren, J. D.; Fendt, S.-M.; Asara, J. M.; DeNicola, G. M.; Lyssiotis, C. A.; Lairson, L. L.; Cantley, L. C., Identification of a small molecule inhibitor of 3-phosphoglycerate dehydrogenase to target serine biosynthesis in cancers. *Proc Natl Acad Sci USA.* **2016,** *113* (11), 1778–1783.

132.   Hamanaka, R. B.; Nigdelioglu, R.; Meliton, A. Y.; Tian, Y.; Witt, L. J.; O'Leary, E.; Sun, K. A.; Woods, P. S.; Wu, D.; Ansbro, B.; Ard, S.; Rohde, J. M.; Dulin, N. O.; Guzy, R. D.; Mutlu, G. M., Inhibition of phosphoglycerate dehydrogenase attenuates bleomycin-induced pulmonary fibrosis. *Am J Respir Cell Mol Biol.* **2018,** *58* (5), 585-593.

133.   Wang, Q.; Liberti, M. V.; Liu, P.; Deng, X.; Liu, Y.; Locasale, J. W.; Lai, L., Rational design of selective allosteric inhibitors of PHGDH and serine synthesis with anti-tumor activity. *Cell Chem Biol.* **2017,** *24* (1), 55-65.

134.   Guo, J.; Gu, X.; Zheng, M.; Zhang, Y.; Chen, L.; Li, H., Azacoccone E inhibits cancer cell growth by targeting 3-phosphoglycerate dehydrogenase. *Bioorg Chem.* **2019,** *87*, 16-22.

135.   Zheng, M.; Guo, J.; Xu, J.; Yang, K.; Tang, R.; Gu, X.; Li, H.; Chen, L., Ixocarpalactone A from dietary tomatillo inhibits pancreatic cancer growth by targeting PHGDH. *Food Funct.* **2019,** *10* (6), 3386-3395.

136.   Mullarky, E.; Xu, J.; Robin, A. D.; Huggins, D. J.; Jennings, A.; Noguchi, N.; Olland, A.; Lakshminarasimhan, D.; Miller, M.; Tomita, D.; Michino, M.; Su, T.; Zhang, G.; Stamford, A. W.; Meinke, P. T.; Kargman, S.; Cantley, L. C., Inhibition of 3-phosphoglycerate dehydrogenase (PHGDH) by indole amides abrogates de novo serine synthesis in cancer cells. *Bioorg Med Chem Lett.* **2019,** *29* (17), 2503-2510.

137.   Spillier, Q.; Ravez, S.; Unterlass, J.; Corbet, C.; Degavre, C.; Feron, O.; Frederick, R., Structure-activity relationships (SARs) of alpha-ketothioamides as inhibitors of phosphoglycerate dehydrogenase (PHGDH). *Pharmaceuticals.* **2020,** *13* (2), 20.

138.   Riccardi, N.; Giacomelli, A.; Canetti, D.; Comelli, A.; Intini, E.; Gaiera, G.; Diaw, M. M.; Udwadia, Z.; Besozzi, G.; Codecasa, L.; Di Biagio, A., Clofazimine: an old drug for never-ending diseases. *Future Microbiol.* **2020,** *15*, 557-566.

139.   Hawkinson, J. E.; Acosta-Burruel, M.; Ta, N. D.; Wood, P. L., Novel phosphoserine phosphatase inhibitors. *Eur J Pharmacol.* **1997,** *337*, 315-324.

140.   Marcus, L.; Soileau, J.; Judge, L. W.; Bellar, D., Evaluation of the effects of two doses of alpha glycerylphosphorylcholine on physical and psychomotor performance. *J Int Soc Sports Nutr.* **2017,** *14*, 39.

141.   Parnetti, L.; Mignini, F.; Tomassoni, D.; Traini, E.; Amenta, F., Cholinergic precursors in the treatment of cognitive impairment of vascular origin: ineffective approaches or need for re-evaluation? *J Neurol Sci.* **2007,** *257* (1-2), 264-269.

142.   Hawkinson, J. E.; Acosta-Burruel, M.; Wood, P. L., The metabotropic glutamate receptor antagonist l-2-amino-3-phosphonopropionic acid inhibits phosphoserine phosphatase. *Eur J Pharmacol.* **1996,** *307* (2), 219-225.

143.   Yadav, G. P.; Shree, S.; Maurya, R.; Rai, N.; Singh, D. K.; Srivastava, K. K.; Ramachandran, R., Characterization of M. tuberculosis SerB2, an essential HAD-family phosphatase, reveals novel properties. *PLoS One.* **2014,** *9* (12), e115409.

144.   McGuire, J. J.; Haile, W. H., Potent inhibition of human folylpolyglutamate synthetase by suramin. *Arch Biochem Biophys.* **1996,** *335*, 139-144.

145.   Konner, J. A.; Bell-McGuinn, K. M.; Sabbatini, P.; Hensley, M. L.; Tew, W. P.; Pandit-Taskar, N.; Vander Els, N.; Phillips, M. D.; Schweizer, C.; Weil, S. C.; Larson, S. M.; Old, L. J., Farletuzumab, a humanized monoclonal antibody against folate receptor alpha, in epithelial ovarian cancer: a phase I study. *Clin Cancer Res.* **2010,** *16* (21), 5288-5295.

146. Armstrong, D. K.; White, A. J.; Weil, S. C.; Phillips, M.; Coleman, R. L., Farletuzumab (a monoclonal antibody against folate receptor alpha) in relapsed platinum-sensitive ovarian cancer. *Gynecol Oncol.* **2013,** *129* (3), 452-458.

147. Vergote, I.; Armstrong, D.; Scambia, G.; Teneriello, M.; Sehouli, J.; Schweizer, C.; Weil, S. C.; Bamias, A.; Fujiwara, K.; Ochiai, K.; Poole, C.; Gorbunova, V.; Wang, W.; O'Shannessy, D.; Herzog, T. J., A randomized, double-blind, placebo-controlled, Phase III study to assess efficacy and safety of weekly farletuzumab in combination with carboplatin and taxane in patients with ovarian cancer in first platinum-sensitive relapse. *J Clin Oncol.* **2016,** *34* (19), 2271-2278.

148. Assaraf, Y. G.; Sierra, E. E.; Babani, S.; Goldman, I. D., Inhibitory effects of prostaglandin A1 on membrane transport of folates mediated by both the reduced folate carrier and ATP-driven exporters. *Biochem Pharmacol.* **1999,** *58*, 1321-1327.

149. Piper, J. R.; McCaleb, G. S.; Montgomery, J. A.; Kisliuk, R. L.; Gaumont, Y.; Sirotnak, F. M., Syntheses and antifolate activity of 5-Methyl-5-deaza analogues of aminopterin, methotrexate, folic acid, and N10-methylfolic acid. *J Med Chem.* **1986,** *29*, 1080-1087.

150. Alqarni, A. M.; Zeidler, M. P., How does methotrexate work? *Biochem Soc Trans.* **2020,** *48* (2), 559-567.

151. Senkovich, O.; Bhatia, V.; Garg, N.; Chattopadhyay, D., Lipophilic antifolate trimetrexate is a potent inhibitor of Trypanosoma cruzi: prospect for chemotherapy of Chagas' disease. *Antimicrob Agents Chemother.* **2005,** *49* (8), 3234-3238.

152. Sirotnak, F. M.; DeGraw, J. I.; Colwell, W. T.; Piper, J. R., A new analogue of 10-deazaaminopterin with markedly enhanced curative effects against human tumor xenografts in mice. *Cancer Chemother Pharmacol.* **1998,** *42*, 313-318.

153. Jackman, A. L.; Taylor, G. A.; Gibson, W.; Kimbell, R.; Brown, M.; Calvert, A. H.; Judson, I. R.; Hughes, L. R., ICI D1694, a quinazoline antifolate thymidylate synthase inhibitor that is a potent inhibitor of L1210 tumor cell growth in vitro and in vivo: a new agent for clinical study. *Cancer Res.* **1991,** *51*, 5579-5586.

154. Cammarata, M.; Thyer, R.; Lombardo, M.; Anderson, A.; Wright, D.; Ellington, A.; Brodbelt, J. S., Characterization of trimethoprim resistant E. coli dihydrofolate reductase mutants by mass spectrometry and inhibition by propargyl-linked antifolates. *Chem Sci.* **2017,** *8* (5), 4062-4072.

155. Wrobel, A.; Arciszewska, K.; Maliszewski, D.; Drozdowska, D., Trimethoprim and other nonclassical antifolates an excellent template for searching modifications of dihydrofolate reductase enzyme inhibitors. *J Antibiot (Tokyo).* **2020,** *73* (1), 5-27.

156. Liu, H.; Qin, Y.; Zhai, D.; Zhang, Q.; Gu, J.; Tang, Y.; Yang, J.; Li, K.; Yang, L.; Chen, S.; Zhong, W.; Meng, J.; Liu, Y.; Sun, T.; Yang, C., Antimalarial drug pyrimethamine plays a

dual role in antitumor proliferation and metastasis through targeting DHFR and TP. *Mol Cancer Ther.* **2019,** *18* (3), 541-555.

157.   Yuthavong, Y.; Tarnchompoo, B.; Vilaivan, T.; Chitnumsub, P.; Kamchonwongpaisan, S.; Charman, S. A.; McLennan, D. N.; White, K. L.; Vivas, L.; Bongard, E.; Thongphanchang, C.; Taweechai, S.; Vanichtanankul, J.; Rattanajak, R.; Arwon, U.; Fantauzzi, P.; Yuvaniyama, J.; Charman, W. N.; Matthews, D., Malarial dihydrofolate reductase as a paradigm for drug development against a resistance-compromised target. *Proc Natl Acad Sci U S A.* **2012,** *109* (42), 16823-16828.

158.   Fry, D. W.; Jackson, R. C., Biological and biochemical properties if new anticancer antagonists. *Cancer Metastasis Rev.* **1987,** *5*, 251-270.

159.   Hassan, G. S.; El-Messery, S. M.; Al-Omary, F. A.; Al-Rashood, S. T.; Shabayek, M. I.; Abulfadl, Y. S.; Habib el, S. E.; El-Hallouty, S. M.; Fayad, W.; Mohamed, K. M.; El-Menshawi, B. S.; El-Subbagh, H. I., Nonclassical antifolates, part 4. 5-(2-aminothiazol-4-yl)-4-phenyl-4H-1,2,4-triazole-3-thiols as a new class of DHFR inhibitors: synthesis, biological evaluation and molecular modeling study. *Eur J Med Chem.* **2013,** *66*, 135-145.

160.   Ewida, M. A.; Abou El Ella, D. A.; Lasheen, D. S.; Ewida, H. A.; El-Gazzar, Y. I.; El-Subbagh, H. I., Thiazolo[4,5-d]pyridazine analogues as a new class of dihydrofolate reductase (DHFR) inhibitors: Synthesis, biological evaluation and molecular modeling study. *Bioorg Chem.* **2017,** *74*, 228-237.

161.   El-Subbagh, H. I.; Hassan, G. S.; El-Messery, S. M.; Al-Rashood, S. T.; Al-Omary, F. A.; Abulfadl, Y. S.; Shabayek, M. I., Nonclassical antifolates, part 5. Benzodiazepine analogs as a new class of DHFR inhibitors: synthesis, antitumor testing and molecular modeling study. *Eur J Med Chem.* **2014,** *74*, 234-245.

162.   El-Messery, S. M.; Hassan, G. S.; Nagi, M. N.; Habib, E. E.; Al-Rashood, S. T.; El-Subbagh, H. I., Synthesis, biological evaluation and molecular modeling study of some new methoxylated 2-benzylthio-quinazoline-4(3H)-ones as nonclassical antifolates. *Bioorg Med Chem Lett.* **2016,** *26* (19), 4815-4823.

163.   Li, H.; Fang, F.; Liu, Y.; Xue, L.; Wang, M.; Guo, Y.; Wang, X.; Tian, C.; Liu, J.; Zhang, Z., Inhibitors of dihydrofolate reductase as antitumor agents: design, synthesis and biological evaluation of a series of novel nonclassical 6-substituted pyrido[3,2-d]pyrimidines with a three-to five-carbon bridge. *Bioorg Med Chem.* **2018,** *26* (9), 2674-2685.

164.   Zhou, X.; Lin, K.; Ma, X.; Chui, W. K.; Zhou, W., Design, synthesis, docking studies and biological evaluation of novel dihydro-1,3,5-triazines as human DHFR inhibitors. *Eur J Med Chem.* **2017,** *125*, 1279-1288.

165.   Nakao, Y.; Fusetani, N., Enzyme inhibitors from marine invertebrates. *J Nat Prod.* **2007,** *70*, 689-710.

166.   Kalogris, C.; Garulli, C.; Pietrella, L.; Gambini, V.; Pucciarelli, S.; Lucci, C.; Tilio, M.; Zabaleta, M. E.; Bartolacci, C.; Andreani, C.; Giangrossi, M.; Iezzi, M.; Belletti, B.; Marchini, C.; Amici, A., Sanguinarine suppresses basal-like breast cancer growth through dihydrofolate reductase inhibition. *Biochem Pharmacol.* **2014,** *90* (3), 226-234.

167.   Singla, P.; Luxami, V.; Paul, K., Synthesis, in vitro antitumor activity, dihydrofolate reductase inhibition, DNA intercalation and structure-activity relationship studies of 1,3,5-triazine analogues. *Bioorg Med Chem Lett.* **2016,** *26* (2), 518-523.

168.   Ng, H. L.; Chen, S.; Chew, E. H.; Chui, W. K., Applying the designed multiple ligands approach to inhibit dihydrofolate reductase and thioredoxin reductase for anti-proliferative activity. *Eur J Med Chem.* **2016,** *115*, 63-74.

169.   Tsukamoto, T.; Kitazume, T.; McGuire, J. J.; Coward, J. K., Synthesis and biological evaluation of DL-4,4-difluoroglutamic acid and DL-γ,γ-difluoromethotrexate. *J Med Chem.* **1996,** *39*, 66-72.

170.   Al-Rashood, S. T.; Aboldahab, I. A.; Nagi, M. N.; Abouzeid, L. A.; Abdel-Aziz, A. A.; Abdel-Hamide, S. G.; Youssef, K. M.; Al-Obaid, A. M.; El-Subbagh, H. I., Synthesis, dihydrofolate reductase inhibition, antitumor testing, and molecular modeling study of some new 4(3H)-quinazolinone analogs. *Bioorg Med Chem.* **2006,** *14* (24), 8608-8621.

171.   Santi, D. V.; McHenry, C. S.; Sommer, H., Mechanism of interaction of thymidylate synthetase with 5-fluorodeoxyuridylate. *Biochemistry.* **1984,** *13*, 471-481.

172.   Jackman, A. L.; Calvert, A. H., Folate-based thymidylate synthase inhibitors as anticancer drugs. *Ann Oncol.* **1995,** *6* (9), 871-881.

173.   Beutel, G.; Glen, H.; Schoffski, P.; Chick, J.; Gill, S.; Cassidy, J.; Twelves, C., Phase I study of OSI-7904L, a novel liposomal thymidylate synthase inhibitor in patients with refractory solid tumors. *Clin Cancer Res.* **2005,** *15*, 5487-5495.

174.   Henderson, E. A.; Bavetsias, V.; Theti, D. S.; Wilson, S. C.; Clauss, R.; Jackman, A. L., Targeting the alpha-folate receptor with cyclopenta[g]quinazoline-based inhibitors of thymidylate synthase. *Bioorg Med Chem.* **2006,** *14* (14), 5020-5042.

175.   Gibbs, D. D.; Theti, D. S.; Wood, N.; Green, M.; Raynaud, F.; Valenti, M.; Forster, M. D.; Mitchell, F.; Bavetsias, V.; Henderson, E.; Jackman, A. L., BGC 945, a novel tumor-selective thymidylate synthase inhibitor targeted to alpha-folate receptor-overexpressing tumors. *Cancer Res.* **2005,** *65* (24), 11721-11728.

176.   Bavetsias, V.; Marriot, J. H.; Melin, C.; Kimbel, R.; Matusiak, Z. S.; Boyle, F. T.; AJackman, A. L., Design and synthesis of cyclopenta[g]quinazoline-based antifolates as inhibitors of thymidylate synthase and potential antitumor agent. *J Med Chem.* **2000,** *43*, 1910-1926.

177.   Zhang, Z.; Tian, C.; Zhou, S.; Wang, W.; Guo, Y.; Xia, J.; Liu, Z.; Wang, B.; Wang, X.; Golding, B. T.; Griff, R. J.; Du, Y.; Liu, J., Mechanism-based design, synthesis and biological studies of N(5)-substituted tetrahydrofolate analogs as inhibitors of cobalamin-dependent methionine synthase and potential anticancer agents. *Eur J Med Chem.* **2012,** *58*, 228-236.

178.   Elshihawy, H.; Helal, M. A.; Said, M.; Hammad, M. A., Design, synthesis, and enzyme kinetics of novel benzimidazole and quinoxaline derivatives as methionine synthase inhibitors. *Bioorg Med Chem.* **2014,** *22* (1), 550-558.

179.   Allen, R. H.; Stabler, S. P.; Lindenbaum, J., Serum betaine, N,N-dimethylglycine and N-methylglycine levels in patients with cobalamin and folate deficiency and related inborn errors of metabolism. *Metabolism.* **1993,** *42* (11), 1448-1460.

180.   Lee, K. H.; Cava, M.; Amiri, P.; Ottoboni, T.; Lindquist, R. N., Betaine-homocysteine methyltransferase from rat liver- Purification and inhibition by a boronic acid substrate analog. *Arch Biochem Biophys.* **1992,** *292*, 77-86.

181.   Sessa, C.; Jong, J. D.; D'Incalci, M.; Hatty, S.; Pagani, O.; Cavalli, F., Phase I study of the antipurine antifolate lometrexol (DDATHF) with folinic acid rescue. *Clin Cancer Res.* **1996,** *2*, 1123-1127.

182.   DeMartino, J. K.; Hwang, I.; Xu, L.; Wilson, I. A.; Boger, D. L., Discovery of a potent, nonpolyglutamatable inhibitor of glycinamide ribonucleotide transformylase. *J Med Chem.* **2006,** *49* (10), 2998-3002.

183.   Boritzki, T. J.; Barlett, C. A.; Howland, E. F., AG2034: a novel inhibitor of glycinamide ribonucleotide formyltransferase. *Invest. New Drugs.* **1996,** *14* (3), 295-303.

184.   Cheong, C. G.; Wolan, D. W.; Greasley, S. E.; Horton, P. A.; Beardsley, G. P.; Wilson, I. A., Crystal structures of human bifunctional enzyme aminoimidazole-4-carboxamide ribonucleotide transformylase/IMP cyclohydrolase in complex with potent sulfonyl-containing antifolates. *J Biol Chem.* **2004,** *279* (17), 18034-18045.

CHAPTER II Transcriptomic Profiling of Genetically Engineered Cell Lines Augmenting One-Carbon Metabolism

Introduction[2]

One carbon metabolism has been a target for anti-cancer therapy for decades and the success of methotrexate (DHFR inhibitor) and 5-fluorouracil (TYMS inhibitor) attest to the reliance on this pathway for carcinogenesis. Lung cancer (e.g. pemetrexed) and leukemias (e.g. cytarabine) have particularly benefited from anti-metabolite chemotherapies.[1-2] In fact, anti-folate chemotherapy revolutionized treatment for acute leukemia.[3] Previous studies have applied metabolomic, transcriptomic, and proteomic techniques to further elucidate signaling pathways and compensation mechanisms associated with SHMT2 and MTHFD2 in the context of cancer, however their roles in lung cancer and leukemic cancers are incompletely understood.[1, 4]

An elegant metabolomic study performed by Ducker and colleagues quantitated metabolic flux in response to knockouts of several folate-dependent enzymes including SHMT2 and MTHFD2.[5] Knockout of either enzyme resulted in drastic increases in the final *de novo* purine biosynthesis intermediate AICAR which requires a folate derivative to be converted to the final product of the pathway.[5] This finding led to the discovery that when the mitochondrial one-carbon metabolism is inhibited, the cytosolic pathway reverses its normal pathway flux to compensate for

---

the reduced one-carbon units.[5] A blind metabolic profiling approach to identify key metabolic pathways in metastatic breast cancer found that there was enhanced dependence on the mitochondrial one-carbon metabolism pathway.[6]

In an effort to identify SHMT2-interacting proteins, proximity-dependent biotinylation identification was carried out with SHMT2-inducible cell lines and nearly all were mitochondrial proteins.[7] Importantly, many are involved in mitochondrial respiration providing a link to SHMT2's role in redox regulation.[8-9] A similar approach was applied to MTHFD2 to identify potential interaction partners as there was previous evidence of a moonlighting function of MTHFD2.[10] In agreement with prior reports of MTHFD2 localizing to the nucleus, many nuclear RNA-related proteins physically interacted with MTHFD2.[10-11] Of particular relevance to our study, a multi-omics investigation led to the identification of SHMT2 as significantly upregulated at the DNA, RNA, and protein level in non-small cell lung cancer (NSCLC) patient samples.[12]

To gain a better understanding of SHMT2's and MTHFD2's involvement in cancer progression, we performed multiple transcriptomic experiments and used the results to guide a review of the current literature while simultaneously identifying several novel connections through bioinformatic approaches. As part of our experimental approach, we developed doxycycline-inducible NSCLC cell lines that overexpress and knockdown SHMT2 and briefly characterize them. We then explore our sequencing data and frame it in the current body of knowledge while also highlighting new discoveries that further underline the importance of these targets in cancer. Our extensive survey of the literature provides a comprehensive review of what is currently known and unknown about these critical enzymes.

Results and discussion

RNA-seq and bioinformatics analysis of SHMT2 KO and MTHFD2 KO cell lines

Significant overlap of differentially expressed genes

To better understand the compensation mechanisms that arise from inhibition of SHMT2 or MTHFD2 we performed RNA-sequencing on three biological replicates of HAP1 WT, SHMT2 KO, and MTHFD2 KO (Horizon Discovery). HAP1 cells are derived from the chronic myelogenous leukemia cell line KBM-7. Knockout of SHMT2 and MTHFD2 both cause a proliferative disadvantage compared to WT cells (Figure II-1A). Validation of protein knockout was performed prior to transcriptomic analysis (Figure II-1B). RNA-sequencing of HAP1 SHMT2 KO yielded 602 significantly differentially expressed genes (DEGs) ($|FC| > 1.5$, q-value < 0.05, and mean RPKM > 0.5), 358 were upregulated and 244 were downregulated. For HAP1 MTHFD2 KO, 1252 genes were significantly differentially expressed, with 818 upregulated and 433 downregulated. The top 25 DEGs sorted by fold change for both KO's can be found in Appendix Tables II-1 and II-2. There was a significant overlap between common up- and downregulated genes ($|FC| \geq 2$) (Figure II-1C/D, Tables II-1 and II-2).
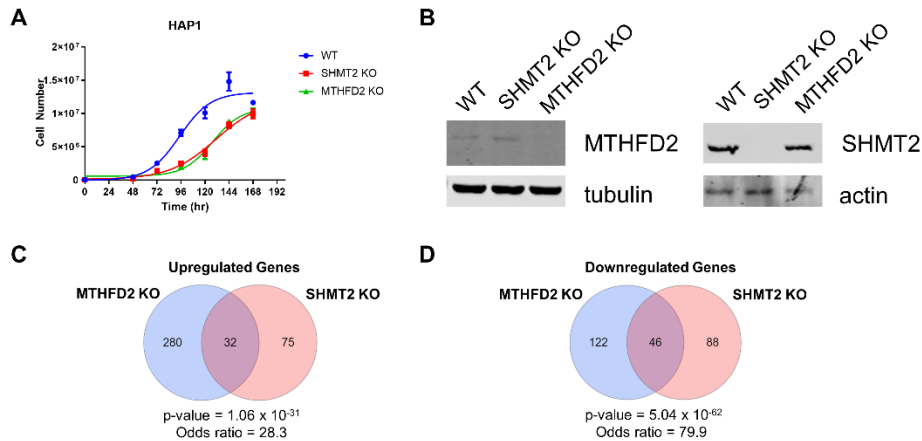
Figure II-1. *In vitro* characterization of HAP1 cell lines and common gene expression changes. (A) Cell proliferation rates for HAP1 WT, SHMT2 KO and MTHFD2 KO. (B) Validation of protein knockouts. (C) Common up- and (D) downregulated differentially expressed genes.

Table II-1. Common upregulated genes of MTHFD2 and SHMT2 KO.

Gene[a]	Description	MTHFD2 KO Fold Change	SHMT2 KO Fold Change
FBXO17	F-box protein 17	11.31	9.44

RENBP	Renin binding protein	6.90	2.55
SHC2	Src Homology 2 Domain Containing Transforming Protein 2	5.77	2.14
CNR1	Cannabinoid receptor 1	5.02	4.27
MPDZ	Multiple PDZ Domain Crumbs Cell Polarity Complex Component	4.70	2.50
ZNF788	Zinc Finger Family Member 788	4.36	2.04
DOC2B	Double C2-like domain-containing protein beta	3.82	2.07
PTHLH	Parathyroid Hormone Like Hormone	3.80	4.12
RNF165	Ring Finger Protein 165	3.74	2.12
KLHL24	Kelch Like Family Member 24	3.68	2.15
MAP2	Microtubule Associated Protein 2	3.60	3.14
ANGPTL2	Angiopoietin Like 2	3.58	2.28
EYA1	EYA transcriptional coactivator and phosphatase 1	3.56	2.95
NACAD	NAC Alpha Domain Containing	2.95	2.46
LYRM9	LYR Motif Containing 9	2.94	2.43
DCHS1	Dachsous Cadherin-Related 1	2.88	2.02
PRPH	Peripherin	2.84	3.01
YPEL1	Yippee Like 1	2.75	2.39
PIFO	Primary Cilia Formation	2.71	2.35
NELL1	Neural EGFL Like 1	2.68	2.81
SMIM14	Small Integral Membrane Protein 14	2.53	2.01
YPEL3	Yippee Like 3	2.52	2.21
BOK	Bcl-2 related ovarian killer	2.41	3.21
RPRM	Reprimo, TP53 Dependent G2 Arrest Mediator Homolog	2.38	2.49
CRACR2B	Calcium Release Activated Channel Regulator 2B	2.33	2.36
PHLDB2	Pleckstrin Homology Like Domain Family B Member 2	2.30	2.17
THSD7A	Thrombospondin Type 1 Domain Containing 7A	2.27	2.53

ZNF704	Zinc Finger Family Member 704	2.26	2.58
HTR6	5-Hydroxytryptamine (Serotonin) Receptor 6, G Protein-Coupled	2.23	2.35
ZFR2	Zinc Finger RNA Binding Protein 2	2.13	2.58
PNMA6A	Paraneoplastic Ma Antigen Family Member 6A	2.05	2.14
CTSO	Cathepsin O	2.04	2.22

[a]Gene input of fold change ≥ |2|

Table II-2. Common downregulated genes of MTHFD2 and SHMT2 KO.

Gene[a]	Description	MTHFD2 KO Fold Change	SHMT2 KO Fold Change
FZD10	Frizzled-10	-725.45	-409.81
SLC17A9	Solute carrier family 17, member 9	-438.95	-475.21
FASTKD2	FAST kinase domain-containing protein 2, mitochondrial	-156.00	-65.66
ALDH1A2	Retinal dehydrogenase 2	-94.39	-10.41
IFI16	Gamma-interferon-inducible protein 16	-79.40	-401.07
TAL1	T-cell acute lymphocytic leukemia protein 1	-72.54	-22.39
IAH1	Isoamyl acetate-hydrolyzing esterase 1 homolog	-53.05	-27.65
BMP7	Bone morphogenetic protein 7	-30.27	-247.64
AMBN	Ameloblastin	-28.81	-232.32
TCEAL9	Transcription elongation factor A protein-like 9	-28.46	-807.89
HOXC9	Homeobox protein Hox-C9	-26.45	-2.25
TCEAL8	Transcription elongation factor A protein-like 8	-22.25	-819.43
SCGB3A2	Secretoglobin family 3A member 2	-19.47	-33.33
CD44	CD44 antigen	-13.49	-22.20
MGMT	Methylated-DNA--protein-cysteine methyltransferase	-11.04	-4.02
PSMB8	Proteasome subunit beta type-8	-8.48	-6.76
RTL8B	Retrotransposon Gag-like protein 8B	-7.61	-12.01

GCNT2	N-acetyllactosaminide beta-1,6-N-acetylglucosaminyl-transferase	-7.14	-6.16
STXBP2	Syntaxin-binding protein 2	-6.81	-31.80
ACTL8	Actin-like protein 8	-5.85	-4.10
TNNI3	Troponin I, cardiac muscle	-5.16	-2.59
SLC1A6	Excitatory amino acid transporter 4	-4.37	-8.05
SLC1A3	Excitatory amino acid transporter 1	-4.14	-2.44
TSPAN7	Tetraspanin-7	-4.14	-3.15
TXNIP	Thioredoxin-interacting protein	-4.05	-2.86
KCTD12	BTB/POZ domain-containing protein KCTD12	-4.04	-2.48
MFAP2	Microfibrillar-associated protein 2	-3.98	-671.75
SYT11	Synaptotagmin-11	-3.85	-3.40
IFITM1	Interferon-induced transmembrane protein 1	-3.72	-2.57
ZNF329	Zinc finger protein 329	-3.63	-6.35
PROM1	Prominin-1	-3.25	-4.66
PPP1R14C	Protein phosphatase 1 regulatory subunit 14C	-2.98	-4.76
TRABD2A	Metalloprotease TIKI1	-2.90	-4.48
HOXD13	Homeobox protein Hox-D13	-2.74	-2.29
ALX4	Homeobox protein aristaless-like 4	-2.66	-32.78
ROR2	Tyrosine-protein kinase transmembrane receptor ROR2	-2.53	-2.54
PTPRE	Receptor-type tyrosine-protein phosphatase epsilon	-2.53	-5.07
DNAAF3	Dynein assembly factor 3, axonemal	-2.34	-2.43
WNT11	Protein Wnt-11	-2.29	-2.49
KLF4	Krueppel-like factor 4	-2.23	-3.74
NMI	N-myc-interactor	-2.20	-748.30
KLHL29	Kelch-like protein 29	-2.16	-2.47
ARRDC4	Arrestin domain-containing protein 4	-2.12	-2.02
SARM1	Sterile alpha and TIR motif-containing protein 1	-2.10	-3.44

| ANPEP | Aminopeptidase N | -2.07 | -2.39 |
| PAPSS2 | Bifunctional 3'-phosphoadenosine 5'-phosphosulfate synthase 2 | -2.03 | -77.30 |

Gene input of fold change $\geq |2|$

The top four common upregulated genes ranked by fold change can be grouped into two categories: glycoprotein- (*FBXO17* and *RENBP*) and nervous system-related (*SHC2* and *CNR1*). The F-box family of proteins are part of an E3-ubiquitin ligase complex and function as the substrate recognition subunit for targeting proteins for proteasomal degradation.[13] Limited literature exists about the commonly upregulated gene *FBXO17* (Appendix Table II-1), but two reports are pertinent to our analysis. FBXO17 is able to bind sulfated and galactose-terminated glycoproteins, but whether these are substrates remains to be determined.[14] Our gene set enrichment analysis established a connection between SHMT2 and glycosylated proteins (Figure II-2C, discussed below). Knockdown of *FBXO17* resulted in downregulation of two serine biosynthesis genes, *PSAT1* and *PHGDH*, in A549 cells.[15] Ectopic expression of FBXO17 activated AKT, an upstream regulator of mTOR, a known regulator of one-carbon metabolism.[15-18] Therefore, it is possible that FBXO17 regulates diverse metabolism genes in different cancer cell types.

N-acylglucosamine 2-epimerase (GlcNAc 2-epimerase), encoded by *RENBP*, is another glycosylation-related protein. *RENBP* was discovered back in 1980, but mainly biochemical studies have been published with some on its role in cardiovascular disease.[19] GlcNAc 2-epimerase, also known as renin-binding protein, catalyzes the conversion between GlcNAc and N-acetylmannosamine and also regulates renin activity.[20-21] Renin plays a key role in blood pressure regulation, hence the studies in cardiovascular contexts. Only one cancer-related study exists; in a study evaluating gene expression differences between epithelial and lung cancer cells *RENBP* was

upregulated ~2-fold. As you will read below, DAVID analysis identified "glycoprotein" as significantly enriched up- and downregulated gene sets (Figure II-2C). Although *RENBP* is a common upregulated gene, the glycoprotein signature seems more specific to knockout of SHMT2. However, we did find that there are cardiovascular gene sets enriched upon knockout of MTHFD2 (Appendix Table II-5).

Like SHC2 and CNR1, SHMT2 and MTHFD2 are important for embryonic development.[22-24] SHC2 is mainly expressed in the nervous system and is required for the development of neurons.[25] However, the relationship between SHC2 and CNR1 with SHMT2 and MTHFD2 is less obvious. The Src homology and collagen (SHC) family of proteins aid in signal transduction with downstream effects on survival, oxidative stress, migration, metastasis, and differentiation.[26] The collagen homology domains are named so because they are rich in glycine (and proline). This is notable because glycine is a product of SHMT2. We also see upregulation of collagen proteins in both KOs (Appendix Tables II-1 and II-2, discussed below). Research on the role of cannabinoid receptors in cancer is conflicting; in some cases, inhibition is favorable and in others, activation.[27] CNR1 (cannabinoid receptor 1) is implicated in regulating axon guidance.[28-29] Axon guidance and other neural-related gene sets were significantly enriched for SHMT2 KO (Figure II-2C, Table II-4). Folate plays a key role in axon regeneration after injury,[30] but how SHMT2 and MTHFD2 fit into that picture is unclear.

FZD10 was the top downregulated gene in common between SHMT2 and MTHFD2 KO and showed especially high fold changes (Table II-2). The frizzled (FZD) family are the receptors for Wnt ligands. The Wnt/β-catenin pathway is critical for embryonic development and dysregulation of the pathway in adult tissues leads to cancer.[31] The Wnt ligand *WNT11* was also present in the common downregulated genes (Table II-2). Neither *FZD10* nor *WNT11* have

established connections to SHMT2 or MTHFD2. The relationship between one carbon metabolism and Wnt signaling is largely unknown. In a doxycycline-inducible system, after 24 h of β-catenin induction, *SHMT2* and *MTHFD1L* expression increased ~2-fold.[32] Knockdown of *MTHFD2* resulted in enrichment of Wnt/β-catenin signaling genes in H1299 cells.[33] Additionally, in agreement with our results, inhibition of the folate pathway with methotrexate inhibited Wnt signaling.[34]

MGMT is a DNA repair suicide enzyme that removes the methyl group from O^6-methylguanine, the most critical DNA lesion. Lower expression of this enzyme renders cancer cells sensitive to alkylating chemotherapy agents.[35] Treatment with cisplatin, an alkylating agent, decreased the expression of *MGMT* and increased the expression of *SHMT2* and *MTHFD2* in the majority of the NCI-60 panel of cell lines at both high and low concentrations, whereas the same was not true for their cytosolic counterparts.[36] An earlier study found the expression of *SHMT2* correlated with sensitivity to oxaliplatin and tetraplatin, but not cisplatin, in the NCI-60 cell lines.[37] In a mouse lymphoma cell line, expression of *MTHFD2* decreased in response to cisplatin treatment.[38] It is not known if there is a correlation with *MGMT* expression and *SHMT2* or *MTHFD2*. These conflicting results reveal that the relationship between DNA repair and one carbon metabolism is likely context dependent.

SHMT2 KO gene set enrichment

Replication-related processes are downregulated

GSEA only identified two significantly downregulated gene sets for SHMT2 KO: GO_RIBOSOME_BIOGENESIS and GO_NEGATIVE_REGULATION_OF_VIRAL_GENOME_REPLICATION (Figure II-2A); there were no significant upregulated gene sets. While SHMT2 has not been linked directly to

ribosomal RNA (rRNA) metabolism, loss of its catalytic activity stalled translation of specific methylated-tRNAs and resulted in decreased expression of respiratory chain enzymes (complexes I, IV, and V) ultimately leading to impaired oxidative phosphorylation.[39] A downstream folate derivative of the SHMT2 reaction is used in the production of formyl-methionine (f-Met). The authors found that the levels of N-terminal f-Met of the mitochondrial protein COX1 were unchanged.[39] A separate study reported that SHMT2 was in fact required for generation of f-Met-tRNAs.[40] However, these were done in different cell lines and so the role that SHMT2 plays in tRNA metabolism may vary by cell type. Furthermore, inhibition of the histone H3 methyltransferase G9A (*EHMT2* gene) caused downregulation of serine biosynthesis genes, including *SHMT2*, and this corresponded with a decrease in monomethylation of their transcription start sites.[41] G9A is required for activation of rRNA transcription,[42] so this finding epigenetically links serine biosynthesis with ribosome biogenesis. However, we did not observe a significant change in the level of *EHMT2* in our RNA-Seq data (data not shown). In line with downregulated ribosome biogenesis, we observed that *FASTKD2* and *PTEN* were in the top 25 downregulated genes upon knockout of *SHMT2* (Appendix Table II-1). Both genes are established in their role of rRNA metabolism.[43-45] Knockdown of *PTEN*, an important tumor suppressor, and specifically the beta isoform, results in an increase of ribosome biogenesis.[44-45] Related, activation of the PI3K pathway through knockdown of *PTEN* caused an increase in the association of mTORC2 to the assembled ribosome and promoted Akt signaling independently of the protein synthesis function of the ribosome.[46] The mTOR complexes (mTORC1 and mTORC2) are important regulators of one carbon metabolism and may act as bridges for DNA and RNA methylation.[18] FASTKD2 is a key regulator of mitochondrial gene expression and RNA metabolism in response to stress.[43] In a study investigating proteins that are essential for oxidative phosphorylation, the authors identified

that FASTKD2 forms part of a 16S rRNA regulatory module.[47] It was later discovered that

mutations in FASTKD2 played a role in impaired mitochondrial function as they were associated

with mitochondrial diseases characterized with defective oxidative phosphorylation.[48]

Additionally, in a pancreatic cancer model, FASTKD2 promoted a pro-cancer phenotype through

transcriptional upregulation of c-MYC.[49] Using proximity biotinylation, Tong et al. identified

FASTKD2 as a SHMT2 associating protein, but this was not validated with western blot.[7] It is

certain that SHMT2 is related to ribosome biogenesis at least through common signaling pathways,

but whether SHMT2 directly contributes to rRNA metabolism remains to be elucidated.

The link between SHMT2 and viral genome replication can partly be explained through its

enzymatic activity. In order for viruses to synthesize their DNA or RNA, nucleotides are required

and therefore 1C units need to be available. A recent study found that the Epstein-Barr virus (EBV)

hijacks 1CM and upregulates mitochondrial 1CM enzymes, including SHMT2.[50] They also

observed that SHIN1, a dual-SHMT inhibitor, was effective at blocking EBV-driven B-cell

proliferation. Another study evaluating the prognostic value of SHMT2 in hepatocellular

carcinoma found that it significantly correlated with hepatitis-B virus (HBV) infection.[51] The small

molecule JIB-04, originally discovered as a Jumonji demethylase inhibitor with anti-cancer

activity,[52] was later found to directly target SHMT2.[53] In this study, the authors were investigating

JIB-04's ability to impede viral replication and inhibit the expression and transactivation HIV-1

Tat, a regulator of viral transcription. The mechanism by which this occurred was through

SHMT2's interaction with BRCC36 K63-specific deubiquitinase. Treatment with JIB-04 caused

an increase in Tat K63-ubiquitin ultimately resulting in autophagy.[53] It is unknown if JIB-04

inhibits the enzymatic activity of SHMT2. Others have also discovered, and further characterized,

SHMT2's involvement in the viral immune response through interferon signaling.[54-57] In sum, targeting SHMT2 for viral infections may be a viable strategy.
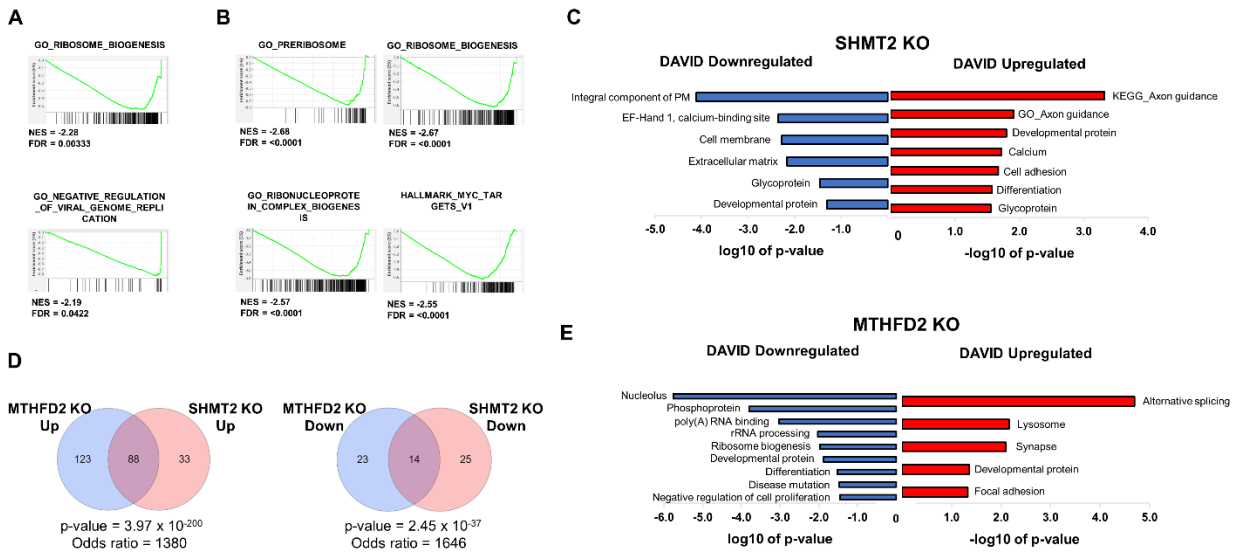
Figure II-2. Enriched gene sets for SHMT2 and MTHFD2 KO. (A) SHMT2 KO downregulated GSEA gene sets. (B) Top four MTHFD2 KO downregulated GSEA gene sets. (C) Significantly enriched gene sets for SHMT2 KO using DAVID. PM = plasma membrane. (D) Comparison of common up- (left) and downregulated gene sets (right). (E) Significantly enriched gene sets for MTHFD2 KO using DAVID.

Neural-related processes are upregulated

The majority of the significantly upregulated gene sets using the DAVID platform indicate that SHMT2 might play a key role in neural development (Figure II-2C). SHMT2 plays a critical role in development as evidenced by embryonic lethality in mice, whereas its cytosolic counterpart is not embryonic lethal.[23, 58] Unlike other folate-dependent enzymes, knockout of *SHMT2* did not produce mitochondrial respiration defects in the brain, but was instead manifested in the livers.[24] Therefore the embryonic lethality was caused by anemia instead of neural tube defects (NTDs).[24] Interestingly, though *SHMT1* knockout does not cause embryonic lethality, combined with folate-deficient conditions mice express NTDs.[59] However, this does not rule out that *SHMT2* knockout could not result in NTDs. To ask this question a conditional knockout in mice brains would be required to avoid the lethal anemia. Recently variants of SHMT2 were found to be associated with a novel syndrome affecting the development of brains and hearts.[60] SHMT2 participates in

development outside of the embryonic stage as well. Importantly, SHMT2 expression was shown to significantly decrease when Ephrin-B receptors were stimulated.[61] This study focused on the similar result with a Ephrin-B (EFNB1/2)-mediated decrease in DHFR, which led to neural stem cell differentiation and revealed that this alteration in 1CM impacted H3K4 methylation.[61] Ephrin receptors promote differentiation of adult neural stem cells, influence tissue morphogenesis and axon guidance, among other important developmental processes.[62] We observed a significant decrease in *EFNB2* (FC = -1.58, p-value = 4.66E-07) and increase in Ephrin type-B receptor 6 (*EPHB6*, FC = 2.21, p-value = 1.96E-12) in our RNA-seq results. While there were not any significant compounds identified with CMAP using the SHMT2 KO data, the knockdown of SHMT2 Bru-seq data (another transcriptomic analysis, discussed below) produced many compounds with significant correlations (Appendix Tables II-7 and II-8). Of note, in the top 25 positively correlated compounds are two potent EphB2 inhibitors: ALW-II-38-3 and ALW-II-49-7 (Appendix Table II-8).[63] Our discovery highlights the importance of pursuing a further understanding of the role of SHMT2 in neural development and differentiation, and specifically in Ephrin signaling.

Glycosylation, membranes and the matrix

It is curious that "developmental protein" and "glycoprotein" keywords also show up in the downregulated gene sets (Figure II-2C). This further emphasizes the possibility of SHMT2's integral role in development and cell-cell communication. Glycosylated proteins are mostly found on the outer cell surface and secreted proteins, but also have a regulatory role in the cytosol and nucleus.[64] *O*-GlcNAcylation is an important regulator of metabolic reprogramming.[65] SHMT2 harbors an *O*-GlcNAcylation in HT29 cells that is regulated by O-GlcNAc transferase (OGT).[66] However, it remains to be determined at which site(s) and for what regulatory purpose. To our

knowledge, GalNAcylation has not been linked to SHMT2. Interestingly, *GALNT5* (Polypeptide N-acetylgalactosaminyltransferase 5, pp-GalNAc-T5) is one of the top upregulated genes for SHMT2 KO (FC = 9.53, Appendix Table II-1). The role of pp-GalNAc-Ts in cancer are becoming better appreciated.[67] pp-GalNac-T5 has been found to be a critical mediator in differentiation of K562 cells (a chronic myeloid leukemia cell line).[68] It is worth noting that B-cell lymphomas were particularly sensitive to SHMT inhibition, and the K562 cell line was among the most sensitive (Compound **2** IC_{50} = 1.60 μM).[69] Moreover, we saw significant downregulation of *GCNT2*, N-acetyllactosaminide beta-1,6-N-acetylglucosaminyl-transferase (FC = -6.16, Table II-2) and *GALNT6* (FC = -4.71, p-value = 9.58E-21). Knockdown of heterogenous nuclear ribonucleoprotein (hnRNP) A2 showed enrichment of genes involved in glycosylation as well as a downregulation of SHMT1.[70] SHMT1 is known to preferentially convert serine to glycine, and hnRNPs have glycine-rich C-terminal domains.[5, 71] Furthermore, we observed significant downregulation of the gene encoding the carbohydrate-binding protein galectin-8 (*LGALS8*, FC = -96.84, Appendix Table II-1). Expression of galectin-8 has been shown to have prognostic value in breast,[72] ovarian,[73-74] gastric,[75-76] and other cancers.[77-78] Suffice to say that the interplay between glycosylation and SHMTs warrants further investigation.

It is our understanding that there has been no previous functional relationship established between SHMT2 and EF-hand proteins or calcium binding sites. It is curious that even though it was a downregulated gene set, we observed an EF-Hand domain gene, *CGREF1*, in one of the top 25 upregulated genes (FC = 6.96, Appendix Table II-1). Not much is known about CGREF functionally, except that it is a secretory protein that inhibits the transcriptional activity of AP-1, a protein complex composed of dimers of JUN, FOS, ATF, and Maf family members and is associated with neoplastic phenotypes.[79-80] In our SHMT2 KO RNA-seq data we saw significant

upregulation of *JUND* (FC = 1.40, p-value = 3.48E-05) and downregulation of *JUNB* (FC = -1.44, p-value = 8.68E-05), so it is possible that SHMT2 expression is controlled by the AP-1 transcriptional program.

There is exciting data concerning SHMT2 and its role at the membrane and contribution to extracellular matrix (ECM). Zheng and colleagues first identified SHMT2's association with the BRISC complex and its role in regulating interferon signaling through deubiquitylation of IFNαR1, preventing internalization and degradation of the receptor.[56] Subsequent simultaneous, independent reports of the Cryo-EM structures of the multi-protein complex revealed the basis of how this occurs.[55, 57] Another study reported that lysine fatty-acylation of SHMT2 regulates its ability to participate in IFN-signaling and that the PTM is removed by HDAC11.[54] They hypothesized that the fatty acyl chain would target SHMT2 to the plasma membrane to be localized near IFNαR1, but they instead found co-localization at the endosome/lysosome.[54] We observed in our data that the immune-related gene coding for interferon-γ-inducible protein 16, *IFI16*, was significantly downregulated (FC = -401.07, Appendix Table II-1). IFI16 has been previously linked to a metabolic response in that it activated the AMPK/p53 pathway in low-glucose conditions,[81] however, there is no established connection with 1CM. It is likely that the "integral component of cell membrane" gene set was enriched as serine is incorporated into phospholipids (phosphatidylserine).

Glycine is a core component of collagen (33%)[82] and it was recently discovered that TGF-β_1 treatment upregulated expression of SHMT2.[17] This pro-fibrotic cytokine mediated the response through mTOR and ATF4 as well as canonical TGF-β_1 signaling (SMAD3).[17] Interestingly, *COL11A1* was among the top upregulated genes in SHMT2 KO (FC = 11.20, Appendix Table II-1). *COL11A1* (collagen type XI alpha 1 chain), is a minor fibrillar collagen that is emerging as a

novel biomarker for many cancers. A recent study found that binding of COL11A1 to its receptors stimulates signaling that results in an increase in fatty acid biosynthesis and oxidation, ultimately leading to cisplatin resistance.[83] They found that glycolysis was not affected by COL11A1, whereas its family member COL1 does upregulate glycolysis.[84] To the best of our knowledge, our analysis is the first to connect any specific collagen protein to 1CM. In addition to *COL11A1*, we observed a marked downregulation of the gene encoding microfibrillar-associated protein 2, *MFAP2* (FC = -671.75, Appendix Table II-1). MFAP2 is an ECM protein emerging as a prognostic biomarker and promotor of metastatic phenotypes.[85-88] It is notable that MFAP2 promoted the epithelial-to-mesenchymal transition through the TGF-β_1/SMAD axis.[87] SHMT2 has been linked to the ECM in another context as well. Exosome-mediated fibroblast activation resulted in an increase in ECM secretion and *SHMT2* expression irrespective of the stage of cancer cell line the exosomes were derived from.[89] Altogether, the ECM in the tumor microenvironment may contribute to 1CM reprogramming.

Non-coding RNA processing

The final gene set enrichment analysis was done using the online tool STRING. This additional analysis was conducted as the STRING database has more GO_biological processes and KEGG terms than DAVID and GSEA. As expected, The STRING database highlighted many of the same pathways detailed above (Tables II-3 and II-4 compared to Figure II-2C). RNA-related processes were particularly enriched in the downregulated biological processes gene sets (Table II-3). Of interest was the presence of non-coding RNA (ncRNA) processing. SHMT2 has been reported to be under the control of several micro-RNAs (miRs) and long intergenic non-coding RNAs (lincRNAs).[90-94] We did not observe significant changes in expression of any of these ncRNAs, however, this makes sense as SHMT2 is not being expressed in the first place. This

prompted us to investigate changes in expression of non-protein coding genes (Appendix Table II-3). Only the top four differentially expressed ncRNAs (both up- and downregulated) are discussed here for brevity purposes.

Table II-3. SHMT2 KO STRING-identified downregulated gene sets.

Gene set	Size	FDR
ribonucleoprotein complex biogenesis	182	3.52E-28
ncRNA metabolic process	187	2.95E-27
ribosome biogenesis	134	1.81E-24
ncRNA processing	146	1.81E-24
rRNA metabolic process	108	2.54E-18
rRNA processing	98	6.12E-18
mRNA metabolic process	184	7.74E-13
mRNA processing	126	1.92E-09
ribonucleoprotein complex subunit organization	80	5.95E-09
ribonucleoprotein complex assembly	79	8.72E-09
translation	100	2.44E-08
RNA splicing, via transesterification reactions	83	5.00E-08
mRNA splicing, via spliceosome	82	7.35E-08
peptide biosynthetic process	104	1.87E-07
nuclear export	52	2.64E-07
RNA splicing	115	2.86E-07
amide biosynthetic process	130	5.04E-07
mitochondrial gene expression	46	5.75E-07

nuclear transport	90	6.13E-07
nucleocytoplasmic transport	89	8.91E-07
peptide metabolic process	129	1.15E-06
protein export from nucleus	48	1.30E-06
ribosomal large subunit biogenesis	38	1.97E-06
RNA modification	44	2.28E-06
ribosomal small subunit biogenesis	36	3.36E-06
KEGG_Spliceosome	43	1.06E-05
KEGG_Ribosome biogenesis in eukaryotes	42	4.05E-05
KEGG_RNA transport	56	4.21E-05
KEGG_Ribosome	33	4.61E-05
KEGG_Pyrimidine metabolism	28	0.0138
KEGG_Purine metabolism	51	0.0461

Table II-4. SHMT2 KO STRING-identified upregulated gene sets.

Gene set	Size	FDR
neuron development	197	6.42E-05
axonogenesis	109	0.00012
axon development	113	0.00019
plasma membrane bounded cell projection morphogenesis	127	0.00019
neuron projection morphogenesis	126	0.00025
cell projection morphogenesis	128	0.00031
neuron projection development	166	0.00034

cell morphogenesis involved in neuron differentiation	124	0.00041
synapse organization	42	0.00045
cell part morphogenesis	132	0.0017
cell morphogenesis	175	0.0019
axon guidance	74	0.0026
Rho protein signal transduction	12	0.0038
trans-synaptic signaling	65	0.0064
positive regulation of neuron projection development	67	0.0065
cell morphogenesis involved in differentiation	151	0.0089
regulation of small GTPase mediated signal transduction	84	0.0097
cellular component morphogenesis	189	0.011
chemical synaptic transmission	63	0.0121
cell adhesion	159	0.0147
central nervous system development	197	0.0153
neuron migration	28	0.0168
signal release	29	0.0178
biological adhesion	161	0.0195
chemotaxis	106	0.0248
KEGG_Axon guidance	48	0.049

HOXC-AS3 (HOXC cluster antisense RNA 3) is becoming increasingly appreciated for its implication in cancer.[95-99] Importantly a study in gastric cancer samples identified two HOXC-AS family members (AS1 and AS3) to be significantly upregulated.[100] Since *HOXC-AS1* was more consistently upregulated among gastric cancer samples and cell lines, only the AS1 transcript was

pursued further for mechanistic studies.[100] The authors found that *HOXC-AS1* participates in a positive feedback loop with MYC, a master regulator of metabolic genes, including 1CM.[100-102] Given our result of upregulation of *HOXC-AS3* (FC = 25.39, Appendix Table II-3) in SHMT2 KO cells, we believe that investigation of this asRNA in the context of cancer metabolism is warranted. Limited information is available for *LINC00649* except for its potential relevance in cancer.[103-104] The same is true for the lncRNA *CAHM* (colon adenocarcinoma hypermethylated).[105-106] It is peculiar that *CAHM* would be upregulated when one-carbon units would presumably be less available, although from our experiment we cannot deduce the methylation status. Some mechanistic data is available for *LINC00365* in addition to its possible application as a cancer biomarker.[107-109] *LINC00365* has been shown to regulate both the Wnt/β-catenin and NF-κB signaling pathways, each important in their contribution to neoplastic disease.[110-112]

The appearance of *FZD10-AS1* (frizzled class receptor 10 - antisense RNA) as the top downregulated non-protein coding gene (FC = -935.51, Appendix Table II-3) grabbed our attention since we also saw significant downregulation of the *FZD10* gene itself (FC = -409.81, Appendix Table II-1). There is only one report on the asRNA in that it was downregulated 4.27-fold in response to the Warburg effect antagonist ginsenoside 20(S)-Rg3 in ovarian cancer cells.[113] *FZD10-AS1* is a divergent antisense transcript, so would most likely not impact the expression of FZD10. Comparison of their mRNA sequences does not show alignment (not shown).

Studies on *LINC01551* have revealed that it targets at least two different miRs: miR-132-5p and miR-122-5p.[114-115] It is unknown what the targets of miR-132-5p are, but miR-122-5p has been observed to target ADAM10 (ADAM metallopeptidase domain 10). ADAM10 is a protease that contributes to development, inflammation, and cancer and has many oncogenic substrates.[116] One notable family of substrates are the Ephrin ligands. As discussed above, SHMT2 expression

decreases upon stimulation of Ephrin-B receptors.[61] Despite the significant change in expression of *LINC01551* (FC = -74.13, Appendix Table II-3), we did not observe a significant change in *ADAM10* expression (data not shown), and the expression of miR-122 was not detected. The exosome study mentioned above that observed an increase in *SHMT2* expression also saw the same for *ADAM10*.[89] Our data provide increasing evidence of the potential role that SHMT2 plays in differentiation. In fact, clinically, SHMT2 expression correlates with differentiation (tumor grade).[8, 51, 117-124] Additionally, differentiated glioma cells harbor low expression of SHMT2.[125] Furthermore, knockout of SHMT2 impairs the differentiation of erythroblasts.[24] We suggest that the mechanism by which the possible SHMT2-mediated differentiation be explored.

Embryonic stem cell related gene (*ESRG*) is a lncRNA implicated in maintaining pluripotency of stem cells,[126-128] and is an early marker of reprogramming of somatic cells towards pluripotent ones.[129] Expression of *ESRG* was found to correlate with overall survival in colon and ovarian cancer.[130-131] A study evaluating the composition of extracellular vesicles derived from KRAS WT or KRAS mutant colon cancer cells found that the levels of *ESRG* in the vesicles were roughly 7-fold higher than the original cells.[132] This is particularly interesting as another study reported that colon cancer-derived exosomes could upregulate the expression of SHMT2 in fibroblasts.[89] The cells lines used in the latter study were both KRAS mutant (G12V). We observed a marked downregulation of *ESRG* (FC = -10.99, Appendix Table II-3) in SHMT2 KO cells. Therefore, we propose that more studies are warranted to understand their relationship.

In a screen to identify HBV-associated liver cancer specific ncRNAs, *LINC01018* was observed to significantly correlate with expression of the gene coding for sideroflexin 1 (*SFXN1*), a mitochondrial serine transporter, presumably through the predicted interaction with miR-4452.[133] In their expanded competing endogenous RNA (ceRNA) network, there was a lncRNA/miR

interaction predicted to target SHMT1 (*LOC157273* and miR-1304-5p).[133] In general, the identified ceRNA network was enriched with genes in metabolic pathways.[133] However, this all remains to be confirmed experimentally. This discovery is exciting because SHMT2 expression also correlates with HBV-associated hepatocellular carcinoma.[51] Another study validated its contribution to metabolic regulation, specifically fatty-acid oxidation.[134] Others have confirmed *LINC01018*'s role in tumorigenesis and is a component of a ncRNA signature correlated with overall survival in gastric cancer.[135-137]

MTHFD2 KO gene set enrichment

Ribosomal RNA and MYC

Congruent with similar transcriptome changes, there were a significant number of gene sets in common between SHMT2 KO and MTHFD2 KO (Figure II-2D). As was the case for the SHMT2 KO condition, there were also no upregulated gene sets identified by GSEA analysis for MTHFD2 KO. However, there were 26 significantly downregulated gene sets (Table II-5); the top four are in Figure II-2B. "Preribosome," "ribosome biogenesis," and "ribonucleoprotein complex biogenesis" (among other rRNA-related processes) all fall under the umbrella of rRNA metabolism. Several studies have come out delving into the moonlighting function of MTHFD2, that is, its role in cancer outside of its enzymatic activity.[10-11, 138] Of relevance here is the discovery by Koufaris and Nilsson that MTHFD2 physically interacts with RNA-related proteins.[10] This study coupled co-immunoprecipitation with mass spectrometry and found that in addition to physical interactions, knockdown of MTHFD2 resulted in a decrease in expression of its partners.[10] To see if this carried over to our study, we evaluated expression changes in these genes (Appendix Table II-4). Not all genes were detected but of those that were, were significantly downregulated, albeit only modestly – roughly -1.2 to -1.6-fold change (Appendix Table II-4). Two studies have

identified that knockout of SHMT2 impairs mitochondrial translation because of its contribution of 1C units, however, the same was not true for MTHFD2.[39-40]

While we saw significant downregulation of two MYC-related gene sets (Table II-5), we did not observe a change in expression of *MYC* itself. MYC activation correlates with the 1CM gene signature in several cancers.[139-140] A similar analysis found that breast cancer samples with a higher expression of *MTHFD2* were more sensitive to MTX and this also correlated with the MYC targets signature.[141] In an inducible mouse model of MYC-driven liver tumorigenesis, MYC induction upregulates expression of *MTHFD2*, and *SHMT2*.[142] The opposite was also found to be true – knockdown of *MYC* downregulated *MTHFD2*.[143-144] A study of the downstream effects of B-cell receptor stimulation in chronic lymphocytic leukemia cells identified that an upregulation of *MYC* was temporally followed by an upregulation of *MTHFD2*, among other genes and miRNAs.[145] The same was true for T-cell stimulation in an mTORC1-dependent manner.[146] In AML cell lines, treatment with JQ1, a BET bromodomain inhibitor, caused a decrease in MYC binding at the *MTHFD2* promoter.[144] Other studies have validated MYC binding at MTHFD2's promoter as well.[50, 147-148] The EBV protein EBNA2 is capable of upregulating MYC in B-cells which in turn upregulated mitochondrial 1C genes, including MTHFD2.[50] Consistent with our results, in colorectal cancer samples with upregulated MTHFD2, "MYC targets_v1" was one of the upregulated gene sets.[147] In addition to being an important regulator of metabolism, MYC also regulates transcription through E2Fs.[149-150] This is notable because we also observed significant downregulation of the "Hallmark_E2F_targets" gene set (Table II-5). Not all E2Fs were detected, but of those that were, were modestly downregulated (E2F2, -1.54; E2F3, -1.22; E2F4, -1.23; E2F7, -1.23; all $p < 0.01$). E2F1 has been linked to glycolytic and oxidative metabolism,[151-152] but to our knowledge, this is the first report connecting E2F with mitochondrial 1CM.

Table II-5. MTHFD2 KO downregulated GSEA gene sets

Gene set	Size	NES	FDR
GO_PRERIBOSOME	72	-2.68	<0.0001
GO_RIBOSOME_BIOGENESIS	269	-2.67	<0.0001
GO_RIBONUCLEOPROTEIN_COMPLEX_BIOGENESIS	385	-2.57	<0.0001
HALLMARK_MYC_TARGETS_V1	194	-2.55	<0.0001
GO_RRNA_METABOLIC_PROCESS	206	-2.53	<0.0001
HALLMARK_MYC_TARGETS_V2	58	-2.48	7.47E-05
GO_RIBOSOMAL_LARGE_SUBUNIT_BIOGENESIS	64	-2.42	1.49E-04
GO_SMALL_SUBUNIT_PROCESSOME	34	-2.35	9.28E-04
GO_NCRNA_PROCESSING	340	-2.29	0.0037
GO_NCRNA_METABOLIC_PROCESS	396	-2.29	0.0035
GO_PRERIBOSOME_LARGE_SUBUNIT_PRECURSOR	23	-2.24	0.0081
GO_BONE_CELL_DEVELOPMENT	23	-2.24	0.0084
GO_WNT_PROTEIN_BINDING	20	-2.23	0.0083
GO_90S_PRERIBOSOME	29	-2.23	0.0084
HALLMARK_E2F_TARGETS	198	-2.20	0.0142
GO_MATURATION_OF_SSU_RRNA_FROM_TRICISTRONIC_RRNA_TRANSCRIPT_SSU_RRNA_5_8S_RRNA_LSU_RRNA	31	-2.16	0.0268
GO_RIBONUCLEOPROTEIN_COMPLEX_SUBUNIT_ORGANIZATION	173	-2.14	0.0341
GO_MITOCHONDRIAL_GENE_EXPRESSION	159	-2.13	0.0353
KEGG_SPLICEOSOME	123	-2.13	0.0339
GO_RIBOSOMAL_SMALL_SUBUNIT_BIOGENESIS	61	-2.13	0.0341
GO_ANAPHASE_PROMOTING_COMPLEX_DEPENDENT_CATABOLIC_PROCESS	76	-2.13	0.0334
GO_MATURATION_OF_SSU_RRNA	43	-2.11	0.0394
GO_RIBOSOME_ASSEMBLY	54	-2.11	0.0387
GO_PLATELET_MORPHOGENESIS	15	-2.11	0.0406

Alternative splicing and focal adhesion

DAVID analysis only identified five significantly upregulated gene sets (Figure II-2E). "Alternative splicing" and "focal adhesion" will be discussed here, but it is notable that MTHFD2 has not been linked to the lysosome or synapses in previous studies. As discussed above, MTHFD2 participates in RNA metabolism, but the connection to alternative splicing has not been explored. Koufaris and Nilsson identified that MTHFD2 interacts with *SF3B3* (splicing factor 3B subunit 3), but the function for this is unknown. The expression of *SF3B3* was not detected in our data (Appendix Table II-4) however, *SF3B4* was significantly downregulated (FC = -1.52, p-value = 5.73E-08). Interestingly, several splicing-related gene sets were significantly enriched as downregulated in our STRING analysis (Table II-6). Investigation of the "KEGG_Spliceosome" genes within our data corroborated Koufaris and Nilsson's identified HSPA8 interaction (Appendix Table II-4), and also revealed other HSPA family members, *HSPA1A* and *HSPA1B* as significantly downregulated (FC = -1.87 and -1.91, p-values = 1.52E-07 and 2.03E-06, respectively). The top upregulated gene of the "KEGG_Spliceosome" gene set was *PRPF40B* with a 1.53-fold change (p-value = 1.84E-06). Most studies on this gene have focused on polymorphisms common in cancer samples, but until recently, its function was unknown.[153-154] Lorenzini and colleagues were the first to disclose a mechanistic role – they discovered that knockout of PRPF40B induced a transcriptomic hypoxia signature.[155] Further studies showed that there was an inverse correlation between *PRPF40B* and *HIF1A* expression in AML.[155] MTHFD2 expression is also regulated by HIF1,[156] so we suggest that the relationship between MTHFD2 and PRPF40B be explored further, in addition to MTHFD2's role in alternative splicing as a whole.

It is clear that MTHFD2 plays a role in migration, but the mechanism is unknown.[148, 157-162] A quick glance at the top 25 upregulated genes reveals three proteins involved in adhesion: *COL5A2*, *VCAM1*, and *RELN* (Appendix Table II-2). *COL5A2* (collagen, type V, alpha 2) is a minor fibrillar collagen that is gaining traction for its clinical significance in terms of poor prognosis.[163-165] In addition to an upregulation of *COL5A2* (FC = 18.15), we saw significant downregulation of *COL11A1* (FC = -145.28, Appendix Table II-2), discussed earlier with SHMT2 KO (FC = 11.20, Appendix Table II-1). In colorectal cancer tissues, these two collagen genes were co-expressed and were higher in the tumor versus the stromal tissue.[166] It is interesting that inhibition of the 1CM pathway causes seemingly opposite effects. Regardless, it is obvious that there is possible restructuring of the ECM. *VCAM1* (vascular cell adhesion molecule 1, FC = 10.07) has been studied in the context of cancer for over 30 years and numerous reports have reported on its clinical significance.[167] Interestingly, treatment with 5FU, a thymidylate synthase inhibitor, upregulated *VCAM1* expression.[168] Additionally, VCAM1 was found to directly interact with CD44,[169] an important marker of cancer stem cells, which we observed strong downregulation of (Appendix Table II-2).[170] *RELN* (reelin, FC = 8.06) is a ECM glycoprotein that regulates neuronal migration in a non-disease state, but also in cancer.[171-173] Importantly, evidence shows that this is a TGF-β dependent process.[172-173] MTHFD2's relationship with TGF-β is discussed below. Reelin is a negative regulator of TGF-β induced migration,[172-173] therefore upregulation would provide a favorable anti-migratory phenotype. Since knockdown of MTHFD2 inhibits migration, it would be interesting to evaluate RELN's involvement, as well as other ECM structural proteins such as the collagen family.

Nucleoli and phosphoproteins

MTHFD2 resides in both mitochondria and nuclei, but not nucleoli.[11] Given its tie to ribosome biogenesis (this study and Koufaris and Nilsson), it would seem that localization to the nucleolus would be ideal since ribosome biogenesis occurs there.[174] Investigation of the genes present in the gene set revealed other ribosomal proteins not previously identified to interact with MTHFD2: *NOP2* (FC = -1.72, q-value = 1.02E-16), *NOP16* (FC = -1.70, q-value = 3.25E-14), and *POLR3K* (FC = -1.69, q-value = 2.76E-08). NOP2 is a nucleolar protein with SAM-dependent RNA-methyltransferase activity.[175-176] NOP16 (also known as HSPC111) is a MYC-regulated, nucleolar protein implicated in tumorigenesis.[177] POLR3K (also known as RPC11) is a subunit of RNA Polymerase III, machinery responsible for transcribing both rRNAs and tRNAs.[178] With the many evidences that link MTHFD2 to ribosomal biogenesis and nuclear localization, we believe it would behoove the field to investigate potential nucleolar localization in a wider variety of cell lines.

Of the genes in the "phosphoprotein" gene set, *CHMP4C* was the top downregulated gene and is one of the top downregulated genes overall (Appendix Table II-2). *CHMP4C* (charged multivesicular body protein 4C) participates in the final step of cell division, namely the separation of daughter cells (abscission) and is regulated by Aurora kinase B through phosphorylation.[179-180] Cytosolic 1CM genes (*TYMS*, *DHFR*, and *SHMT1*) correlated with expression of Aurora kinases A and B, but not *MTHFD2*.[181] Five sites of phosphorylation on MTHFD2 have been identified through phosphoproteomics (S149, T187, T191, T306, and T324).[182] However, it is unknown what kinases catalyze these phosphorylations or what purpose they serve. PTMs in general can act as a switch for metabolic enzymes to take on their moonlighting functions.[183] For example, phosphorylation of superoxide dismutase 1 (SOD1) causes its translocation to the nucleus where it is able to transcriptionally upregulate antioxidant-related genes.[184] As MTHFD2 has been shown

77

to be present at DNA replication sites,[11] it would be interesting to see if PTMs regulated this function.

ncRNA processing and immune signaling

As expected, the STRING analysis complemented what was found in GSEA and DAVID (Tables II-6 and II-7), but a couple differences will be discussed here. Like we saw for SHMT2 KO, MTHFD2 KO downregulated gene sets contained ncRNA processing as significantly enriched. NcRNAs are reported to regulate MTHFD2 expression including miR-9 (along with lncRNA *TUG1*), miR-92a, miR-940, miR-33a-5p, rno-miR-126a-5p (rno, *Rattus norvegicus*), and *LIN28B* and miR-22.[162, 185-191] MTHFD2 is a predicted target gene of miR-99a-3p, miR-186-5p, and hsa-miR-202.[192-194] No changes in expression level were detected for these ncRNAs except for *LIN28B* (FC = -1.50, p-value = 1.26E-10). *LIN28B* is emerging as a prognostic biomarker for many cancers.[195] Knockdown of *LIN28B* in AML cells reduced the expression of *MTHFD2* by about 2-fold, in addition to other 1CM-related genes.[189] As described previously, MTHFD2 has been reported to be involved in RNA-related processes,[10] but this is the first report to identify an alteration in ncRNA processing when MTHFD2 is knocked out.

Many gene sets enriched in the KEGG pathways in our STRING analysis validate known changes in mechanistic pathways when 1CM is inhibited (Table II-6), e.g. purine and pyrimidine metabolism and mTOR signaling. However, not much is known about MTHFD2's role in relation to immunology ("cytokine-cytokine receptor interaction," Appendix Table II-5). Knockdown of insulin-like growth factor 2 (IGF2) caused a downregulation of *MTHFD2* expression in colorectal cancer cells.[196] The successful use of anti-folate therapy for the treatment of rheumatic diseases underlies the importance of 1CM in inflammation.[197] In the top 25 differentially expressed gene lists (Appendix Table II-2), three cytokine-related genes caught our attention: *THBS1* (FC = 6.85),

IFI16 (FC = -79.40), and *CD44* (FC = -13.49). Thrombospondin-1 (*THBS1*) is a matricellular protein involved in the epithelial-to-mesenchymal transition (EMT) and is speculated to play a role in metabolism as it mediates various stress-responses.[198-199] *IFI16* was briefly discussed above. The downregulation of *CD44* is particularly exciting (also seen for SHMT2 KO, see Table II-2). CD44 is a well-known marker of cancer stem cells.[170] Knockdown of MTHFD2 decreased the population of CD44$^+$ metastatic breast cancer cells.[158] The same study found that treatment with TGF-β induced the expression of *MTHFD2*.[158] In fact, all three of these genes have something in common: TGF-β.[170, 200-201] Transforming growth factor (TGF)-β is a cytokine responsible for mediating many cancer-related processes such as the EMT, immune evasion, invasion, migration, and metastasis.[202] We observed significant changes in expression of ligands, receptors, and effectors involved in TGF-β signaling (for full list, see Appendix Table II-6). At the top of the pathway, we see changes in *TGFB2* (FC = -2.60, p-value = 5.10E-11), *TGFB1* (FC = -1.29, p-value = 4.81E-04), but not *TGFB3* (Appendix Table II-6). Interestingly, we don't see a change in expression of the TGF-β receptors *TGFBR1 or TGFBR2,* but we do for *TGFBR3* (FC = -1.84, p-value = 2.45E-10) (Appendix Table II-6). An adjacent pathway that regulates other SMAD proteins, which are downstream canonical effectors of TGF-β signaling, is the bone morphogenic protein (BMP) superfamily. Importantly, we observed a marked downregulation for BMP7 (FC = -30.27, Table II-2). Given the number of components that significantly change in the TGF-β signaling (Appendix Table II-6), we recommend that the role of MTHFD2 in the context of immune regulation and cancer stem cells be explored.

Table II-6. MTHFD2 KO STRING-identified downregulated gene sets.

Gene set	Size	FDR
ncRNA processing	182	2.55E-25

ribosome biogenesis	165	3.36E-25
rRNA metabolic process	128	5.94E-21
rRNA processing	115	8.99E-19
amide biosynthetic process	184	1.67E-14
RNA splicing	187	1.67E-14
mRNA processing	193	1.72E-13
RNA splicing, via transesterification reactions	137	3.00E-13
translation	147	5.34E-13
mRNA splicing, via spliceosome	134	9.61E-13
peptide biosynthetic process	155	1.23E-11
peptide metabolic process	187	7.17E-10
ribonucleoprotein complex subunit organization	113	9.68E-10
mitochondrial gene expression	73	9.68E-10
nuclear transport	112	9.68E-10
tRNA metabolic process	80	1.04E-09
nucleocytoplasmic transport	111	1.28E-09
ribonucleoprotein complex assembly	111	1.85E-09
KEGG_splicesome	65	2.61E-09
nuclear export	72	7.82E-09
KEGG_ RNA transport	80	1.17E-08
RNA localization	92	4.15E-08
RNA export from nucleus	61	5.32E-08
mitochondrial translation	56	6.13E-08

translational termination	51	1.02E-07
protein export from nucleus	66	1.18E-07
ribonucleoprotein complex localization	59	1.21E-07
KEGG_ Ribosome biogenesis in eukaryotes	53	5.28E-07
KEGG_ Ribosome	48	1.92E-06
KEGG_ Purine metabolism	70	4.18E-05
KEGG_ Pyrimidine metabolism	42	0.00033
KEGG_ Proteasome	25	0.0007
KEGG_ mRNA surveillance pathway	34	0.0016
KEGG_ Herpes simplex infection	45	0.0037
KEGG_ Epstein-Barr virus infection	78	0.0196

Table II-7. MTHFD2 KO STRING-identified upregulated gene sets.

Gene set	Size	FDR
plasma membrane bounded cell projection morphogenesis	142	0.002
synapse organization	48	0.0022
neuron projection morphogenesis	141	0.0026
cell projection morphogenesis	143	0.0029
KEGG_ Autophagy - animal	50	0.004
axon guidance	71	0.0043
cell morphogenesis involved in neuron differentiation	132	0.0046
axon development	117	0.0047
neuron projection guidance	72	0.0055

post-Golgi vesicle-mediated transport	36	0.0057
neuron projection development	182	0.0061
KEGG_ Lysosome	50	0.0065
axonogenesis	110	0.0075
B cell differentiation	21	0.0078
artery morphogenesis	17	0.008
positive regulation of cell projection organization	105	0.0085
positive regulation of neuron differentiation	106	0.0085
regulation of neuron differentiation	196	0.0137
regulation of macroautophagy	60	0.0147
regulation of cell projection organization	193	0.0159
regulation of GTPase activity	142	0.0211
regulation of plasma membrane bounded cell projection organization	189	0.0222
cell part morphogenesis	151	0.0224
cell morphogenesis	194	0.0242
endocytosis	135	0.0249
middle ear morphogenesis	11	0.0255
positive regulation of neuron projection development	77	0.033
KEGG_ mTOR signaling pathway	46	0.0336

HDAC and mTOR inhibitors

Several histone deacetylase (HDAC) inhibitors showed a similar profile to knockout of MTHFD2 (Appendix Table II-9). Treatment with vorinostat, a HDAC inhibitor, decreased the expression of *MTHFD2* in the majority of the NCI-60 panel of cell lines at both high and low

concentrations.[36] Outside of the CMAP database,[148] there are no other studies linking HDAC inhibitors to MTHFD2. The remainder of the compounds also have no previous connection to MTHFD2. The presence of an mTOR inhibitor however is not surprising as mTOR is a regulator of 1CM.[16-18] Activation of mTOR significantly upregulates the expression of MTHFD2, and the addition of rapamycin or torin, both mTOR inhibitors, prevents this effect.[16] Interestingly, treatment with rapamaycin in the HAP1 WT and KO cells lines showed differential activity with MTHFD2 KO and with SHMT2 KO (Figure II-3). Both KOs conferred resistance of cell growth inhibition by rapamycin, but KO of SHMT2 was more significant. Previous literature showed that rapamycin inhibited the expression of SHMT2, and MTHFD2, in activated T-cells.[146] Furthermore in a liver regeneration model, knockdown of SHMT2 inhibited the phosphorylation of mTOR, but not total levels of mTOR; likewise, overexpression of SHMT2 increased phosphorylation of mTOR.[203] However, there is no existing evidence that inhibition of SHMT2 and MTHFD2 provides resistance cell growth inhibition via mTOR inhibition.
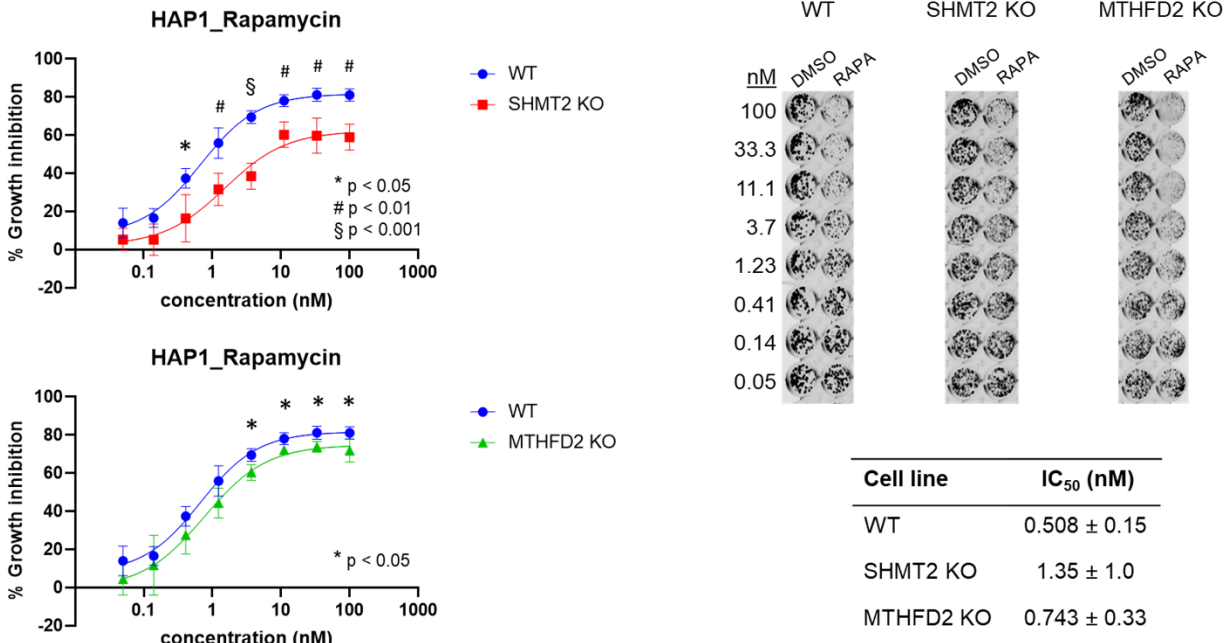
Figure II-3. Knockout of SHMT2 and MTHFD2 confer resistance to rapamycin compared to WT HAP1 cells in the colony formation assay. * $p < 0.05$, # $p < 0.01$, § $p < 0.001$.

Generation and characterization of SHMT2-inducible cell lines

Four NSCLC cell lines (H1299, A549, H226, and H460) were engineered to either overexpress or knockdown SHMT2 (OES and KDS), as well as controls (OEC and KDC) (Figure II-4, Appendix Figure II-1). Two separate overexpression controls were constructed, one for GFP and the other for the gene encoding β-galactosidase, LacZ (OEC^{GFP} and OEC^{LacZ}). Successful overexpression was obtained for all cell lines (Figure II-4A/B, Appendix Figure II-1A/B), with A549 being the least robust. Overexpression of SHMT2 appeared as early as 24 h after doxycycline exposure, but the maximum was achieved after 72 h. (Figure II-4D, Appendix Figure II-1D). Near complete knockdown was observed after 72 h treatment with doxycycline (Figure II-4C, Appendix Figure II-1C), except for H226 which did not show appreciable knockdown until after 120 h (Appendix Figure II-1E).

H1299 and A549 KDS grow significantly slower than OES, OEC, and KDC lines (Figure II-4F, Appendix Figure II-1F). However, no difference was seen for the H460 set (Appendix

Figure II-1F). Overexpression of SHMT2 only provided a proliferative advantage in the A549 cell line (Appendix Figure II-1F). The H1299 engineered lines showed the best overexpression and knockdown of SHMT2 coupled with significant differences in proliferation rates and thus was chosen for further studies (Figure II-4).
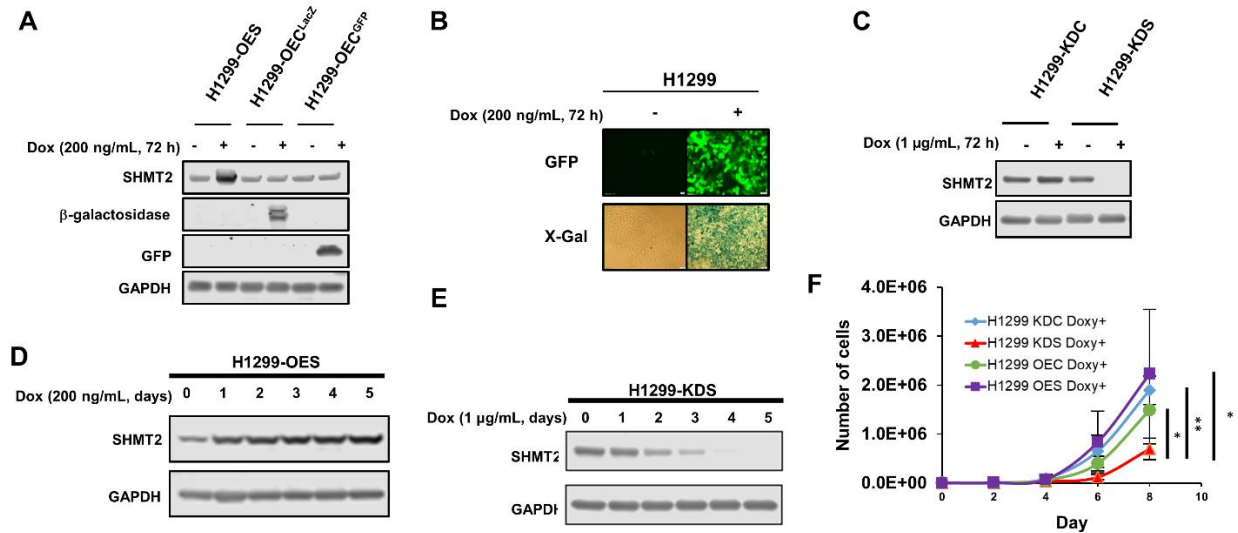
Figure II-4. Generation of H1299 cell line with inducible overexpression or knockdown of SHMT2. (A) Dox-induced overexpression of SHMT2, LacZ, and GFP. (B) Micrographs of Dox-induced GFP and LacZ expression in control cell lines. Dox-induced GFP expression was monitored using fluorescent microscopy. The activity of LacZ-encoded β-galactosidase was measured by the conversion of colorless X-Gal into an insoluble blue product that was visualized under bright-field microscopy. (C) Dox-induced SHMT2 knockdown. (D) Time-dependent overexpression of SHMT2 with doxycycline treatment. (E) Time-dependent knockdown of SHMT2. (F) Doubling time of engineered H1299 cells; OEC used was LacZ. *$p < 0.05$, **$p < 0.01$.

Nascent RNA-seq and bioinformatics analysis of SHMT2-inducible cell lines

We chose to measure the nascent transcriptome of the engineered H1299 cell lines to better understand how the cells respond to active overexpression or knockdown in real-time. The experiment was performed as previously described.[204] A total of five comparisons were explored; active overexpression versus matched control (OESvOEC), active knockdown versus matched control (KDSvKDC), recovery of overexpression versus control (OES-RecvOEC), recovery of knockdown versus control (KDS-RecvKDC), and active overexpression versus active knockdown (OESvKDS). Validation of knockdown and overexpression of SHMT2 via western blot can be found in Appendix Figure II-2. As expected, removal of doxycycline allowed expression of

SHMT2 to progress towards a normal level, however, we were surprised that the knockdown still retained a significantly lower level of SHMT2 than the control even after seven days without doxycycline (Appendix Figure II-2).

DEGs for overexpression and knockdown of SHMT2

Sequencing of libraries derived from the capturing of Bru-labeled nascent RNA from H1299 OES yielded 57 significantly DEGs ($|FC| > 1.5$ and mean RPKM > 0.5), 25 were upregulated and 32 were downregulated compared to OEC. H1299 KDS showed a much higher gene count change. For H1299 KDS, 241 genes were significantly differentially expressed, with 117 upregulated and 124 downregulated compared to KDC. The top 25 DEGs for both samples can be found in Tables II-8 and II-9. Interestingly, there were a few genes that were common between the treatments (bold-faced in Tables II-8 and II-9) and are discussed. Gratifyingly, *SHMT2* was among the significantly upregulated for OES and downregulated for KDS, validating the inducible expression systems.

Table II-8. H1299 OES top 25 differentially expressed genes compared to OEC[LacZ].

Gene[a]	Description	FC	Gene[a]	Description	FC
SHMT2	Serine hydroxymethyltransferase 2 (mitochondrial)	3.96	EIF4EBP3	Eukaryotic translation initiation factor 4E-binding protein 3	-4.50
HIST1H2AK	histone cluster 1, H2AK	3.60	C19orf33	Uncharacterized protein C19orf33	-3.75
HIST1H2AB	histone cluster 1, H2AB	2.29	AC092718.3	Uncharacterized protein AC092718.3	-3.75
CARD17	Caspase recruitment domain-containing protein 17	2.00	**COG8**	Conserved oligomeric Golgi complex subunit 8	-3.50

KIAA0408	Uncharacterized protein KIAA0408	2.00	**AP001931.1**	Uncharacterized protein AP001931.1	-3.30
ANKDD1A	ankyrin repeat and death domain containing 1A	1.92	**PRR4**	Proline-rich protein 4	-3.00
HOXB9	Homeobox protein Hox-B9	1.81	**GPR21**	Probable G-protein coupled receptor 21	-3.00
HIST1H3J	histone cluster 1, H3J	1.76	**PRH1**	Salivary acidic proline-rich phosphoprotein 1/2	-2.14
AC106886.5	Uncharacterized protein AC106886.5	1.73	MIF	Macrophage migration inhibitory factor	-2.00
GAGE2A	G antigen 2A	1.71	**PILRB**	Paired immunoglobin-like type 2 receptor beta	-2.00
UBALD2	UBA-like domain-containing protein 2	1.66	MSH5-SAPCD1	MSH5-SAPCD1 Readthrough (NMD Candidate)	-2.00
CKLF	Chemokine-like factor	1.64	**EGR1**	early growth response 1	-1.83
HIST1H2AL	histone cluster 1, H2AL	1.63	NEDD8-MDP1	NEDD8-MDP1 readthrough	-1.76
ZC2HC1B	Zinc finger C2HC-type containing 1B	1.62	**SLC10A5**	solute carrier family 10 (sodium/bile acid cotransporter family), member 5	-1.68
MRPS2	mitochondrial ribosomal protein S2	1.60	FKBPL	FK506-binding protein-like	-1.63

ZYX	zyxin	1.58	ZNF799	Zinc finger protein 799	-1.59
AD000671.1	Uncharacterized protein AD000671.1	1.55	**DDX39B**	Spliceosome RNA helicase DDX39B	-1.59
MSH5	MutS protein homolog 5	1.55	CDO1	cysteine dioxygenase, type I	-1.58
RING1	E3 ubiquitin-protein ligase RING1	1.54	**PMF1**	Polyamine-modulated factor 1	-1.58
HIST1H2BM	histone cluster 1, H2BM	1.52	AL031708.1	Uncharacterized protein AL031708.1	-1.54
MRPL40	Mitochondrial ribosomal protein L40	1.52	ZNF564	Zinc finger protein 564	-1.52
PPP1R14B	Protein phosphatase 1 regulatory subunit 14B	1.52	NR2C2AP	Nuclear receptor 2C2-associated protein	-1.52
SENP3	Sentrin-specific protease 3	1.52	TMEM179B	Transmembrane protein 179B	-1.52
DDTL	D-dopachrome tautomerase-like	1.52	**LIN37**	Protein lin-37 homolog	-1.50
BEX1	Protein BEX1	1.50	**MATR3**	Matrin-3	-1.50

[a]Genes with mean RPKM > 0.5

Table II-9. H1299 KDS top 25 differentially expressed genes compared to KDC.

Gene[a]	Description	FC	Gene[a]	Description	FC
SPP1	secreted phosphoprotein 1	9.04	**PRR4**	Proline-rich protein 4	-7.38
RHOB	ras homolog family member B	5.60	EEF1G	Elongation factor 1-gamma	-5.73
IPO4	Importin-4	5.21	ANKRD1	ankyrin repeat domain 1 (cardiac muscle)	-3.96
GPR21	Probable G-protein coupled receptor 21	3.79	ZNF404	zinc finger protein 404	-3.31

CHMP4A	Charged multivesicular body protein 4a	3.32	**COG8**	Conserved oligomeric Golgi complex subunit 8	-3.16
ERRFI1	ERBB receptor feedback inhibitor 1	3.29	AARSD1	Alanyl-tRNA editing protein Aarsd1	-3.16
ARL4C	ADP-ribosylation factor-like 4C	3.10	ZNF582	zinc finger protein 582	-3.03
EGR1	early growth response 1	2.61	**PILRB**	Paired immunoglobin-like type 2 receptor beta	-2.85
WNT16	wingless-type MMTV integration site family, member 16	2.55	**AD000671.2**	Uncharacterized protein AD000671.2	-2.81
ARHGAP29	Rho GTPase activating protein 29	2.47	NTM	neurotrimin	-2.81
GPAT3	Glycerol-3-phosphate acyltransferase 3	2.41	ZNF781	zinc finger protein 781	-2.52
RAP2B	RAP2B, member of RAS oncogene family	2.28	SALL3	sal-like 3 (Drosophila)	-2.28
PRH1	Salivary acidic proline-rich phosphoprotein 1/2	2.27	ZNF45	zinc finger protein 45	-2.27
CIART	Circadian-associated transcriptional repressor	2.21	**DDX39B**	Spliceosome RNA helicase DDX39B	-2.23
JUN	jun proto-oncogene	2.20	HIST1H4D	histone cluster 1, H4D	-2.22
GAGE2A	G antigen 2A	2.15	ZNF221	zinc finger protein 221	-2.21
TMSB4X	Thymosin beta-4	2.12	KRBA2	KRAB-A domain containing 2	-2.17
BHLHE41	basic helix-loop-helix family, member e41	2.12	ATF5	activating transcription factor 5	-2.17

MUC15	mucin 15, cell surface associated	2.11	INSIG1	insulin induced gene 1	-2.16
TMEM256	Transmembrane protein 256	2.09	IER3	Radiation-inducible immediate-early gene IEX-1	-2.15
AP001931.1	Uncharacterized protein AP001931.1	2.05	ZNF283	zinc finger protein 283	-2.13
EMP1	epithelial membrane protein 1	2.04	CHAC1	ChaC, cation transport regulator homolog 1 (E. coli)	-2.12
KLF2	Krueppel-like factor 2	2.02	HTD2	Hydroxyacyl-thioester dehydratase type 2, mitochondrial	-2.11
ADRA1B	Alpha-1B adrenergic receptor	1.99	UCHL3	Ubiquitin carboxyl-terminal hydrolase isozyme L3	-2.06
TNIK	TRAF2 and NCK-interacting protein kinase	1.93	LACTB	lactamase, beta	-2.05

[a]Genes with mean RPKM > 0.5

There were only two genes commonly upregulated between the two samples: *GAGE2A* and *MSH5*. We were surprised that there were any commonly up- or downregulated genes since SHMT2's expression was going in opposing directions. The GAGE family of proteins are part of the cancer/testis (CT) antigen class of cell-surface markers and are commonly upregulated in cancer.[205] There is considerable interest in targeting CT antigens for cancer immunotherapy as evidenced by clinical trials for other CT proteins and preclinical efforts for GAGE.[205-206] Despite the promise as a potential target for immunotherapy, the function of GAGE2A is unknown and there is little known about its biology; this includes a link to SHMT2 or metabolism in general. MutS homolog 5, MSH5, is a member of the DNA mismatch repair family of proteins that is crucial for chromosome pairing in meiosis. Despite being part of the mismatch repair family,

MSH5 has not experimentally been shown to participate in it although there is some evidence to suggest that MSH5 may play a role in mitotic DNA damage response and repair.[207] Di Bernardo et al. analyzed the changes in expression of *MSH5* when incubated with the histone deacetylase inhibitors SAHA and MS-257 and found that its expression significantly increased after 24 h treatment, but then subsequently decreased over the next 48 h.[208] CMAP analysis of the KDS data revealed that many HDAC inhibitors positively correlated with gene expression changes caused by knockdown of SHMT2 (Appendix Table II-8).

Two of the top three commonly downregulated genes are *COG8* and *PILRB*. COG8 is a subunit of a multi-protein Golgi complex that participates in glycosylation of proteins.[209-210] Our RNA-Seq analysis of SHMT2 KO revealed significant changes in expression of glycosylated proteins (Figure II-2C), so it would be interesting to see what role, if any, COG8 played specifically in relation to SHMT2, and how the glycosylome in general changes in response to manipulation of SHMT2 expression. It is notable that the mRNA transcript of *COG8* overlaps with peptide deformylase (*PDF*).[211] PDF removes the formyl group from methionine in the mitochondria and interference with its activity negatively impacts translation and by extension, oxidative phosphorylation.[211] *PILRB* (paired immunoglobulin-like type 2 receptor) contributes to immune regulation by binding the sialylated O-glycosylated ligand CD99, which is expressed on activated T cells.[212] PILRB also has a role in the central nervous system in responding to injury, mainly axonal regeneration and synaptic plasticity.[213] We also observed enrichment of axon-related genes with SHMT2 KO (Figure II-2C, Table II-4).

GPR21 and *PRH1* were among the genes that were downregulated when SHMT2 was overexpressed and upregulated when it was knocked down. GPR21 is an orphan G-protein-coupled receptor with an unknown ligand. The expression of GPR21 seems to shift in metabolic disorders

such as diabetes.[214-215] There are conflicting reports on GPR21's direct involvement in glucose tolerance.[216-217] There is no reported link between GPR21 and 1CM. *PRH1*, proline-rich protein HaeIII subfamily 1, encodes for a family of acidic salivary proteins.[218] In addition to having high proline content, glycine is also a major component.[218] Based on this fact, one would expect that knockdown of *SHMT2* would cause a downregulation of *PRH1*, and vice versa, but this is the opposite of our result. We observed a downregulation of another proline-rich protein encoding gene, *PRR4*, in both our OES and KDS samples. Little is known about *PRR4*, but was recently shown to be associated with laryngeal cancer.[219]

HOXB9 and *DDTL* were the only other genes, besides *SHMT2* itself, that were upregulated when SHMT2 was overexpressed and downregulated when it was knocked down. HOXB9 is a transcription factor important for embryonic development and is an important prognostic biomarker in several cancers including lung.[220-221] Expression of HOXB9 is associated with a more aggressive phenotype, and interestingly this is intricately regulated by a PTM of acetylation.[221] Importantly, deprivation of essential amino acids induced the expression of HOXB9 in activated T-cells.[222] Glycine is a conditionally non-essential amino acid, meaning that cells are able to synthesize it, but in times of rapid growth, stress, or illness, the body might require a supplement.[223] We suggest that deconvolution of which essential amino acids induce the expression of HOXB9 in activated T-cells to be explored, and also to evaluate if this translates to cancer cells as well. As overexpression of HOXB9 negatively correlates with survival, the fact that we observe downregulation when SHMT2 is knocked down is a positive result.

DDTL, or D-dopachrome tautomerase-like protein, is believed to play a role in oxidative metabolism due to its neighboring genes' functions.[224] However, there is no experimental evidence to support this. DDTL was among genes whose amplification was associated with erlotinib

resistance in NSCLC cells.[225] In breast cancer cells, SHMT2 was upregulated in response to a different EGFR tyrosine kinase inhibitor, lapatinib.[226] Given that SHMT2 also participates in redox homeostasis,[8-9, 227] it would be interesting to see if DDTL contributes to resistance through this mechanism as well.

SHMT2 overexpression gene set enrichment

Novel transcription factor associations

Gene set enrichment analysis of H1299 OES resulted in no downregulated and 14 significantly upregulated gene sets, the top four are shown in Figure II-5. The SOX9_B1 gene set contains genes that have a SOX9 binding site. SOX9 is a transcription factor responsible for regulating chondrogenesis and myriad cancer-related processes.[228-229] SOX9 has not been linked to SHMT2 or 1CM, but given its role in cartilage formation of which collagen is a main component, it is possible that SHMT2 may be a part of this program through glycine production, much like the case for TGF-β.[17, 228] Interestingly, in the comparison of OESvKDS, SOX9 is one of the top 25 downregulated genes (FC = -2.48), indicating the opposite case for knockdown of SHMT2. We speculate that SOX9 may be downregulated when SHMT2 is overexpressed because glycine may be abundant. Conversely, SOX9 may be upregulated when SHMT2 is knocked down as a compensation mechanism. In this case, it would be interesting to investigate the interplay of SHMT1/SHMT2 in relation to SOX9. Importantly, another SOX family member, SOX7, plays a repressive role against *MTHFD2* in breast cancer.[230]

RTAAACA_FREAC2_01 describes a list of genes that are regulated by the transcription factor FREAC2, more commonly known as FOXF2. SHMT2 is not listed in this gene set. FOXF2 controls several cancer processes including metabolic reprogramming.[231-232] Of interest, in breast cancer FOXF2 differentially regulates genes involved in pyrimidine (*CAD*), folate (*MTHFR*), and

glycan metabolism (*GALNTL4*).[231] These changes were not validated at the protein level, but with our finding we suggest that the role of FOXF2 in regulation of 1CM be explored further.

ZBTB44_TARGET_GENES contain genes that have predicted binding sites for the putative transcription factor ZBTB44. Little is known about the gene or protein. One important finding is that it was upregulated in response to low maternal folate intake.[233] This is in line with our experiment. Decreased activity of SHMT2 would limit the carbon units available to be conjugated to THF and therefore affect many cellular biosynthetic processes. ZBTB44 may act as a sensor for folate pathway fitness.

The HALLMARK_G2M_CHECKPOINT gene set is composed of genes involved in cell cycle progression past the G2M checkpoint. Knockdown of SHMT2 has previously been shown to induce cell cycle arrest.[234-235] Jain and colleagues found that knockdown of SHMT2 resulted in accumulation of cells in the G1 phase in HeLa cells.[234] Importantly, using a lung cancer model, Paone et al. showed that knockdown of SHMT2 in H1299 cells did result in a significant accumulation of sub-G1 cells, but knockdown of SHMT1 had a more pronounced effect.[235] Our data supports the notion that SHMT2 overexpression facilitates cell cycle progression.

Chromatin, ethanol, and lupus

DAVID and STRING both identified many chromatin related gene sets (Figure II-5, Table II-10). This is supported by the presence of HDAC inhibitors in the CMAP analysis (Appendix Table II-7). Through donation of 1C units, 1CM impacts epigenetic modifications of histones, with most focusing on H3 methylation.[41, 61] There are many variants of histone H2A with several identified as being altered in the context of cancer, including *HIST1H2AK* (FC = 3.60, Table II-8).[236]

Table II-10. H1299 OES STRING gene sets compared to OEC[LacZ].

Gene set	FDR

94

nucleosome	0.0013
nuclear chromosome part	0.0071
chromosomal part	0.0224
chromatin	0.0305
nuclear chromatin	0.0305
nucleus	0.0329

The interplay of folate and ethanol has been extensively studied in the context of cancer, but there is still much to learn.[237] Many folate-metabolizing enzymes have been linked to effects of alcohol exposure, but to our knowledge SHMT2 has not.[237] Much like ethanol, folate-deficiency and loss of serine hydroxymethyltransferase has a teratogenic effect (NTDs).[59] Additionally, alcohol consumption induces folate-deficiency, therefore it is not surprising that decreasing of SHMT2 expression would produce a similar response, so it is interesting that we see the similarity with overexpression.

Systemic lupus erythematosus (SLE) is an autoimmune disease of unknown etiology.[238] Polymorphisms for folate enzymes are associated with systemic lupus erythematosus, however it is unknown if SHMT2 is among them.[239] mTOR signaling contribute to the pathogenesis of SLE, and mTOR inhibitors are showing efficacy in the clinic.[238] SHMT2 is a downstream target of mTOR and therefore its involvement in SLE is not impossible.[17] As discussed above, SHMT2 forms a complex with BRISC that works to regulate IFN signaling.[55-56] IFNαR1 signaling is elevated in SLE and neutralizing antibodies of IFN are currently undergoing clinical trials.[240] Inhibition of SHMT2 could be an interesting alternative to decreasing IFN signaling by allowing receptor internalization and degradation.[56]
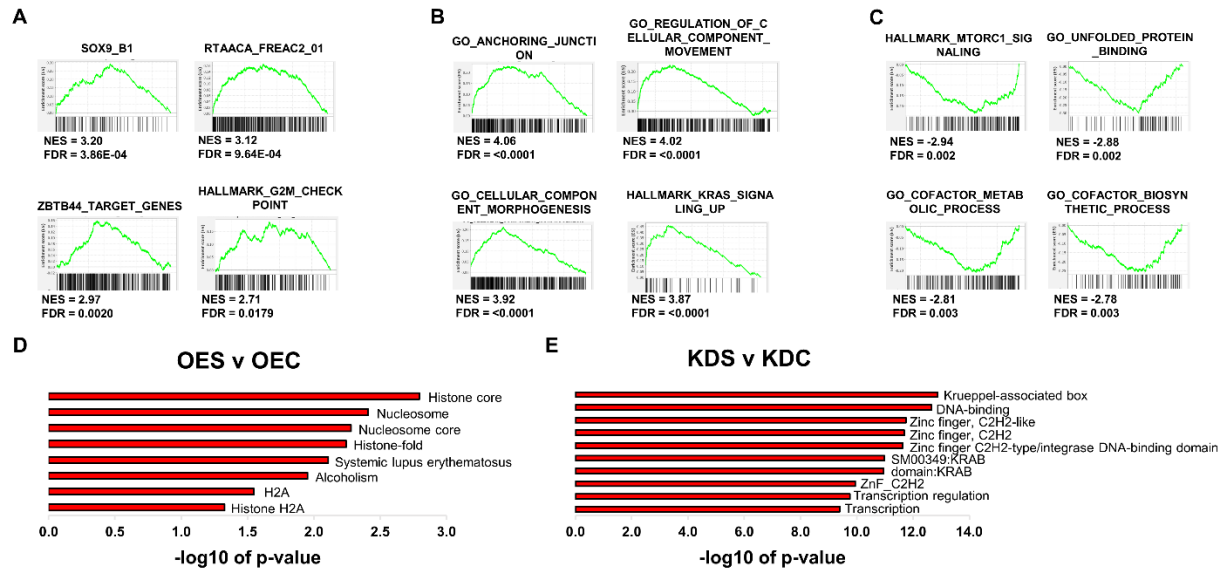
Figure II-5. Enriched gene sets for H1299 OES and KDS versus OEC and KDC, respectively. (A) Top four H1299 OES upregulated GSEA gene sets. (B) Top four H1299 KDS upregulated GSEA gene sets. (C) Top four H1299 KDS downregulated GSEA gene sets. (D) Significantly enriched gene sets for H1299 OES using DAVID. (E) Significantly enriched gene sets for H1299 KDS using DAVID.**SHMT2 knockdown gene set enrichment**

Cell-cell interactions and morphogenesis

The top four significantly upregulated enriched gene sets through GSEA can be found in Figure II-5B. GO_ANCHORING_JUNCTION and GO_REGULATION_OF_CELLULAR_COMPONENT_MOVEMENT both contain genes that mediate cell-cell interactions and movement. The top upregulated gene for H1299 KDS encodes for a protein that is important for cell adhesion and migration, *SPP1* (FC = 9.04, Table II-9). The protein encoded by the *SPP1* gene is known as osteopontin. Osteopontin participates in several immune- and cancer-related processes in multiple cancer types, including lung cancer.[241-242] Osteopontin majorly carries out its function through interaction with various integrins and CD44.[242] Osteopontin is highly post-translationally modified including glycosylation, however, glycosylation status is understudied in the lungs.[241] Our RNA-Seq results suggest that SHMT2 may be related to protein glycosylation so we believe that the relationship between SHMT2 and the glycosylation status of SPP1 be further explored since we observed an inverse relationship in

the H1299 lung cancer cell line. We did not observe a difference in expression of osteopontin at the protein level (Figure II-6A), but we evaluated soluble osteopontin and not the secreted form. The antibody used does not distinguish between the three different splice variants of osteopontin. Interestingly, *SPP1* expression correlated with pemetrexed sensitivity, expanding the evidence that osteopontin expression may be affected by folate metabolism.[243]
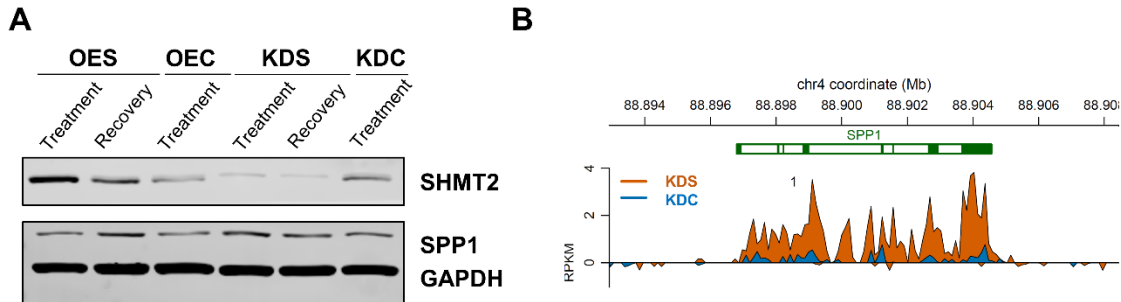
Figure II-6. Expression of SPP1. (A) Expression of SPP1 in cell lysates of all Bru-seq samples. (B) Trace diagram of nascent mRNA expression of SPP1 in SHMT2 and control knockdown H1299 cells.

Three of the top 25 upregulated genes are part of the GO_CELLULAR_COMPONENT_MORPHOGENESIS gene set: *RHOB* (FC = 5.60), *KLF2* (FC = 2.02), and *TNIK* (FC = 1.93) (Table II-9). Ras homolog family member B (RhoB), as its name reveals, is part of the Ras superfamily of GTPases. It is well-established that the Rho family of proteins regulate actin organization in the cell, however the role that RhoB plays in the context of cancer is not well-defined.[244] Interestingly, RhoB expression was found to be epitranscriptomically regulated by methylation of the N^6-adenosine on the mRNA transcript.[245] Methylation of the mRNA can either increase or decrease stability of the transcript, depending on the accompanying protein.[245] Given that the *RHOB* transcript has a short half-life (~30 min), it is significant that we observe a 5.6-fold increase in expression.[244] We believe that the methylation status of *RHOB* as a regulation mechanism in metabolically reprogrammed cancer cells warrants investigation. KLF2 is a tumor suppressive zinc finger transcription factor found to regulate glutamine consumption in NSCLC cells and overexpression negatively impacts cell proliferation.[246] *KLF6* and *KLF7* are

also in the upregulated genes (FC = 1.79 and 1.67 respectively). The KLF family is a group of transcription factors with a zinc finger structure implicated in metabolism regulation and carcinogenesis.[247-248] KLF2, KLF6, and KLF7 are all in Class II within the larger family.[247, 249] Interestingly, all of the top ten significantly enriched gene sets by DAVID analysis are related to zinc-fingers and transcription (Figure II-5E) and is discussed below. TNIK, also known as Traf2- and Nck-interacting kinase, can specifically activate the JNK and Wnt pathways.[250-251] Related, we also see upregulation of *JUN* and *JUND* (Table II-9). As discussed above, Wnt signaling is inhibited when 1CM is inhibited, so it is possible that the upregulation of *TNIK* is in response to this inhibition.[34]

Knockdown of KRAS caused downregulation of SHMT2 in KRAS-mutant cells.[143] RAS-mutant cells were more sensitive to anti-folates including H1299 (KRAS WT, NRAS[Q61K]), underlining the dependence on folate metabolism.[143] Our observed upregulation of the KRAS signaling gene set when SHMT2 is knocked down suggests a potential compensation mechanism.

Canonical pathways validated

Three of the top four significantly enriched downregulated gene sets are in line with the canonical function of SHMT2 (Figure II-5C): HALLMARK_MTORC1_SIGNALING, GO_COFACTOR_METABOLIC_PROCESS, and GO_COFACTOR_BIOSYNTHETIC_PROCESS. SHMT2 is a well-known target of mTOR and therefore knockdown of SHMT2 would mimic a downregulation of mTOR signaling.[17-18, 252] The downregulation of the cofactor processes gene sets supports the knockdown of SHMT2. Folate is a critical cofactor, contributing to many biosynthetic pathways (Figure I-1).[253] Without SHMT2 to conjugate a 1C unit to THF, nucleotide biosynthesis, PTMs and epigenetics are all affected as a consequence.

A large portion of genes in the GO_UNFOLDED_PROTEIN_BINDING gene set are protein folding chaperones or cochaperones (heat shock proteins, HSPs). The HSP70 family are the major chaperones in the cell and facilitate folding of nascent polypeptides. This protein processing can be assisted by the HSP40 (also known as DNAJ) family of proteins.[254] DNAJA1 was shown to be negatively regulated by an oxidative environment.[254] We observed a downregulation of *DNAJA1* (FC = -1.50) with knockdown of SHMT2. As discussed previously, SHMT2 plays a key role in redox homeostasis.[8-9, 227] Recently *SHMT2* expression was found to be increased upon induction of the unfolded protein response (UPR).[255] Additionally, knockout of a key UPR transcription factor XBP1 caused an upregulation of SHMT2 in dendritic cells.[256] We observed a modest decrease in *XBP1* expression (FC = -1.30). It is interesting that there seems to be crosstalk between these two pathways.

Zinc-finger transcription factors

As mentioned above, all the significantly enriched gene sets by DAVID analysis are related to zinc-fingers and transcription (Figure II-5E). The C_2H_2-type zinc finger domain is a very common motif of transcription factors and is present in all KLF family members.[247] Krüppel-like and SP-1-like transcription factors share high similarity.[249] SHMT2 has SP-1 binding site in its promoter.[257] The DNA-binding motifs of these two families are GC rich; for KLFs it is 5'-CACCC-3'.[247] Inspection of the SHMT2 promoter using the GeneCards source revealed the presence of this sequence. KLFs are involved in several cancer-related processes including proliferation, differentiation, and apoptosis.[247] For example, KLF6 induces G_1 cell cycle arrest and is a tumor suppressor like KLF2.[246-247] In general, KLFs regulate adipogenesis, but also participate in other metabolic processes. As mentioned above, KLF2 regulates glutamine metabolism in

NSCLC cells.[246] Additionally, KLF15 has also been linked to glucose and amino acid metabolism.[248] This is the first study to propose a connection between *KLF2*, *6*, and *7* and 1CM.

STRING analysis of the SHMT2 knockdown data did not yield anything unexpected (Table II-11). Regulation of various biosynthetic processes dominate the list. Since 1CM contributes to many different ones, it's not surprising that we observe broad changes in processes such as macromolecules, nucleic acids, small molecules, and transcription.

Table II-11. H1299 KDS STRING gene sets compared to KDC.

Gene set	FDR
regulation of biosynthetic process	5.45E-12
regulation of transcription, DNA-templated	1.58E-11
regulation of cellular biosynthetic process	1.58E-11
regulation of gene expression	1.97E-11
regulation of cellular macromolecule biosynthetic process	3.81E-11
regulation of macromolecule biosynthetic process	5.07E-11
regulation of metabolic process	1.29E-10
regulation of RNA metabolic process	1.29E-10
regulation of primary metabolic process	1.29E-10
regulation of nucleobase-containing compound metabolic process	2.18E-10
regulation of transcription by RNA polymerase II	2.29E-10
regulation of cellular metabolic process	2.95E-10
regulation of macromolecule metabolic process	1.55E-09
regulation of nitrogen compound metabolic process	2.78E-09
transcription, DNA-templated	3.91E-09

organic cyclic compound biosynthetic process	7.30E-09
nucleobase-containing compound biosynthetic process	1.56E-08
cellular macromolecule biosynthetic process	6.24E-08
cellular nitrogen compound biosynthetic process	6.88E-08
nucleic acid metabolic process	4.35E-07
organic substance biosynthetic process	1.21E-06
RNA metabolic process	1.28E-06
cellular biosynthetic process	2.04E-06
organic cyclic compound metabolic process	2.90E-06
nucleobase-containing compound metabolic process	7.27E-06

Kinase inhibitors show similar profile

Several kinase inhibitors both positively and negatively correlated with gene expression changes caused by knockdown of SHMT2 (Appendix Table II-8). Many reports have shown metabolic reprogramming occurs in response to tyrosine kinase inhibitors.[258-259] This includes amino acid metabolism, and serine and glycine in particular.[258] A previous study found a negative correlation between high SHMT2 expression and sensitivity to sunitinib across a panel of 635 cell lines.[181] In agreement with that result, our data show that sunitinib-induced gene expression changes negatively correlate with knockdown of SHMT2 (Appendix Table II-8). In a breast cancer study, the transcription factor ERRα targets SHMT2 as a mechanism to overcome sensitivity to lapatinib.[226] In just these two works SHMT2 is associated with chemosensitivity and chemoresistance, supporting our result of both negative and positive correlations to knockdown of SHMT2. There are many tyrosine kinase inhibitors that have not previously been linked to SHMT2 that deserve attention such as motesanib, cediranib, tozasertib, BIBX-1382, and TG-101348.

DEGs for recovery of overexpression and knockdown of SHMT2

We performed the recovery experiments to evaluate if we would observe the same changes when SHMT2 expression was decreasing (OES-Rec and KDS) or increasing (KDS-Rec and OES), albeit from different starting levels (e.g. high to "normal" and "normal" to low). H1299 OES-Rec had 150 upregulated and 62 downregulated genes (Table II-12 contains the top 25 from each). H1299 KDS-Rec had 46 and 40 upregulated and downregulated genes respectively (top 25 in Table II-13). By simply looking at the numbers, it is apparent that a decrease in expression of SHMT2 (KDS and OES-Rec) had a stronger impact on H1299 cells than an increase in expression (OES and KDS-Rec).

Table II-12. H1299 OES-Rec top 25 differentially expressed genes compared to OEC[LacZ].

Gene[a]	Description	FC	Gene[a]	Description	FC
TRIB3	tribbles homolog 3 (Drosophila)	8.60	AC018630.6	Uncharacterized protein AC018630.6	-5.68
DDIT4	DNA-damage-inducible transcript 4	5.41	CHMP4A	Charged multivesicular body protein 4a	-5.68
SESN2	sestrin 2	3.99	PRR4	Proline-rich protein 4	-4.26
CHAC1	ChaC, cation transport regulator homolog 1 (E. coli)	3.37	EIF4EBP3	Eukaryotic translation initiation factor 4E-binding protein 3	-4.26
CDKN2B	cyclin-dependent kinase inhibitor 2B (p15, inhibits CDK4)	3.26	KRTAP2-3	Keratin associated protein 2-3	-2.98
SLFN5	schlafen family member 5	2.94	NDUFA7	NADH dehydrogenase [ubiquinone] 1 alpha subcomplex subunit 7	-2.56
GAGE2A	G antigen 2A	2.82	PRH1	Salivary acidic proline-rich phosphoprotein 1/2	-2.37

SLC7A11	solute carrier family 7 (anionic amino acid transporter light chain, xc- system), member 11	2.57	DDX39B	Spliceosome RNA helicase DDX39B	-2.13
HIST1H2AK	histone cluster 1, H2AK	2.53	PILRB	Paired immunoglobin-like type 2 receptor beta	-1.85
IDH1	isocitrate dehydrogenase 1 (NADP+), soluble	2.43	NR2C2AP	nuclear receptor 2C2-associated protein	-1.84
UPP1	uridine phosphorylase 1	2.42	SLC10A5	solute carrier family 10 (sodium/bile acid cotransporter family), member 5	-1.83
ALDH1L2	aldehyde dehydrogenase 1 family, member L2	2.40	HSPA8	heat shock 70kDa protein 8	-1.83
BHLHE40	basic helix-loop-helix family, member e40	2.40	RRP8	ribosomal RNA processing 8, methyltransferase, homolog (yeast)	-1.82
ASNS	asparagine synthetase (glutamine-hydrolyzing)	2.39	NOL6	nucleolar protein family 6 (RNA-associated)	-1.81
TCTEX1D2	Tctex1 domain-containing protein 2	2.29	ANKRD1	ankyrin repeat domain 1 (cardiac muscle)	-1.78
RTL8A	Retrotransposon Gag-like protein 8A	2.27	MATR3	Matrin-3	-1.78
CEBPB	CCAAT/enhancer binding protein (C/EBP), beta	2.25	IPO4	Importin-4	-1.78
BEX4	brain expressed, X-linked 4	2.25	AC092587.1	Uncharacterized protein AC018630.6	-1.78
FAM129A	Protein Niban	2.24	TAX1BP3	Tax1-binding protein 3	-1.76

Gene	Description				
MMP24-AS1	MMP24-AS1-EDEM2 Readthrough	2.24	ZNF564	zinc finger protein 564	-1.75
CLDN1	Claudin-1	2.23	AP001931.1	Uncharacterized protein AP001931.1	-1.74
STC2	Stanniocalcin-2	2.20	TOR1B	torsin family 1, member B (torsin B)	-1.74
GOT1	Aspartate aminotransferase, cytoplasmic	2.18	ZNF544	zinc finger protein 544	-1.70
HOXB9	Homeobox protein Hox-B9	2.18	MATR3	Matrin-3	-1.68
CCNG2	Cyclin-G2	2.17	NEDD8-MDP1	NEDD8-MDP1 readthrough	-1.67

[a]Genes with mean RPKM > 0.5

Table II-13. H1299 KDS-Rec top 25 differentially expressed genes compared to KDC.

Gene[a]	Description	FC	Gene[a]	Description	FC
EIF4EBP3	Eukaryotic translation initiation factor 4E-binding protein 3	4.34	EEF1G	Elongation factor 1-gamma	-5.43
TXNDC5	Thioredoxin domain-containing protein 5	3.84	TAX1BP3	Tax1-binding protein 3	-2.73
CDK11A	Cyclin dependent kinase 11A	3.00	AD000671.2	Uncharacterized protein AD000671.2	-2.67
CHMP4A	Charged multivesicular body protein 4a	2.50	DDX39B	Spliceosome RNA helicase DDX39B	-2.37
ARHGAP29	Rho GTPase activating protein 29	2.46	KRTAP2-3	Keratin associated protein 2-3	-2.15
AC018630.6	Uncharacterized protein AC018630.6	2.33	STC1	stanniocalcin 1	-2.00

WNT16	wingless-type MMTV integration site family, member 16	2.19	ANKRD1	ankyrin repeat domain 1 (cardiac muscle)	-2.00
HSPB1	heat shock 27kDa protein 1	2.03	PPAN	Suppressor of SWI4 1 homolog	-2.00
CDKN2B	cyclin-dependent kinase inhibitor 2B (p15, inhibits CDK4)	2.02	LIN37	Protein lin-37 homolog	-2.00
C2orf74	chromosome 2 open reading frame 74	2.00	AL662899.3	Uncharacterized protein AL662899.3	-2.00
RTL8C	Retrotransposon Gag-like protein 8C	1.97	HBEGF	heparin-binding EGF-like growth factor	-1.96
CIART	Circadian-associated transcriptional repressor	1.95	ZNF404	zinc finger protein 404	-1.95
ARL4C	ADP-ribosylation factor-like 4C	1.94	C7orf25	chromosome 7 open reading frame 25	-1.87
NDUFA13	NADH dehydrogenase [ubiquinone] 1 alpha subcomplex subunit 13	1.92	MARCH3	E3 ubiquitin-protein ligase MARCH3	-1.83
ZNF593	zinc finger protein 593	1.92	POLR3GL	DNA-directed RNA polymerase III subunit RPC7-like	-1.80
HIST2H2BE	histone cluster 2, H2BE	1.85	PRR4	Proline-rich protein 4	-1.75
C1orf50	chromosome 1 open reading frame 50	1.79	CD274	CD274 molecule	-1.74
NPHP3	Nephrocystin-3	1.76	AC009779.3	Uncharacterized protein AC009779.3	-1.70
GAGE2A	G antigen 2A	1.73	HIST1H2AD	histone cluster 1, H2AD	-1.66

TMEM158	transmembrane protein 158	1.72	KBTBD8	kelch repeat and BTB (POZ) domain containing 8	-1.64
CENPS	Centromere protein S	1.72	NPM3	nucleophosmin/nucleoplasmin 3	-1.63
TMEM81	transmembrane protein 81	1.71	ZNF626	zinc finger protein 626	-1.63
JUND	jun D proto-oncogene	1.71	PRAF2	PRA1 family protein 2	-1.58
HIST1H2AI	histone cluster 1, H2AI	1.70	SOGA3	SOGA family member 3	-1.58
HIST4H4	histone cluster 4, H4	1.69	AC005837.2	Uncharacterized protein AC005837.2	-1.56

[a]Genes with mean RPKM > 0.5

Between OES-Rec and KDS, there were a total of 29 commonly differentially expressed genes. The upregulated ones were: *TRIB3, CDKN2B, GAGE2A, CLDN1, RHOB, SPRY2, ARHGEF2, TMEM158, PHLDA1, JUND, AHNAK2, IRF2BP2, FAM3C, WNT16, VGF, JUN, KLF7, CCDC71L,* and *KLF6.* The genes *CLDN1* and *RHOB* were also upregulated in SHMT2 KO (FC = 2.95 and 2.86, respectively); see above for discussion on *RHOB.* Claudin-1, encoded by *CLDN-1*, is a membrane protein involved in endo- or epithelial tight junctions.[260] Unsurprisingly, deregulation of this protein in cancer is associated with metastatic phenotypes because cell adhesion precludes invasion and migration. However, there is a context-dependency on whether CLDN-1 functions as a tumor promoter or suppressor.[260] Modulation of expression of glycosylation-related proteins has been shown to impact CLDN-1 expression.[261-262] Interestingly, CLDN-1 levels were significantly increased in response to prolonged exposure to 5FU, and knockdown re-sensitized cells to 5FU treatment.[263] *TRIB3* is a pseudokinase involved in regulating the unfolded protein and endoplasmic reticulum stress responses, insulin signaling, glycogen synthesis, and PI3K/AKT/mTOR signaling, among others.[264] In fact, TRIB3 expression is induced

in the absence of glucose and amino acids.[265] We observed an 8.6-fold change in expression of *TRIB3* for OES-Rec, while only a modest 1.6-fold change for KDS.

The common downregulated genes between OES-Rec and KDS were: *DESI1, AL022238.4, TAX1BP3, MATR3, ANKRD1, SLC10A5, PILRB, DDX39B, KRTAP2-3,* and *PRR4. DESI1* encodes for the protein deSUMOylating isopeptidase 1, which removes small ubiquitin-like modifier (SUMO) from substrates.[266] SHMT1 has been shown to be SUMOylated and localize to the nucleus for de novo thymidylate synthesis.[267-269] This translocation occurs during S-phase, or in response to DNA damage.[270-271] Interestingly, the SHMT2 isoform lacking the mitochondrial-targeting sequence (SHMT2α) localized to the nucleus when SHMT1 was knocked out,[268] however it is not known whether this translocation is SUMO-dependent. Substrates of DESI1 are unknown as are the conjugating and de-conjugating enzymes for SHMT1. Notably, inhibition of the SUMO pathway induces TRIB3 upregulation.[272]

There were only six genes that were significantly in common between KDS-Rec and OES: *PIGM*, *LIN37*, *DDX39B*, *SLC10A5*, *PRR4*, and *AD000671.2*. Phosphatidylinositol glycan anchor biosynthesis class M (PIGM) is an endoplasmic reticulum transmembrane protein that catalyzes addition of the first mannose moiety of the GPI core which is responsible for anchoring proteins to the cell surface.[273] We also observed glycosylation-modifying enzymes as significantly differentially expressed in our SHMT2 KO RNA-Seq data (Figure II-2C, Tables II-1 and II-2, Appendix Table II-1). Like *SHMT2*, *PIGM* also has a SP-1 binding site in its promoter.[273] DDX39B is a DECD-box helicase that regulates pre-ribosomal RNA synthesis and stability, mRNA processing, and alternative splicing.[274-275] Additionally, DDX39B participates in regulation of factors that control the ECM and the NF-κB-mediated inflammatory response.[276] As discussed previously, glycine is a major component of the ECM and SHMT2 has also been linked to the

immune response.[55, 57, 82] The function of SLC10A5 has not been determined at this point but based on sequence identity and tissue distribution it is expected that it participates in bile acid transport.[277] Bile acids play a key role in digestion of fat-soluble vitamins and nutrients and therefore are critical regulators of metabolic homeostasis. Glycine is a common conjugate of bile acids and in addition to improving water solubility, it also increases affinity of the bile acids for certain transporters.[277] Beyond this link, SHMT2 has not been connected to SLC10A5.

Gene set enrichment for recovery of overexpression of SHMT2

Hypoxia, immune signaling, and fatty acid synthesis

The top four upregulated gene sets can be found in Figure II-7A. Several studies have reported on SHMT2's involvement in response to hypoxia. Hypoxia induces *SHMT2*'s expression.[9] A key transcription factor that regulates the cell's response to hypoxia is HIF1-α. HIF1-α and SHMT2's expression positively correlate with each other,[8, 203] and the upregulation of SHMT2 by HIF1-α is through the transcription factor MYC.[8] Expression of SHMT2 is necessary to maintain redox homeostasis and brain cancer cell survival under hypoxic conditions *in vitro* and *in vivo*.[8, 125] In contrast, in colon cancer cells, inhibition of SHMT2 enhanced growth under hypoxia.[227] Therefore SHMT2's role in response to hypoxia is context-dependent. In our data, we did not observe a significant change in expression of HIF1-α, but MYC was upregulated (FC = 1.75).

Tumor necrosis factor alpha (TNF-α) is a key cytokine that regulates immune responses in healthy persons and in diseased conditions. In cancer, TNF-α can elicit myriad effects depending on the context, such as proliferation, apoptosis, necrosis, migration, angiogenesis, or invasion.[278] Very little is known about the relationship between cancer cell metabolism reprogramming and TNF-α signaling through NF-κB. To our knowledge, there are only a couple studies have been

published investigating metabolic changes of cancer cells in response to TNF-α. In non-cancerous and malignant breast epithelial cells, TNF-α induced a shift to reliance on aerobic glycolysis, however it is unknown if it was NF-κB dependent.[279] Also, in cooperation with interleukin-17, TNF-α induced glycolysis in colorectal cancer cells.[280] Similarly, another study reported metabolic reprogramming of hepatocytes towards the Warburg-effect phenotype in response to viral infection mediated by macrophage-secreted TNF-α.[281] In adipocytes, sustained exposure to TNF-α altered mitochondrial metabolism, notably reducing the NAD/NADH ratio.[282] Despite the observations toward the Warburg effect, no mechanisms have been elucidated. Given this knowledge gap, it is uncertain as to how folate metabolism is relevant to NF-κB signaling. Interestingly, a nanoparticle containing NF-κB targeted siRNA and MTX, a standard drug for treatment of rheumatoid arthritis, reduced TNF-α secretion and suppressed arthritis progression in a mouse model.[283]

Of the top four downregulated gene sets (Figure II-7B), HSD17B8_TARGET_GENES, was the only one that had not yet appeared in our analyses. The *HSD17B8* gene encodes for the mitochondrial NAD-dependent enzyme estradiol 17-β-dehydrogenase 8. In addition to oxidizing estradiol to estrone, HSD17B8 also contributes to fatty acid synthesis (FAS).[284] 1CM has previously been reported to be important for providing NADPH for this process.[140] It is possible that as SHMT2 expression decreases, less redox power is available for FAS and therefore there is a downregulation in FAS-related genes. HSD17B8 expression is able to be induced by estradiol through estrogen receptor-α.[285] Interestingly, estrogen-related receptor-α was shown to activate transcription of SHMT2 in response to lapatinib and this conferred resistance.[226]

Leucine-zipper transcription factors

Basic leucine-zipper (bZIP) domains facilitate dimerization of bZIP proteins, bringing their basic N-terminal domains together to produce a contiguous interface that recognizes specific DNA

sequences. Notable bZIP proteins include Nrf1/2, c-Jun, FOS, ATF4, ATF5, XBP1, CREB, and C/EBP.[286] Nrf2 and ATF4 are well-established transcription factors that mediate metabolic processes.[16, 287-288] Oncogenic and tumor-suppressive associations with ATF5 have been established in different cancers.[286] ATF5's role in metabolism is not as well understood, but is known to participate in lipid metabolism and is upregulated in liver cells in response to nutrient deprivation *in vivo.*[289-290] ATF5 was also shown to upregulate asparagine synthetase (*ASNS*) expression.[291] While we observed downregulation of *ATF5* when SHMT2 was knocked down (FC = -2.17), *ASNS* was in the top 25 upregulated genes for OES-Rec (FC = 2.38, Table II-12). We also observed an upregulation of *ATF5* with OES compared to KDS (FC = 2.64). Another bZIP gene *CEBPB*, CCAAT/enhancer binding protein (C/EBP)-β, was also one of the top 25 upregulated genes for OES-Rec (FC = 2.25, Table II-12). Several STRING-identified enriched gene sets for OES-Rec contained *JUN* or *JUND* (Appendix Table II-10, bold faced). These two genes were among the common downregulated genes between OES-Rec and KDS (see above). STRING analysis did not reveal anything that has not already been discussed (Appendix Tables II-10 and II-11), but the appearance of amino acid related pathways as significantly enriched validated our experimental approach.
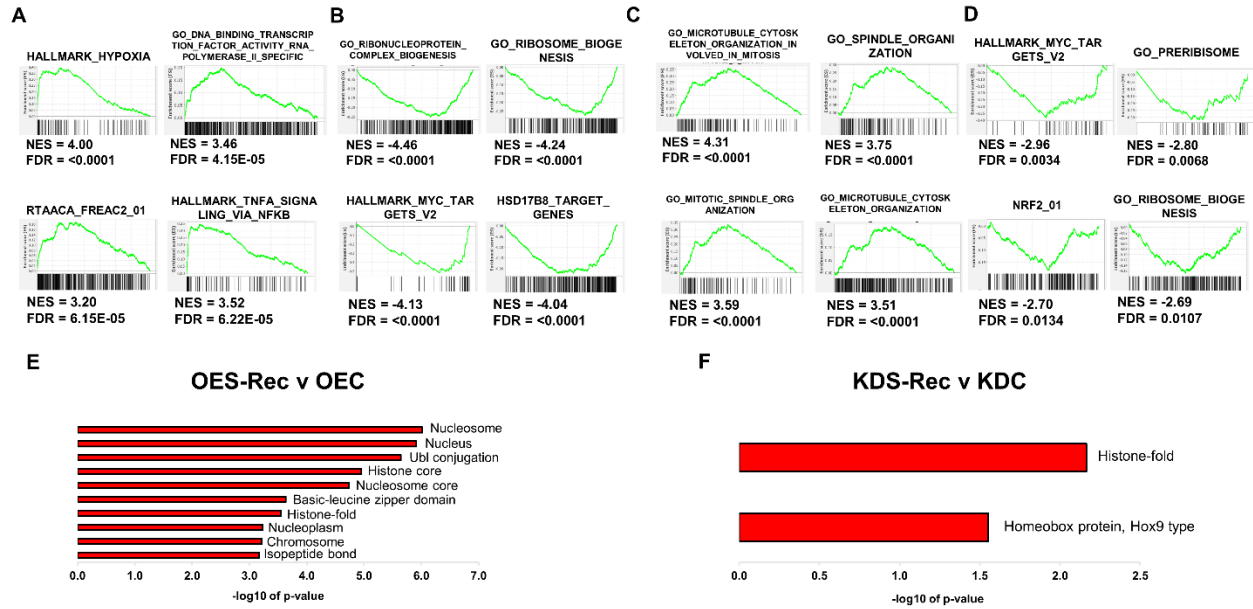
Figure II-7. Enriched gene sets for H1299 OES-Rec and KDS-Rec versus OEC and KDC, respectively. (A) Top four H1299 OES-Rec upregulated GSEA gene sets. (B) Top four H1299 OES-Rec downregulated GSEA gene sets. (C) Top four H1299 KDS-Rec upregulated GSEA gene sets. (D) Top four H1299 KDS-Rec downregulated GSEA gene sets. (E) Significantly enriched gene sets for H1299 OES-Rec using DAVID. (F) Significantly enriched gene sets for H1299 KDS-Rec using DAVID. **Gene set**

enrichment for recovery of knockdown of SHMT2

Cytoskeleton arrangement

The top four upregulated gene sets are all related to the organization of the cytoskeleton during mitosis (Figure II-7C). Folate deficiency was shown to lead to chromosomal instability through several mechanisms and led to deregulation of the spindle assembly checkpoint of mitosis [292]. Folate deficiency also causes uracil misincorporation, and knockdown of SHMT2 has been shown to elicit this effect as well in NSCLC cell lines.[235, 293] It would be interesting to evaluate what effect knockdown of SHMT2 would have on spindle organization and if similar mitotic aberrations would be seen as with general folate deficiency.

The top four downregulated gene sets are familiar to what we have seen previously (Figure II-7D). It is interesting that in both the OES-Rec and KDS-Rec conditions we observe that the HALLMARK_MYC_TARGETS_V2 and GO_RIBOSOME_BIOGENESIS gene sets are downregulated. We currently do not firmly understand why this could be the case. Our RNA-Seq

111

data for SHMT2 KO also showed enrichment of the GO_RIBOSOME_BIOGENESIS gene set. Despite the increase in expression of SHMT2 in KDS-Rec compared to the KDS treatment condition, the level of SHMT2 is still considerably lower than the negative control. NRF2 has been shown to regulate SHMT2 in both NSCLC and glioblastoma cell lines.[9, 287] NRF2-mediated activation of SHMT2 promotes serine flux through the folate cycle,[287] so it makes sense that reduced levels of SHMT2 would correspond with a downregulation of genes related to NRF2.

HOX genes

Only two gene sets were identified as significantly enriched using the DAVID platform (Figure II-7F). The HOX family of genes are extremely important for proper embryonic development and are also dysregulated in cancer. A recent bioinformatics-informed analysis reported on the known and predicted involvement of HOX genes in the hallmarks of cancer as described by Hanahan and Weinberg.[294] The HOX9 cluster is involved in the majority of hallmarks, but one in which there is no prior connection is 'deregulating cellular energetics,' which refers to metabolic reprogramming. In fact there is very little known about HOX genes' roles in regulation of metabolic pathways in cancer.[294] As you might recall, *HOXB9* specifically was upregulated when SHMT2 was overexpressed and downregulated when SHMT2 was knocked down. Additionally, asRNA for HOXC was also upregulated in SHMT2 KO (Appendix Table II-3). Our study is the first to suggest a connection between 1CM and HOX proteins and think HOXB9 deserves special attention.

Conclusions

In summary, we have provided a comprehensive overview of the roles of SHMT2 and MTHFD2 in the context of cancer. In addition to data that is in support of prior literature, we have identified several novel avenues we believe are worth exploring. Our data showed changes in genes

and gene sets related to hypoxia, MYC, mTOR, all of which are well-established 1CM-related pathways. Prior research has connected SHMT2 and MTHFD2 to RNA metabolism, and we built upon that work. We identified similar trends in RNA-related proteins with MTHFD2 KO as Koufaris and Nilsson, but also saw changes in novel genes such as *NOP2*, *NOP16*, and *POLR3K*. Moreover, this is the first report to link MTHFD2 to alternative splicing, with notable changes in expression of *SF3B4*, *PRPF40B*, *HSPA1A*, and *HSPA1B*. Furthermore, we observed enrichment of ncRNA processing with both knockouts of SHMT2 and MTHFD2 which has not previously been connected to these 1CM proteins. Glycosylation was a strong theme in both the RNA-Seq and Bru-Seq for SHMT2 with changes in genes such as *RENBP*, *GALNT5*, *GALNT6*, *GCNT2*, *LGALS8*, *COG8*, *PIGM*, and *SPP1*. In terms of signaling pathways, we saw significant changes in genes related to TGF-β signaling for both KOs (Appendix Table II-6), Wnt signaling for both KOs (*FZD10* and *WNT11,* Table II-2), and TNF-α/NF-kB for SHMT2 OES-Rec (Figure II-7A). Additionally, we observed changes in expression of Ephrin-related genes (e.g. *EFNB2* and *EPHB6*) building on previous work that connected 1CM to Ephrin signaling and differentiation.[61] Moreover, CMAP analysis identified Ephrin inhibitors as positively correlating with knockdown of SHMT2 (Appendix Table II-8). Previous work has illustrated that SHMT2 plays a role in chemosensitivity and resistance to kinase inhibitors,[181, 226] and we identified several novel kinase inhibitors that correlate with SHMT2 expression patterns (Appendix Table II-7 and II-8). Collectively, there is no shortage of data that supports the targeting of SHMT2 and MTHFD2 for cancer therapy and therein lies considerable optimism surrounding current pharmacological agents.

Methods

Cell culture. H226, H460, H1299, and A549 were cultured in RPMI 1640, and the HAP1 cell lines (Horizon Discovery) were cultured in IMDM + 1% Pen-Strep., all were supplemented with 10% FBS (Gibco). For the engineered cell lines, doxycycline was only added in preparation for experiments and then supplemented every 48 h. Cells were grown at 37 °C in a humidified atmosphere of 5% CO_2 and maintained in culture under 30 passages. Cell lines were tested for *Mycoplasma* contamination with the *Mycoplasma* detection kit, PlasmoTest (InvivoGen, San Diego, California).

Doxycycline-inducible shRNA and expression systems. The sequence for shRNA oligonucleotides used in this study are: shSHMT2 (TRCN0000238795): CGGAGAGTTGTGGACTTTATA, and shCtrl (TRCN0000072181): ACAACAGCCACAACGTCTATA. Oligonucleotides were annealed and ligated into pENTR™/H1/TO vector (Invitrogen #K4920-00) following the BLOCK-iT™ Inducible H1 RNAi Entry Vector Kit manual. Resulting shRNA constructs were recombined into pLentipuro/BLOCK-iT-DEST using Gateway® LR Clonase II® (Invitrogen #11791-020). pLentipuro/BLOCK-iT-DEST is a modification of pLenti4/BLOCK-iT-DEST (Invitrogen #K4925-00) wherein the SV40 promoter/zeocin resistance cassette was replaced with the human PGK promoter/puromycin resistance gene and the cPPT/WPRE elements were added, and was kindly provided by Dr. Andrew Aplin (Thomas Jefferson University, Kimmel Cancer Center).[295-296] Inducible GFP and LacZ protein were expression from pLentipuro3/TO/GW/GFP and pLentipuro3/TO/V5-GW/LacZ lentiviral plasmids, which were constructed by Dr. Ethan Abel and was kindly provided by Dr. Diane M. Simeone (University of Michigan, Translational Oncology Program). The SHMT2 cDNA was subcloned from a SHMT2 lentiviral plasmid (Applied Biological Materials Inc. #LV792797) into the pENTR/D-TOPO vector (Invitrogen, #K2400-20) following the

manufacture's manual. Resulting constructs were recombined into pLentipuro3/TO/V5-DEST using Gateway® LR Clonase II® (Invitrogen #11791-020). pLentipuro3/TO/V5-DEST is a modification of pLenti4/TO/V5-DEST (Invitrogen #V498-10) wherein the SV40 promoter/zeocin resistance cassette was replaced with the human PGK promoter/puromycin resistance gene and the cPPT/WPRE elements were added and was kindly provided by Dr. Andrew Aplin. Recombinant lentiviruses were packaged in 293FT cells (Invitrogen #R700-07) by co-transfecting 6×10^6 cells with 4 μg each of lentivirus plasmid (shRNA or cDNA), and packaging plasmids pLP1, pLP2, and pLP/VSV-G (Invitrogen #K4975-00), using 48 μl FuGENE®6 (Promega #E2691, Fitchburg, Wisconsin) as a transfection reagent. Viral supernatants were collected after 72 h of transfection. Indicated cells were transduced with viral supernatant for 72 h, followed by selection with puromycin (5 μg/ml) for at least 2 weeks. The doxycycline induction of knockdown is controlled by the Tet repressor (TetR) protein expressed from the pLenti0.3/EF/GW/IVS-Kozak-TetR-P2A-Bsd vector, which was constructed by Dr. Ethan Abel and was kindly provided by Dr. Diane M. Simeone (University of Michigan, Translational Oncology Program).

Microscopy. Dox-induced GFP expression was monitored using fluorescent microscopy (Olympus Corporation) using a 10x objective. The activity of LacZ-encoded β-galactosidase was measured by the conversion of colorless X-Gal into an insoluble blue product that was visualized under bright-field microscopy. Cells were treated with Dox at the indicated concentrations and time points. Cells were then fixed in 0.1 M phosphate buffer (pH 7.3) supplemented with 5 mM EGTA, 2 mM MgCl2, and 0.2% glutaraldehyde for 15 min, followed by overnight staining with X-Gal solution (#B1690, ThermoFisher Scientific) at 37 ºC.

Doubling time assay. For the engineered cell lines, cells were first pre-treated with doxycycline for 72 h, and during the experiment were supplemented with fresh doxycycline every 48 h. Cells

were seeded at 1,000-5,000 cells/well. At the indicated day, cells were trypsinized and neutralized with 3x volume of trypsin used. Wells were washed with additional volume of media to ensure collection of all cells. After centrifugation, cells were resuspended in DPBS and counted using trypan blue. The experiment was conducted a minimum of three independent times.

Western blotting. Protein concentration of whole-cell lysate was determined by BCA protein assay kit (ThermoFisher). Proteins were resolved in 10% SDS-PAGE gels and electrotransferred to ImmunBlot PVDF membranes (BioRad). After blocking with StartingBlock (ThermoFisher) membranes were probed with primary antibodies. Fluorescent-conjugated secondary antibodies (DyLight 800, ThermoFisher) were incubated with the membranes for 1 h. Protein expression was visualized using an Odyssey CLx imager (LI-COR Biosciences). Antibodies: SHMT2 (GeneTex, GTX125939), MTHFD2 (Abcam, ab56772), SPP1 (Pierce, PA5-34579), actin (Santa Cruz, sc-56499), tubulin (Santa Cruz, sc-101527), GAPDH (Cell Signaling, 2118S).

Colony formation assay. Cells were seeded in 96-well plates at 100 (WT) or 300 (SHMT2 KO and MTHFD2 KO) cells/well and allowed to attach overnight. Compounds were added to the indicated concentrations and incubated with the cells continuously until the vehicle control reached ~90% confluency (~7 days). At the end of treatment, media was removed, and cells were fixed and stained with crystal violet solution (0.05% crystal violet, 2% formaldehyde, 40% methanol) for 30 minutes. Wells were washed with water and allowed to dry overnight before imaging with the Odyssey CLx imager (LI-COR Biosciences).

Bromouridine RNA-sequencing (Bru-seq). Bru-seq was performed as previously described.[204] H1299 engineered cell lines (OES, OEC, KDS, and KDC) were treated with doxycycline (500 ng/mL) every other day for one week. Separate samples of H1299 OES and KDS were allowed to recover from doxycycline treatment for an additional 7 days. After the respective treatments, 2

116

mM Bru was incubated with the cells for 30 min. Collected cells were lysed with TRIzol reagent to isolate RNA. Bru-labeled RNA was captured from total RNA by incubation with anti-BrdU antibodies (BD Biosciences) conjugated to magnetic beads (Dynabeads, goat antimouse IgG; Invitrogen). The Bru-containing RNA population was isolated and sequenced. Sequencing reads were mapped to the GRCh38 reference genome.

Fold changes were calculated for five different comparisons described in the paper (OES v. OEC, OES-Rec v. OEC, KDS v. KDC, KDS-Rec v. KDC, and OES v. KDS) with a single Bru-Seq profile being generated for each treatment without biological replicates. Differential expression fold changes were calculated using DESeq2 with protein coding genes having |fold change| ≥ 1.5, gene size > 300 bp, and mean RPKM > 0.5 considered significant.[297] Gene set enrichment was performed using STRING,[298-301] GSEA v4.0.3 with v7.0 gene sets sourced from MSigDB,[302-303] and over-representation (ORA) gene set enrichment was performed using DAVID v6.8.[304-305] For GSEA, preranked gene lists were generated for each treatment by ranking genes using fold changes generated with DESeq2. GSEA was run using 10,000 permutations, maximum gene set size set to 500, minimum gene set size set to 15, weighted mode on Hallmark, GO all, transcription factor target genes, and KEGG pathways. STRING and DAVID enrichment was performed for significant expressed up and down regulated genes separately using all genes with Entrez identifiers measured in the Bru-Seq annotation. DAVD enrichment was performed on GO, OMIM_DISEASE, COG_ONTOLOGY, UP_KEYWORDS, UP_SEQ_FEATURE, BBID, BIOCARTA, INTERPRO, PIR_SUPERFAMILY, SMART, and KEGG pathway gene sets. For all enrichment analyses gene sets were considered significantly enriched if FDR-adjusted p-values were < 0.05. The data sets were also interrogated with Connectivity Map (CMAP) to identify small

molecules that showed similar transcriptomic profiles, the input were genes with $|FC| > 1.5$.[306-307] Only compounds with scores ≥ 90 or ≤ -90 were considered significant.

RNA-seq. RNA sequencing of HAP1 WT, SHMT2 KO, and MTHFD2 KO (Horizon) were profiled three independent times. Cells were lysed with TRIzol® Reagent (ThermoFisher Scientific) at room temperature. RNA was further purified with DirectZol kit (Zymo Research, Irvine, CA). The RNA libraries were sequenced on the HiSeq 4000 at the University of Michigan DNA Sequencing Core using 50bp single-end sequencing. Reads were mapped to GRCh38 using STAR v2.5.2a and gene quantifications were calculated using Cufflinks v2.2.1 to quantify refGene annotations.[308-309] Three biological replicates were profiled for each KO and control. After PCA and clustering log2 expression values it was determined that one of the MTHFD2 samples was an outlier and should be excluded from differential expression analysis—as a result MTHFD2 KO replicate #2 was excluded from subsequent analysis. Gene read counts calculated using featureCounts v1.5.0 were used to evaluate differential expression using DESeq2 v1.16.1.[297, 310] Protein coding genes were considered significantly differentially expressed with a mean RPKM > 0.5, absolute fold change > 1.5, and FDR adjusted p-value < 0.05.

Gene set enrichment was performed using STRING, GSEA, and DAVID as described above for the Bru-Seq data except for STRING and DAVID an additional filter for gene input was applied (FDR < 0.05). CMAP was used to identify compounds with similar impacts on gene expression. The top/bottom 150 differentially expressed genes were used as input to CMAP and scores for summary cell line are highlighted. Compounds with scores ≥ 90 or ≤ -90 were considered significant.
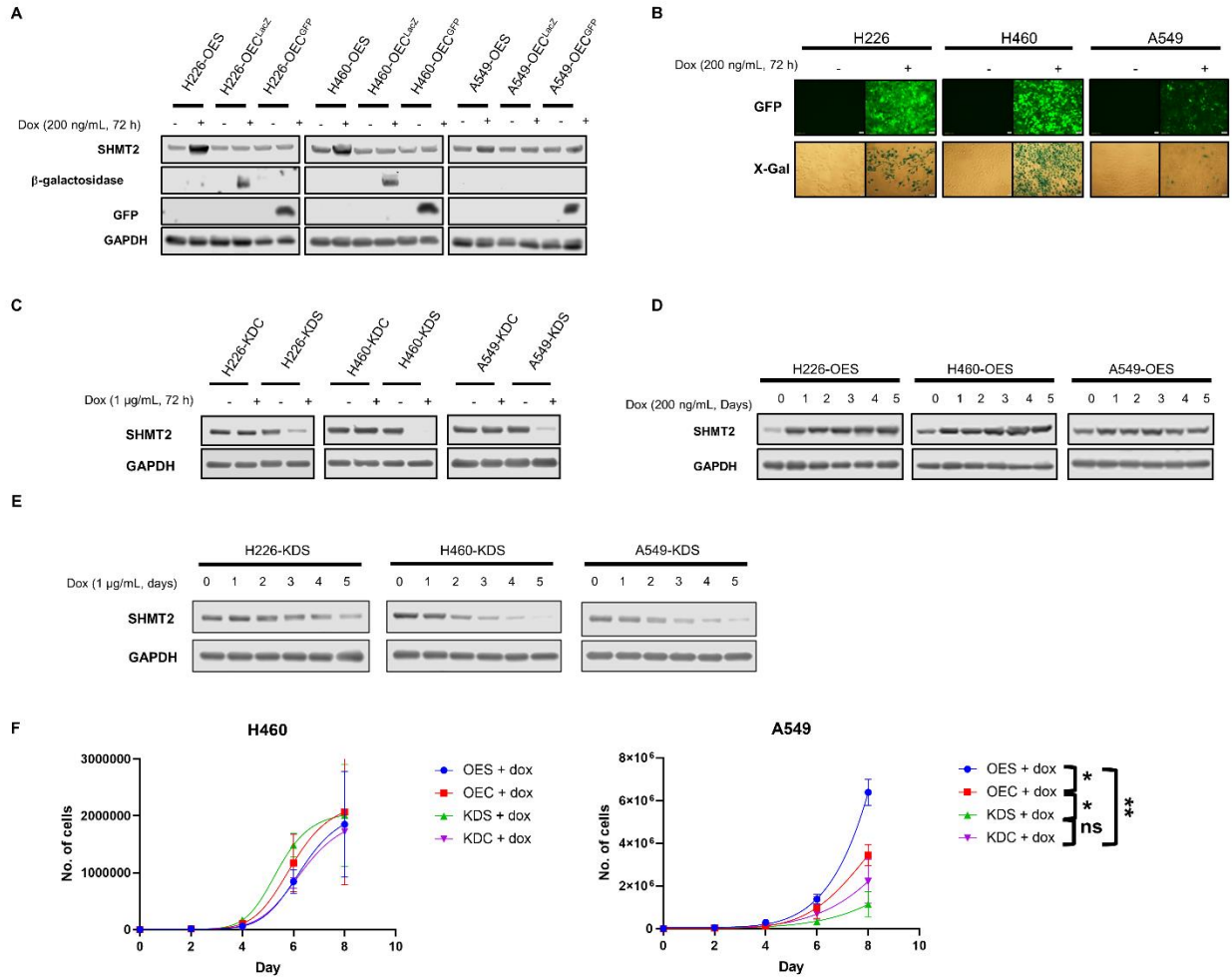
Appendix

Appendix Figure II-1. Generation of H226, H460, and A549 NSCLC cell lines with Dox-inducible overexpression and knockdown of SHMT2. (A) Dox-induced overexpression of SHMT2, LacZ, and GFP. (B) Micrographs of Dox-induced GFP and LacZ expression in control cell lines. Dox-induced GFP expression was monitored using fluorescent microscopy. The activity of LacZ-encoded β-galactosidase was measured by the conversion of colorless X-Gal into an insoluble blue product that was visualized under bright-field microscopy. (C) Dox-induced SHMT2 knockdown. (D) Time-dependent overexpression of SHMT2 with doxycycline treatment. E) Time-dependent knockdown of SHMT2. F) Doubling time of engineered cells; OEC used was LacZ. H460 cell line data is from only two independent experiments. *p < 0.01, **p < 0.001.

119
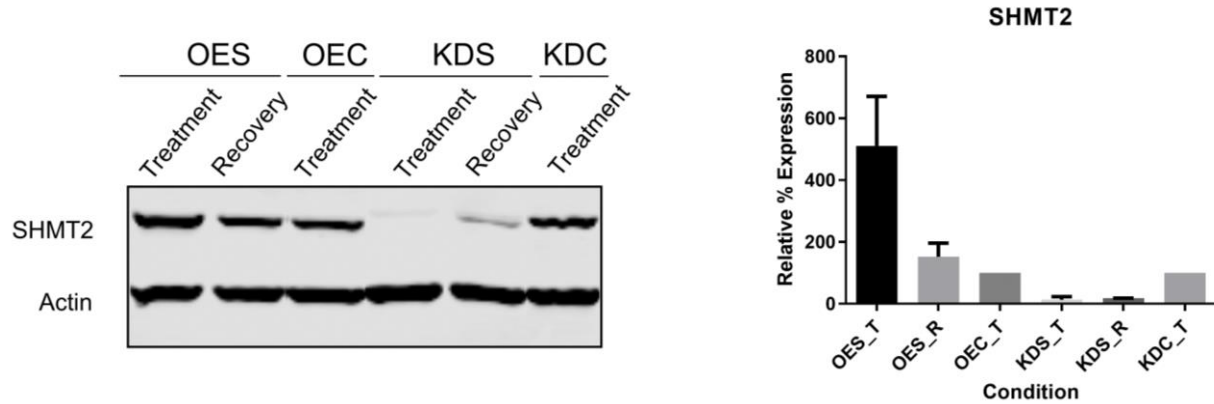
Appendix Figure II-2. Validation of overexpression and knockdown of SHMT2 for Bru-Seq samples.

Appendix Table II-1. SHMT2 KO top 25 differentially expressed protein-coding genes.

Gene[a]	Description	FC	Gene[a]	Description	FC
RHOD	Ras homolog family member D	406.41	SLC7A3	Solute carrier family 7 (cationic amino acid transporter, γ+ system), member 3	-2287.0
SYT1	Synaptotagmin I	20.30	ATAD1	ATPase family, AAA domain containing 1	-2045.4
COL11A1	Collage, type XI, α-1	11.20	PTEN	Phosphatase and tensin homolog	-1010.2
GALNT5	Polypeptide N-acetlygalactosaminyltransferase	9.53	TCEAL8	Transcription elongation factor A (SII)-like 8	-819.43
FBXO17	F-box protein 17	9.44	TCEAL9	WW domain binding protein 5	-807.89
LPAR4	Lysophosphatidic acid receptor 4	8.57	NMI	N-myc (and (STAT) interactor	-748.30
CHMP4C	Charged multivesicular body protein 4C	8.54	LAYN	Layilin	-674.41
GRIA2	Glutamate receptor, ionotropic, AMPA-2	7.66	MFAP2	Microfibrillar-associated protein 2	-671.75
KIF5A	Kinesin family member 5A	7.54	SLC17A9	Solute carrier family 19, member 9	-475.21
ZNF214	Zinc finger protein 214	7.34	FZD10	Frizzled family receptor 10	-409.81
CGREF1	Cell growth regulator with EF-hand domain 1	6.96	IFI16	Interferon, gamma-inducible protein 16	-401.07
SOX1	SRY (sex determining region Y)-box 1	6.18	GABRA5	Gamma-aminobutyric acid (GABA) A receptor, alpha 5	-257.88
GNG11	Guanine nucleotide binding protein, γ-11	6.09	BMP7	Bone morphogenic protein 7	-247.64
TMEM47	Transmembrane protein 47	6.07	AMBN	Ameloblastin (enamel matrix protein)	-232.32
CHL1	Cell adhesion molecule with homology to L1CAM	6.01	EYA4	Eyes absent homolog 4 (Drosophila)	-121.88
SFTA3	Surfactant associated 3	5.84	NUAK2	NUAK family, SNF-like kinase, 2	-97.39

CRYM	Crystallin, μ	5.22	LGALS8	Lectin, galactoside-binding, soluble, 8	-96.84
PIPOX	Pipecolic acid oxidase	5.16	APOBEC3C	Apolipoprotein B mRNA editing enzyme, catalytic polypeptide-like 3C	-96.17
GSAP	Gamma-secretase activating protein	5.04	PRLR	Prolactin receptor	-83.09
NKX2-1	NK2 homeobox 1	4.82	PAPSS2	3'-phosphoadenosine 5'-phosphosulfate synthase 2	-77.30
HMSD	Histocompatibility (minor) serpin domain containing	4.81	FASTKD2	FAST kinase domain 2	-65.66
CSMD1	CUB and Sushi multiple domains 1	4.65	SNX19	Sorting nexin 19	-58.98
ATP8A2	ATPase, aminophospholipid transporter, class I, type 8A, member 2	4.55	SLITRK5	SLIT and NTRK-like family, member 5	-50.52
JAKMIP3	Janus kinase and microtubule interacting protein 3	4.54	HRASLS5	HRAS-like suppressor family, member 5	-49.09
CNR1	Cannabinoid receptor 1	4.27	PTPN3	Protein tyrosine phosphatase, non-receptor type 3	-42.20

[a]Genes with mean RPKM > 0.5 and q-value < 0.05

Appendix Table II-2. MTHFD2 KO differentially expressed protein-coding genes.

Gene[a]	Description	FC	Gene[a]	Description	**FC**
EFS	Embryonal Fyn-associated substrate	30.29	FZD10	Frizzled family receptor 10	-725.4
PRRX1	Paired related homeobox 1	26.26	SLC17A9	Solute carrier family 17, member 9	-438.9
COL5A2	Collagen, type V, alpha 2	18.15	CHMP4C	Charged multivesicular body protein 4C	-216.0
TMEM163	Transmembrane protein 163	15.59	FAM20C	Family with sequence similarity 20, member C	-180.0
CRYAB	Crystallin, alpha B	14.61	BCHE	Butyrylcholinesterase	-166.9
NEUROG2	Neurogenin 2	12.46	FASTKD2	FAST kinase domains 2	-156.0
FABP3	Fatty acid binding protein 3, muscle and heart (mammary-derived growth inhibitor)	12.04	COL11A1	Collagen, type XI, alpha 1	-145.3
TMEM132E	Transmembrane protein 132E	11.92	ALDH1A2	Aldehyde dehydrogenase 1 family, member A2	-94.39
FBXO17	F-box protein 17	11.31	FAM124B	Family with sequence similarity 124B	-88.79
PGM5	Phosphoglucomutase 5	11.24	LGSN	Lengsin, lens protein with glutamine synthetase domain	-80.33
APOE	Apolipoprotein E	10.58	IFI16	Interferon, gamma-inducible protein 16	-79.40
VCAM1	Vascular cell adhesion molecule 1	10.07	CGREF1	Cell growth regulator with EF-hand domain 1	-73.02
HRASLS5	HRAS-like suppressor family, member 5	8.53	TAL1	T-cell acute lymphocytic leukemia 1	-72.54
CADPS	Ca^{2+}- dependent secretion activator	8.44	IAH1	Isoamyl acetate-hydrolyzing esterase 1 homolog (S. cerevisiae)	-53.05

RELN	Reelin	8.06	ABCB1	ATP-binding cassette, subfamily B (MDR/TAP), member 1	-33.29
EPHX2	Epoxide hydrolase 2	7.57	BMP7	Bone morphogenic protein 7	-30.27
MLF1	Myeloid leukemia factor 1	7.36	AMBN	Ameloblastin (enamel matrix protein)	-28.81
KCND3	Potassium voltage-gated channel, Shal-related subfamily, member 3	7.31	TCEAL9	WW domain binding protein 5	-28.46
HIST4H4	Histone cluster, H4	7.14	HOXC9	Homeobox C9	-26.45
FAM189A2	Family with sequence similarity 189, member A2	6.99	TCEAL8	Transcription elongation factor A (SII)-like 8	-22.25
RENBP	Renin binding protein	6.90	SCGB3A2	Secretoglobin, family 3A, member 2	-19.47
THBS1	Thrombospondin 1	6.85	NPNT	Nephronectin	-17.66
OLIG1	Oligodendrocyte transcription factor 1	6.51	SFRP1	Secreted frizzled-related protein 1	-16.61
C9orf135	Chromosome 9 open reading frame 135	6.21	SLITRK3	SLIT and NTRK-like family, member 3	-15.36
ALDH3B1	Aldehyde dehydrogenase family 3, member B1 (ALDH7)	6.20	CD44	CD44 molecule; receptor for hyaluronic acid	-13.49

[a]Genes with mean RPKM > 0.5 and q-value < 0.05

Appendix Table II-3. SHMT2 KO top 25 differentially expressed non-protein-coding genes.

Gene[a]	Description	FC	Gene[a]	Description	FC
HOXC-AS3	HOXC Cluster Antisense RNA 3	25.39	FZD10-AS1	Frizzled Class Receptor 10 - Antisense RNA 1	-935.5
LINC00649	Long Intergenic Non-Protein Coding RNA 649	3.20	LINC01551	Long Intergenic Non-Protein Coding RNA 1551	-74.13
CAHM	Colon Adenocarcinoma Hypermethylated	2.93	ESRG	Embryonic Stem Cell Related	-10.99
LINC00365	Long Intergenic Non-Protein Coding RNA 365	2.46	LINC01018	Long Intergenic Non-Protein Coding RNA 1018	-5.38
HCG27	HLA Complex Group 27	2.46	LINC00632	Long Intergenic Non-Protein Coding RNA 632	-3.10
MSL3P1	Male-Specific Lethal 3 Homolog Pseudogene 1	2.34	MIR4435-2HG	MIR4435-2 Host Gene	-2.84
TOB1-AS1	Transducer of ERBB2, 1 - Antisense RNA 1	2.29	RHOXF1P1	Rhox Homeobox Family Member 1 Pseudogene 1	-2.62
PYY2	Peptide YY 2 (Pseudogene)	2.29	SNORD83A	Small Nucleolar RNA, C/D Box 83A	-2.00
SDAD1P1	SDA1 Domain Containing 1 Pseudogene 1	2.20	NR2F1-AS1	Nuclear Receptor Subfamily 2 Group F Member 1 - Antisense RNA 1	-1.90
CBR3-AS1	Carbonyl reductase 3 - Antisense RNA 1	2.10	LINC02449	Long Intergenic Non-Protein Coding RNA 2449	-1.88
PKN2-AS1	Protein Kinase N2 - Antisense RNA 1	2.02	SNORA52	Small Nucleolar RNA, H/ACA Box 52	-1.83
PRSS30P	Serine Protease 30, Pseudogene	1.98	SNORA33	Small Nucleolar RNA, H/ACA Box 33	-1.78

DICER1-AS1	Dicer 1, Ribonuclease III - Antisense RNA 1	1.92	LINC01788	Long Intergenic Non-Protein Coding RNA 1788	-1.62
MHENCR	Melanoma Highly Expressed Competing Endogenous LncRNA For MiR-425 And MiR-489	1.90	TPM3P9	Tropomyosin 3 Pseudogene 9	-1.55
MAGI2-AS3	Membrane Associated Guanylate Kinase, WW And PDZ Domain Containing 2 - Antisense RNA 3	1.85	MIR22HG	MIR22 Host Gene	-1.52
BOLA3-AS1	BolA Family Member 3 - Antisense RNA 1	1.83	SCARNA12	Small Cajal Body-Specific RNA 12	-1.51
PAXIP1-AS2	PAX Interacting Protein 1 - Antisense RNA 2	1.82			
TUNAR	TCL1 Upstream Neural Differentiation-Associated RNA	1.79			
OSER1-AS1	Oxidative Stress Responsive Serine Rich 1 - Antisense RNA 1	1.77			
LINC01011	Long Intergenic Non-Protein Coding RNA 1011	1.73			
DDX11-AS1	DEAD/H-Box Helicase 11 - Antisense RNA 1	1.73			
C1orf220	Chromosome 1 open reading frame 220	1.71			
CEBPA-AS1	CCAAT Enhancer Binding Protein Alpha - Antisense RNA 1	1.71			
ARRDC3-AS1	Arrestin Domain Containing 3 - Antisense RNA 1	1.63			
ATP1A1-AS1	ATPase Na+/K+ Transporting Subunit Alpha 1 - Antisense RNA 1	1.63			

[a]Genes with mean RPKM > 0.5, |FC| > 1.5, and q-value < 0.05

Appendix Table II-4. Expression changes in MTHFD2 interaction partners identified by Koufaris and Nilsson.[10]

Gene	Description	Fold Change	q-value
HSPA8	Heat shock cognate 71 kDa protein	-1.58	3.56E-05
HSPA9	Stress-70 protein, mitochondrial	-1.23	0.0192
HSPB1	Heat shock protein β-1	ND[a]	NA[b]
HSPD1	60 kDa heat shock protein	-1.27	0.0191
NPMI	Nucleophosmin	-1.27	2.09E-04
HIST1H3A	Histone cluster 1 H3 family member A	ND	NA
HIST2H3A	Histone cluster 2 H3 family member A	ND	NA
HIST3H3	H3 Histone Family, Member T	ND	NA
H3F3A	H3 Histone, Family 3A	ND	NA
XRCC6	X-ray repair cross-complementing protein 6	-1.26	0.0178
RPA1	Replication protein A 70 kDa DNA-binding subunit	ND	NA

HNRNPK	Heterogeneous nuclear ribonucleoprotein K		-1.20	0.0233
HNRNPM	Heterogeneous nuclear ribonucleoprotein M		-1.44	0.00159
SYNCRIP	Heterogeneous nuclear ribonucleoprotein Q		-1.33	1.33E-06
HNRNPR	Heterogeneous nuclear ribonucleoprotein R		ND	NA
HNRNPU	Heterogeneous nuclear ribonucleoprotein U		-1.32	4.51E-04
SF3B3	Splicing factor 3B subunit 3		ND	NA
LRPPRC	Leucine-rich PPR motif-containing protein, mitochondrial		ND	NA
ILF2	Interleukin enhancer-binding factor 2		-1.39	8.46E-06
NUFIP2	Nuclear fragile X mental retardation-interacting protein 2		-1.17	0.00276
DDX3X	ATP-dependent RNA helicase DDX3X		ND	NA
RPL18	60S ribosomal protein L18a		ND	NA
RPS13	40S ribosomal protein S13		ND	NA
RPS3A	40S ribosomal protein S3a		ND	NA
RPS5	40S ribosomal protein S5		ND	NA
RPS8	40S ribosomal protein S8		ND	NA
ENO1	Alpha-enolase		-1.41	9.55E-07
EZR	Ezrin		-1.18	0.0499
RPN1	Dolichyl-diphosphooligosaccharide--protein glycosyltransferase subunit 1		-1.27	0.00865

[a]ND, not detected
[b]NA, not applicable

Appendix Table II-5. MTHFD2 KO bidirectional STRING-identified gene sets.

Gene set	Size	FDR
KEGG_Neuroactive ligand-receptor interaction	23	0.00033
cell adhesion	166	0.00084
biological adhesion	168	0.0012
outflow tract morphogenesis	21	0.0016
nervous system process	183	0.0018
KEGG_Cytokine-cytokine receptor interaction	33	0.0019
regulation of inflammatory response	57	0.0036
G protein-coupled receptor signaling pathway	125	0.0039
positive regulation of hemopoiesis	48	0.0053
positive regulation of leukocyte differentiation	34	0.0055
blood circulation	77	0.0059
renal system development	96	0.0076
heart morphogenesis	69	0.0098
kidney development	94	0.0111
negative regulation of cell motility	66	0.0113
negative regulation of cellular component movement	70	0.0117
negative regulation of cell migration	63	0.0137
regulation of cell migration	196	0.0145
trans-synaptic signaling	83	0.0168
sensory perception	96	0.0173
urogenital system development	109	0.0184
KEGG_ECM-receptor interaction	28	0.0185

circulatory system process			81	0.019
regulation of myeloid leukocyte differentiation			25	0.0213
behavior			145	0.0224
cardiac chamber development			53	0.0224
chemical synaptic transmission			81	0.0224
cardiac chamber morphogenesis			40	0.0227

Appendix Table II-6. Expression changes in TGF-β signaling genes as illustrated by Ahmadi et al.[202] and related isoforms.

Member	Gene	Description	Fold Change	q-value
Ligands	TGFB1	Transforming growth factor beta-1	1.98	5.01E-17
	TGFB2	Transforming growth factor beta-2	2.60	1.46 E-09
	TGFB3	Transforming growth factor beta-3	1.08	0.636
	BMP1	Bone morphogenetic protein 1	1.06	0.511
	BMP2	Bone morphogenetic protein 2	-59.0	3.527E-15
	BMP3	Bone morphogenetic protein 3	23.0	0.001
	BMP4	Bone morphogenetic protein 4	-2.07	2.128E-06
	BMP5	Bone morphogenetic protein 5	ND[a]	NA[b]
	BMP6	Bone morphogenetic protein 6	-1.08	0.877
	BMP7	Bone morphogenetic protein 7	-30.3	2.81E-50
	BMP8A	Bone morphogenetic protein 8A	-3.20	0.582
	BMP8B	Bone morphogenetic protein 8B	-1.07	0.669
	BMP10	Bone morphogenetic protein 10	ND	NA
	BMP15	Bone morphogenetic protein 15	ND	NA
Receptors	TGFBR1	TGF-beta receptor type-1	-1.01	0.912
	TGFBR2	TGF-beta receptor type-2	-1.02	0.937
	TGFBR3	TGF-beta receptor type-3	-1.83	6.28E-09
	BMPR1A	Bone morphogenetic protein receptor type-1A	1.19	0.07
	BMPR1B	Bone morphogenetic protein receptor type-1B	1.26	0.048
	BMPR2	Bone morphogenetic protein receptor type-2	1.15	0.086
Canonical effectors	SMAD1	Mothers against decapentaplegic homolog 1	-1.08	0.257
	SMAD2	Mothers against decapentaplegic homolog 2	1.23	0.0003
	SMAD3	Mothers against decapentaplegic homolog 3	1.18	0.0041
	SMAD4	Mothers against decapentaplegic homolog 4	1.09	0.221
	SMAD5	Mothers against decapentaplegic homolog 5	1.03	0.682
	SMAD6	Mothers against decapentaplegic homolog 6	1.53	0.008
	SMAD7	Mothers against decapentaplegic homolog 7	1.20	0.126
	SMAD8	Mothers against decapentaplegic homolog 8	ND	NA
	SMAD9	Mothers against decapentaplegic homolog 9	1.41	0.0001
Non-canonical effectors[c]	MAP2K3	Dual specificity mitogen-activated protein kinase kinase 3	-1.52	1.04E-09
	MAPK6	Mitogen-activated protein kinase 6	-1.08	0.354
	MAPK7	Mitogen-activated protein kinase 7	1.27	0.005
	MAPK8	Mitogen-activated protein kinase 8	1.24	0.008
	MAPK10	Mitogen-activated protein kinase 10	6.16	4.05E-06
	MAPK11	Mitogen-activated protein kinase 11	1.53	2.04E-05

MAPK14	Mitogen-activated protein kinase 14	1.00	0.910
MAPK15	Mitogen-activated protein kinase 15	2.81	0.018
AKT3	RAC-gamma serine/threonine-protein kinase	1.69	2.01E-07

[a]ND, not detected
[b]NA, not applicable
[c]For MAP2Ks and MAPKs, only select genes are included

Appendix Table II-7. Top 25 compounds in CMAP database showing positive or negative correlations with H1299 OES.

Compound	Description	Score	Compound	Description	Score
imatinib	BCR-ABL kinase inhibitor	99.82	depudecin	HDAC inhibitor	-99.89
BRD-K08502430	Angiogenesis inhibitor	99.75	XAV-939	Tankyrase inhibitor	-99.86
zosuquidar	P-glycoprotein inhibitor	99.72	OM-137	Aurora kinase inhibitor	-99.79
perospirone	Dopamine receptor antagonist	99.72	fluprostenol	Prostanoid receptor agonist	-99.79
benzbromarone	Chloride channel blocker	99.72	XE-991	Potassium channel blocker	-99.79
D-64406	PDGFR receptor inhibitor	99.68	terconazole	Sterol demethylase inhibitor	-99.75
UK-356618	Metalloproteinase inhibitor	99.65	ruxolitinib	JAK inhibitor	-99.74
vemurafenib	RAF inhibitor	99.54	ZM-306416	ABL inhibitor	-99.72
BRD-K09991945	PKC inhibitor	99.51	piperine	Monoamine oxidase inhibitor	-99.68
SB-415286	Glycogen synthase kinase inhibitor	99.47	clonidine	Adrenergic receptor agonist	-99.68
phenprobamate	Muscle relaxant	99.40	forskolin	Adenylyl cyclase activator	-99.65
penitrem-a	Potassium channel blocker	99.40	purvalanol-b	Tyrosine kinase inhibitor	-99.65
lenalidomide	Antineoplastic	99.37	BRD-K72541103	JAK inhibitor	-99.61
BRD-K04923131	Glycogen synthase kinase inhibitor	99.33	osthol	Calcium channel blocker	-99.61
indirubin	CDK inhibitor	99.30	estradiol-cypionate	Estrogen receptor agonist	-99.61
pentobarbital	Barbiturate antiepileptic	99.22	EMF-bca1-57	caspase inhibitor	-99.58
gliquidone	Sulfonylurea	99.22	BRD-K29313308	HDAC inhibitor	-99.50
ABT-737	BCL inhibitor	99.19	mecillinam	Bacterial cell wall synthesis inhibitor	-99.37
kinetin-riboside	Apoptosis stimulant	99.19	bemegride	Chemoreceptor agonist	-99.33
GANT-58	GLI antagonist	99.15	VX-702	p38 MAPK inhibitor	-99.30
PD-173074	FGFR inhibitor	99.12	estrone	Estrogen receptor agonist	-99.22
SB-216763	Glycogen synthase kinase inhibitor	99.12	dantrolene	Calcium channel blocker	-99.21
U-0124	MEK inhibitor	99.12	cilostazol	Phosphodiesterase inhibitor	-99.19
vindesine	Tubulin inhibitor	99.08	BMS-191011	Potassium channel activator	-99.17
buphenine	Adrenergic receptor agonist	98.98	dibenzoylmethane	Antineoplastic	-99.15

Gene input: >|1.5|-fold change compared to OEC[LacZ]

Appendix Table II-8. Top 25 compounds in CMAP database showing positive or negative correlations with H1299 KDS.

Compound	Description	Score	Compound	Description	Score
QS-11	ARFGAP inhibitor	99.51	bisindolylmaleimide	CDK inhibitor, PKC inhibitor, leucine rich repeat kinase inhibitor	-98.38
tubastatin-a	HDAC inhibitor	99.44	TG-101348	JAK inhibitor, FLT3 inhibitor, RET tyrosine kinase inhibitor	-98.38
droxinostat	HDAC inhibitor	98.91	XMD-885	leucine rich repeat kinase inhibitor, MAP kinase inhibitor	-97.15
pyroxamide	HDAC inhibitor, cell cycle inhibitor	98.84	maprotiline	norepinephrine reputake inhibitor, tricyclic antidepressant (TCA)	-96.12
BRD-A16820783	phosphodiesterase inhibitor	98.77	cediranib	VEGFR inhibitor, KIT inhibitor, angiogenesis inhibitor, VEGFR antagonist	-95.77
Merck60	HDAC inhibitor	98.56	BI-2536	PLK inhibitor, apoptosis stimulant, cell cycle inhibitor, protein kinase inhibitor	-95.07
HU-211	glutamate receptor antagonist, apoptosis stimulant, NFkB pathway inhibitor, reducing agent	98.28	tozasertib	Aurora kinase inhibitor, Bcr-Abl kinase inhibitor, FLT3 inhibitor, JAK inhibitor, Abl kinase inhibitor, mitotic inhibitor	-94.54
SA-63133	casein kinase inhibitor, tubulin inhibitor	98.17	enzastaurin	PKC inhibitor, AKT inhibitor, angiogenesis inhibitor, apoptosis stimulant, PI3K inhibitor	-94.02
purmorphamine	smoothened receptor agonist	97.94	fluphenazine	dopamine receptor antagonist, acetylcholine receptor ligand, dopamine receptor, histamine receptor antagonist, serotonin receptor antagonist	-93.15
entinostat	HDAC inhibitor, cell cycle inhibitor	97.9	dilazep	adenosine reuptake inhibitor, calcium channel antagonist, platelet aggregation inhibitor	-93.11
PP-30	RAF inhibitor	97.84	BIBX-1382	EGFR inhibitor, tyrosine kinase inhibitor	-93.09
ON-01910	PLK inhibitor, cell cycle inhibitor, MCL1	97.39	sunitinib	FLT3 inhibitor, KIT inhibitor, PDGFR tyrosine kinase	-92.38

	inhibitor, protein kinase inhibitor	
rucaparib	PARP inhibitor	97.36
phorbol-12-myristate-13-acetate	PKC activator, CD antagonist	97.32
motesanib	KIT inhibitor, PDGFR tyrosine kinase receptor inhibitor, VEGFR inhibitor, angiogenesis inhibitor, RET tyrosine kinase inhibitor, vascular endothelial growth factor receptor (VEGFR) inhibitor, VEGFR antagonist	97.04
depudecin	HDAC inhibitor	96.84
WT-171	HDAC inhibitor	96.58
ALW-II-38-3	ephrin inhibitor	96.34
tacedinaline	HDAC inhibitor, cell cycle inhibitor	96.29
VU-0365114-2	acetylcholine receptor allosteric modulator, M5 modulator	95.92
epothilone-a	microtubule stabilizing agent	95.88

	receptor inhibitor, RET tyrosine kinase inhibitor, VEGFR inhibitor, angiogenesis inhibitor, colony stimulating factor receptor antagonist, colony stimulating factor receptor inhibitor, platelet-derived growth factor receptor (PDGFR) inhibitor, vascular endothelial growth factor receptor (VEGFR) inhibitor, vascular endothelial growth factor receptor 1 (VEGFR1) inhibitor, vascular endothelial growth factor receptor 2 (VEGFR2) inhibitor, VEGFR antagonist	
tamoxifen	estrogen receptor antagonist, selective estrogen receptor modulator (SERM), estrogen receptor agonist, estrogen receptor modulator, PKC inhibitor	-91.42

ALW-II-49-7	ephrin inhibitor	95.88
ingenol	PKC activator	95.84
APHA-compound-8	HDAC inhibitor	95.84
BRD-K29313308	HDAC inhibitor	95.80

Gene input: >|1.5|-fold change compared to KDC

Appendix Table II-9. Compounds in CMAP database showing positive or negative correlations with MTHFD2 KO.

Compound	Description	Score[a]
BI-2536	PLK inhibitor, apoptosis stimulant, cell cycle inhibitor, protein kinase inhibitor	97.65
apicidin	HDAC inhibitor	97.32
XMD-892	MAP kinase inhibitor, BMK inhibitor, leucine rich repeat kinase inhibitor	96.55
XMD-885	leucine rich repeat kinase inhibitor, MAP kinase inhibitor	96.43
KU-0060648	DNA dependent protein kinase, DNA dependent protein kinase inhibitor, PI3K inhibitor	94.89
panobinostat	HDAC inhibitor, apoptosis stimulant, cell cycle inhibitor	94.72
ISOX	HDAC inhibitor	94.53
TG-101348	JAK inhibitor, FLT3 inhibitor, RET tyrosine kinase inhibitor	94.47
XMD-1150	leucine rich repeat kinase inhibitor	94.33
NU-7441	DNA dependent protein kinase, DNA dependent protein kinase inhibitor, P glycoprotein inhibitor	93.83
JWE-035	Aurora kinase inhibitor	93.70
U-0126	MEK inhibitor, JAK inhibitor, MAP kinase inhibitor	92.88
trichostatin-a	HDAC inhibitor, CDK expression enhancer, ID1 expression inhibitor	92.30
MEK1-2-inhibitor	MEK inhibitor	91.94
emetine	protein synthesis inhibitor	91.10
WYE-354	mTOR inhibitor	90.71
homoharringtonine	apoptosis stimulant, protein synthesis inhibitor	90.59
PI-828	PI3K inhibitor	90.30
kinetin-riboside	apoptosis inducer	-90.03

[a]Scores ≥ 90 or ≤ -90

Appendix Table II-10. H1299 OES-Rec STRING KEGG gene sets compared to OEC[LacZ].

Gene set	FDR	Genes
MicroRNAs in cancer	0.0070	CCNE2, CDKN1B, DDIT4, MARCKS, MYC, PDCD4, PIM1, SPRY2, VEGFA
Biosynthesis of amino acids	0.0077	CTH, GOT1, IDH1, PHGDH, PSAT1, SHMT2
p53 signaling pathway	0.0077	CCNE2, CCNG2, GADD45A, IGFBP3, SESN2, TNFRSF10B
Systemic lupus erythematosus	0.0077	H2AFJ, HIST1H2AB, HIST1H2AL, HIST1H2BE, HIST1H2BK, HIST1H2BL, HIST2H2BE
Transcriptional misregulation in cancer	0.0184	CDKN1B, CEBPB, DDIT3, DUSP6, GADD45A, IGFBP3, MYC, WNT16
Glycine, serine and threonine metabolism	0.0253	CTH, PHGDH, PSAT1, SHMT2
MAPK signaling pathway	0.0253	DDIT3, DUSP5, DUSP6, GADD45A, HSPA8, **JUN**, **JUND**, MYC, RAPGEF2, VEGFA
Alcoholism	0.0253	H2AFJ, HIST1H2AB, HIST1H2AL, HIST1H2BE, HIST1H2BK, HIST1H2BL, HIST2H2BE
Viral carcinogenesis	0.0253	CCNE2, CDKN1B, CDKN2B, HIST1H2BE, HIST1H2BK, HIST1H2BL, HIST2H2BE, **JUN**

Gastric cancer	0.0253	CCNE2, CDKN1B, CDKN2B, GADD45A, MYC, WNT16, WNT5B
Aminoacyl-tRNA biosynthesis	0.0255	AARS, EPRS, GARS, WARS
ErbB signaling pathway	0.0336	CAMK2D, CDKN1B, EIF4EBP1, **JUN**, MYC
Small cell lung cancer	0.0474	CCNE2, CDKN1B, CDKN2B, GADD45A, MYC

Appendix Table II-11. H1299 OES-Rec STRING biological processes gene sets compared to OEC^{LacZ}.

Gene set	FDR
regulation of biosynthetic process	6.55E-07
negative regulation of metabolic process	7.88E-07
regulation of cellular biosynthetic process	7.88E-07
negative regulation of cellular metabolic process	7.96E-07
negative regulation of macromolecule metabolic process	9.42E-07
regulation of gene expression	1.05E-06
regulation of metabolic process	1.05E-06
negative regulation of nitrogen compound metabolic process	1.05E-06
regulation of primary metabolic process	1.05E-06
cellular response to external stimulus	1.97E-06
response to endoplasmic reticulum stress	2.59E-06
negative regulation of biosynthetic process	2.81E-06
regulation of macromolecule metabolic process	3.39E-06
regulation of cellular metabolic process	3.46E-06
regulation of nitrogen compound metabolic process	3.46E-06
negative regulation of cellular biosynthetic process	4.33E-06
regulation of macromolecule biosynthetic process	1.12E-05
negative regulation of gene expression	1.12E-05
cellular response to nutrient levels	1.12E-05
regulation of cellular macromolecule biosynthetic process	1.12E-05
negative regulation of cellular protein metabolic process	1.24E-05
negative regulation of protein metabolic process	1.28E-05
negative regulation of biological process	1.96E-05
response to stress	3.83E-05
cellular response to starvation	4.45E-05

Notes

The authors would like to thank Michelle Paulsen for running the Bru-seq experiments and for other members of the Ljungman lab for helpful discussions and mapping of the sequencing results, especially Dr. Brian Magnuson and Karan Bedi. We would also like to thank Dr. Ethan Abel and Dr. Diane Simeone (University of Michigan, Translational Oncology Program) and Dr. Andrew Aplin (Thomas Jefferson University, Kimmel Cancer Center) for constructing and kindly providing plasmids instrumental in developing the SHMT2-inducuble cell lines. We would also like to thank Dr. Shuai Hu for critical reading of the manuscript.

Data from Bru-sequencing of the H1299 cell line is only from one biological replicate, so care should be taken when drawing conclusions and the results should be validated experimentally. For Bru-seq, a significantly differentially expressed gene was defined as having an absolute fold change greater than 1.5-fold and mean RPKM > 0.5, but this experiment should be repeated to obtain p-values to determine true significance.

References

1.   Majem, B.; Nadal, E.; Munoz-Pinedo, C., Exploiting metabolic vulnerabilities of non small cell lung carcinoma. *Semin Cell Dev Biol.* **2020,** *98*, 54-62.

2.   Kantarjian, H., Acute myeloid leukemia--major progress over four decades and glimpses into the future. *Am J Hematol.* **2016,** *91* (1), 131-145.

3.   Farber, S.; Diamond, L. K.; Mercer, R. D.; Sylvester Jr, R. F.; Wolff, J. A., Temporary remissions in acute leukemia in children produced by folic acid antagonist, 4-aminopteroyl-glutamic acid (aminopterin). *N Engl J Med.* **1948,** *238*, 787-793.

4.   Stuani, L.; Sabatier, M.; Sarry, J. E., Exploiting metabolic vulnerabilities for personalized therapy in acute myeloid leukemia. *BMC Biol.* **2019,** *17* (1), 57.

5.   Ducker, G. S.; Chen, L.; Morscher, R. J.; Ghergurovich, J. M.; Esposito, M.; Teng, X.; Kang, Y.; Rabinowitz, J. D., Reversal of cytosolic one-carbon flux compensates for loss of the mitochondrial folate pathway. *Cell Metab.* **2016,** *23* (6), 1140-1153.

6.   Li, A. M.; Ducker, G. S.; Li, Y.; Seoane, J. A.; Xiao, Y.; Melemenidis, S.; Zhou, Y.; Liu, L.; Vanharanta, S.; Graves, E. E.; Rankin, E. B.; Curtis, C.; Massague, J.; Rabinowitz, J. D.; Thompson, C. B.; Ye, J., Metabolic profiling reveals a dependency of human metastatic breast cancer on mitochondrial serine and one-carbon unit metabolism. *Mol Cancer Res.* **2020,** *18* (4), 599-611.

7.   Tong, J.; Krieger, J. R.; Taylor, P.; Bagshaw, R.; Kang, J.; Jeedigunta, S.; Wybenga-Groot, L. E.; Zhang, W.; Badr, H.; Mirhadi, S.; Pham, N. A.; Coyaud, E.; Yu, M.; Li, M.; Cabanero, M.; Raught, B.; Maynes, J. T.; Hawkins, C.; Tsao, M. S.; Moran, M. F., Cancer proteome and metabolite changes linked to SHMT2. *PLoS One.* **2020,** *15* (9), e0237981.

8.   Ye, J.; Fan, J.; Venneti, S.; Wan, Y. W.; Pawel, B. R.; Zhang, J.; Finley, L. W.; Lu, C.; Lindsten, T.; Cross, J. R.; Qing, G.; Liu, Z.; Simon, M. C.; Rabinowitz, J. D.; Thompson, C. B., Serine catabolism regulates mitochondrial redox control during hypoxia. *Cancer Discov.* **2014,** *4* (12), 1406-1417.

9.   Engel, A. L.; Lorenz, N. I.; Klann, K.; Munch, C.; Depner, C.; Steinbach, J. P.; Ronellenfitsch, M. W.; Luger, A. L., Serine-dependent redox homeostasis regulates glioblastoma cell survival. *Br J Cancer.* **2020,** *122* (9), 1391-1398.

10.   Koufaris, C.; Nilsson, R., Protein interaction and functional data indicate MTHFD2 involvement in RNA processing and translation. *Cancer Metab.* **2018,** *6*, 12.

11.   Gustafsson Sheppard, N.; Jarl, L.; Mahadessian, D.; Strittmatter, L.; Schmidt, A.; Madhusudan, N.; Tegner, J.; Lundberg, E. K.; Asplund, A.; Jain, M.; Nilsson, R., The folate-coupled enzyme MTHFD2 is a nuclear protein and promotes cell proliferation. *Sci Rep.* **2015,** *5*, 15029.

12.   Li, L.; Wei, Y.; To, C.; Zhu, C. Q.; Tong, J.; Pham, N. A.; Taylor, P.; Ignatchenko, V.; Ignatchenko, A.; Zhang, W.; Wang, D.; Yanagawa, N.; Li, M.; Pintilie, M.; Liu, G.; Muthuswamy, L.; Shepherd, F. A.; Tsao, M. S.; Kislinger, T.; Moran, M. F., Integrated omic analysis of lung cancer reveals metabolism proteome signatures with prognostic impact. *Nat Commun.* **2014,** *5*, 5469.

13.   Wang, Z.; Liu, P.; Inuzuka, H.; Wei, W., Roles of F-box proteins in cancer. *Nat Rev Cancer.* **2014,** *14* (4), 233-247.

14.   Glenn, K. A.; Nelson, R. F.; Wen, H. M.; Mallinger, A. J.; Paulson, H. L., Diversity in tissue expression, substrate binding, and SCF complex formation for a lectin family of ubiquitin ligases. *J Biol Chem.* **2008,** *283* (19), 12717-12729.

15.   Suber, T. L.; Nikolli, I.; O'Brien, M. E.; Londino, J.; Zhao, J.; Chen, K.; Mallampalli, R. K.; Zhao, Y., FBXO17 promotes cell proliferation through activation of Akt in lung adenocarcinoma cells. *Respir Res.* **2018,** *19* (1), 206.

16.   Ben-Sahra, I.; Hoxhaj, G.; Ricoult, S. J. H.; Asara, J. M.; Manning, B. D., mTORC1 induces purine synthesis through control of the mitochondrial tetrahydrofolate cycle. *Science.* **2016,** *351* (6274), 728-733.

17.   Selvarajah, B.; Azuelos, I.; Platé, M.; Guillotin, D.; Forty, E. J.; Contento, G.; Woodcock, H. V.; Redding, M.; Taylor, A.; Brunori, G.; Durrenberger, P. F.; Ronzoni, R.; Blanchard, A. D.; Mercer, P. F.; Anastasiou, D.; Chambers, R. C., mTORC1 amplifies the ATF-dependent de novo serine-glycine pathway to supply glycine during TGF-β-induced collagen biosynthesis. *Sci Signal.* **2019,** *12*, eaav3048.

18.   Zeng, J. D.; Wu, W. K. K.; Wang, H. Y.; Li, X. X., Serine and one-carbon metabolism, a bridge that links mTOR signaling and DNA methylation in cancer. *Pharmacol Res.* **2019,** *149*, 104352.

19.   Hellmann, G. M.; Fields, W. R.; Doolittle, D. J., Gene expression profiling of cultured human bronchial epithelial and lung carcinoma cells. *Toxicol. Sci.* **2001,** *61*, 154-163.

20.   Takahashi, S.; Ohsawa, T.; Miura, R.; Miyake, Y., Purification of high molecular weight (HMW) renin from porcine kidney and direct evidence that the HMW renin is a complex of renin with renin binding protein (RnBP). *J Biochem.* **1983,** *93*, 265-274.

21.   Takahashi, S.; Takahashi, K.; Kaneko, T.; Ogasawara, H.; Shindo, S.; Kobayashi, M., Human renin-binding protein is the enzyme N-acetyl-D-glucosamine 2-epimerase. *J Biochem.* **1999,** *125*, 348-353.

22.   Di Pietro, E.; Sirois, J.; Tremblay, M. L.; MacKenzie, R. E., Mitochondrial NAD-dependent methylenetetrahydrofolate dehydrogenase-methenyltetrahydrofolate cyclohydrolase is essential for embryonic development. *Mol Cell Biol.* **2002,** *22* (12), 4158-4166.

23. Tani, H.; Ohnishi, S.; Shitara, H.; Mito, T.; Yamaguchi, M.; Yonekawa, H.; Hashizume, O.; Ishikawa, K.; Nakada, K.; Hayashi, J. I., Mice deficient in the Shmt2 gene have mitochondrial respiration defects and are embryonic lethal. *Sci Rep.* **2018,** *8* (1), 425.

24. Tani, H.; Mito, T.; Velagapudi, V.; Ishikawa, K.; Umehara, M.; Nakada, K.; Suomalainen, A.; Hayashi, J. I., Disruption of the mouse Shmt2 gene confers embryonic anaemia via foetal liver-specific metabolomic disorders. *Sci Rep.* **2019,** *9* (1), 16054.

25. Sakai, R.; Henderson, J. T.; O'Bryan, J. P.; Elia, A. J.; Saxton, T. M.; Pawson, T., The mammalian ShcB and ShcC phosphotyrosine docking proteins function in the maturation of sensory and sympathetic neurons. *Neuron.* **2000,** *28*, 819-833.

26. Ahmed, S. B. M.; Prigent, S. A., Insights into the Shc family of adaptor proteins. *J Mol Signal.* **2017,** *12* (2), 1-17.

27. Moreno, E.; Cavic, M.; Krivokuca, A.; Casado, V.; Canela, E., The endocannabinoid system as a target in cancer diseases: are we there yet? *Front Pharmacol.* **2019,** *10*, 339.

28. Argaw, A.; Duff, G.; Zabouri, N.; Cecyre, B.; Chaine, N.; Cherif, H.; Tea, N.; Lutz, B.; Ptito, M.; Bouchard, J. F., Concerted action of CB1 cannabinoid receptor and deleted in colorectal cancer in axon guidance. *J Neurosci.* **2011,** *31* (4), 1489-1499.

29. Berghuis, P.; Rajnicek, A. M.; Morozov, Y. M.; Ross, R. A.; Mulder, J.; Urbán, G. M.; Monoroy, K.; Marsicano, G.; Matteoli, M.; Canty, A.; Irving, A. J.; Katona, I.; Yanagawa, Y.; Rakic, P.; Lutz, B.; Mackie, K.; Harkany, T., Hardwiring the brain: endocannabinoids shape neuronal connectivity. *Science.* **2007,** *316*, 1212-1216.

30. Iskandar, B. J.; Rizk, E.; Meier, B.; Hariharan, N.; Bottiglieri, T.; Finnell, R. H.; Jarrard, D. F.; Banerjee, R. V.; Skene, J. H.; Nelson, A.; Patel, N.; Gherasim, C.; Simon, K.; Cook, T. D.; Hogan, K. J., Folate regulation of axonal regeneration in the rodent central nervous system through DNA methylation. *J Clin Invest.* **2010,** *120* (5), 1603-1616.

31. Zhong, Z.; Virshup, D. M., Wnt signaling and drug resistance in cancer. *Mol Pharmacol.* **2020,** *97* (2), 72-89.

32. Hirata, A.; Utikal, J.; Yamashita, S.; Aoki, H.; Watanabe, A.; Yamamoto, T.; Okano, H.; Bardeesy, N.; Kunisada, T.; Ushijima, T.; Hara, A.; Jaenisch, R.; Hochedlinger, K.; Yamada, Y., Dose-dependent roles for canonical Wnt signalling in de novo crypt formation and cell cycle properties of the colonic epithelium. *Development.* **2013,** *140* (1), 66-75.

33. Yu, C.; Yang, L.; Cai, M.; Zhou, F.; Xiao, S.; Li, Y.; Wan, T.; Cheng, D.; Wang, L.; Zhao, C.; Huang, X., Down-regulation of MTHFD2 inhibits NSCLC progression by suppressing cycle-related genes. *J Cell Mol Med.* **2020,** *24* (2), 1568-1577.

34.   Albrecht, L. V.; Bui, M. H.; De Robertis, E. M., Canonical Wnt is inhibited by targeting one-carbon metabolism through methotrexate or methionine deprivation. *Proc Natl Acad Sci U S A.* **2019,** *116* (8), 2987-2995.

35.   Kaina, B.; Christmann, M., DNA repair in personalized brain cancer therapy with temozolomide and nitrosoureas. *DNA Repair (Amst).* **2019,** *78,* 128-141.

36.   Krushkal, J.; Zhao, Y.; Hose, C.; Monks, A.; Doroshow, J. H.; Simon, R., Concerted changes in transcriptional regulation of genes involved in DNA methylation, demethylation, and folate-mediated one-carbon metabolism pathways in the NCI-60 cancer cell line panel in response to cancer drug treatment. *Clin Epigenetics.* **2016,** *8,* 73.

37.   Puyo, S.; Houede, N.; Kauffmann, A.; Richaud, P.; Robert, J.; Pourquier, P., Gene expression signature predicting high-grade prostate cancer responses to oxaliplatin. *Mol Pharmacol.* **2012,** *82* (6), 1205-1216.

38.   Hu, T.; Gibson, D. P.; Carr, G. J.; Torontali, S. M.; Tiesman, J. P.; Chaney, J. G.; Aardema, M. J., Identification of a gene expression profile that discriminates indirect-acting genotoxins from direct-acting genotoxins. *Mutat Res.* **2004,** *549* (1-2), 5-27.

39.   Morscher, R. J.; Ducker, G. S.; Li, S. H.; Mayer, J. A.; Gitai, Z.; Sperl, W.; Rabinowitz, J. D., Mitochondrial translation requires folate-dependent tRNA methylation. *Nature.* **2018,** *554* (7690), 128-132.

40.   Minton, D. R.; Nam, M.; McLaughlin, D. J.; Shin, J.; Bayraktar, E. C.; Alvarez, S. W.; Sviderskiy, V. O.; Papagiannakopoulos, T.; Sabatini, D. M.; Birsoy, K.; Possemato, R., Serine catabolism by SHMT2 is required for proper mitochondrial translation initiation and maintenance of formylmethionyl-tRNAs. *Mol Cell.* **2018,** *69* (4), 610-621.

41.   Ding, J.; Li, T.; Wang, X.; Zhao, E.; Choi, J. H.; Yang, L.; Zha, Y.; Dong, Z.; Huang, S.; Asara, J. M.; Cui, H.; Ding, H. F., The histone H3 methyltransferase G9A epigenetically activates the serine-glycine synthesis pathway to sustain cancer cell survival and proliferation. *Cell Metab.* **2013,** *18* (6), 896-907.

42.   Yuan, X.; Feng, W.; Imhof, A.; Grummt, I.; Zhou, Y., Activation of RNA polymerase I transcription by cockayne syndrome group B protein and histone methyltransferase G9a. *Mol Cell.* **2007,** *27* (4), 585-595.

43.   Jourdain, A. A.; Popow, J.; de la Fuente, M. A.; Martinou, J. C.; Anderson, P.; Simarro, M., The FASTK family of proteins: emerging regulators of mitochondrial RNA biology. *Nucleic Acids Res.* **2017,** *45* (19), 10941-10947.

44.   Li, P.; Wang, D.; Li, H.; Yu, Z.; Chen, X.; Fang, J., Identification of nucleolus-localized PTEN and its function in regulating ribosome biogenesis. *Mol Biol Rep.* **2014,** *41* (10), 6383-6390.

45.   Liang, H.; Chen, X.; Yin, Q.; Ruan, D.; Zhao, X.; Zhang, C.; McNutt, M. A.; Yin, Y., PTENbeta is an alternatively translated isoform of PTEN that regulates rDNA transcription. *Nat Commun.* **2017,** *8*, 14771.

46.   Zinzalla, V.; Stracka, D.; Oppliger, W.; Hall, M. N., Activation of mTORC2 by association with the ribosome. *Cell.* **2011,** *144* (5), 757-768.

47.   Arroyo, J. D.; Jourdain, A. A.; Calvo, S. E.; Ballarano, C. A.; Doench, J. G.; Root, D. E.; Mootha, V. K., A genome-wide CRISPR death screen identifies genes essential for oxidative phosphorylation. *Cell Metab.* **2016,** *24* (6), 875-885.

48.   Wei, X.; Du, M.; Li, D.; Wen, S.; Xie, J.; Li, Y.; Chen, A.; Zhang, K.; Xu, P.; Jia, M.; Wen, C.; Zhou, H.; Lyu, J.; Yang, Y.; Fang, H., Mutations in FASTKD2 are associated with mitochondrial disease with multi-OXPHOS deficiency. *Hum Mutat.* **2020,** *41* (5), 961-972.

49.   Fang, R.; Zhang, B.; Lu, X.; Jin, X.; Liu, T., FASTKD2 promotes cancer cell progression through upregulating Myc expression in pancreatic ductal adenocarcinoma. *J Cell Biochem.* **2020,** *121* (3), 2458-2466.

50.   Wang, L. W.; Shen, H.; Nobre, L.; Ersing, I.; Paulo, J. A.; Trudeau, S.; Wang, Z.; Smith, N. A.; Ma, Y.; Reinstadler, B.; Nomburg, J.; Sommermann, T.; Cahir-McFarland, E.; Gygi, S. P.; Mootha, V. K.; Weekes, M. P.; Gewurz, B. E., Epstein-Barr-virus-induced one-carbon metabolism drives B cell transformation. *Cell Metab.* **2019,** *30*, 539–555.

51.   Ji, L.; Tang, Y.; Pang, X.; Zhang, Y., Increased expression of serine hydroxymethyltransferase 2 (SHMT2) is a negative prognostic marker in patients with hepatocellular carcinoma and is associated with proliferation of HepG2 cells. *Med Sci Monit.* **2019,** *25*, 5823-5832.

52.   Wang, L.; Chang, J.; Varghese, D.; Dellinger, M.; Kumar, S.; Best, A. M.; Ruiz, J.; Bruick, R.; Pena-Llopis, S.; Xu, J.; Babinski, D. J.; Frantz, D. E.; Brekken, R. A.; Quinn, A. M.; Simeonov, A.; Easmon, J.; Martinez, E. D., A small molecule modulates Jumonji histone demethylase activity and selectively inhibits cancer growth. *Nat Commun.* **2013,** *4*, 2035.

53.   Xu, M.; Moresco, J. J.; Chang, M.; Mukim, A.; Smith, D.; Diedrich, J. K.; Yates, J. R., 3rd; Jones, K. A., SHMT2 and the BRCC36/BRISC deubiquitinase regulate HIV-1 Tat K63-ubiquitylation and destruction by autophagy. *PLoS Pathog.* **2018,** *14* (5), e1007071.

54.   Cao, J.; Sun, L.; Aramsangtienchai, P.; Spiegelman, N. A.; Zhang, X.; Huang, W.; Seto, E.; Lin, H., HDAC11 regulates type I interferon signaling through defatty-acylation of SHMT2. *Proc Natl Acad Sci USA.* **2019,** *116* (12), 5487-5492.

55.   Walden, M.; Tian, L.; Ross, R. L.; Sykora, U. M.; Byrne, D. P.; Hesketh, E. L.; Masandi, S. K.; Cassel, J.; George, R.; Ault, J. R.; El Oualid, F.; Pawlowski, K.; Salvino, J. M.; Eyers, P. A.; Ranson, N. A.; Del Galdo, F.; Greenberg, R. A.; Zeqiraj, E., Metabolic control of BRISC-SHMT2 assembly regulates immune signalling. *Nature.* **2019,** *570* (7760), 194-199.

56.   Zheng, H.; Gupta, V.; Patterson-Fortin, J.; Bhattacharya, S.; Katlinski, K.; Wu, J.; Varghese, B.; Carbone, C. J.; Aressy, B.; Fuchs, S. Y.; Greenberg, R. A., A Novel BRISC-SHMT complex deubiquitinates IFNAR1 and regulates interferon responses. *Cell Rep.* **2013,** *5* (1), 180-193.

57.   Rabl, J.; Bunker, R. D.; Schenk, A. D.; Cavadini, S.; Gill, M. E.; Abdulrahman, W.; Andres-Pons, A.; Luijsterburg, M. S.; Ibrahim, A. F. M.; Branigan, E.; Aguirre, J. D.; Marceau, A. H.; Guerillon, C.; Bouwmeester, T.; Hassiepen, U.; Peters, A.; Renatus, M.; Gelman, L.; Rubin, S. M.; Mailand, N.; van Attikum, H.; Hay, R. T.; Thoma, N. H., Structural basis of BRCC36 function in DNA repair and immune regulation. *Mol Cell.* **2019,** *75* (3), 483-497.

58.   MacFarlane, A. J.; Liu, X.; Perry, C. A.; Flodby, P.; Allen, R. H.; Stabler, S. P.; Stover, P. J., Cytoplasmic serine hydroxymethyltransferase regulates the metabolic partitioning of methylenetetrahydrofolate but is not essential in mice. *J Biol Chem.* **2008,** *283* (38), 25846-25853.

59.   Beaudin, A. E.; Abarinov, E. V.; Noden, D. M.; Perry, C. A.; Chu, S.; Stabler, S. P.; Allen, R. H.; Stover, P. J., Shmt1 and de novo thymidylate biosynthesis underlie folate-responsive neural tube defects in mice. *Am J Clin Nutr.* **2011,** *93* (4), 789-798.

60.   Garcia-Cazorla, A.; Verdura, E.; Julia-Palacios, N.; Anderson, E. N.; Goicoechea, L.; Planas-Serra, L.; Tsogtbaatar, E.; Dsouza, N. R.; Schluter, A.; Urreizti, R.; Tarnowski, J. M.; Gavrilova, R. H.; Group, S. W.; Ruiz, M.; Rodriguez-Palmero, A.; Fourcade, S.; Cogne, B.; Besnard, T.; Vincent, M.; Bezieau, S.; Folmes, C. D.; Zimmermann, M. T.; Klee, E. W.; Pandey, U. B.; Artuch, R.; Cousin, M. A.; Pujol, A., Impairment of the mitochondrial one-carbon metabolism enzyme SHMT2 causes a novel brain and heart developmental syndrome. *Acta Neuropathol.* **2020**.

61.   Fawal, M. A.; Jungas, T.; Kischel, A.; Audouard, C.; Iacovoni, J. S.; Davy, A., Cross talk between one-carbon metabolism, Eph signaling, and histone methylation promotes neural stem cell differentiation. *Cell Rep.* **2018,** *23* (10), 2864-2873.

62.   Kania, A.; Klein, R., Mechanisms of ephrin-Eph signalling in development, physiology and disease. *Nat Rev Mol Cell Biol.* **2016,** *17* (4), 240-256.

63.   Choi, Y.; Syeda, F.; Walker, J. R.; Finerty, P. J., Jr.; Cuerrier, D.; Wojciechowski, A.; Liu, Q.; Dhe-Paganon, S.; Gray, N. S., Discovery and structural analysis of Eph receptor tyrosine kinase inhibitors. *Bioorg Med Chem Lett.* **2009,** *19* (15), 4467-4470.

64.   Reily, C.; Stewart, T. J.; Renfrow, M. B.; Novak, J., Glycosylation in health and disease. *Nat Rev Nephrol.* **2019,** *15* (6), 346-366.

65.   Jozwiak, P.; Forma, E.; Brys, M.; Krzeslak, A., O-GlcNAcylation and metabolic reprograming in cancer. *Front Endocrinol (Lausanne).* **2014,** *5*, 145.

66.   Chaiyawat, P.; Chokchaichamnankit, D.; Lirdprapamongkol, K.; Srisomsap, C.; Svasti, J.; Champattanachai, V., Alteration of O-GlcNAcylation affects serine phosphorylation and regulates gene expression and activity of pyruvate kinase M2 in colorectal cancer cells. *Oncol Rep.* **2015,** *34* (4), 1933-1942.

67.   Hussain, M. R. M.; Hoessli, D. C.; Fang, M., N-acetylgalactosaminyltransferases in cancer. *Oncotarget.* **2016,** *7* (33), 54067-54081.

68.   Qiu, H.; Guo, X. H.; Mo, J. H.; Jin, M. F.; Wu, S. L.; Chen, H. L., Expressions of polypeptide: N-acetylgalactosaminyltransferase in leukemia cell lines during 1,25-dihydroxyvitamin D3 induced differentiation. *Glycoconj J.* **2006,** *23* (7-8), 575-584.

69.   Ducker, G. S.; Ghergurovich, J. M.; Mainolfi, N.; Suri, V.; Jeong, S. K.; Hsin-Jung Li, S.; Friedman, A.; Manfredi, M. G.; Gitai, Z.; Kim, H.; Rabinowitz, J. D., Human SHMT inhibitors reveal defective glycine import as a targetable metabolic vulnerability of diffuse large B-cell lymphoma. *Proc Natl Acad Sci USA.* **2017,** *114* (43), 11404-11409.

70.   Yeh, Y. M.; Chen, C. Y.; Huang, P. R.; Hsu, C. W.; Wu, C. C.; Wang, T. C., Proteomic analyses of genes regulated by heterogeneous nuclear ribonucleoproteins A/B in Jurkat cells. *Proteomics.* **2014,** *14* (11), 1357-1366.

71.   Geuens, T.; Bouhy, D.; Timmerman, V., The hnRNP family: insights into their role in health and disease. *Hum Genet.* **2016,** *135* (8), 851-867.

72.   Grosset, A. A.; Labrie, M.; Vladoiu, M. C.; Yousef, E. M.; Gaboury, L.; St-Pierre, Y., Galectin signatures contribute to the heterogeneity of breast cancer and provide new prognostic information and therapeutic targets. *Oncotarget.* **2016,** *7*, 18183-18203.

73.   Labrie, M.; De Araujo, L. O. F.; Communal, L.; Mes-Masson, A. M.; St-Pierre, Y., Tissue and plasma levels of galectins in patients with high grade serous ovarian carcinoma as new predictive biomarkers. *Sci Rep.* **2017,** *7* (1), 13244.

74.   Schulz, H.; Kuhn, C.; Hofmann, S.; Mayr, D.; Mahner, S.; Jeschke, U.; Schmoeckel, E., Overall survival of ovarian cancer patients is determined by expression of galectins-8 and -9. *Int J Mol Sci.* **2018,** *19* (1), 323.

75.   Wu, S.; Liu, H.; Zhang, H.; Lin, C.; Li, R.; Cao, Y.; He, H.; Li, H.; Shen, Z.; Qin, J.; Xu, J., Galectin-8 is associated with recurrence and survival of patients with non-metastatic gastric cancer after surgery. *Tumour Biol.* **2016,** *37* (9), 12635-12642.

76.   Long, B.; Yu, Z.; Zhou, H.; Ma, Z.; Ren, Y.; Zhan, H.; Li, L.; Cao, H.; Jiao, Z., Clinical characteristics and prognostic significance of galectins for patients with gastric cancer: A meta-analysis. *Int J Surg.* **2018,** *56*, 242-249.

77.   Elola, M. T.; Ferragut, F.; Cardenas Delgado, V. M.; Nugnes, L. G.; Gentilini, L.; Laderach, D.; Troncoso, M. F.; Compagno, D.; Wolfenstein-Todel, C.; Rabinovich, G. A.,

Expression, localization and function of galectin-8, a tandem-repeat lectin, in human tumors. *Histol Histopathol.* **2014,** *29* (9), 1093-1105.

78.   Liu, Y.; Xu, L.; Zhu, Y.; Zhang, W.; Liu, W.; Liu, H.; Xu, J., Galectin-8 predicts postoperative recurrence of patients with localized T1 clear cell renal cell carcinoma. *Urol Oncol-Semin Ori.* **2015,** *33* (3), 112.e111-112.e118.

79.   Deng, W.; Wang, L.; Xiong, Y.; Li, J.; Wang, Y.; Shi, T.; Ma, D., The novel secretory protein CGREF1 inhibits the activation of AP-1 transcriptional activity and cell proliferation. *Int J Biochem Cell Biol.* **2015,** *65*, 32-39.

80.   Gazon, H.; Barbeau, B.; Mesnard, J. M.; Peloponese, J. M., Jr., Hijacking of the AP-1 signaling pathway during development of ATL. *Front Microbiol.* **2017,** *8*, 2686.

81.   Duan, X.; Ponomareva, L.; Veeranki, S.; Choubey, D., IFI16 induction by glucose restriction in human fibroblasts contributes to autophagy through activation of the ATM/AMPK/p53 pathway. *PLoS One.* **2011,** *6* (5), e19532.

82.   de Paz-Lugo, P.; Lupianez, J. A.; Melendez-Hevia, E., High glycine concentration increases collagen synthesis by articular chondrocytes in vitro: acute glycine deficiency could be an important cause of osteoarthritis. *Amino Acids.* **2018,** *50* (10), 1357-1365.

83.   Nallanthighal, S.; Rada, M.; Heiserman, J. P.; Cha, J.; Sage, J.; Zhou, B.; Yang, W.; Hu, Y.; Korgaonkar, C.; Hanos, C. T.; Ashkavand, Z.; Norman, K.; Orsulic, S.; Cheon, D. J., Inhibition of collagen XI alpha 1-induced fatty acid oxidation triggers apoptotic cell death in cisplatin-resistant ovarian cancer. *Cell Death Dis.* **2020,** *11* (4), 258.

84.   Zhao, X.; Psarianos, P.; Ghoraie, L. S.; Yip, K.; Goldstein, D.; Gilbert, R.; Witterick, I.; Pang, H.; Hussain, A.; Lee, J. H.; Williams, J.; Bratman, S. V.; Ailles, L.; Haibe-Kains, B.; Liu, F. F., Metabolic regulation of dermal fibroblasts contributes to skin extracellular matrix homeostasis and fibrosis. *Nature Metabolism.* **2019,** *1*, 147-157.

85.   Sun, T.; Wang, D.; Ping, Y.; Sang, Y.; Dai, Y.; Wang, Y.; Liu, Z.; Duan, X.; Tao, Z.; Liu, W., Integrated profiling identifies SLC5A6 and MFAP2 as novel diagnostic and prognostic biomarkers in gastric cancer patients. *Int J Oncol.* **2020,** *56* (2), 460-469.

86.   Yao, L. W.; Wu, L. L.; Zhang, L. H.; Zhou, W.; Wu, L.; He, K.; Ren, J. C.; Deng, Y. C.; Yang, D. M.; Wang, J.; Mu, G. G.; Xu, M.; Zhou, J.; Xiang, G. A.; Ding, Q. S.; Yang, Y. N.; Yu, H. G., MFAP2 is overexpressed in gastric cancer and promotes motility via the MFAP2/integrin alpha5beta1/FAK/ERK pathway. *Oncogenesis.* **2020,** *9* (2), 17.

87.   Wang, J. K.; Wang, W. J.; Cai, H. Y.; Du, B. B.; Mai, P.; Zhang, L. J.; Ma, W.; Hu, Y. G.; Feng, S. F.; Miao, G. Y., MFAP2 promotes epithelial-mesenchymal transition in gastric cancer cells by activating TGF-beta/SMAD2/3 signaling pathway. *Onco Targets Ther.* **2018,** *11*, 4001-4017.

88.   Chen, Z.; Lv, Y.; Cao, D.; Li, X.; Li, Y., Microfibril-associated protein 2 (MFAP2) potentiates invasion and migration of melanoma by EMT and Wnt/β-catenin pathway. *Med Sci Mon Int Med J Exp Clin Res.* **2020,** *26*, 923808.

89.   Rai, A.; Greening, D. W.; Chen, M.; Xu, R.; Ji, H.; Simpson, R. J., Exosomes derived from human primary and metastatic colorectal cancer cells contribute to functional heterogeneity of activated fibroblasts by reprogramming their proteome. *Proteomics.* **2019,** *19* (8), e1800148.

90.   Lin, C.; Zhang, Y.; Chen, Y.; Bai, Y.; Zhang, Y., Long noncoding RNA LINC01234 promotes serine hydroxymethyltransferase 2 expression and proliferation by competitively binding miR-642a-5p in colon cancer. *Cell Death Dis.* **2019,** *10* (2), 137.

91.   Wu, X.; Deng, L.; Tang, D.; Ying, G.; Yao, X.; Liu, F.; Liang, G., miR-615-5p prevents proliferation and migration through negatively regulating serine hydromethyltransferase 2 (SHMT2) in hepatocellular carcinoma. *Tumour Biol.* **2016,** *37* (5), 6813-6821.

92.   Pinweha, P.; Rattanapornsompong, K.; Charoensawan, V.; Jitrapakdee, S., MicroRNAs and oncogenic transcriptional regulatory networks controlling metabolic reprogramming in cancers. *Comput Struct Biotechnol J.* **2016,** *14*, 223-233.

93.   Leivonen, S. K.; Rokka, A.; Ostling, P.; Kohonen, P.; Corthals, G. L.; Kallioniemi, O.; Perala, M., Identification of miR-193b targets in breast cancer cells and systems biological analysis of their functional impact. *Mol Cell Proteomics.* **2011,** *10* (7), M110.005322.

94.   Qi, C.; Qin, X.; Zhou, Z.; Wang, Y.; Yang, Q.; Liao, T., Circ_0072995 promotes cell carcinogenesis via up-regulating miR-149-5p-mediated SHMT2 in breast cancer. *Cancer Manag Res.* **2020,** *12*, 11169-11181.

95.   Zhang, E.; He, X.; Zhang, C.; Su, J.; Lu, X.; Si, X.; Chen, J.; Yin, D.; Han, L.; De, W., A novel long noncoding RNA HOXC-AS3 mediates tumorigenesis of gastric cancer by binding to YBX1. *Genome Biol.* **2018,** *19* (1), 154.

96.   Wang, X.; Sun, Y.; Xu, T.; Qian, K.; Huang, B.; Zhang, K.; Song, Z.; Qian, T.; Shi, J.; Li, L., HOXB13 promotes proliferation, migration, and invasion of glioblastoma through transcriptional upregulation of lncRNA HOXC-AS3. *J Cell Biochem.* **2019,** *120* (9), 15527-15537.

97.   Shi, S. H.; Jiang, J.; Zhang, W.; Sun, L.; Li, X. J.; Li, C.; Ge, Q. D.; Zhuang, Z. G., A novel lncRNA HOXC-AS3 acts as a miR-3922-5p sponge to promote breast cancer metastasis. *Cancer Invest.* **2020,** *38* (1), 1-12.

98.   Yang, Z.; Hu, T., Long noncoding RNA HOXC-AS3 facilitates the progression of invasive mucinous adenocarcinomas of the lung via modulating FUS/FOXM1. *In Vitro Cell Dev Biol Anim.* **2020,** *56* (1), 15-23.

99.   Fu, T.; Ji, X.; Bu, Z.; Zhang, J.; Wu, X.; Zong, X.; Fan, B.; Jia, Z.; Ji, J., Identification of key long non-coding RNAs in gastric adenocarcinoma. *Cancer Biomark.* **2020,** *27*, 541-553.

100.   Dong, Y.; Li, X.; Lin, Z.; Zou, W.; Liu, Y.; Qian, H.; Jia, J., HOXC-AS1-MYC regulatory loop contributes to the growth and metastasis in gastric cancer. *J Exp Clin Cancer Res.* **2019,** *38* (1), 502.

101.   Xia, Y.; Ye, B.; Ding, J.; Yu, Y.; Alptekin, A.; Thangaraju, M.; Prasad, P. D.; Ding, Z. C.; Park, E. J.; Choi, J. H.; Gao, B.; Fiehn, O.; Yan, C.; Dong, Z.; Zha, Y.; Ding, H. F., Metabolic reprogramming by MYCN confers dependence on the serine-glycine-one-carbon biosynthetic pathway. *Cancer Res.* **2019,** *79* (15), 3837-3850.

102.   Marengo, B.; Garbarino, O.; Speciale, A.; Monteleone, L.; Traverso, N.; Domenicotti, C., MYC expression and metabolic redox changes in cancer cells: a synergy able to induce chemoresistance. *Oxid Med Cell Longev.* **2019,** *2019*, 7346492.

103.   He, M.; Lin, Y.; Xu, Y., Identification of prognostic biomarkers in colorectal cancer using a long non-coding RNA-mediated competitive endogenous RNA network. *Oncol Lett.* **2019,** *17* (3), 2687-2694.

104.   Zhu, T. G.; Xiao, X.; Wei, Q.; Yue, M.; Zhang, L. X., Revealing potential long non-coding RNA biomarkers in lung adenocarcinoma using long non-coding RNA-mediated competitive endogenous RNA network. *Braz J Med Biol Res.* **2017,** *50* (9), e6297.

105.   Pedersen, S. K.; Mitchell, S. M.; Graham, L. D.; McEvoy, A.; Thomas, M. L.; Baker, R. T.; Ross, J. P.; Xu, Z. Z.; Ho, T.; LaPointe, L. C.; Young, G. P.; Molloy, P. L., CAHM, a long non-coding RNA gene hypermethylated in colorectal neoplasia. *Epigenetics.* **2014,** *9* (8), 1071-1082.

106.   Li, X. X.; Wang, L. J.; Hou, J.; Liu, H. Y.; Wang, R.; Wang, C.; Xie, W. H., Identification of long noncoding RNAs as predictors of survival in triple-negative breast cancer based on network analysis. *Biomed Res Int.* **2020,** *2020*, 8970340.

107.   Fan, Q.; Liu, B., Identification of a RNA-seq based 8-long non-coding RNA signature predicting survival in esophageal cancer. *Med Sci Monit.* **2016,** *22*, 5163-5172.

108.   Zhu, Y.; Bian, Y.; Zhang, Q.; Hu, J.; Li, L.; Yang, M.; Qian, H.; Yu, L.; Liu, B.; Qian, X., Construction and analysis of dysregulated lncRNA-associated ceRNA network in colorectal cancer. *J Cell Biochem.* **2019,** *120* (6), 9250-9263.

109.   Li, Y.; He, Y.; Han, S.; Liang, Y., Identification and functional inference for tumor-associated long non-coding RNA. *IEEE/ACM Trans Comput Biol Bioinform.* **2019,** *16*, 1288-1301.

110.   Zhu, Y.; Bian, Y.; Zhang, Q.; Hu, J.; Li, L.; Yang, M.; Qian, H.; Yu, L.; Liu, B.; Qian, X., LINC00365 promotes colorectal cancer cell progression through the Wnt/beta-catenin signaling pathway. *J Cell Biochem.* **2020,** *121* (2), 1260-1272.

111.   Yan, X. Y.; Zhang, J. J.; Zhong, X. R.; Yu, S. H.; Xu, L.; Tian, R.; Sun, L. K.; Su, J., The LINC00365/SCGB2A1 (mammaglobin B) axis down-regulates NF-kappaB signaling and is associated with the progression of gastric cancer. *Cancer Manag Res.* **2020,** *12*, 621-631.

112.   Zhang, L.; Yan, X.; Yu, S.; Zhong, X.; Tian, R.; Xu, L.; Bian, X.; Su, J., LINC00365-SCGB2A1 axis inhibits the viability of breast cancer through targeting NF-kappaB signaling. *Oncol Lett.* **2020,** *19* (1), 753-762.

113.   Zheng, X.; Zhou, Y.; Chen, W.; Chen, L.; Lu, J.; He, F.; Li, X.; Zhao, L., Ginsenoside 20(S)-Rg3 prevents PKM2-targeting miR-324-5p from H19 sponging to antagonize the Warburg effect in ovarian cancer cells. *Cell Physiol Biochem.* **2018,** *51* (3), 1340-1353.

114.   Xue, M.-Y.; Cao, H.-X., LINC01551 promotes metastasis of nasopharyndeal carcinoma through targeting microRNA-132-5p. *Eur Rev Med Pharmacol Sci.* **2020,** *24*, 3724-3733.

115.   Gao, J.; Yin, X.; Yu, X.; Dai, C.; Zhou, F., Long noncoding LINC01551 promotes hepatocellular carcinoma cell proliferation, migration, and invasion by acting as a competing endogenous RNA of microRNA-122-5p to regulate ADAM10 expression. *J Cell Biochem.* **2019,** *120* (10), 16393-16407.

116.   Saha, N.; Robev, D.; Himanen, J. P.; Nikolov, D. B., ADAM proteases: Emerging role and targeting of the non-catalytic domains. *Cancer Lett.* **2019,** *467*, 50-57.

117.   Yin, K., Positive correlation between expression level of mitochondrial serine hydroxymethyltransferase and breast cancer grade. *Onco Targets Ther.* **2015,** *8*, 1069-1074.

118.   Liu, Y.; Yin, C.; Deng, M.-M.; Wang, Q.; He, X.-Q.; Li, M.-T.; Li, C.-P.; Wu, H., High expression of SHMT2 is correlated with tumor progression and predicts poor prognosis in gastrointestinal tumors. *Eur Rev Med Pharmacol Sci.* **2019,** *23*, 9379-9392.

119.   Shi, H.; Fang, X.; Li, Y.; Zhang, Y., High expression of serine hydroxymethyltransferase 2 indicates poor prognosis of gastric cancer patients. *Med Sci Monit.* **2019,** *25*, 7430-7438.

120.   Wu, M.; Wanggou, S.; Li, X.; Liu, Q.; Xie, Y., Overexpression of mitochondrial serine hydroxyl-methyltransferase 2 is associated with poor prognosis and promotes cell proliferation and invasion in gliomas. *Onco Targets Ther.* **2017,** *10*, 3781-3788.

121.   Bernhardt, S.; Bayerlova, M.; Vetter, M.; Wachter, A.; Mitra, D.; Hanf, V.; Lantzsch, T.; Uleer, C.; Peschel, S.; John, J.; Buchmann, J.; Weigert, E.; Burrig, K. F.; Thomssen, C.; Korf, U.; Beissbarth, T.; Wiemann, S.; Kantelhardt, E. J., Proteomic profiling of breast cancer metabolism identifies SHMT2 and ASCT2 as prognostic factors. *Breast Cancer Res.* **2017,** *19* (1), 112.

122.   Zhang, L.; Chen, Z.; Xue, D.; Zhang, Q.; Liu, X.; Luh, F.; Hong, L.; Zhang, H.; Pan, F.; Liu, Y.; Chu, P.; Zheng, S.; Lou, G.; Yen, Y., Prognostic and therapeutic value of mitochondrial serine hydroxyl-methyltransferase 2 as a breast cancer biomarker. *Oncol Rep.* **2016,** *36* (5), 2489-2500.

123.   Ning, S.; Ma, S.; Saleh, A. Q.; Guo, L.; Zhao, Z.; Chen, Y., SHMT2 overexpression predicts poor prognosis in intrahepatic cholangiocarcinoma. *Gastroenterol Res Pract.* **2018,** *2018*, 4369253.

124.   Wang, B.; Wang, W.; Zhu, Z.; Zhang, X.; Tang, F.; Wang, D.; Liu, X.; Yan, X.; Zhuang, H., Mitochondrial serine hydroxymethyltransferase 2 is a potential diagnostic and prognostic biomarker for human glioma. *Clin Neurol Neurosurg.* **2017,** *154*, 28-33.

125.   Kim, D.; Fiske, B. P.; Birsoy, K.; Freinkman, E.; Kami, K.; Possemato, R. L.; Chudnovsky, Y.; Pacold, M. E.; Chen, W. W.; Cantor, J. R.; Shelton, L. M.; Gui, D. Y.; Kwon, M.; Ramkissoon, S. H.; Ligon, K. L.; Kang, S. W.; Snuderl, M.; Vander Heiden, M. G.; Sabatini, D. M., SHMT2 drives glioma cell survival in ischaemia but imposes a dependence on glycine clearance. *Nature.* **2015,** *520* (7547), 363-367.

126.   Chen, J.; Lin, M.; Foxe, J. J.; Pedrosa, E.; Hrabovsky, A.; Carroll, R.; Zheng, D.; Lachman, H. M., Transcriptome comparison of human neurons generated using induced pluripotent stem cells derived from dental pulp and skin fibroblasts. *PLoS One.* **2013,** *8* (10), e75682.

127.   Stelcer, E.; Kulcenty, K.; Rucinski, M.; Jopek, K.; Trzeciak, T.; Richter, M.; Wroblewska, J. P.; Suchorska, W. M., Expression of pluripotency genes in chondrocyte-like cells differentiated from human induced pluripotent stem cells. *Int J Mol Sci.* **2018,** *19* (2), 550.

128.   Han, X.; Chen, H.; Huang, D.; Chen, H.; Fei, L.; Cheng, C.; Huang, H.; Yuan, G. C.; Guo, G., Mapping human pluripotent stem cell differentiation pathways using high throughput single-cell RNA-sequencing. *Genome Biol.* **2018,** *19* (1), 47.

129.   Rand, T. A.; Sutou, K.; Tanabe, K.; Jeong, D.; Nomura, M.; Kitaoka, F.; Tomoda, E.; Narita, M.; Nakamura, M.; Nakamura, M.; Watanabe, A.; Rulifson, E.; Yamanaka, S.; Takahashi, K., MYC releases early reprogrammed human cells from proliferation pause via retinoblastoma protein inhibition. *Cell Rep.* **2018,** *23* (2), 361-375.

130.   Li, F.; Li, Q.; Wu, X., Construction and analysis for differentially expressed long non-coding RNAs and microRNAs mediated competing endogenous RNA network in colon cancer. *PLoS One.* **2018,** *13* (2), e0192494.

131.   Filippov-Levy, N.; Cohen-Schussheim, H.; Trope, C. G.; Hetland Falkenthal, T. E.; Smith, Y.; Davidson, B.; Reich, R., Expression and clinical role of long non-coding RNA in high-grade serous carcinoma. *Gynecol Oncol.* **2018,** *148* (3), 559-566.

132.	Hinger, S. A.; Cha, D. J.; Franklin, J. L.; Higginbotham, J. N.; Dou, Y.; Ping, J.; Shu, L.; Prasad, N.; Levy, S.; Zhang, B.; Liu, Q.; Weaver, A. M.; Coffey, R. J.; Patton, J. G., Diverse long RNAs are differentially sorted into extracellular vesicles secreted by colorectal cancer cells. *Cell Rep.* **2018,** *25* (3), 715-725.

133.	Quan, W.; Yao, Y.; Xianhua, C.; Xiaodong, P.; Qi, H.; Dong, W.; Youcai, D.; Xiaohui, L.; Jun, Y.; Jihong, Z., Competing endogenous RNA screening based on long noncoding RNA-messenger RNA co-expression profile in Hepatitis B virus-associated hepatocarcinogenesis. *J Tradit Chin Med.* **2017,** *37*, 510-521.

134.	Ruan, X.; Li, P.; Chen, Y.; Shi, Y.; Pirooznia, M.; Seifuddin, F.; Suemizu, H.; Ohnishi, Y.; Yoneda, N.; Nishiwaki, M.; Shepherdson, J.; Suresh, A.; Singh, K.; Ma, Y.; Jiang, C. F.; Cao, H., In vivo functional analysis of non-conserved human lncRNAs associated with cardiometabolic traits. *Nat Commun.* **2020,** *11* (1), 45.

135.	Zhang, W.; Fei, J.; Yu, S.; Shen, J.; Zhu, X.; Sadhukhan, A.; Lu, W.; Zhou, J., LINC01088 inhibits tumorigenesis of ovarian epithelial cells by targeting miR-24-1-5p. *Sci Rep.* **2018,** *8* (1), 2876.

136.	Wang, S.; Xu, M.; Sun, Z.; Yu, X.; Deng, Y.; Chang, H., LINC01018 confers a novel tumor suppressor role in hepatocellular carcinoma through sponging microRNA-182-5p. *Am J Physiol Gastrointest Liver Physiol.* **2019,** *317* (2), G116-G126.

137.	Miao, Y.; Sui, J.; Xu, S.-Y.; Liang, G.-Y.; Pu, Y.-P.; Yin, L.-H., Comprehensive analysis of a novel four-lncRNA signature as a prognostic biomarker for human gastric cancer. *Oncotarget.* **2017,** *8*, 75007-75024.

138.	Green, N. H.; Galvan, D. L.; Badal, S. S.; Chang, B. H.; LeBleu, V. S.; Long, J.; Jonasch, E.; Danesh, F. R., MTHFD2 links RNA methylation to metabolic reprogramming in renal cell carcinoma. *Oncogene.* **2019,** *38* (34), 6211-6225.

139.	Markert, E. K.; Levine, A. J.; Vazquez, A., Proliferation and tissue remodeling in cancer: the hallmarks revisited. *Cell Death Dis.* **2012,** *3*, e397.

140.	Tedeschi, P. M.; Markert, E. K.; Gounder, M.; Lin, H.; Dvorzhinski, D.; Dolfi, S. C.; Chan, L. L.; Qiu, J.; DiPaola, R. S.; Hirshfield, K. M.; Boros, L. G.; Bertino, J. R.; Oltvai, Z. N.; Vazquez, A., Contribution of serine, folate and glycine metabolism to the ATP, NADPH and purine requirements of cancer cells. *Cell Death Dis.* **2013,** *4*, e877.

141.	Vazquez, A.; Tedeschi, P. M.; Bertino, J. R., Overexpression of the mitochondrial folate and glycine-serine pathway: a new determinant of methotrexate selectivity in tumors. *Cancer Res.* **2013,** *73* (2), 478-482.

142.	Vazquez, A.; Markert, E. K.; Oltvai, Z. N., Serine biosynthesis with one carbon catabolism and the glycine cleavage system represents a novel pathway for ATP generation. *PLoS One.* **2011,** *6* (11), e25881.

143. Moran, D. M.; Trusk, P. B.; Pry, K.; Paz, K.; Sidransky, D.; Bacus, S. S., KRAS mutation status is associated with enhanced dependency on folate metabolism pathways in non-small cell lung cancer cells. *Mol Cancer Ther.* **2014,** *13* (6), 1611-1624.

144. Pikman, Y.; Puissant, A.; Alexe, G.; Furman, A.; Chen, L. M.; Frumm, S. M.; Ross, L.; Fenouille, N.; Bassil, C. F.; Lewis, C. A.; Ramos, A.; Gould, J.; Stone, R. M.; DeAngelo, D. J.; Galinsky, I.; Clish, C. B.; Kung, A. L.; Hemann, M. T.; Vander Heiden, M. G.; Banerji, V.; Stegmaier, K., Targeting MTHFD2 in acute myeloid leukemia. *J Exp Med.* **2016,** *213* (7), 1285-1306.

145. Pede, V.; Rombout, A.; Vermeire, J.; Naessens, E.; Mestdagh, P.; Robberecht, N.; Vanderstraeten, H.; Van Roy, N.; Vandesompele, J.; Speleman, F.; Philippe, J.; Verhasselt, B., CLL cells respond to B-cell receptor stimulation with a microRNA/mRNA signature associated with MYC activation and cell cycle progression. *PLoS One.* **2013,** *8* (4), e60275.

146. Tan, H.; Yang, K.; Li, Y.; Shaw, T. I.; Wang, Y.; Blanco, D. B.; Wang, X.; Cho, J. H.; Wang, H.; Rankin, S.; Guy, C.; Peng, J.; Chi, H., Integrative proteomics and phosphoproteomics profiling reveals dynamic signaling networks and bioenergetics pathways underlying T cell activation. *Immunity.* **2017,** *46* (3), 488-503.

147. Ju, H. Q.; Lu, Y. X.; Chen, D. L.; Zuo, Z. X.; Liu, Z. X.; Wu, Q. N.; Mo, H. Y.; Wang, Z. X.; Wang, D. S.; Pu, H. Y.; Zeng, Z. L.; Li, B.; Xie, D.; Huang, P.; Hung, M. C.; Chiao, P. J.; Xu, R. H., Modulation of redox homeostasis by inhibition of MTHFD2 in colorectal cancer: mechanisms and therapeutic implications. *J Natl Cancer Inst.* **2018,** *111*, 584-596.

148. Cheung, C. H. Y.; Hsu, C. L.; Tsuei, C. Y.; Kuo, T. T.; Huang, C. T.; Hsu, W. M.; Chung, Y. H.; Wu, H. Y.; Hsu, C. C.; Huang, H. C.; Juan, H. F., Combinatorial targeting of MTHFD2 and PAICS in purine synthesis as a novel therapeutic strategy. *Cell Death Dis.* **2019,** *10* (11), 786.

149. Chen, H.; Liu, H.; Qing, G., Targeting oncogenic Myc as a strategy for cancer treatment. *Signal Transduct Target Ther.* **2018,** *3*, 5.

150. Kent, L. N.; Leone, G., The broken cycle: E2F dysfunction in cancer. *Nat Rev Cancer.* **2019,** *19* (6), 326-338.

151. Blanchet, E.; Annicotte, J. S.; Lagarrigue, S.; Aguilar, V.; Clape, C.; Chavey, C.; Fritz, V.; Casas, F.; Apparailly, F.; Auwerx, J.; Fajas, L., E2F transcription factor-1 regulates oxidative metabolism. *Nat Cell Biol.* **2011,** *13* (9), 1146-1152.

152. Wu, M.; Seto, E.; Zhang, J., E2F1 enhances glycolysis through suppressing Sirt6 transcription in cancer cells. *Oncotarget.* **2015,** *6*, 11252-11263.

153. Yoshida, K.; Sanada, M.; Shiraishi, Y.; Nowak, D.; Nagata, Y.; Yamamoto, R.; Sato, Y.; Sato-Otsubo, A.; Kon, A.; Nagasaki, M.; Chalkidis, G.; Suzuki, Y.; Shiosaka, M.; Kawahata, R.;

Yamaguchi, T.; Otsu, M.; Obara, N.; Sakata-Yanagimoto, M.; Ishiyama, K.; Mori, H.; Nolte, F.; Hofmann, W. K.; Miyawaki, S.; Sugano, S.; Haferlach, C.; Koeffler, H. P.; Shih, L. Y.; Haferlach, T.; Chiba, S.; Nakauchi, H.; Miyano, S.; Ogawa, S., Frequent pathway mutations of splicing machinery in myelodysplasia. *Nature.* **2011,** *478* (7367), 64-69.

154.   Tian, J.; Liu, Y.; Zhu, B.; Tian, Y.; Zhong, R.; Chen, W.; Lu, X.; Zou, L.; Shen, N.; Qian, J.; Li, H.; Miao, X.; Wang, L., SF3A1 and pancreatic cancer: new evidence for the association of the spliceosome and cancer. *Oncotarget.* **2015,** *6*, 37750-37757.

155.   Lorenzini, P. A.; Chew, R. S. E.; Tan, C. W.; Yong, J. Y.; Zhang, F.; Zheng, J.; Roca, X., Human PRPF40B regulates hundreds of alternative splicing targets and represses a hypoxia expression signature. *RNA.* **2019,** *25*, 905-920.

156.   Samanta, D.; Semenza, G. L., Maintenance of redox homeostasis by hypoxia-inducible factors. *Redox Biol.* **2017,** *13*, 331-335.

157.   Wei, Y.; Liu, P.; Li, Q.; Du, J.; Chen, Y.; Wang, Y.; Shi, H.; Wang, Y.; Zhang, H.; Xue, W.; Gao, Y.; Li, D.; Feng, Y.; Yan, J.; Han, J.; Zhang, J., The effect of MTHFD2 on the proliferation and migration of colorectal cancer cell lines. *Onco Targets Ther.* **2019,** *12*, 6361-6370.

158.   Lehtinen, L.; Ketola, K.; Makela, R.; Mpindi, J. P.; Viitala, M.; Kallioniemi, O.; Iljin, K., High-throughput RNAi screening for novel modulators of vimentin expression identifies MTHFD2 as a regulator of breast cancer cell migration and invasion. *Oncotarget.* **2013,** *4* (1), 48-63.

159.   Li, S. M.; Zhao, Y. Q.; Hao, Y. L.; Liang, Y. Y., Upregulation of miR-504-3p is associated with favorable prognosis of acute myeloid leukemia and may serve as a tumor suppressor by targeting MTHFD2. *Eur Rev Med Pharmacol Sci.* **2019,** *23* (3), 1203-1213.

160.   Lin, H.; Huang, B.; Wang, H.; Liu, X.; Hong, Y.; Qiu, S.; Zheng, J., MTHFD2 overexpression predicts poor prognosis in renal cell carcinoma and is associated with cell proliferation and vimentin-modulated migration and invasion. *Cell Physiol Biochem.* **2018,** *51* (2), 991-1000.

161.   Liu, X.; Huang, Y.; Jiang, C.; Ou, H.; Guo, B.; Liao, H.; Li, X.; Yang, D., Methylenetetrahydrofolate dehydrogenase 2 overexpression is associated with tumor aggressiveness and poor prognosis in hepatocellular carcinoma. *Dig Liver Dis.* **2016,** *48* (8), 953-960.

162.   Yan, Y.; Zhang, D.; Lei, T.; Zhao, C.; Han, J.; Cui, J.; Wang, Y., MicroRNA-33a-5p suppresses colorectal cancer cell growth by inhibiting MTHFD2. *Clin Exp Pharmacol Physiol.* **2019,** *46* (10), 928-936.

163.   Meng, X. Y.; Shi, M. J.; Zeng, Z. H.; Chen, C.; Liu, T. Z.; Wu, Q. J.; Li, S.; Li, S., The role of COL5A2 in patients with muscle-invasive bladder cancer: a bioinformatics analysis of public datasets involving 787 subjects and 29 cell lines. *Front Oncol.* **2018,** *8*, 659.

164.   Zeng, X. T.; Liu, X. P.; Liu, T. Z.; Wang, X. H., The clinical significance of COL5A2 in patients with bladder cancer: A retrospective analysis of bladder cancer gene expression data. *Medicine (Baltimore).* **2018,** *97* (10), e0091.

165.   Chen, H. C.; Tseng, Y. K.; Shu, C. W.; Weng, T. J.; Liou, H. H.; Yen, L. M.; Hsieh, I. C.; Wang, C. C.; Wu, P. C.; Shiue, Y. L.; Fu, T. Y.; Tsai, K. W.; Ger, L. P.; Liu, P. F., Differential clinical significance of COL5A1 and COL5A2 in tongue squamous cell carcinoma. *J Oral Pathol Med.* **2019,** *48* (6), 468-476.

166.   Fischer, H.; Stenling, R.; Rubio, C.; Lindblom, A., Colorectal carcinogenesis is associated with stromal expression of COL11A1 and COL5A2. *Carcinogenesis.* **2001,** *22*, 875-878.

167.   Schlesinger, M.; Bendas, G., Vascular cell adhesion molecule-1 (VCAM-1)--an increasing insight into its role in tumorigenicity and metastasis. *Int J Cancer.* **2015,** *136* (11), 2504-2514.

168.   Altieri, P.; Murialdo, R.; Barisione, C.; Lazzarini, E.; Garibaldi, S.; Fabbi, P.; Ruggeri, C.; Borile, S.; Carbone, F.; Armirotti, A.; Canepa, M.; Ballestrero, A.; Brunelli, C.; Montecucco, F.; Ameri, P.; Spallarossa, P., 5-fluorouracil causes endothelial cell senescence: potential protective role of glucagon-like peptide 1. *Br J Pharmacol.* **2017,** *174* (21), 3713-3726.

169.   Wang, P. C.; Weng, C. C.; Hou, Y. S.; Jian, S. F.; Fang, K. T.; Hou, M. F.; Cheng, K. H., Activation of VCAM-1 and its associated molecule CD44 leads to increased malignant potential of breast cancer cells. *Int J Mol Sci.* **2014,** *15* (3), 3560-3579.

170.   Najafi, M.; Farhood, B.; Mortezaee, K., Cancer stem cells (CSCs) in cancer progression and therapy. *J Cell Physiol.* **2019,** *234* (6), 8381-8395.

171.   Schulze, M.; Violonchi, C.; Swoboda, S.; Welz, T.; Kerkhoff, E.; Hoja, S.; Bruggemann, S.; Simburger, J.; Reinders, J.; Riemenschneider, M. J., RELN signaling modulates glioblastoma growth and substrate-dependent migration. *Brain Pathol.* **2018,** *28* (5), 695-709.

172.   Luo, Y.; Huang, K.; Zheng, J.; Zhang, J.; Zhang, L., TGF-beta1 promotes cell migration in hepatocellular carcinoma by suppressing reelin expression. *Gene.* **2019,** *688*, 19-25.

173.   Yuan, Y.; Chen, H.; Ma, G.; Cao, X.; Liu, Z., Reelin is involved in transforming growth factor-beta1-induced cell migration in esophageal carcinoma cells. *PLoS One.* **2012,** *7* (2), e31802.

174. Hernandez-Verdun, D.; Roussel, P.; Thiry, M.; Sirri, V.; Lafontaine, D. L., The nucleolus: structure/function relationship in RNA metabolism. *Wiley Interdiscip Rev RNA.* **2010,** *1* (3), 415-431.

175. Wang, H.; Wang, L.; Wang, Z.; Dang, Y.; Shi, Y.; Zhao, P.; Zhang, K., The nucleolar protein NOP2 is required for nucleolar maturation and ribosome biogenesis during preimplantation development in mammals. *FASEB J.* **2020,** *34* (2), 2715-2729.

176. Sharma, S.; Yang, J.; Watzinger, P.; Kotter, P.; Entian, K. D., Yeast Nop2 and Rcm1 methylate C2870 and C2278 of the 25S rRNA, respectively. *Nucleic Acids Res.* **2013,** *41* (19), 9062-9076.

177. Zhang, C.; Yin, C.; Wang, L.; Zhang, S.; Qian, Y.; Ma, J.; Zhang, Z.; Xu, Y.; Liu, S., HSPC111 governs breast cancer growth by regulating ribosomal biogenesis. *Mol Cancer Res.* **2014,** *12* (4), 583-594.

178. Landrieux, E.; Alic, N.; Ducrot, C.; Acker, J.; Riva, M.; Carles, C., A subcomplex of RNA polymerase III subunits involved in transcription termination and reinitiation. *EMBO J.* **2006,** *25* (1), 118-128.

179. Carlton, J. G.; Caballe, A.; Agromayor, M.; Kloc, M.; Martin-Serrano, J., ESCRT-III governs the Aurora B-mediated abscission checkpoint through CHMP4C. *Science.* **2012,** *336* (6078), 220-225.

180. Capalbo, L.; Montembault, E.; Takeda, T.; Bassi, Z. I.; Glover, D. M.; D'Avino, P. P., The chromosomal passenger complex controls the function of endosomal sorting complex required for transport-III Snf7 proteins during cytokinesis. *Open Biol.* **2012,** *2* (5), 120070.

181. Min, D. J.; Vural, S.; Krushkal, J., Association of transcriptional levels of folate-mediated one-carbon metabolism-related genes in cancer cell lines with drug treatment response. *Cancer Genet.* **2019,** *237*, 19-38.

182. Hornbeck, P. V.; Kornhauser, J. M.; Tkachev, S.; Zhang, B.; Skrzypek, E.; Murray, B.; Latham, V.; Sullivan, M., PhosphoSitePlus: a comprehensive resource for investigating the structure and function of experimentally determined post-translational modifications in man and mouse. *Nucleic Acids Res.* **2012,** *40* (Database issue), D261-270.

183. Snaebjornsson, M. T.; Schulze, A., Non-canonical functions of enzymes facilitate cross-talk between cell metabolic and regulatory pathways. *Exp Mol Med.* **2018,** *50* (4), 34.

184. Banks, C. J.; Andersen, J. L., Mechanisms of SOD1 regulation by post-translational modifications. *Redox Biol.* **2019,** *26*, 101270.

185. Selcuklu, S. D.; Donoghue, M. T.; Rehmet, K.; de Souza Gomes, M.; Fort, A.; Kovvuru, P.; Muniyappa, M. K.; Kerin, M. J.; Enright, A. J.; Spillane, C., MicroRNA-9 inhibition of cell

proliferation and identification of novel miR-9 targets by transcriptome profiling in breast cancer cells. *J Biol Chem.* **2012,** *287* (35), 29516-29528.

186.   Gu, Y.; Si, J.; Xiao, X.; Tian, Y.; Yang, S., miR-92a inhibits proliferation and induces apoptosis by regulating methylenetetrahydrofolate dehydrogenase 2 (MTHFD2) expression in acute myeloid leukemia. *Oncol Res.* **2017,** *25* (7), 1069-1079.

187.   Xu, T.; Zhang, K.; Shi, J.; Huang, B.; Wang, X.; Qian, K.; Ma, T.; Qian, T.; Song, Z.; Li, L., MicroRNA-940 inhibits glioma progression by blocking mitochondrial folate metabolism through targeting of MTHFD2. *Am J Cancer Res.* **2019,** *9* (2), 250-269.

188.   Zou, Z. Y.; Liu, J.; Chang, C.; Li, J. J.; Luo, J.; Jin, Y.; Ma, Z.; Wang, T. H.; Shao, J. L., Biliverdin administration regulates the microRNA-mRNA expressional network associated with neuroprotection in cerebral ischemia reperfusion injury in rats. *Int J Mol Med.* **2019,** *43* (3), 1356-1372.

189.   Zhou, J.; Bi, C.; Ching, Y. Q.; Chooi, J. Y.; Lu, X.; Quah, J. Y.; Toh, S. H.; Chan, Z. L.; Tan, T. Z.; Chong, P. S.; Chng, W. J., Inhibition of LIN28B impairs leukemia cell growth and metabolism in acute myeloid leukemia. *J Hematol Oncol.* **2017,** *10* (1), 138.

190.   Zhao, X. B.; Ren, G. S., LncRNA taurine-upregulated gene 1 promotes cell proliferation by inhibiting microRNA-9 in MCF-7 cells. *J Breast Cancer.* **2016,** *19* (4), 349-357.

191.   Tong, D.; Zhang, J.; Wang, X.; Li, Q.; Liu, L.; Lu, A.; Guo, B.; Yang, J.; Ni, L.; Qin, H.; Zhao, L.; Huang, C., MiR-22, regulated by MeCP2, suppresses gastric cancer cell proliferation by inducing a deficiency in endogenous S-adenosylmethionine. *Oncogenesis.* **2020,** *9* (11), 99.

192.   Wei, G. G.; Guo, W. P.; Tang, Z. Y.; Li, S. H.; Wu, H. Y.; Zhang, L. C., Expression level and prospective mechanism of miRNA-99a-3p in head and neck squamous cell carcinoma based on miRNA-chip and miRNA-sequencing data in 1, 167 cases. *Pathol Res Pract.* **2019,** *215* (5), 963-976.

193.   Jones, D. Z.; Schmidt, M. L.; Suman, S.; Hobbing, K. R.; Barve, S. S.; Gobejishvili, L.; Brock, G.; Klinge, C. M.; Rai, S. N.; Park, J.; Clark, G. J.; Agarwal, R.; Kidd, L. R., Micro-RNA-186-5p inhibition attenuates proliferation, anchorage independent growth and invasion in metastatic prostate cancer cells. *BMC Cancer.* **2018,** *18* (1), 421.

194.   Gamazon, E. R.; Trendowski, M. R.; Wen, Y.; Wing, C.; Delaney, S. M.; Huh, W.; Wong, S.; Cox, N. J.; Dolan, M. E., Gene and microRNA perturbations of cellular response to pemetrexed implicate biological networks and enable imputation of response in lung adenocarcinoma. *Sci Rep.* **2018,** *8* (1), 733.

195.   Zhang, J.; Xu, A.; Miao, C.; Yang, J.; Gu, M.; Song, N., Prognostic value of Lin28A and Lin28B in various human malignancies: a systematic review and meta-analysis. *Cancer Cell Int.* **2019,** *19*, 79.

196.   Rogers, M. A.; Kalter, V.; Strowitzki, M.; Schneider, M.; Lichter, P., IGF2 knockdown in two colorectal cancer cell lines decreases survival, adhesion and modulates survival-associated genes. *Tumour Biol.* **2016,** *37* (9), 12485-12495.

197.   Cronstein, B. N.; Aune, T. M., Methotrexate and its mechanisms of action in inflammatory arthritis. *Nat Rev Rheumatol.* **2020,** *16* (3), 145-154.

198.   Her, N. G.; Kesari, S.; Nurmemmedov, E., Thrombospondin-1 counteracts the p97 inhibitor CB-5083 in colon carcinoma cells. *Cell Cycle.* **2020,** *19* (13), 1590-1601.

199.   Liu, X.; Xu, D.; Liu, Z.; Li, Y.; Zhang, C.; Gong, Y.; Jiang, Y.; Xing, B., THBS1 facilitates colorectal liver metastasis through enhancing epithelial-mesenchymal transition. *Clin Transl Oncol.* **2020,** *22* (10), 1730-1740.

200.   Scharenberg, M. A.; Pippenger, B. E.; Sack, R.; Zingg, D.; Ferralli, J.; Schenk, S.; Martin, I.; Chiquet-Ehrismann, R., TGF-beta-induced differentiation into myofibroblasts involves specific regulation of two MKL1 isoforms. *J Cell Sci.* **2014,** *127* (Pt 5), 1079-1091.

201.   Pal, S. K.; Nguyen, C. T.; Morita, K. I.; Miki, Y.; Kayamori, K.; Yamaguchi, A.; Sakamoto, K., THBS1 is induced by TGFB1 in the cancer stroma and promotes invasion of oral squamous cell carcinoma. *J Oral Pathol Med.* **2016,** *45* (10), 730-739.

202.   Ahmadi, A.; Najafi, M.; Farhood, B.; Mortezaee, K., Transforming growth factor-beta signaling: Tumorigenesis and targeting for cancer therapy. *J Cell Physiol.* **2019,** *234* (8), 12173-12187.

203.   Wang, M.; Yuan, F.; Bai, H.; Zhang, J.; Wu, H.; Zheng, K.; Zhang, W.; Miao, M.; Gong, J., SHMT2 promotes liver regeneration through glycine-activated Akt/mTOR pathway. *Transplantation.* **2019,** *103* (7), e188-e197.

204.   Paulsen, M. T.; Veloso, A.; Prasad, J.; Bedi, K.; Ljungman, E. A.; Tsan, Y. C.; Chang, C. W.; Tarrier, B.; Washburn, J. G.; Lyons, R.; Robinson, D. R.; Kumar-Sinha, C.; Wilson, T. E.; Ljungman, M., Coordinated regulation of synthesis and stability of RNA during the acute TNF-induced proinflammatory response. *Proc Natl Acad Sci USA.* **2013,** *110* (6), 2240-2245.

205.   Gjerstorff, M. F.; Ditzel, H. J., An overview of the GAGE cancer/testis antigen family with the inclusion of newly identified members. *Tissue Antigens.* **2008,** *71* (3), 187-192.

206.   Kular, R. K.; Yehiely, F.; Deiss, L. P., Rational drug design: a GAGE derived peptide kills tumor cells. *Cancer Biol Ther.* **2010,** *9* (10), 825-831.

207.   Clark, N.; Wu, X.; Her, C., MutS homologues hMSH4 and hMSH5: genetic variations, functions, and implications in human diseases. *Curr Genomics.* **2013,** *14*, 81-90.

208.   Di Bernardo, G.; Alessio, N.; Dell'Aversana, C.; Casale, F.; Teti, D.; Cipollaro, M.; Altucci, L.; Galderisi, U., Impact of histone deacetylase inhibitors SAHA and MS-275 on DNA repair pathways in human mesenchymal stem cells. *J Cell Physiol.* **2010,** *225* (2), 537-544.

209.   Smith, R. D.; Lupashin, V. V., Role of the conserved oligomeric Golgi (COG) complex in protein glycosylation. *Carbohydr Res.* **2008,** *343* (12), 2024-2031.

210.   Pokrovskaya, I. D.; Willett, R.; Smith, R. D.; Morelle, W.; Kudlyk, T.; Lupashin, V. V., Conserved oligomeric Golgi complex specifically regulates the maintenance of Golgi glycosylation machinery. *Glycobiology.* **2011,** *21* (12), 1554-1569.

211.   Pereira-Castro, I.; Costa, L. T.; Amorim, A.; Azevedo, L., Transcriptional regulation of the human mitochondrial peptide deformylase (PDF). *Biochem Biophys Res Commun.* **2012,** *421* (4), 825-831.

212.   Tato, C. M.; Joyce-Shaikh, B.; Banerjee, A.; Chen, Y.; Sathe, M.; Ewald, S. E.; Liu, M. R.; Gorman, D.; McClanahan, T. K.; Phillips, J. H.; Heyworth, P. G.; Cua, D. J., The myeloid receptor PILRbeta mediates the balance of inflammatory responses through regulation of IL-27 production. *PLoS One.* **2012,** *7* (3), e31680.

213.   Peng, W. S.; Qi, C.; Zhang, H.; Gao, M. L.; Wang, H.; Ren, F.; Li, X. Q., Distribution of paired immunoglobulin-like receptor B in the nervous system related to regeneration difficulties after unilateral lumbar spinal cord injury. *Neural Regen Res.* **2015,** *10* (7), 1139-1146.

214.   Leonard, S.; Kinsella, G. K.; Benetti, E.; Findlay, J. B. C., Regulating the effects of GPR21, a novel target for type 2 diabetes. *Sci Rep.* **2016,** *6*, 27002.

215.   Romero-Nava, R.; Garcia, N.; Aguayo-Ceron, K. A.; Sanchez Munoz, F.; Huang, F.; Hong, E.; Villafana, S., Modifications in GPR21 and GPR82 genes expression as a consequence of metabolic syndrome etiology. *J Recept Signal Transduct Res.* **2020**, 1-7.

216.   Gardner, J.; Wu, S.; Ling, L.; Danao, J.; Li, Y.; Yeh, W. C.; Tian, H.; Baribault, H., G-protein-coupled receptor GPR21 knockout mice display improved glucose tolerance and increased insulin response. *Biochem Biophys Res Commun.* **2012,** *418* (1), 1-5.

217.   Wang, J.; Pan, Z.; Baribault, H.; Chui, D.; Gundel, C.; Veniant, M., GPR21 KO mice demonstrate no resistance to high fat diet induced obesity or improved glucose tolerance. *F1000Res.* **2016,** *5*, 136.

218.   Kim, H. S.; Lyons, K. M.; Saitoh, E.; Azen, E. A.; Smithies, O.; Maeda, N., The structure and evolution of the human salivary proline-rich protein gene family. *Mamm Genome.* **1993,** *4*, 3-14.

219.   Ekizoglu, S.; Ulutin, T.; Guliyev, J.; Buyru, N., PRR4: A novel downregulated gene in laryngeal cancer. *Oncol Lett.* **2018,** *15* (4), 4669-4675.

220.   Zhan, J.; Wang, P.; Niu, M.; Wang, Y.; Zhu, X.; Guo, Y.; Zhang, H., High expression of transcriptional factor HoxB9 predicts poor prognosis in patients with lung adenocarcinoma. *Histopathology.* **2015,** *66* (7), 955-965.

221.   Wan, J.; Xu, W.; Zhan, J.; Ma, J.; Li, X.; Xie, Y.; Wang, J.; Zhu, W. G.; Luo, J.; Zhang, H., PCAF-mediated acetylation of transcriptional factor HOXB9 suppresses lung adenocarcinoma progression by targeting oncogenic protein JMJD6. *Nucleic Acids Res.* **2016,** *44* (22), 10662-10675.

222.   Hayashi, K.; Ouchi, M.; Endou, H.; Anzai, N., HOXB9 acts as a negative regulator of activated human T cells in response to amino acid deficiency. *Immunol Cell Biol.* **2016,** *94* (6), 612-617.

223.   Razak, M. A.; Begum, P. S.; Viswanath, B.; Rajagopal, S., Multifarious beneficial effect of nonessential amino acid, glycine: a review. *Oxid Med Cell Longev.* **2017,** *2017*, 1716701.

224.   Nakamura, T.; Ohnuma, T.; Hanzawa, R.; Takebayashi, Y.; Takeda, M.; Nishimon, S.; Sannohe, T.; Katsuta, N.; Higashiyama, R.; Shibata, N.; Arai, H., Associations of common copy number variants in glutathione S-transferase mu 1 and D-dopachrome tautomerase-like protein genes with risk of schizophrenia in a Japanese population. *Am J Med Genet B Neuropsychiatr Genet.* **2015,** *168* (7), 630-636.

225.   Serizawa, M.; Takahashi, T.; Yamamoto, N.; Koh, Y., Genomic aberrations associated with erlotinib resistance in non-small cell lung cancer cells. *Anticancer Res.* **2013,** *33*, 5223-5234.

226.   Li, X.; Zhang, K.; Hu, Y.; Luo, N., ERRalpha activates SHMT2 transcription to enhance the resistance of breast cancer to lapatinib via modulating the mitochondrial metabolic adaption. *Biosci Rep.* **2020,** *40* (1), BSR20192465.

227.   Yang, L.; Garcia Canaveras, J. C.; Chen, Z.; Wang, L.; Liang, L.; Jang, C.; Mayr, J. A.; Zhang, Z.; Ghergurovich, J. M.; Zhan, L.; Joshi, S.; Hu, Z.; McReynolds, M. R.; Su, X.; White, E.; Morscher, R. J.; Rabinowitz, J. D., Serine catabolism feeds NADH when respiration is impaired. *Cell Metab.* **2020,** *31* (4), 809-821.

228.   Song, H.; Park, K. H., Regulation and function of SOX9 during cartilage development and regeneration. *Semin Cancer Biol.* **2020**.

229.   Jana, S.; Madhu Krishna, B.; Singhal, J.; Horne, D.; Awasthi, S.; Salgia, R.; Singhal, S. S., SOX9: The master regulator of cell fate in breast cancer. *Biochem Pharmacol.* **2020,** *174*, 113789.

230.   Zhu, Z.; Leung, G. K. K., More than a metabolic enzyme: MTHFD2 as a novel target for anticancer therapy? *Front Oncol.* **2020,** *10*, 658.

231.   Lo, P. K., FOXF2 differentially regulates expression of metabolic genes in non-cancerous and cancerous breast epithelial cells. *Trends Diabetes Metab.* **2018,** *1* (1).

232.   He, W.; Kang, Y.; Zhu, W.; Zhou, B.; Jiang, X.; Ren, C.; Guo, W., FOXF2 acts as a crucial molecule in tumours and embryonic development. *Cell Death Dis.* **2020,** *11* (6), 424.

233.   McKay, J. A.; Xie, L.; Adriaens, M.; Evelo, C. T.; Ford, D.; Mathers, J. C., Maternal folate depletion during early development and high fat feeding from weaning elicit similar changes in gene expression, but not in DNA methylation, in adult offspring. *Mol Nutr Food Res.* **2017,** *61* (4), 1600713.

234.   Jain, M. N., R.; Sharma, S.; Madhusuhan, N.; Kitami, T.; Souza, A.L.; Kafri, R.; Kirschner, M.W.; Clish, C.B. Mootha, V.K., Metabolite profiling identifies a key role for glycine in rapid cancer cell proliferation. *Science.* **2012,** *336*, 1040-1044.

235.   Paone, A.; Marani, M.; Fiascarelli, A.; Rinaldo, S.; Giardina, G.; Contestabile, R.; Paiardini, A.; Cutruzzola, F., SHMT1 knockdown induces apoptosis in lung cancer cells by causing uracil misincorporation. *Cell Death Dis.* **2014,** *5*, e1525.

236.   Monteiro, F. L.; Baptista, T.; Amado, F.; Vitorino, R.; Jerónimo, C.; Helguero, L. A., Expression and functionality of histone H2A variants in cancer. *Oncotarget.* **2014,** *5*, 3428-3443.

237.   Sharma, J.; Krupenko, S. A., Folate pathways mediating the effects of ethanol in tumorigenesis. *Chem Biol Interact.* **2020,** *324*, 109091.

238.   He, J.; Ma, J.; Ren, B.; Liu, A., Advances in systemic lupus erythematosus pathogenesis via mTOR signaling pathway. *Semin Arthritis Rheum.* **2020,** *50* (2), 314-320.

239.   Salimi, S.; Keshavarzi, F.; Mohammadpour-Gharehbagh, A.; Moodi, M.; Mousavi, M.; Karimian, M.; Sandoughi, M., Polymorphisms of the folate metabolizing enzymes: association with SLE susceptibility and in silico analysis. *Gene.* **2017,** *637*, 161-172.

240.   Kalunian, K. C.; Merrill, J. T.; Maciuca, R.; McBride, J. M.; Townsend, M. J.; Wei, X.; Davis Jr, J. C.; Kennedy, W. P., A Phase II study of the efficacy and safety of rontalizumab (rhuMAb interferon-α) in patients with systemic lupus erythematosus (ROSE). *Ann Rheum Dis.* **2016,** *75*, 196-202.

241.   Lamort, A. S.; Giopanou, I.; Psallidas, I.; Stathopoulos, G. T., Osteopontin as a link between inflammation and cancer: the thorax in the spotlight. *Cells.* **2019,** *8*, 815.

242.   Zhao, H.; Chen, Q.; Alam, A.; Cui, J.; Suen, K. C.; Soo, A. P.; Eguchi, S.; Gu, J.; Ma, D., The role of osteopontin in the progression of solid organ tumour. *Cell Death Dis.* **2018,** *9* (3), 356.

243.   Takeuchi, S.; Seike, M.; Noro, R.; Soeno, C.; Sugano, T.; Zou, F.; Uesaka, H.; Nishijima, N.; Matsumoto, M.; Minegishi, Y.; Kubota, K.; Gemma, A., Significance of osteopontin in the

sensitivity of malignant pleural mesothelioma to pemetrexed. *Int J Oncol.* **2014,** *44* (6), 1886-1894.

244.   Ju, J. A.; Gilkes, D. M., RhoB: team oncogene or team tumor suppressor? *Genes (Basel).* **2018,** *9* (2), 67.

245.   Yang, Y. Y.; Yu, K.; Li, L.; Huang, M.; Wang, Y., Proteome-wide interrogation of small GTPases regulated by N(6)-methyladenosine modulators. *Anal Chem.* **2020,** *92* (14), 10145-10152.

246.   Xiao, S.; Jin-Xiang, Y.; Long, T.; Xiu-Rong, L.; Hong, G.; Jie-Cheng, Y.; Fei, Z., Kruppel-like factor 2 disturb non-small cell lung cancer energy metabolism by inhibited glutamine consumption. *J Pharm Pharmacol.* **2020,** *72* (6), 843-851.

247.   McConnell, B. B.; Yang, V. W., Mammalian Kruppel-like factors in health and diseases. *Physiol Rev.* **2010,** *90* (4), 1337-1381.

248.   Hsieh, P. N.; Fan, L.; Sweet, D. R.; Jain, M. K., The Kruppel-like factors and control of energy homeostasis. *Endocr Rev.* **2019,** *40* (1), 137-152.

249.   Kaczynski, J.; Cook, T.; Urrutia, R., Sp1- and Krüppel-like transcription factors. *Genome Biol.* **2003,** *4*, 206.

250.   Fu, C. A.; Shen, M.; Huang, B. C. B.; Lasaga, J.; Payan, D. G.; Luo, Y., TNIK, a novel member of the germinal center kinase family that activates the c-Jun N-terminal kinase pathway and regulates the cytoskeleton. *J Biol Chem.* **1999,** *274*, 30729-30737.

251.   Mahmoudi, T.; Li, V. S.; Ng, S. S.; Taouatas, N.; Vries, R. G.; Mohammed, S.; Heck, A. J.; Clevers, H., The kinase TNIK is an essential activator of Wnt target genes. *EMBO J.* **2009,** *28* (21), 3329-3340.

252.   Rosenzweig, A.; Blenis, J.; Gomes, A. P., Beyond the Warburg effect: how do cancer cells regulate one-carbon metabolism? *Front Cell Dev Biol.* **2018,** *6*, 90.

253.   Ducker, G. S.; Rabinowitz, J. D., One-carbon metabolism in health and disease. *Cell Metab.* **2017,** *25* (1), 27-42.

254.   Choi, H. I.; Lee, S. P.; Kim, K. S.; Hwang, C. Y.; Lee, Y. R.; Chae, S. K.; Kim, Y. S.; Chae, H. Z.; Kwon, K. S., Redox-regulated cochaperone activity of the human DnaJ homolog Hdj2. *Free Radic Biol Med.* **2006,** *40* (4), 651-659.

255.   Reich, S.; Nguyen, C. D. L.; Has, C.; Steltgens, S.; Soni, H.; Coman, C.; Freyberg, M.; Bichler, A.; Seifert, N.; Conrad, D.; Knobbe-Thomsen, C. B.; Tews, B.; Toedt, G.; Ahrends, R.; Medenbach, J., A multi-omics analysis reveals the unfolded protein response regulon and stress-induced resistance to folate-based antimetabolites. *Nat Commun.* **2020,** *11* (1), 2936.

256.   Osorio, F.; Tavernier, S. J.; Hoffmann, E.; Saeys, Y.; Martens, L.; Vetters, J.; Delrue, I.; De Rycke, R.; Parthoens, E.; Pouliot, P.; Iwawaki, T.; Janssens, S.; Lambrecht, B. N., The unfolded-protein-response sensor IRE-1alpha regulates the function of CD8alpha+ dendritic cells. *Nat Immunol.* **2014,** *15* (3), 248-257.

257.   Stover, P. J.; Chen, L. H.; Suh, J. R.; Stover, D. M.; Keymarsi, K.; Shane, B., Molecular cloning, characterization, and regulation of the human mitochondrial serine hydroxymethyltransferase gene. *J Biol Chem.* **1997,** *272*, 1842-1848.

258.   Poliakova, M.; Aebersold, D. M.; Zimmer, Y.; Medova, M., The relevance of tyrosine kinase inhibitors for global metabolic pathways in cancer. *Mol Cancer.* **2018,** *17* (1), 27.

259.   Rodriguez-Hernandez, M. A.; de la Cruz-Ojeda, P.; Lopez-Grueso, M. J.; Navarro-Villaran, E.; Requejo-Aguilar, R.; Castejon-Vega, B.; Negrete, M.; Gallego, P.; Vega-Ochoa, A.; Victor, V. M.; Cordero, M. D.; Del Campo, J. A.; Barcena, J. A.; Padilla, C. A.; Muntane, J., Integrated molecular signaling involving mitochondrial dysfunction and alteration of cell metabolism induced by tyrosine kinase inhibitors in cancer. *Redox Biol.* **2020,** *36*, 101510.

260.   Bhat, A. A.; Syed, N.; Therachiyil, L.; Nisar, S.; Hashem, S.; Macha, M. A.; Yadav, S. K.; Krishnankutty, R.; Muralitharan, S.; Al-Naemi, H.; Bagga, P.; Reddy, R.; Dhawan, P.; Akobeng, A.; Uddin, S.; Frenneaux, M. P.; El-Rifai, W.; Haris, M., Claudin-1, a double-edged sword in cancer. *Int J Mol Sci.* **2020,** *21* (2), 569.

261.   Zhang, G.; Isaji, T.; Xu, Z.; Lu, X.; Fukuda, T.; Gu, J., N-acetylglucosaminyltransferase-I as a novel regulator of epithelial-mesenchymal transition. *FASEB J.* **2019,** *33* (2), 2823-2835.

262.   Detarya, M.; Sawanyawisuth, K.; Aphivatanasiri, C.; Chuangchaiya, S.; Saranaruk, P.; Sukprasert, L.; Silsirivanit, A.; Araki, N.; Wongkham, S.; Wongkham, C., The O-GalNAcylating enzyme GALNT5 mediates carcinogenesis and progression of cholangiocarcinoma via activation of AKT/ERK signaling. *Glycobiology.* **2020,** *30* (5), 312-324.

263.   Tong, H.; Li, T.; Qiu, W.; Zhu, Z., Claudin-1 silencing increases sensitivity of liver cancer HepG2 cells to 5-fluorouracil by inhibiting autophagy. *Oncol Lett.* **2019,** *18* (6), 5709-5716.

264.   Mondal, D.; Mathur, A.; Chandra, P. K., Tripping on TRIB3 at the junction of health, metabolic dysfunction and cancer. *Biochimie.* **2016,** *124*, 34-52.

265.   Schwarzer, R.; Dames, S.; Tondera, D.; Klippel, A.; Kaufmann, J., TRB3 is a PI 3-kinase dependent indicator for nutrient starvation. *Cell Signal.* **2006,** *18* (6), 899-909.

266.   Shin, E. J.; Shin, H. M.; Nam, E.; Kim, W. S.; Kim, J. H.; Oh, B. H.; Yun, Y., DeSUMOylating isopeptidase: a second class of SUMO protease. *EMBO Rep.* **2012,** *13* (4), 339-346.

267.   Woeller, C. F.; Anderson, D. D.; Szebenyi, D. M.; Stover, P. J., Evidence for small ubiquitin-like modifier-dependent nuclear import of the thymidylate biosynthesis pathway. *J Biol Chem.* **2007,** *282* (24), 17623-17631.

268.   Anderson, D. D.; Stover, P. J., SHMT1 and SHMT2 are functionally redundant in nuclear de novo thymidylate biosynthesis. *PLoS One.* **2009,** *4* (6), e5839.

269.   Anderson, D. D.; Eom, J. Y.; Stover, P. J., Competition between sumoylation and ubiquitination of serine hydroxymethyltransferase 1 determines its nuclear localization and its accumulation in the nucleus. *J Biol Chem.* **2012,** *287* (7), 4790-4799.

270.   Kamynina, E.; Lachenauer, E. R.; DiRisio, A. C.; Liebenthal, R. P.; Field, M. S.; Stover, P. J., Arsenic trioxide targets MTHFD1 and SUMO-dependent nuclear de novo thymidylate biosynthesis. *Proc Natl Acad Sci USA.* **2017,** *114* (12), E2319-E2326.

271.   Fox, J. T.; Shin, W. K.; Caudill, M. A.; Stover, P. J., A UV-responsive internal ribosome entry site enhances serine hydroxymethyltransferase 1 expression for DNA damage repair. *J Biol Chem.* **2009,** *284* (45), 31097-31108.

272.   Lorente, M.; Garcia-Casas, A.; Salvador, N.; Martinez-Lopez, A.; Gabicagogeascoa, E.; Velasco, G.; Lopez-Palomar, L.; Castillo-Lluva, S., Inhibiting SUMO1-mediated SUMOylation induces autophagy-mediated cancer cell death and reduces tumour cell invasion via RAC1. *J Cell Sci.* **2019,** *132* (20), jcs234120.

273.   Kinoshita, T., Congenital defects in the expression of the glycosylphosphatidylinositol-anchored complement regulatory proteins CD59 and decay-accelerating factor. *Semin Hematol.* **2018,** *55* (3), 136-140.

274.   Meng, T.; Huang, R.; Zeng, Z.; Huang, Z.; Yin, H.; Jiao, C.; Yan, P.; Hu, P.; Zhu, X.; Li, Z.; Song, D.; Zhang, J.; Cheng, L., Identification of prognostic and metastatic alternative splicing signatures in kidney renal clear cell carcinoma. *Front Bioeng Biotechnol.* **2019,** *7*, 270.

275.   Awasthi, S.; Chakrapani, B.; Mahesh, A.; Chavali, P. L.; Chavali, S.; Dhayalan, A., DDX39B promotes translation through regulation of pre-ribosomal RNA levels. *RNA Biol.* **2018,** *15* (9), 1157-1166.

276.   Szymura, S. J.; Bernal, G. M.; Wu, L.; Zhang, Z.; Crawley, C. D.; Voce, D. J.; Campbell, P. A.; Ranoa, D. E.; Weichselbaum, R. R.; Yamini, B., DDX39B interacts with the pattern recognition receptor pathway to inhibit NF-kappaB and sensitize to alkylating chemotherapy. *BMC Biol.* **2020,** *18* (1), 32.

277.   Claro da Silva, T.; Polli, J. E.; Swaan, P. W., The solute carrier family 10 (SLC10): beyond bile acid transport. *Mol Aspects Med.* **2013,** *34* (2-3), 252-269.

278.   Sharif, P. M.; Jabbari, P.; Razi, S.; Keshavarz-Fathi, M.; Rezaei, N., Importance of TNF-alpha and its alterations in the development of cancers. *Cytokine.* **2020,** *130*, 155066.

279.   Vaughan, R. A.; Garcia-Smith, R.; Dorsey, J.; Griffith, J. K.; Bisoffi, M.; Trujillo, K. A., Tumor necrosis factor alpha induces Warburg-like metabolism and is reversed by anti-inflammatory curcumin in breast epithelial cells. *Int J Cancer.* **2013,** *133* (10), 2504-2510.

280.   Straus, D. S., TNFα and IL-17 cooperatively stimulate glucose metabolism and growth factor production in human colorectal cancer cells. *Mol Cancer.* **2013,** *12*, 78.

281.   Tarasenko, T. N.; Jestin, M.; Matsumoto, S.; Saito, K.; Hwang, S.; Gavrilova, O.; Trivedi, N.; Zerfas, P. M.; Barca, E.; DiMauro, S.; Senac, J.; Venditti, C. P.; Cherukuri, M.; McGuire, P. J., Macrophage derived TNFalpha promotes hepatic reprogramming to Warburg-like metabolism. *J Mol Med (Berl).* **2019,** *97* (9), 1231-1243.

282.   Hahn, W. S.; Kuzmicic, J.; Burrill, J. S.; Donoghue, M. A.; Foncea, R.; Jensen, M. D.; Lavandero, S.; Arriaga, E. A.; Bernlohr, D. A., Proinflammatory cytokines differentially regulate adipocyte mitochondrial metabolism, oxidative stress, and dynamics. *Am J Physiol Endocrinol Metab.* **2014,** *306* (9), E1033-1045.

283.   Duan, W.; Li, H., Combination of NF-kB targeted siRNA and methotrexate in a hybrid nanocarrier towards the effective treatment in rheumatoid arthritis. *J Nanobiotechnology.* **2018,** *16* (1), 58.

284.   Hiltunen, J. K.; Kastaniotis, A. J.; Autio, K. J.; Jiang, G.; Chen, Z.; Glumoff, T., 17B-hydroxysteroid dehydrogenases as acyl thioester metabolizing enzymes. *Mol Cell Endocrinol.* **2019,** *489*, 107-118.

285.   Rotinen, M.; Celay, J.; Alonso, M. M.; Arrazola, A.; Encio, I.; Villar, J., Estradiol induces type 8 17beta-hydroxysteroid dehydrogenase expression: crosstalk between estrogen receptor alpha and C/EBPbeta. *J Endocrinol.* **2009,** *200* (1), 85-92.

286.   Sears, T. K.; Angelastro, J. M., The transcription factor ATF5: role in cellular differentiation, stress responses, and cancer. *Oncotarget.* **2017,** *8* (48), 84595-84609.

287.   DeNicola, G. M.; Chen, P. H.; Mullarky, E.; Sudderth, J. A.; Hu, Z.; Wu, D.; Tang, H.; Xie, Y.; Asara, J. M.; Huffman, K. E.; Wistuba, II; Minna, J. D.; DeBerardinis, R. J.; Cantley, L. C., NRF2 regulates serine biosynthesis in non-small cell lung cancer. *Nat Genet.* **2015,** *47* (12), 1475-1481.

288.   Celardo, I.; Lehmann, S.; Costa, A. C.; Loh, S. H.; Miguel Martins, L., dATF4 regulation of mitochondrial folate-mediated one-carbon metabolism is neuroprotective. *Cell Death Differ.* **2017,** *24* (4), 638-648.

289.   Jiang, J.-H.; Zhao, Y.; Xiao, L.-L.; Zhu, C.-S.; Li, S.-F.; Li, X., Activating transcription factor 5 regulates lipid metabolism in adipocytes. *Sci Bull.* **2016,** *61* (23), 1802-1809.

290.   Shimizu, Y. I.; Morita, M.; Ohmi, A.; Aoyagi, S.; Ebihara, H.; Tonaki, D.; Horino, Y.; Iijima, M.; Hirose, H.; Takahashi, S.; Takahashi, Y., Fasting induced up-regulation of activating transcription factor 5 in mouse liver. *Life Sci.* **2009,** *84* (25-26), 894-902.

291.   Al Sarraj, J.; Vinson, C.; Thiel, G., Regulation of asparagine synthetase gene transcription by the basic region leucine zipper transcription factors ATF5 and CHOP. *Biol Chem.* **2005,** *386* (9), 873-879.

292.   Guo, X.; Ni, J.; Zhu, Y.; Zhou, T.; Ma, X.; Xue, J.; Wang, X., Folate deficiency induces mitotic aberrations and chromosomal instability by compromising the spindle assembly checkpoint in cultured human colon cells. *Mutagenesis.* **2017,** *32* (6), 547-560.

293.   Blount, B. C.; Mack, M. M.; Wehr, C. M.; MacGregor, J. T.; Hiatt, R. A.; Wang, G.; Wickramasinghe, S. N.; Everson, R. B.; Ames, B. N., Folate deficiency causes uracil misincorporation into human DNA and chromosome breakage: Implications for cancer and neuronal damage. *Proc Natl Acad Sci USA.* **1997,** *94*, 3290-3295.

294.   Brotto, D. B.; Siena, A. D. D.; de, B., II; Carvalho, S.; Muys, B. R.; Goedert, L.; Cardoso, C.; Placa, J. R.; Ramao, A.; Squire, J. A.; Araujo, L. F.; Silva, W. A. D., Jr., Contributions of HOX genes to cancer hallmarks: Enrichment pathway analysis and review. *Tumour Biol.* **2020,** *42* (5), 1-16.

295.   Abel, E. V.; Basile, K. J.; Kugel, C. H., 3rd; Witkiewicz, A. K.; Le, K.; Amaravadi, R. K.; Karakousis, G. C.; Xu, X.; Xu, W.; Schuchter, L. M.; Lee, J. B.; Ertel, A.; Fortina, P.; Aplin, A. E., Melanoma adapts to RAF/MEK inhibitors through FOXD3-mediated upregulation of ERBB3. *J Clin Invest.* **2013,** *123* (5), 2155-2168.

296.   Basile, K. J.; Abel, E. V.; Dadpey, N.; Hartsough, E. J.; Fortina, P.; Aplin, A. E., In vivo MAPK reporting reveals the heterogeneity in tumoral selection of resistance to RAF inhibitors. *Cancer Res.* **2013,** *73* (23), 7101-7110.

297.   Love, M. I.; Huber, W.; Anders, S., Moderated estimation of fold change and dispersion for RNA-seq data with DESeq2. *Genome Biol.* **2014,** *15* (12), 550.

298.   Snel, B.; Lehman, G.; Bork, P.; Huynen, M. A., STRING: a web-server to retrieve and display the repeatedly occuring neighbourhood of a gene. *Nucleic Acids Res.* **2000,** *28* (18), 3442-3444.

299.   von Mering, C.; Huynen, M.; Jaeggi, D.; Schmidt, S.; Bork, P.; Snel, B., STRING: a database of predicted functional associations between proteins. *Nucleic Acids Res.* **2003,** *31* (1), 258-261.

300.   von Mering, C.; Jensen, L. J.; Snel, B.; Hooper, S. D.; Krupp, M.; Foglierini, M.; Jouffre, N.; Huynen, M. A.; Bork, P., STRING: known and predicted protein-protein associations, integrated and transferred across organisms. *Nucleic Acids Res.* **2005,** *33* (Database issue), D433-437.

301.   Szklarczyk, D.; Gable, A. L.; Lyon, D.; Junge, A.; Wyder, S.; Huerta-Cepas, J.; Simonovic, M.; Doncheva, N. T.; Morris, J. H.; Bork, P.; Jensen, L. J.; Mering, C. V., STRING v11: protein-protein association networks with increased coverage, supporting functional discovery in genome-wide experimental datasets. *Nucleic Acids Res.* **2019,** *47* (D1), D607-D613.

302.   Mootha, V. K.; Lindgren, C. M.; Eriksson, K. F.; Subramanian, A.; Sihag, S.; Lehar, J.; Puigserver, P.; Carlsson, E.; Ridderstråle, M.; Laurila, E.; Houstis, N.; Daly, M. J.; Patterson, N.; Mesirov, J. P.; Golub, T. R.; Tamayo, P.; Spiegelman, B.; Lander, E. S.; Hirschhorn, J. N.; Altshuler, D.; Groop, L. C., PGC-1α-responsive genes involved in oxidative phosphorylation are coordinately downregulated in human diabetes. *Nat Genet.* **2003,** *34* (3), 267-273.

303.   Subramanian, A.; Tamayo, P.; Mootha, V. K.; Mukherjee, S.; Ebert, B. L.; Gillette, M. A.; Paulovich, A.; Pomeroy, S. L.; Golub, T. R.; Lander, E. S.; Mesirov, J. P., Gene set enrichment analysis: A knowledge-based approach for interpreting genome-wide expression profiles. *Proc Natl Acad Sci USA.* **2005,** *102* (43), 15545-15550.

304.   Huang, D. W.; Sherman, B. T.; Lempicki, R. A., Bioinformatics enrichment tools: paths toward the comprehensive functional analysis of large gene lists. *Nucleic Acids Res.* **2009,** *37* (1), 1-13.

305.   Huang, D. W.; Sherman, B. T.; Lempicki, R. A., Systematic and integrative analysis of large gene lists using DAVID bioinformatics resources. *Nat Protoc.* **2009,** *4* (1), 44-57.

306.   Subramanian, A.; Narayan, R.; Corsello, S. M.; Peck, D. D.; Natoli, T. E.; Lu, X.; Gould, J.; Davis, J. F.; Tubelli, A. A.; Asiedu, J. K.; Lahr, D. L.; Hirschman, J. E.; Liu, Z.; Donahue, M.; Julian, B.; Khan, M.; Wadden, D.; Smith, I. C.; Lam, D.; Liberzon, A.; Toder, C.; Bagul, M.; Orzechowski, M.; Enache, O. M.; Piccioni, F.; Johnson, S. A.; Lyons, N. J.; Berger, A. H.; Shamji, A. F.; Brooks, A. N.; Vrcic, A.; Flynn, C.; Rosains, J.; Takeda, D. Y.; Hu, R.; Davison, D.; Lamb, J.; Ardlie, K.; Hogstrom, L.; Greenside, P.; Gray, N. S.; Clemons, P. A.; Silver, S.; Wu, X.; Zhao, W. N.; Read-Button, W.; Wu, X.; Haggarty, S. J.; Ronco, L. V.; Boehm, J. S.; Schreiber, S. L.; Doench, J. G.; Bittker, J. A.; Root, D. E.; Wong, B.; Golub, T. R., A next generation Connectivity Map: L1000 platform and the first 1,000,000 profiles. *Cell.* **2017,** *171* (6), 1437-1452.

307.   Lamb, J.; Crawford, E. D.; Peck, D.; Modell, J. W.; Blat, I. C.; Wrobel, M. J.; Lerner, J.; Brunet, J. P.; Subramanian, A.; Ross, K. N.; Reich, M.; Hieronymus, H.; Wei, G.; Armstrong, S. A.; Haggarty, S. J.; Clemons, P. A.; Wei, R.; Carr, S. A.; Lander, E. S.; Golub, T. R., The connectivity map: using gene-expression signatures to connect small molecules, genes, and diseases. *Science.* **2006,** *313*, 1929-1935.

308.   Dobin, A.; Davis, C. A.; Schlesinger, F.; Drenkow, J.; Zaleski, C.; Jha, S.; Batut, P.; Chaisson, M.; Gingeras, T. R., STAR: ultrafast universal RNA-seq aligner. *Bioinformatics.* **2013,** *29* (1), 15-21.

309.   Trapnell, C.; Williams, B. A.; Pertea, G.; Mortazavi, A.; Kwan, G.; van Baren, M. J.; Salzberg, S. L.; Wold, B. J.; Pachter, L., Transcript assembly and quantification by RNA-Seq reveals unannotated transcripts and isoform switching during cell differentiation. *Nat Biotechnol.* **2010,** *28* (5), 511-515.

310.   Liao, Y.; Smyth, G. K.; Shi, W., featureCounts: an efficient general purpose program for assigning sequence reads to genomic features. *Bioinformatics.* **2014,** *30* (7), 923-930.

CHAPTER III   The DHODH Inhibitor Brequinar is Synergistic with ENT1/2

Inhibitors

Introduction[3]

To generate the required concentrations of nucleotides for DNA replication and rapid cell growth, cancer cells often use *de novo* synthesis pathways.[1] This differs from normal cells that maintain nucleotide concentrations through nucleoside salvage pathways. This metabolic difference has led to the development of many inhibitors that can selectively target cancer cells by disrupting *de novo* synthesis.[2-3] *De novo* purine biosynthesis inhibitors have become standard-of-care chemotherapies for cancer, and part of their success is due to their transport across the cell membrane by nucleoside transporters.[4] 5-Fluorouracil (5FU), PALA, acivin, brequinar (BREQ), and leflunomide (LEF)/teriflunomide (TERF) are notable examples of pyrimidine biosynthesis inhibitors. While antimetabolites against purine metabolism have largely been successful, their pyrimidine counterparts have not, with the exception of 5FU, and the reason for this is not clear. LEF/TERF and BREQ all target the enzyme dihydroorotate dehydrogenase (DHODH). LEF, and its active metabolite TERF, are FDA-approved for the treatment of autoimmune diseases such as arthritis and multiple sclerosis.[5] Along with autoimmune diseases, DHODH plays a critical role in cancer, which has recently been extensively reviewed.[6-9] Despite BREQ's higher potency and

---

specificity over LEF/TERF (Appendix Table III-1), it failed all cancer clinical trials in solid tumors in the late 1980s and early 1990s. We are interested in exploring the potential to improve the effectiveness of the DHODH inhibitor BREQ by identifying synergistic proteins or pathways for a combination therapy.

DHODH is responsible for the oxidation of dihydroorotic acid to orotic acid. This reaction is the fourth, and committed, step in *de novo* pyrimidine synthesis and its inhibition via BREQ has potent anticancer properties in murine and human xenograft models of cancer.[10] Its promising anticancer potential led to multiple clinical trials, but BREQ failed to provide a significant objective response to patients with solid tumors.[11-16] *In vitro*, cells grown in nucleoside-supplemented media become insensitive to BREQ,[17-18] suggesting a compensatory mechanism exists. A Phase I trial found that after dosing of BREQ, DHODH activity was undetectable in lymphocytes within 15 min and even up to a week afterward,[19] but it is not known if tumor samples showed a similar profile. Moreover, as we show and others have seen, continuous treatment of BREQ as a single agent is necessary to observe a cellular effect, so the dosing regimen is also critical.[20] Additionally, lack of DHODH activity prevented nearly all tumor growth.[21] Clinical trials evaluated efficacy of IV infusions on a bi-weekly basis or for one week on, three weeks off, so it is unlikely that sustained inhibition was achieved. Additionally, plasma uridine levels rebounded after a significant initial decrease.[19] This suggests that BREQ's clinical trial failures might have resulted from the salvage pathway importing extracellular nucleosides to sustain cell viability. While the reason that BREQ failed human clinical trials is likely a complicated one, we were interested in gaining further understanding of the role of the salvage transporters as a compensation mechanism as a potential combination strategy.

De novo pyrimidine salvage pathways rely on two families of membrane bound transporters to import extracellular nucleosides: equilibrative nucleoside transporters (ENT1-4/SLC29A1-4) and concentrative nucleoside transporters (CNT1-3/SLC28A1-3).[22-23] Since their expression varies with subcellular localization and tissue distribution, normal cells utilize a combination of these two families to import nucleosides as fuel for salvage pathways. However, the ENT is a more effective nucleoside/nucleobase transporter and may present an important synergistic target (ENT1: 200 uridine molecules/s vs CNT1: 10 uridine molecules/s).[23-24] The differential expression of the ENTs is cancer-dependent. ENT1 was found to be overexpressed in colon cancer and some pancreatic cancer samples.[25-29] There are also numerous reports on the downregulation of ENT1 in pancreatic cancer,[30-32] with the majority attributed to a resistance mechanism developed from treatment with purine biosynthesis inhibitors (i.e., gemcitabine).[33-46] Therefore, it is possible that these tumors would be more sensitive to pyrimidine biosynthesis inhibition as they would be more reliant on *de novo* pathways.

The combination of ENT inhibitors with antipyrimidines has been investigated previously in colon and pancreatic cancer including dipyridamole (DPM) + acivicin,[47-48] DPM + PALA,[49-50] and DPM + PALA + 5FU.[51] In fact, in a study exploring the combination of BREQ and 5FU, DPM was found to enhance BREQ's growth inhibition.[20] This was rescued in the presence of 50 μM uridine, but that is well above the estimated physiological concentration of 5 μM,[52] which did not rescue the cytotoxicity. In this study, we evaluate synergistic effects of ENT/CNT inhibition concomitantly with DHODH inhibition in colon and pancreatic cancer cells using a small-molecule approach (Figure III-1).
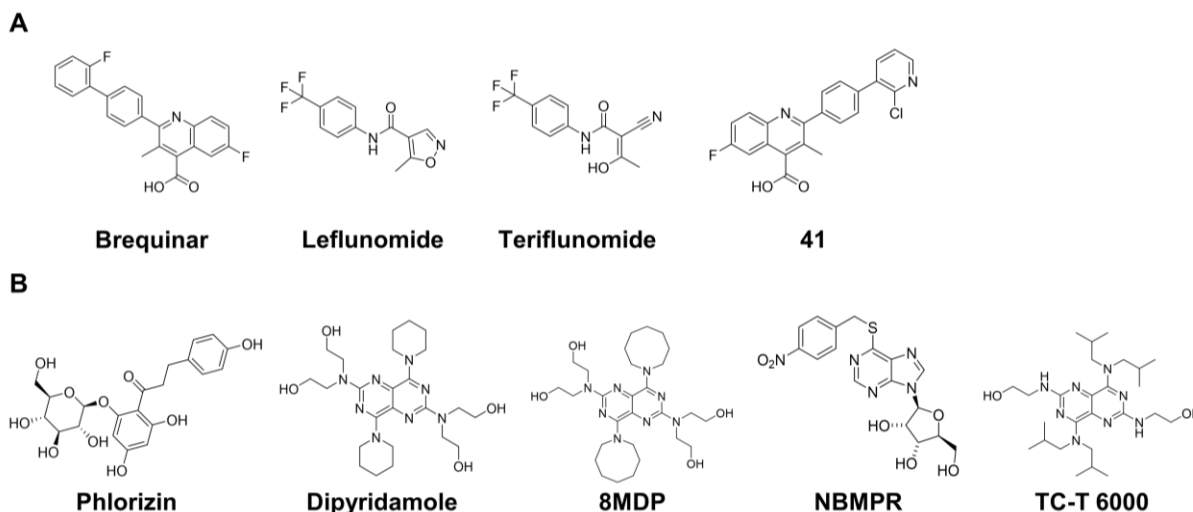
Figure III-1. Structures of DHODH and nucleoside transporter inhibitors used in this study. (A) DHODH inhibitors. (B) Transporter inhibitors.

Results and discussion

Brequinar is synergistic with ENT inhibitor dipyridamole but not CNT inhibitor phlorizin

We first sought to determine the role of the pyrimidine salvage pathway transporters (CNTs versus ENTs) in the compensatory mechanism for DHODH inhibition. We chose colon and pancreatic cancer cell lines for this study as these are the most well-studied pharmacologically in the context of nucleoside transporters. To accomplish this, we combined BREQ with either phlorizin (PHZ, pan-CNT inhibitor) or dipyridamole (DPM, ENT inhibitor). DPM is selective for ENT1/2, but also inhibits ENT4 at higher concentrations. As single agents, PHZ and DPM are not toxic up to 50 µM (Figure III-2A-C). The combination of BREQ + PHZ does not affect the activity of BREQ in the colony formation assay (Figure III-2A-C, Figure III-2G-I) or MTT assay (Appendix Figure III-1A-C) even with continuous and simultaneous treatment. However, treatment of BREQ + DPM for only 24 h is enough to produce significant cytotoxicity (Figure III-2A-C). Importantly, this synergy is seen at 100-fold lower concentration of DPM to PHZ. This synergy increases with continuous treatment (Figure III-2G-I). The cell lines used in this study show a spectrum of sensitivity to BREQ, with HCT 116 being the most sensitive (Table III-1).

164

Even in this cell line, the maximal growth inhibition is roughly 60% (Figure III-2D), suggesting that BREQ is a cytostatic drug and that the salvage pathway may sustain ~40% viability. Regardless of sensitivity to BREQ alone, all of the tested cell lines were sensitive to the combination. A valid concern is that this combination would be toxic to all cells, but, as evidenced by the lack of toxicity in the *in vivo* study (see below), we believe that with the optimal dosing regimen, systemic toxicity is avoidable. Surprisingly, increasing concentrations of DPM does not affect the IC_{50} of BREQ, but instead increases the efficacy in a dose-dependent manner (Figure III-2D-F), even up to a concentration of 25 μM DPM (Appendix Figure III-1D). A similar phenomenon was observed when brequinar was combined with doxorubicin.[53] Furthermore, it is interesting to note that neither the order of addition (Figure III-2J) nor treatment duration (Figure III-2K) significantly affected the IC_{50} of BREQ. We believe this is due the intrinsic cytostatic nature of DHODH inhibitors. Inhibition of DHODH results in a stall of cell-cycle progression at S-phase;[17, 21] cells are able to remain viable because of the salvage pathway. Therefore, when the supply of pyrimidine nucleosides is cut off from both arms, the remaining viable but non-proliferating cells are forced to die (Appendix Figure III-1E/F). To validate the cytotoxicity, we carried out MTT assays with compound treatment for only the first 24 h or the full 72 h. Any growth inhibition from the 24 h treatment would be due to cytotoxicity as fresh medium was replaced after compound removal. As can be seen in Appendix Figure III-1E, 24 h treatment of BREQ in the MTT assay has a minimal effect, whereas significant growth inhibition is seen with continuous treatment in agreement with BREQ's cytostatic mechanism of action. Short-term and continuous treatment of BREQ + DPM produces the same effect, indicating a cytotoxic mechanism. Importantly, comparison of both 24 h treatments reveals a significant difference of cell growth inhibition. Additionally, in an apoptosis assay measuring ATP levels, there was not a

significant difference in the viability of BREQ-treated cells, signifying that while the cell's growth inhibited, the cells were still viable. In contrast, treatment with the BREQ + DPM combination significantly reduced cell viability for 24 h and continuous treatment. These initial studies showed that BREQ is synergistic with DPM but not PHZ, suggesting that CNTs do not play a major role in the salvage pathway when *de novo* pyrimidine biosynthesis is inhibited in colon and pancreatic cancer cell lines.

There are a few possibilities as to why we saw synergy between BREQ and DPM but not PHZ. While all CNTs are able to transport uridine, they do so at a less efficient rate than the ENTs.[23-24] The transport also requires coupled transport of sodium or protons across their concentration gradient. Additionally, PHZ is not as potent as the ENT inhibitors used in this study. So as to not exceed toxic concentrations of DMSO, we were limited by a maximum concentration of 50 μM. This is 2.5-5-fold lower than the IC_{50} values of CNT1 and CNT2. Therefore more potent CNT inhibitors such as compound 22 or siRNA for the CNTs could be used in the future to assess whether combination of DHODH and CNT inhibition is synergistic.[54]
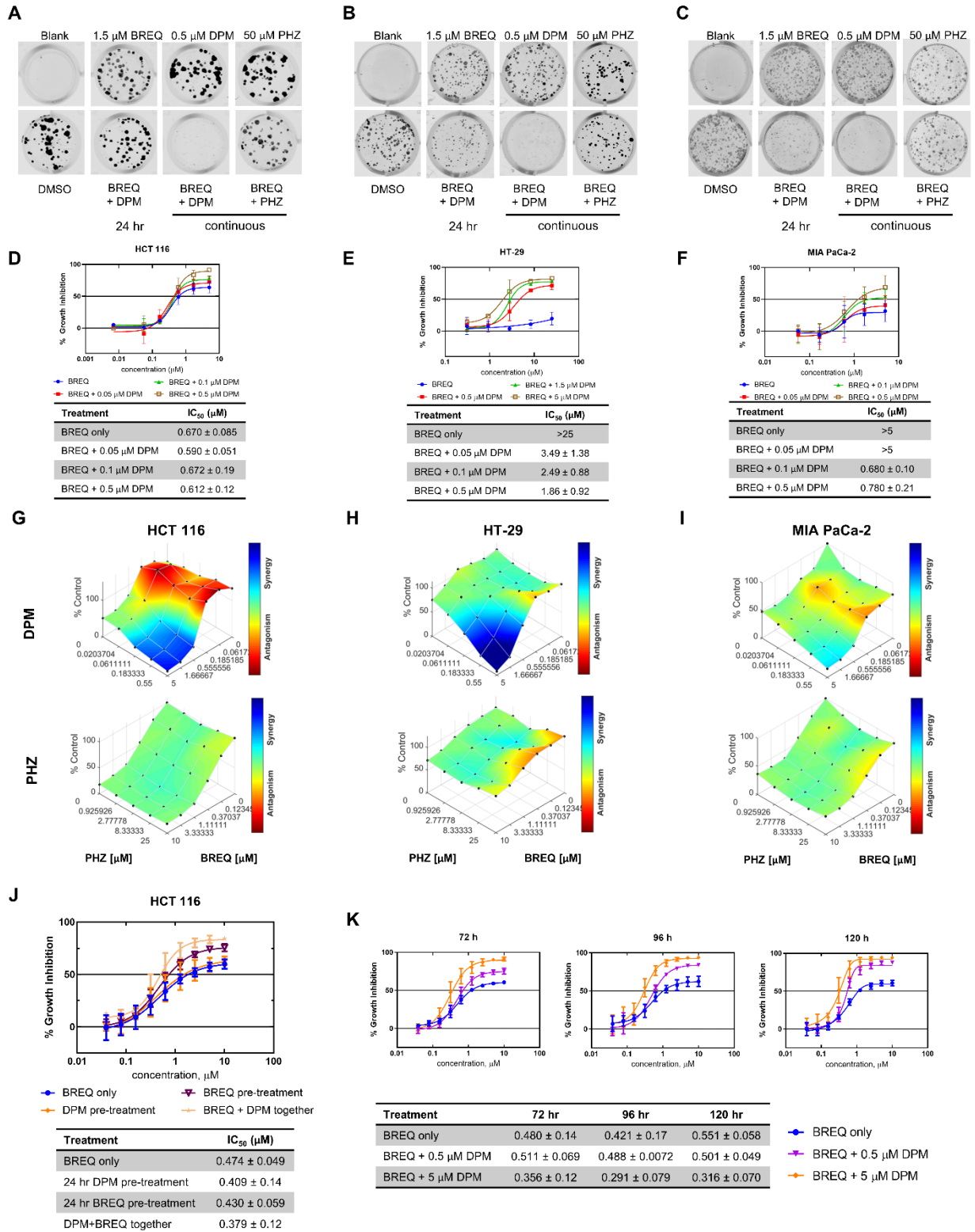
Figure III-2. BREQ is synergistic with ENT antagonist DPM, but not CNT antagonist PHZ. (A-C) Colony formation assay (CFA) at single doses. Continuous and 24 h designations are for combinations only; single drugs are continuous treatments. (D-F) IC50 dependence of BREQ in presence of DPM in the MTT assay. (G-I) Bliss synergy plots using CFA data. Cells were continuously treated with compounds. (J) Order of addition of BREQ+DPM in the MTT assay in HCT 116. Concentration of DPM = 1 μM. (K) Time-dependence of BREQ+DPM treatment in the MTT assay in HCT 116. BREQ and DPM were added at the same time.

BREQ is synergistic with other, but not all, ENT inhibitors

Beyond DPM, additional ENT inhibitors with varying specificities were tested for synergy with BREQ: TC-T 6000 (ENT4 inhibitor), NMBPR (ENT1 inhibitor), and 8MDP (ENT1/2 inhibitor) (Appendix Table III-1). The ENT1/2 specific inhibitors were synergistic with BREQ whereas the ENT4-specific inhibitor TC-T 6000 was not (Figure III-3, Appendix Figure III-2). This indicates that ENT4 does not play an important role in salvage of nucleosides in response to DHODH inhibition. All CNTs and ENTs except for ENT4 transport uridine; ENT4 specifically transports adenosine.[23] This explains why inhibition by TC-T 6000 did not amount to any synergistic, or even additive, effect. Unlike DPM, 8MDP and TC-T 6000 showed cytotoxicity in all three cell lines (Table III-1). This could be due to their higher potency against the ENT isoforms, however, the most selective ENT inhibitor, NBMPR, was not cytotoxic up to 50 μM. It is interesting that these ENT inhibitors show cytotoxicity since not all cell lines are sensitive to BREQ, suggesting that HT-29 and MIA PaCa-2 are more reliant on salvage than *de novo* pathways. Similar to DPM, 8MDP and NBMPR did not affect BREQ's IC_{50}, but instead increased its efficacy (Figure III-3D/E; Appendix Figure III-2C/F). For HCT 116, the synergy is more pronounced with 24 h treatment than continuous (Figure III-3G, H) because BREQ also shows growth inhibition with longer treatment times. For MIA PaCa-2, significant synergy is observed with 24 h and continuous treatment, and for HT-29 only with continuous treatment (Appendix Figure III-2). This can be attributed to their intrinsic resistance to BREQ.
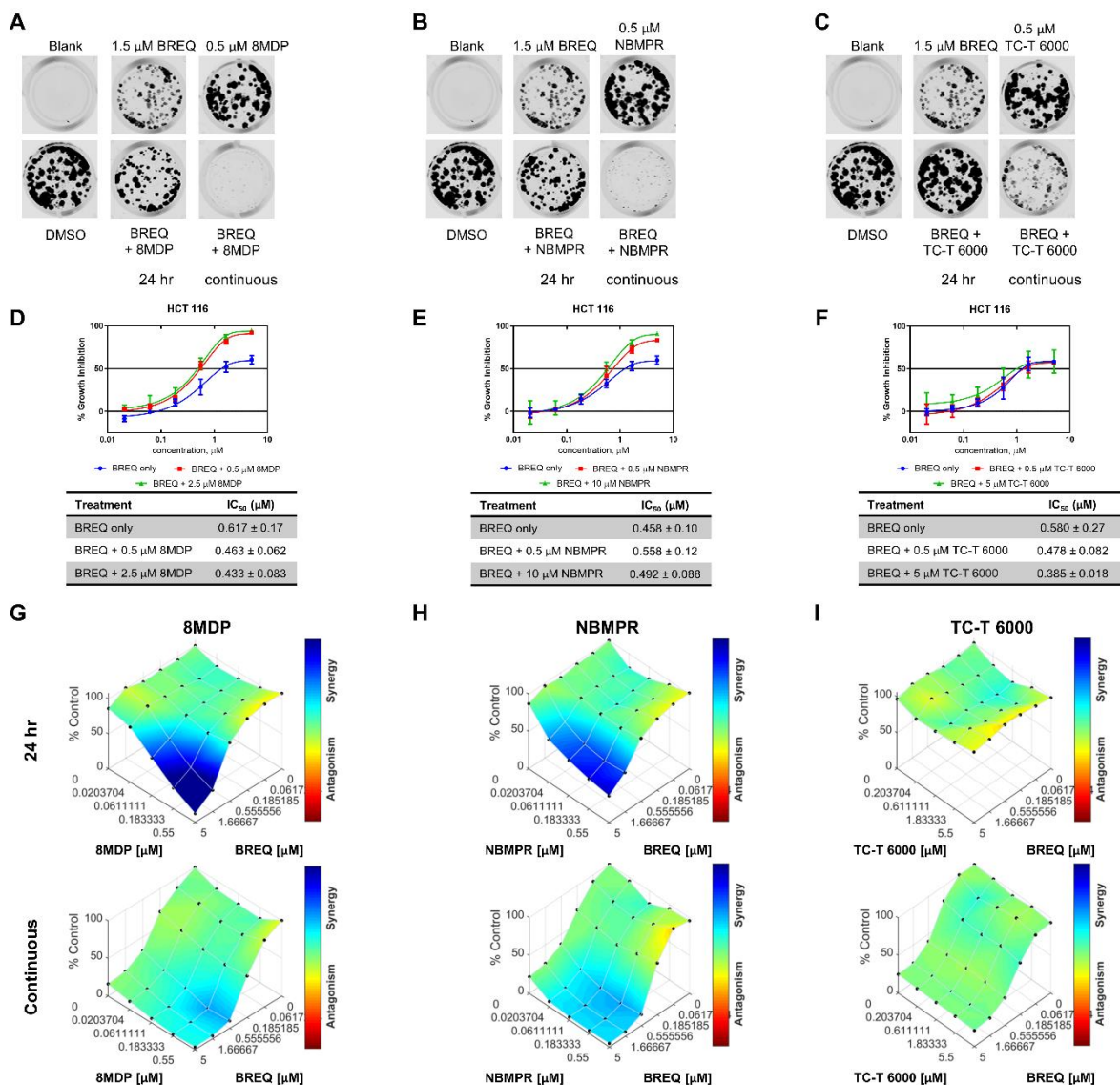
Figure III-3. BREQ is synergistic with ENT1/2 but not ENT4 inhibitors in HCT 116. (A-C) CFA at single doses. Continuous and 24 h designations are for combinations only; single drugs are continuous treatments. (D-F) IC50 dependence of BREQ in presence of ENT inhibitors in the MTT assay. (G-I) Bliss synergy plots using CFA data.

Table III-1. IC$_{50}$ values of DHODH and nucleoside transporter inhibitors against cancer cell lines. Values listed are in μM.

Compound	HCT 116		HT-29		MIA PaCa-2	
	MTT	CFA	MTT	CFA	MTT	CFA
BREQ	0.480 ± 0.14	0.218 ± 0.24	>25	>25	0.680 ± 0.25	0.590 ± 0.36
LEF	>50	14.1 ± 2.4	>50	>50	>50	>50
TERF	>50	11.8 ± 5.7	>50	>50	>50	23.7 ± 19
41	2.86 ± 0.96	NT[a]	NT	NT	7.18 ± 2.3^{55}	NT
PHZ	>50	>50	>50	>50	>50	>50
DPM	>50	>50	>50	>50	>50	>50
8MDP	5.73 ± 2.1	8.30 ± 3.7	>50	>50	16.0 ± 5.0	13.6 ± 6.6
TC-T 6000	11.2 ± 3.9	8.06 ± 3.0	17.9 ± 8.1	6.09 ± 4.0	10.1 ± 2.6	12.0 ± 0.36
NBMPR	>50	>50	>50	>50	>50	>50

[a]NT = not tested

169

Other DHODH inhibitors show mixed synergy with DPM

Additional DHODH inhibitor LEF, and its active metabolite TERF, were also evaluated for synergy with DPM. While only modest cell growth inhibition was observed in the colony formation assay for LEF and TERF alone, combination with DPM did show a significant improvement (Figure III-4A/D; Appendix Figure III-3A/D). Both LEF and TERF were inactive in the MTT assay with IC_{50}'s > 50 μM (Table III-1), but in HCT 116, combination with DPM increased activity (Figure III-4B/E). However, these combinations showed no significant differences in HT-29 or MIA PaCa-2 (Figure III-3B/E). Continuous treatment of LEF/TERF with DPM in the colony formation was synergistic but not with 24 h treatment in HCT 116 (Figure III-4C/F). In HT-29 and MIA PaCa-2, there was no observed synergy at concentrations lower than 50 μM for both LEF and TERF (Appendix Figure III-3). Since LEF/TERF are minimally active to begin with, when DPM is added an IC_{50} is produced. In HCT 116, comparison of the Bliss synergy plots for continuous treatments of BREQ + DPM to LEF/TERF+DPM, the trends are quite similar (Figure III-1G to Figure III-4C/F). By simply looking at the highest concentration of these compounds (25 μM for LEF/TERF or 5 μM BREQ) without DPM, the cell growth inhibition is ~50-70%. Addition of 0.55 μM DPM increases the cell growth inhibition to >95%, thereby increasing the efficacy without a shift in IC_{50}. This is not apparent in the MTT assay because the cells are only treated with the compounds for 3 days, versus 6-7 days in the colony formation assays. LEF and TERF have a much lower affinity for DHODH compared to BREQ (K_i = 4.6 μM and 2.7 μM versus 25 nM, respectively),[56-57] which could account for the lack of synergy in HT-29 and MIA PaCa-2 as these cell lines are more resistant to DHODH inhibition.

We previously published optimized BREQ analog **41**,[55] and were interested whether this molecule would also exhibit synergy when combined with DPM. The cytotoxicity trends with **41**

matched those of BREQ + DPM (Appendix Figure III-4). Significant synergy is present with both 24 h and continuous treatment (Appendix Figure III-4A). Furthermore, DPM dose-dependently increases the efficacy of **41** but does not shift its IC_{50} value (Appendix Figure III-4B). Summaries of all combinations can be found in Appendix Tables III-2, III-3, and III-4.
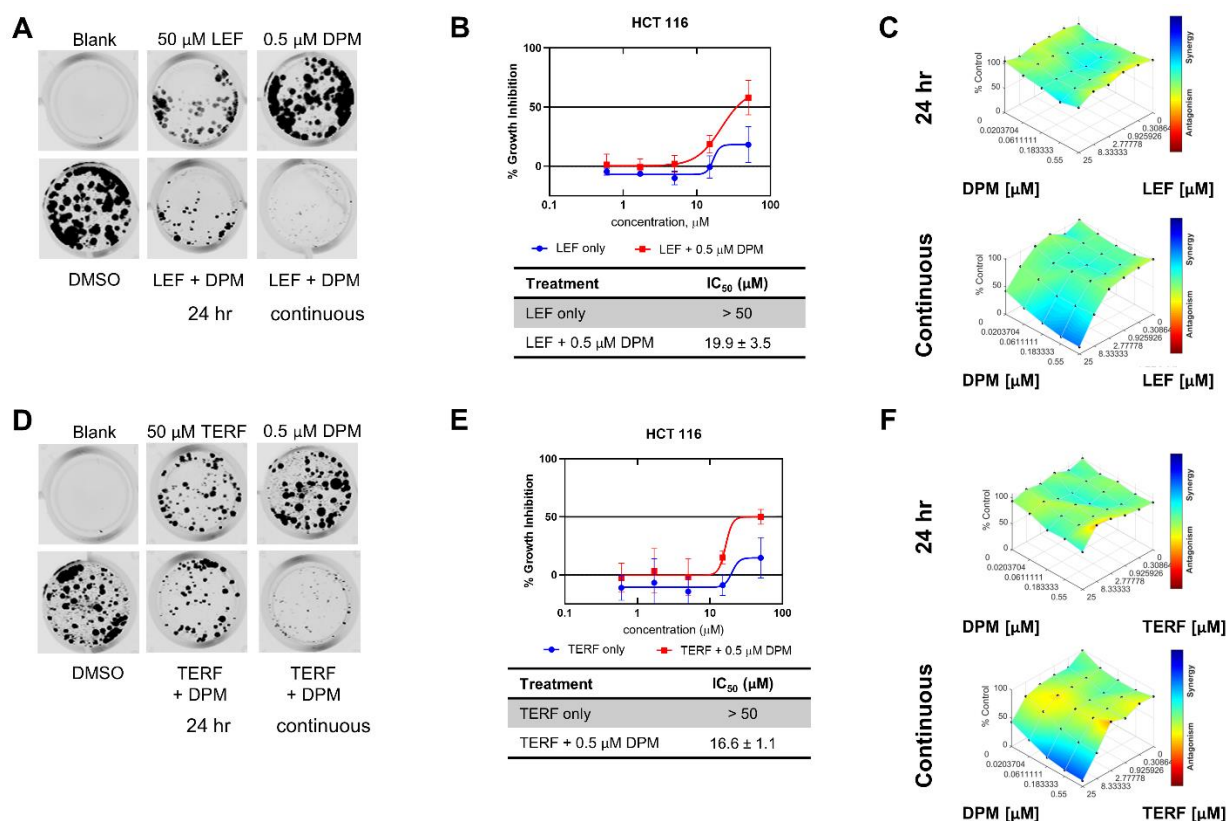

Figure III-4. LEF and TERF are synergistic with DPM in HCT 116. (A, D) CFA at single doses. Continuous and 24 h designations are for combinations only; single drugs are continuous treatments. (B, E) IC_{50} dependence of LEF or TERF in presence of DPM in the MTT assay. (C, F) Bliss synergy plots using CFA data.

Nucleoside depletion confirms synergistic mechanism of action

Removal of nucleosides from the media is a surrogate for inhibition of all nucleoside transporters. Under these conditions, BREQ, TERF and LEF treatment reproduces the synergy that is seen with combined DPM or NBMPR treatment in nutrient-rich media (Figure III-5A). In the MTT assay, removal of nucleosides from the media significantly enhanced activity (Figure III-5B). As expected, BREQ was more cytotoxic in nucleoside-free media, and this media did not impact the drug combinations nor the nucleoside transport inhibitors DPM and NBMPR. When

171

uridine was added to the nucleoside-free media (precursor to the end product of pyrimidine biosynthesis) at a physiological concentration (5 μM), BREQ-induced cell growth inhibition was rescued, but not LEF or TERF (Figure III-5C). This indicates that the mechanisms of action for LEF and TERF extend beyond DHODH inhibition, and that BREQ's lies with inhibition of pyrimidine biosynthesis, all supporting previous literature.
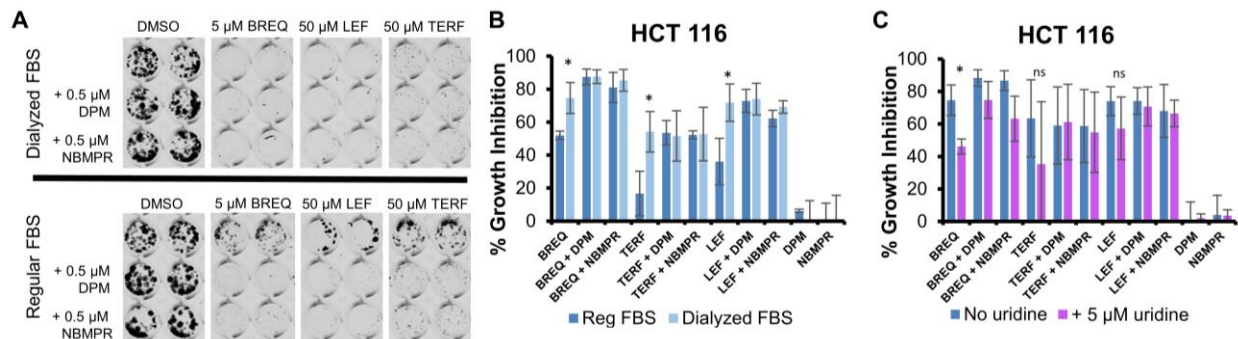

Figure III-5. Nucleoside depletion confirms synergistic mechanism of action. (A) Colony formation assay assessing drug dependence of nucleoside presence in medium. (B) MTT assay assessing drug dependence of nucleoside presence in medium. Drug concentrations are the same as in panel A. *p < 0.05. (C) MTT assay assessing drug dependence of uridine supplementation in dialyzed FBS. Drug concentrations are the same as in panel A. *p < 0.01.

In vitro synergy was not observed in vivo

To evaluate if the *in vitro* synergy would translate *in vivo*, the antitumor effects of DPM, BREQ, **41**, DPM + BREQ, and DPM + **41** were examined using an HCT 116 mouse xenograft model with i.p. administration (Figure III-6A, Appendix Figure III-5A). During the study, no significant body weight was lost in any group (Figure III-6B, Appendix Figure III-5B). While DPM + BREQ showed significant inhibition of tumor growth compared to vehicle control, there was no statistical significance between the combination and BREQ alone (Figure III-6C, Appendix Figure III-5C). Previous *in vivo* studies with PALA + DPM found that the combination was able to significantly reduce nucleotide levels in the tumors greater than either agent alone and that addition of DPM reduced PALA's LD$_{50}$ in mice.[58-59] Therefore, we do not expect tumor penetrance of DPM to be an issue. A possible explanation as to why we did not observe synergy is that plasma uridine concentrations were higher than what was used in cell culture. In mouse plasma the

concentration of uridine is ~5 µM,[52] and in Figure 5C, we show that 5 µM does not rescue growth

inhibition, therefore we do not expect that plasma uridine levels contributed to the lack of synergy.

However, future *in vivo* studies monitoring plasma uridine levels are warranted as 50 µM was

previously shown to rescue the combination effect *in vitro*,[20] and treatment with a sub-toxic dose

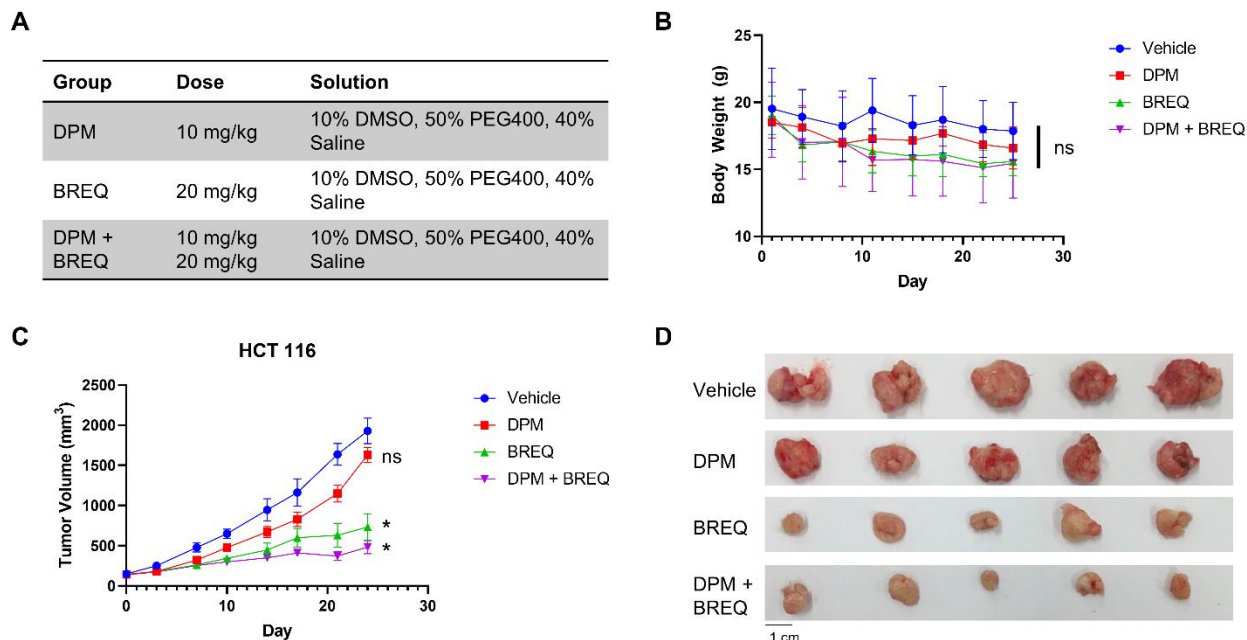of brequinar in mice resulted in a roughly 3-fold increase in uridine concentrations.[19]

Figure III-6. Anticancer effect of DPM + BREQ in a mouse xenograft model (n = 5, mean ± SEM). (A) Formulations of DPM and BREQ. (B) Body weight change throughout the study. (C) Tumor volume of each group. (D) Harvested tumors after sacrifice. *p < 0.001 versus control (t-test).

Disappointingly, **41** showed no antitumor activity alone or in combination with DPM

(Appendix Figure III-5C). However, as was discussed above, the dosing regimen is important. In

this study we only tried one dose combination of BREQ with DPM. In the future it would be

important to establish the optimal ratio of DPM:BREQ as well as the schedule-dependency. We

were pleased to see that the combination group of DPM + BREQ was not toxic to the mice as

measured by body weight. Despite having a favorable pharmacokinetic profile,[55] **41** did not elicit

any tumor growth inhibition. *In vitro*, **41**'s IC_{50} against DHODH is on par with BREQ but

possesses a roughly 6-fold higher IC_{50} in cells (HCT 116). Our previous work speculated that even

with similar solubility to and a lower cLogP than BREQ, **41** may not be as cell-permeable.[55] The computational permeability tool PerMM predicted a 49-fold difference in permeability coefficients between BREQ and **41** (Appendix Table III-5), where BREQ is predicted to more favorably cross the phospholipid bilayer (BLM).[60-61] Similarly, the $logD^{7.4}$ of **41** is more than a full log unit lower than that of BREQ (0.631 ± 0.07 versus 1.83 ± 0.02).[62] Moreover, we used a dose of 10 mg/kg for **41** versus 20 mg/kg for BREQ, so it is possible that a higher dose would be more effective. Likewise, the half-life of **41** is ~2-fold lower than BREQ's, therefore increasing the dosing schedule to every 12 hours instead of daily could potentially overcome the lack of activity. No increased activity was observed in combination with DPM, further indicating a failure to reach the tumor or an inadequate dose. Therefore, future studies are warranted to further elucidate **41**'s *in vivo* efficacy.

Conclusion

This is the first study to thoroughly investigate inhibition of nucleoside transporters in conjunction with DHODH inhibitors. The combination of DPM with BREQ has been studied before, albeit with brevity.[20] Through using a small molecule approach, we found that the equilibrative nucleoside transporters seem to play a greater role in nucleotide salvage rather that the concentrative nucleoside transporters when the *de novo* pathway is inhibited. Experiments using more potent inhibitors of CNTs or siRNA targeting these proteins combined with brequinar are necessary to further validate this result. We identified that the ENT1 and ENT2 isoforms together are responsible for salvage through the use of potent ENT1/2 inhibitors 8MDP and NBMPR. Furthermore, the synergy extended beyond brequinar to other established DHODH inhibitors leflunomide and teriflunomide. The results of our study highlight the possibility to improve brequinar's efficacy in the clinic by using a combination strategy to inhibit nucleotide

salvage from the extracellular environment. Future studies will determine optimal dosing regimens for *in vivo* studies to obtain a synergistic effect.

Methods

Chemicals. DPM, BREQ, and uridine were purchased from Sigma. Compound **41** was prepared as previously described.[55] NBMPR, TC-T 6000, and 8MDP were purchased from Tocris. All stock solutions were prepared in DMSO except for uridine which was dissolved in water. The purity was established by integration of the areas of major peaks detected at 254 nm, and all tested compounds have >95% purity.

Cell Culture. HCT 116 and MIA PaCa-2 were cultured in RPMI 1640, and HT-29 was cultured in McCoy's 5A, all were supplemented with 10% FBS (Gibco). Dialyzed FBS was purchased from GE Healthcare. Cells were grown at 37 °C in a humidified atmosphere of 5% CO_2 and maintained in culture under 30 passages. Cell lines were tested for *Mycoplasma* contamination with the *Mycoplasma* detection kit, PlasmoTest (InvivoGen, San Diego, California). All cell lines were authenticated with STR DNA profiling (University of Michigan, Michigan, USA) and matched to reference profiles from the ATCC database.

Colony formation assay. Cells were seeded in 96-well plates at 200-500 cells/well and allowed to attach overnight. Compounds were added to the indicated concentrations and incubated with the cells for 24 h or continuously until the vehicle control reached ~80% confluency (5-7 days). At the end of treatment, media was removed, and cells were fixed and stained with crystal violet solution (0.05% crystal violet, 2% formaldehyde, 40% methanol) for 30 minutes. Wells were washed with water and allowed to dry overnight before imaging with the Odyssey CLx imager (LI-COR Biosciences).

MTT assay. Cytotoxicity of compounds was evaluated with the MTT assay. Cells were seeded in 96-well plates at 2000-4000 cells/well. After overnight attachment, compounds were added to the wells at sequential dilutions. After 72, 96, or 120 h the tetrazolium dye MTT was added to the media to a final concentration of 300 μg/mL and incubated for 3-4 h at 37 °C. The media was removed, and the insoluble formazan was dissolved in 100 μL of DMSO. Absorbance at 570 nm was read by microplate reader (Molecular Devices, Sunnyvale, CA). Cytotoxicity of compounds is presented as inhibition of cell proliferation against DMSO-treated controls. All compound incubation periods were 72 h unless otherwise indicated.

Apoptosis assay. Apoptosis was measured via quantification of ATP levels using the APOSensor assay (BioVision Incorpoorated) according to the manufacturer's protocol. Briefly, HCT 116 cells were seeded in white 96-well plates at 3,000 c/w. After overnight attachment, compounds were added to the wells and incubated with the cells continuously or for 24 h. After 72 h the media was removed and 100 μL of nucleotide releasing buffer was added to the wells. ATP monitoring enzyme (10 μL) was added to the wells after the plate was gently shaken for 5 min. Luminescence was read by a CLARIOstar Plus microplate reader (BMG LabTech). Cell viability is presented as a percentage compared to DMSO-treated controls.

Data analysis. IC_{50} values were calculated using GraphPad Prism 8. For synergy experiments, data were analyzed for synergistic interactions by the Bliss synergy and antagonism method using the software Combenefit (University of Cambridge).[63-64] All experiments were performed at least three independent times.

PerMM analysis. BREQ and **41** were prepared in MOE using the Amber forcefield for energy minimizations. Compounds were submitted for analysis by the PerMM server using the default settings (T = 298 K, pH 7.4).[60-61]

LogD (pH 7.4) determination. The logD of **41** was first estimated using ADMET Predictor (Simulations Plus, version 9.5.0.16) to inform the appropriate partitions to be used below. The partition coefficient of **41** between n-octanol and PBS at pH 7.4 (log $D^{7.4}$) was obtained using the shake-flask technique as previously described with some alterations.[65] Mutually saturated solutions were prepared by shaking at room temperature overnight. Excess buffer or octanol was removed following centrifugation for 30 min at 3500 rpm. Compound **41** was diluted in 500 μL or 1 mL in octanol-saturated PBS to 200 μM. Aliquots of these standard solutions were transferred to a Corning 3680 plate along with a blank. PBS-saturated octanol was then added to the tubes in 1:1 and 1:10 ratios. The tubes were shaken for 1 h at room temperature and then centrifuged for 5 min at 7000 rpm. Aliquots of the aqueous layers were transferred to the plate and the absorption spectra for all samples were obtained. The area under the curves (AUC) were calculated in Microsoft Excel. Equation 1 was used to determine the logD and the reported value is an average of six experiments.

$$\log D = \log\left(\left(\frac{AUCst}{AUCaq}\right) - 1\right)\frac{Vaq}{Voct} \qquad (1)$$

Xenograft study. All animal studies were approved by the animal care facility at the University of Michigan-Ann Arbor (Protocol number: PRO00009185) and were handled in accordance with the Institutional Animal Use and Care Committee. HCT 116 cells (5×10^6) in a suspension of PBS were injected subcutaneously into dorsal flanks of NSG mice. Tumor size was monitored twice a week through caliper measurement using the following equation: $V = l \times w \times w/2$, where l represents length and w represents width of the tumor. Mice were randomly grouped (n = 5 per group) when the average tumor size reached 150 mm^3. Daily treatment was given at 5 days on, 2 days off cycles. DPM was given at 10 mg/kg, compound **41** at 10 mg/kg, and BREQ was given at 20 mg/kg (10% DMSO, 50% PEG400, 40% saline) by intraperitoneal injection. Study was

concluded on day 25 when the average tumor size in the vehicle-treated group reached 2000 mm^3.

An unpaired *t*-test was performed for data analysis, and $p < 0.05$ was considered significant.
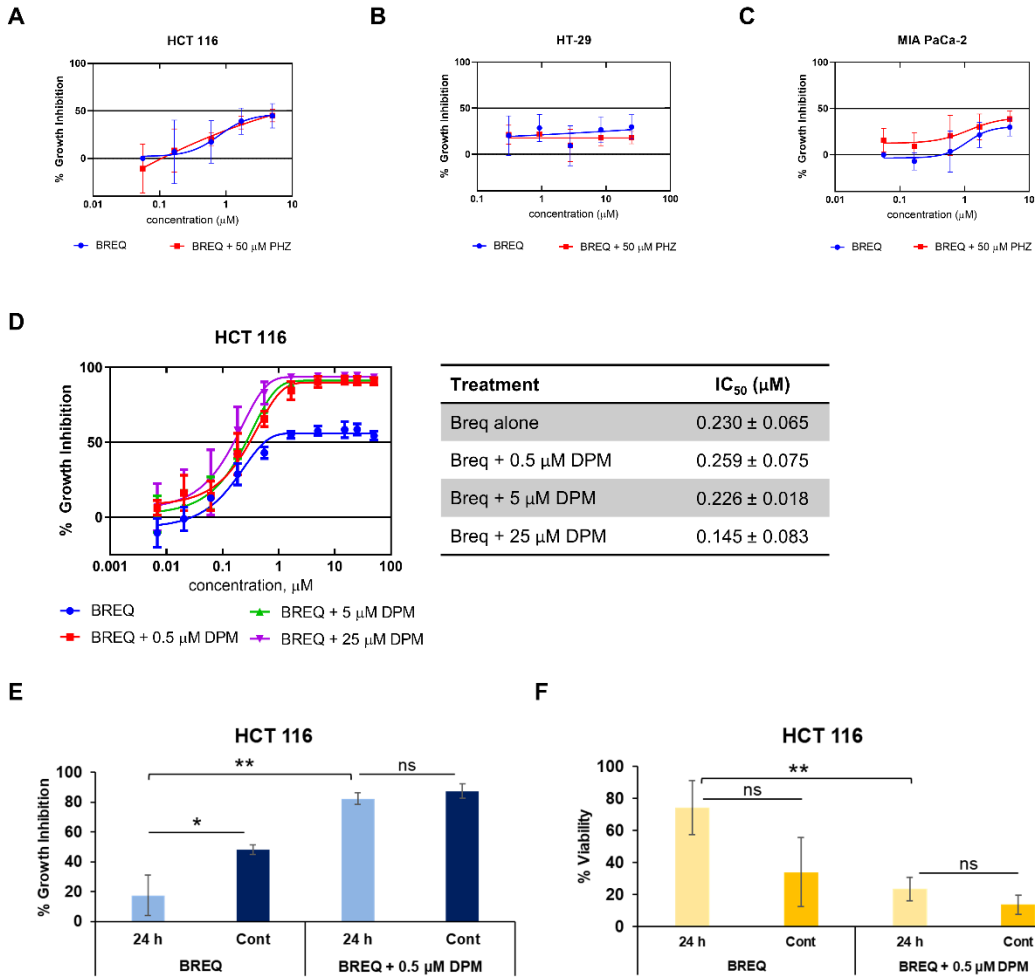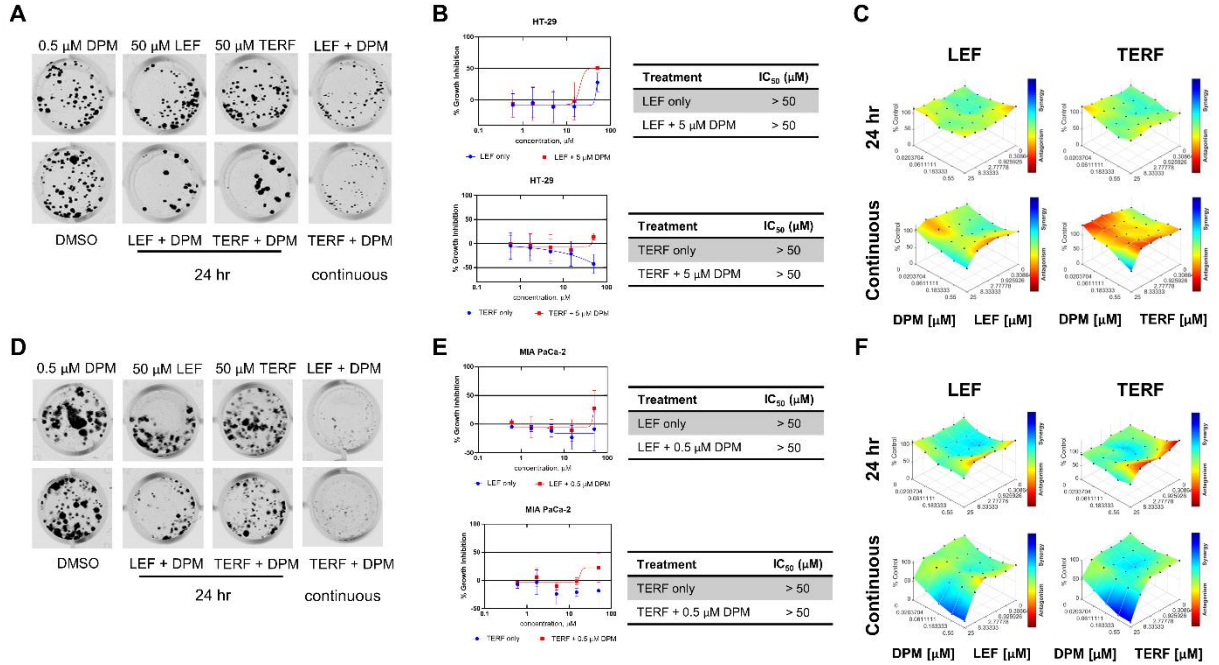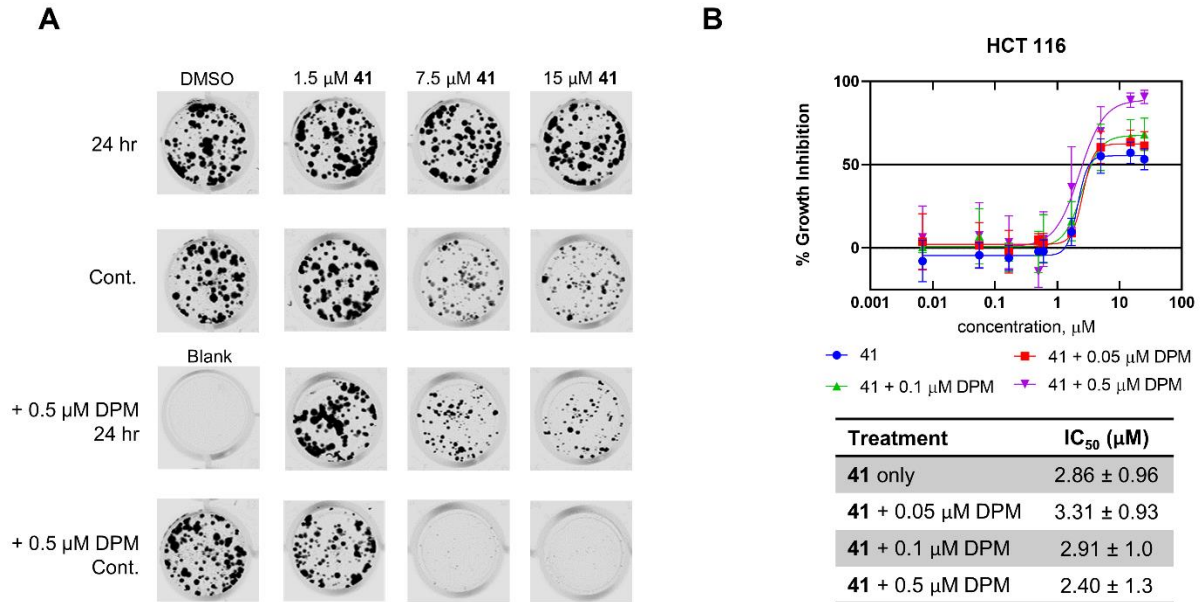
Appendix

Appendix Figure III-1. (A-C) PHZ does not affect cytotoxicity of BREQ. (D) High concentrations of DPM do not shift BREQ's IC50. (E-F) BREQ + DPM elicits cell growth inhibition through a cytotoxic and apoptotic mechanism as measured by the (E) MTT and (F) APOSensor assays.
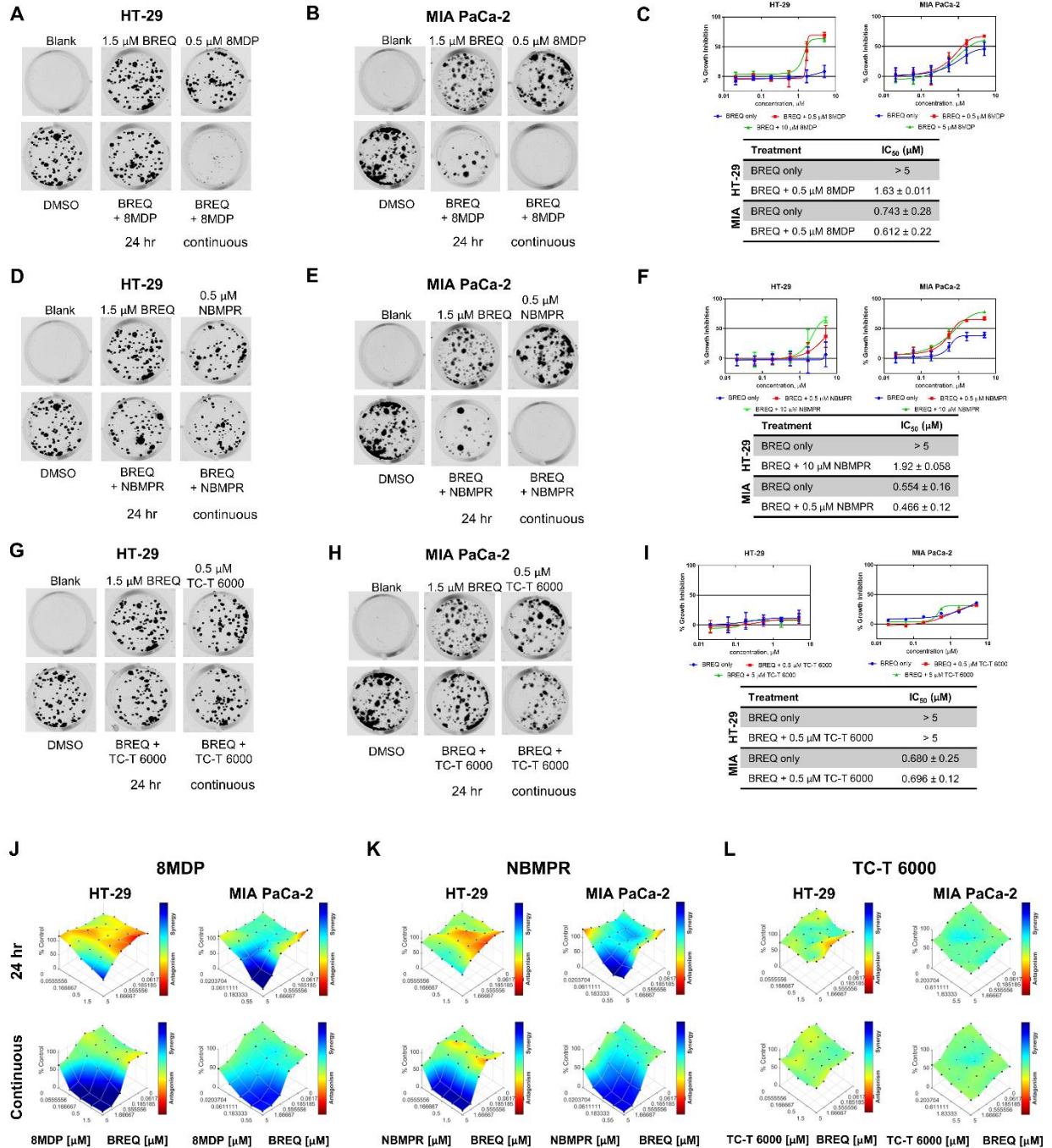
Appendix Figure III-2. BREQ is synergistic with ENT1/2 but not ENT4 inhibitors in HT-29 and MIA PaCa-2. (A, D, G) CFA at single doses in HT-29. (B, E, H) CFA at single doses in MIA PaCa-2. (C) and MTT IC50 curves of BREQ + 8MDP. (F) MTT IC50 curves of BREQ + NBMPR. (I) MTT IC50 curves of BREQ + TC-T 6000. (A, B, D, E, G, H) Continuous and 24 h designations are for combinations only; single drugs are continuous treatments. (J-L) Bliss synergy plots using CFA data.

Appendix Figure III-3. LEF and TERF are synergistic with DPM in HT-29 (A-C) and MIA PaCa-2 (D-F). (A, D) CFA at single doses. Continuous and 24 h designations are for combinations only; single drugs are continuous treatments. (B, E) IC50 dependence of LEF or TERF in presence of DPM in the MTT assay. (C, F) Bliss synergy plots using CFA data.
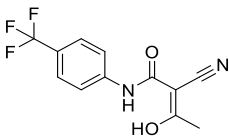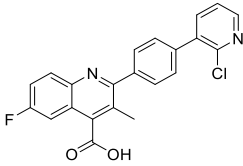

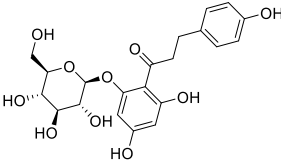| Treatment	IC$_{50}$ (µM)
41 only	2.86 ± 0.96
41 + 0.05 µM DPM	3.31 ± 0.93
41 + 0.1 µM DPM	2.91 ± 1.0
41 + 0.5 µM DPM	2.40 ± 1.3

Appendix Figure III-4. DHODH inhibitor **41** is synergistic with DPM in HCT 116. (A) CFA at single doses. (B) IC$_{50}$ dependence of **41** in presence of DPM in the MTT assay.
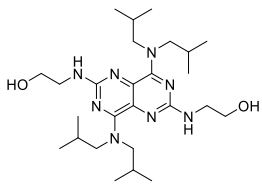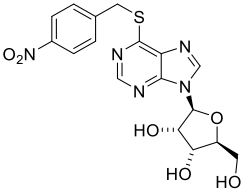
181
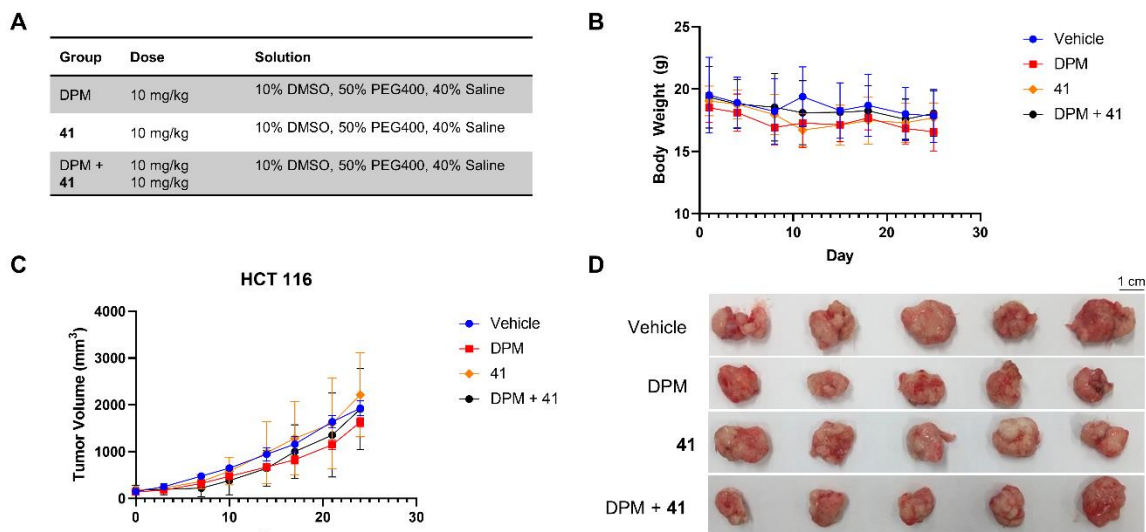
Appendix Figure III-5. Anticancer effect of DPM+**41** in a mouse xenograft model (n = 5, mean ± SEM). (A) Formulations of DPM and **41**. (B) Body weight change throughout the study. (C) Tumor volume of each group. (D) Harvested tumors after sacrifice.

Appendix Table III-1. DHODH, CNT, and ENT inhibitors used in this study.

Compound	Structure	Target	Activity	Status[a]
BREQ		DHODH	$K_i = 25$ nM[56] $IC_{50} = 6\text{-}10$ nM[66]	Not FDA-approved AML Phase IA/IIB (NCT03760666)
LEF		DHODH	$K_i = 4.6$ μM[57]	FDA-approved for rheumatoid and psoriatic arthritis Breast cancer Phase I/II (NCT03709446) Prostate cancer Phase II/III (NCT00004071) Henoch-Schoenlein purpura nephritis Phase II (NCT02532777) Myasthenia gravis Phase III (NCT01727193) Polymyalgia rheumatica Phase III (NCT03576794) Nephropathy Phase IV (NCT04020328)

			IgG4-RD Phase IV (NCT03715699 and NCT02703194)\n\nTakayasu's arteritis (NCT02981979 and NCT03893136)\n\nMultiple myeloma Phase II (NCT02509052)\n\nHIV Phase I (NCT00101374)\n\nUveitis Phase II (NCT00001863)\n\nAnaplastic astrocytoma Phase II (NCT00003775)\n\nSystemic lupus erythematosus Phase II (NCT00637819); Phase II/III (NCT00268567)	
TERF		DHODH	K_i = 2.7 μM[57]\n\n$IC_{50}$ = 230 nM[67]	FDA-approved for multiple sclerosis
41		DHODH	IC_{50} = 9.71 nM[55]	Preclinical
PHZ		CNTs SGLTs	CNT1 IC_{50} = 247 μM[68]\n\nCNT2 IC_{50} = 121 μM[68]\n\nCNT3 K_i = 15 μM[69]\n\nSGLT1 K_i = 140 nM[70]\n\nSGLT2 K_i = 11 nM[70]	Preclinical[b]

				FDA-approved for thromboembolism prophylaxis following surgery, secondary prevention of transient ischemic attack, and prevention of reoccurrence of myocardial infarctions (in combination with aspirin)
DPM		ENT1,2 PDE3,5[c]	ENT1 IC_{50} = 5 nM[71] ENT2 IC_{50} = 356 nM[71] ENT4 IC_{50} = 2.80 μM[72] PDE1A IC_{50} = 2.5 μM[73] PDE1C IC_{50} = >300 μM[73] PDE2 IC_{50} = 50 μM[73] PDE3 IC_{50} = 85 μM[73] PDE4 IC_{50} = 6 μM[73] PDE5 IC_{50} = 800 nM[74]	Cerebral hemorrhage Phase III (NCT02966119) HIV Phase I/II (NCT02121756) Cardiovascular diseases Phase II (NCT00000527) Phase III (NCT00000510, NCT00000496) Phase IV (NCT01295567, NCT00457405, NCT00767663, NCT00129038) Acute mania Phase IV (NCT00560079) Schizophrenia (NCT00349973) Brain ischemia Phase IV (NCT00161070) Endotoxemia Phase IV (NCT01091571) Systemic lupus erythematosus (NCT01781611) Hyperemia/hypoxia (NCT00268554)
8MDP		ENT1, ENT2	ENT1 IC_{50} = 0.49 nM[75] ENT2 IC_{50} = 90.8 nM[72] ENT4 IC_{50} = 404 nM[72]	Preclinical

TC-T 6000		ENT4	ENT1 IC_{50} = 5.95 μM[72] ENT2 IC_{50} = 1.41 uM[72] ENT4 IC_{50} = 74.4 nM[72]	Preclinical
NBMPR		ENT1	ENT1 K_i = 0.4 nM[71] ENT1 IC_{50} = 0.65 nM[72] ENT2 K_i = 2.8 μM[71] ENT2 IC_{50} = 1.35 μM[72] ENT4 IC_{50} = 2.33 μM[72]	Preclinical

[a]Source: clinicaltrials.gov, for recruiting, active, not recruiting, or completed, as single agents or in addition to standard-of-care.
[b]Found to be unsuitable for people but is still used as a probe.[76]
[c]Phosphodiesterase isoforms that are responsible for the cardiovascular effects.[77]

Appendix Table III-2. Summary of MTT and continuous-treatment CFA synergy combination results for HCT 116.

	MTT				CFA			
Compound	BREQ	LEF	TERF	**41**	BREQ	LEF	TERF	**41**
PHZ	no	NT[a]	NT	NT	no	NT	NT	NT
DPM	yes	yes	yes	yes	yes	yes	yes	yes
8MDP	yes	NT	NT	NT	yes	NT	NT	NT
TC-T 6000	no	NT	NT	NT	no	NT	NT	NT
NBMPR	yes	NT	NT	NT	yes	NT	NT	NT

[a]NT = not tested

Appendix Table III-3. Summary of MTT synergy combination results for HT-29 and MIA PaCa-2.

	HT-29			MIA PaCa-2		
Compound	BREQ	LEF	TERF	BREQ	LEF	TERF
PHZ	no	NT[a]	NT	no	NT	NT
DPM	yes	yes	no	yes	no	no
8MDP	yes	NT	NT	yes	NT	NT
TC-T 6000	no	NT	NT	no	NT	NT
NBMPR	yes	NT	NT	yes	NT	NT

[a]NT = not tested

Appendix Table III-4. Summary of CFA synergy combination results for continuous treatments in HT-29 and MIA PaCa-2.

	HT-29			MIA PaCa-2		
Compound	BREQ	LEF	TERF	BREQ	LEF	TERF
PHZ	no	NT[a]	NT	no	NT	NT
DPM	yes	yes	yes	yes	yes	yes
8MDP	yes	NT	NT	yes	NT	NT
TC-T 6000	no	NT	NT	no	NT	NT
NBMPR	yes	NT	NT	yes	NT	NT

[a]NT = not tested

Appendix Table III-5. Permeability predictions as calculated using the PerMM server.[60-61]

Compound	Free energy of binding (DOPC)	Log of PC[a] – BLM[b]	Log of PC – BBB[c]	Log of PC – Caco-2	Log of PC - PAMPA
BREQ	-6.58 kcal/mol	0.93	-2.57	-3.24	-0.37
41	-5.38 kcal/mol	-0.76	-3.16	-3.67	-1.93

[a]PC, permeability coefficient
[b]BLM, bilipid membrane
[c]BBB, blood brain barrier

Notes

References

1.   Villa, E.; Ali, E. S.; Sahu, U.; Ben-Sahra, I., Cancer cells tune the signaling pathways to empower de novo synthesis of nucleotides. *Cancers.* **2019,** *11* (5), 688.

2.   Christopherson, R. L.; Lyons, S. D.; Wilson, P. K., Inhibitors of de novo nucleotide biosynthesis as drugs. *Acc. Chem. Res.* **2002,** *35*, 961-971.

3.   Christopherson, R. L.; Lyons, S. D., Potent inhibitors of de novo pyrimidine and purine biosynthesis as chemotherapeutic agents. *Med. Res. Rev.* **1990,** *10* (4), 505-548.

4.   Koczor, C. A.; Torres, R. A.; Lewis, W., The role of transporters in the toxicity of nucleoside and nucleotide analogs. *Expert Opin. Drug Metab. Toxicol.* **2012,** *8* (6), 665-676.

5.   Fragoso, Y. D.; Brooks, J. B., Leflunomide and teriflunomide: altering the metabolism of pyrimidines for the treatment of autoimmune diseases. *Expert Rev. Clin. Pharmacol.* **2015,** *8* (3), 315-320.

6.   Loffler, M.; Carrey, E. A.; Knecht, W., The pathway to pyrimidines: The essential focus on dihydroorotate dehydrogenase, the mitochondrial enzyme coupled to the respiratory chain. *Nucleos. Nucleot. Nucl.* **2020**, 1-25.

7.   Madak, J. T.; Bankhead, A., 3rd; Cuthbertson, C. R.; Showalter, H. D.; Neamati, N., Revisiting the role of dihydroorotate dehydrogenase as a therapeutic target for cancer. *Pharmacol. Ther.* **2019,** *195*, 111-131.

8.   Boschi, D.; Pippione, A. C.; Sainas, S.; Lolli, M. L., Dihydroorotate dehydrogenase inhibitors in anti-infective drug research. *Eur. J. Med. Chem.* **2019,** *183*, 111681.

9.   Boukalova, S.; Hubackova, S.; Milosevic, M.; Ezrova, Z.; Neuzil, J.; Rohlena, J., Dihydroorotate dehydrogenase in oxidative phosphorylation and cancer. *Biochim. Biophys. Acta Mol. Basis Dis.* **2020,** *1866* (6), 165759.

10.   Dexter, D. L.; Hesson, D. P.; Ardecky, R. J.; Rao, G. V.; Tippett, D. L.; Dusak, B. A.; Paull, K. D.; Plowman, J.; DeLarco, B. M.; Narayanan, V. L.; Forbes, M., Activity of a novel 4-quinolinecarboxylic acid, NSC 368390 [6-Fluoro-2-(2'-fluoro-1,1'-biphenyl-4-yl)-3-methyl-4-quinolinecarboxylic acid sodium salt], against experimental tumors. *Cancer Res.* **1985,** *45*, 5563-5568.

11.   Cody, R.; Stewart, D.; DeForni, M.; Moore, M.; Dallaire, B.; Azarnia, N.; Gyves, J., Multicenter Phase II study of brequinar sodium in patients with advanced breast cancer. *Am. J. Clin. Oncol.* **1993,** *16* (6), 526-528.

12.   Dodion, P. F.; Wagener, T.; Stoter, G.; Drozd, A.; Lev, L. M.; Skovsgaard, T.; Renard, J.; Cavalli, F., Phase II trial with brequinar (DUP-785, NSC 368390) in patients with metastatic

colorectal cancer: a study of the Early Clinical Trials Group of the EORTC. *Ann. Oncol.* **1990,** *1* (1), 79-80.

13.   Urba, S.; Doroshow, J.; Cripps, C.; Robert, F.; Velez-Garcia, E.; Dallaire, B.; Adams, D.; Carlson, R.; Grillo-Lopez, A.; Gyves, J., Multicenter phase II trial of brequinar sodium in patients with advanced squamous-cell carcinoma of the head and neck. *Cancer Chemother. Pharmacol.* **1992,** *31*, 167-169.

14.   Moore, M.; Maroun, J.; Robert, F.; Natale, R.; Neidhart, J.; Dallaire, B.; Sisk, R.; Gyves, J., Multicenter phase II study of brequinar sodium in patients with advanced gastrointestinal cancer. *Invest. New Drugs.* **1993,** *11*, 61-65.

15.   Maroun, J.; Ruckdeschel, J.; Natale, R.; Morgan, R.; Dallaire, B.; Sisk, R.; Gyves, J., Multicenter phase II study of brequinar sodium in patients with advanced lung cancer. *Cancer Chemother. Pharmacol.* **1993,** *32*, 64-66.

16.   Natale, R.; Wheeler, R.; Moore, M.; Dallaire, B.; Lynch, W.; Carlson, R.; Grillo-Lopez, A.; Gyves, J., Multicenter phase II trial of brequinar sodium in patients with advanced melanoma. *Ann. Oncol.* **1992,** *3* (8), 659-660.

17.   Schwartsmann, G.; Peters, G. J.; Laurensse, E.; de Waal, F. C.; Loonen, A. H.; Leyva, A.; Pinedo, H. M., DUP-785 (NSC 368390): schedule-dependency of growth-inhibitory and anti-pyrimidine effects. *Biochem. Pharmacol.* **1988,** *37*, 3257-3266.

18.   Peters, G. J.; Sharma, S. L.; Laurensse, E.; Pinedo, H. M., Inhibition of pyrimidine de novo synthesis by DUP-785 (NSC 368390). *Invest. New Drugs.* **1987,** *5*, 235-244.

19.   Peters, G. J.; Schwartsmann, G.; Nadal, J. C.; Laurensse, E. J.; van Groeningen, C. J.; van der Vijgh, W. J. F.; Pinedo, H. M., In vivo inhibition of the pyrimidine de novo enzyme dihydroorotic acid dehydrogenase by brequinar sodium (DUP-785; NSC 368390) in mice and patients. *Cancer Res.* **1990,** *50*, 4644-4649.

20.   Peters, G. J.; Kraal, I.; Pinedo, H. M., In vitro and in vivo studies on the combination of brequinar sodium (DUP-785; NSC 368390) with 5-fluorouracil; effects of uridine. *Br. J. Cancer.* **1992,** *65*, 229-233.

21.   Bajzikova, M.; Kovarova, J.; Coelho, A. R.; Boukalova, S.; Oh, S.; Rohlenova, K.; Svec, D.; Hubackova, S.; Endaya, B.; Judasova, K.; Bezawork-Geleta, A.; Kluckova, K.; Chatre, L.; Zobalova, R.; Novakova, A.; Vanova, K.; Ezrova, Z.; Maghzal, G. J.; Magalhaes Novais, S.; Olsinova, M.; Krobova, L.; An, Y. J.; Davidova, E.; Nahacka, Z.; Sobol, M.; Cunha-Oliveira, T.; Sandoval-Acuna, C.; Strnad, H.; Zhang, T.; Huynh, T.; Serafim, T. L.; Hozak, P.; Sardao, V. A.; Koopman, W. J. H.; Ricchetti, M.; Oliveira, P. J.; Kolar, F.; Kubista, M.; Truksa, J.; Dvorakova-Hortova, K.; Pacak, K.; Gurlich, R.; Stocker, R.; Zhou, Y.; Berridge, M. V.; Park, S.; Dong, L.; Rohlena, J.; Neuzil, J., Reactivation of dihydroorotate dehydrogenase-driven pyrimidine biosynthesis restores tumor growth of respiration-deficient cancer cells. *Cell Metab.* **2019,** *29* (2), 399-416 e310.

22.   Rehan, S.; Shahid, S.; Salminen, T. A.; Jaakola, V. P.; Paavilainen, V. O., Current progress on equilibrative nucleoside transporter function and inhibitor design. *SLAS Discov.* **2019,** *24* (10), 953-968.

23.   Young, J. D., The SLC28 (CNT) and SLC29 (ENT) nucleoside transporter families: a 30-year collaborative odyssey. *Biochem. Soc. Trans.* **2016,** *44* (3), 869-876.

24.   Smith, K. M.; Ng, A. M.; Yao, S. Y.; Labedz, K. A.; Knaus, E. E.; Wiebe, L. I.; Cass, C. E.; Baldwin, S. A.; Chen, X. Z.; Karpinski, E.; Young, J. D., Electrophysiological characterization of a recombinant human Na+-coupled nucleoside transporter (hCNT1) produced in Xenopus oocytes. *J. Physiol.* **2004,** *558* (Pt 3), 807-823.

25.   Snezhkina, A. V.; Krasnov, G. S.; Zaretsky, A. R.; Zhavoronkov, A.; Nyushko, K. M.; Moskalev, A. A.; Karpova, I. Y.; Afremova, A. I.; Lipatova, A. V.; Kochetkov, D. V.; Fedorova, M. S.; Volchenko, N. N.; Sadritdinova, A. F.; Melnikova, N. V.; Sidorov, D. V.; Popov, A. Y.; Kalinin, D. V.; Kaprin, A. D.; Alekseev, B. Y.; Dmitriev, A. A.; Kudryavtseva, A. V., Differential expression of alternatively spliced transcripts related to energy metabolism in colorectal cancer. *BMC Genomics.* **2016,** *17* (Suppl 14), 1011.

26.   Hagmann, W.; Jesnowski, R.; Lohr, J. M., Interdependence of gemcitabine treatment, transporter expression, and resistance in human pancreatic carcinoma cells. *Neoplasia.* **2010,** *12* (9), 740-747.

27.   Liu, Y.; Zuo, T.; Zhu, X.; Ahuja, N.; Fu, T., Differential expression of hENT1 and hENT2 in colon cancer cell lines. *Genet. Mol. Res.* **2017,** *16* (1), 1-8.

28.   Kunicka, T.; Prochazka, P.; Krus, I.; Bendova, P.; Protivova, M.; Susova, S.; Hlavac, V.; Liska, V.; Novak, P.; Schneiderova, M.; Pitule, P.; Bruha, J.; Vycital, O.; Vodicka, P.; Soucek, P., Molecular profile of 5-fluorouracil pathway genes in colorectal carcinoma. *BMC Cancer.* **2016,** *16* (1), 795.

29.   Santini, D.; Vincenzi, B.; Fratto, M. E.; Perrone, G.; Lai, R.; Catalano, V.; Cass, C.; Ruffini, P. A.; Spoto, C.; Muretto, P.; Rizzo, S.; Muda, A. O.; Mackey, J. R.; Russo, A.; Tonini, G.; Graziano, F., Prognostic role of human equilibrative transporter 1 (hENT1) in patients with resected gastric cancer. *J. Cell. Physiol.* **2010,** *223* (2), 384-388.

30.   Tavano, F.; Fontana, A.; Pellegrini, F.; Burbaci, F. P.; Rappa, F.; Cappello, F.; Copetti, M.; Maiello, E.; Lombardi, L.; Graziano, P.; Vinciguerra, M.; di Mola, F. F.; di Sebastiano, P.; Andriulli, A.; Pazienza, V., Modeling interactions between human equilibrative nucleoside transporter-1 and other factors involved in the response to gemcitabine treatment to predict clinical outcomes in pancreatic ductal adenocarcinoma patients. *J. Transl. Med.* **2014,** *12*, 248.

31.   Mohelnikova-Duchonova, B.; Brynychova, V.; Hlavac, V.; Kocik, M.; Oliverius, M.; Hlavsa, J.; Honsova, E.; Mazanec, J.; Kala, Z.; Melichar, B.; Soucek, P., The association

between the expression of solute carrier transporters and the prognosis of pancreatic cancer. *Cancer Chemother. Pharmacol.* **2013,** *72* (3), 669-682.

32.   Kim, R.; Tan, A.; Lai, K. K.; Jiang, J.; Wang, Y.; Rybicki, L. A.; Liu, X., Prognostic roles of human equilibrative transporter 1 (hENT-1) and ribonucleoside reductase subunit M1 (RRM1) in resected pancreatic cancer. *Cancer.* **2011,** *117* (14), 3126-3134.

33.   Guo, Z.; Wang, F.; Di, Y.; Yao, L.; Yu, X.; Fu, D.; Li, J.; Jin, C., Antitumor effect of gemcitabine-loaded albumin nanoparticle on gemcitabine-resistant pancreatic cancer induced by low hENT1 expression. *Int. J. Nanomedicine.* **2018,** *13*, 4869-4880.

34.   Liu, Z. Q.; Han, Y. C.; Zhang, X.; Chu, L.; Fang, J. M.; Zhao, H. X.; Chen, Y. J.; Xu, Q., Prognostic value of human equilibrative nucleoside transporter1 in pancreatic cancer receiving gemcitabin-based chemotherapy: a meta-analysis. *PLoS One.* **2014,** *9* (1), e87103.

35.   Greenhalf, W.; Ghaneh, P.; Neoptolemos, J. P.; Palmer, D. H.; Cox, T. F.; Lamb, R. F.; Garner, E.; Campbell, F.; Mackey, J. R.; Costello, E.; Moore, M. J.; Valle, J. W.; McDonald, A. C.; Carter, R.; Tebbutt, N. C.; Goldstein, D.; Shannon, J.; Dervenis, C.; Glimelius, B.; Deakin, M.; Charnley, R. M.; Lacaine, F.; Scarfe, A. G.; Middleton, M. R.; Anthoney, A.; Halloran, C. M.; Mayerle, J.; Olah, A.; Jackson, R.; Rawcliffe, C. L.; Scarpa, A.; Bassi, C.; Buchler, M. W.; European Study Group for Pancreatic, C., Pancreatic cancer hENT1 expression and survival from gemcitabine in patients from the ESPAC-3 trial. *J. Natl. Cancer Inst.* **2014,** *106* (1), djt347.

36.   Farrell, J. J.; Elsaleh, H.; Garcia, M.; Lai, R.; Ammar, A.; Regine, W. F.; Abrams, R.; Benson, A. B.; Macdonald, J.; Cass, C. E.; Dicker, A. P.; Mackey, J. R., Human equilibrative nucleoside transporter 1 levels predict response to gemcitabine in patients with pancreatic cancer. *Gastroenterology.* **2009,** *136* (1), 187-195.

37.   Tsujie, M.; Nakamori, S.; Nakahira, S.; Takahashi, Y.; Hayashi, N.; Okami, J.; Nagano, H.; Dono, K.; Umeshita, K.; Sakon, M.; Monden, M., Human equilibrative nucleoside transporter 1, as a predictor of 5-fluorouracil resistance in human pancreatic cancer. *Anticancer Res.* **2007,** *27*, 2241-2250.

38.   Mori, R.; Ishikawa, T.; Ichikawa, Y.; Taniguchi, K.; Matsuyama, R.; Ueda, M.; Fujii, Y.; Endo, I.; Togo, S.; Danenberg, P. V.; Shimada, H., Human equilibrative nucleoside transporter 1 is associated with the chemosensitivity of gemcitabine in human pancreatic adenocarcinoma and biliary tract carcinoma cells. *Oncol. Rep.* **2007,** *17*, 1201-1205.

39.   Giovannetti, E.; Del Tacca, M.; Mey, V.; Funel, N.; Nannizzi, S.; Ricci, S.; Orlandini, C.; Boggi, U.; Campani, D.; Del Chiaro, M.; Iannopollo, M.; Bevilacqua, G.; Mosca, F.; Danesi, R., Transcription analysis of human equilibrative nucleoside transporter-1 predicts survival in pancreas cancer patients treated with gemcitabine. *Cancer Res.* **2006,** *66* (7), 3928-3935.

40.   Marechal, R.; Bachet, J. B.; Mackey, J. R.; Dalban, C.; Demetter, P.; Graham, K.; Couvelard, A.; Svrcek, M.; Bardier-Dupas, A.; Hammel, P.; Sauvanet, A.; Louvet, C.; Paye, F.; Rougier, P.; Penna, C.; Andre, T.; Dumontet, C.; Cass, C. E.; Jordheim, L. P.; Matera, E. L.;

Closset, J.; Salmon, I.; Deviere, J.; Emile, J. F.; Van Laethem, J. L., Levels of gemcitabine transport and metabolism proteins predict survival times of patients treated with gemcitabine for pancreatic adenocarcinoma. *Gastroenterology.* **2012,** *143* (3), 664-674 e666.

41.   Marechal, R.; Mackey, J. R.; Lai, R.; Demetter, P.; Peeters, M.; Polus, M.; Cass, C. E.; Young, J.; Salmon, I.; Deviere, J.; Van Laethem, J. L., Human equilibrative nucleoside transporter 1 and human concentrative nucleoside transporter 3 predict survival after adjuvant gemcitabine therapy in resected pancreatic adenocarcinoma. *Clin. Cancer Res.* **2009,** *15* (8), 2913-2919.

42.   Murata, Y.; Hamada, T.; Kishiwada, M.; Ohsawa, I.; Mizuno, S.; Usui, M.; Sakurai, H.; Tabata, M.; Ii, N.; Inoue, H.; Shiraishi, T.; Isaji, S., Human equilibrative nucleoside transporter 1 expression is a strong independent prognostic factor in UICC T3-T4 pancreatic cancer patients treated with preoperative gemcitabine-based chemoradiotherapy. *J. Hepatobiliary Pancreat. Sci.* **2012,** *19* (4), 413-425.

43.   Aoyama, T.; Kazama, K.; Miyagi, Y.; Murakawa, M.; Yamaoku, K.; Atsumi, Y.; Shiozawa, M.; Ueno, M.; Morimoto, M.; Oshima, T.; Yukawa, N.; Yoshikawa, T.; Rino, Y.; Masuda, M.; Morinaga, S., Predictive role of human equilibrative nucleoside transporter 1 in patients with pancreatic cancer treated by curative resection and gemcitabine-only adjuvant chemotherapy. *Oncol. Lett.* **2017,** *14* (1), 599-606.

44.   Morinaga, S.; Nakamura, Y.; Watanabe, T.; Mikayama, H.; Tamagawa, H.; Yamamoto, N.; Shiozawa, M.; Akaike, M.; Ohkawa, S.; Kameda, Y.; Miyagi, Y., Immunohistochemical analysis of human equilibrative nucleoside transporter-1 (hENT1) predicts survival in resected pancreatic cancer patients treated with adjuvant gemcitabine monotherapy. *Ann. Surg. Oncol.* **2012,** *19 Suppl 3*, S558-564.

45.   Fujita, H.; Ohuchida, K.; Mizumoto, K.; Itaba, S.; Ito, T.; Nakata, K.; Yu, J.; Kayashima, T.; Souzaki, R.; Tajiri, T.; Manabe, T.; Ohtsuka, T.; Tanaka, M., Gene expression levels as predictive markers of outcome in pancreatic cancer after gemcitabine-based adjuvant chemotherapy. *Neoplasia.* **2010,** *12* (10), 807-817.

46.   Spratlin, J.; Sangha, R.; Glubrecht, D.; Dabbagh, L.; Young, J. D.; Dumontet, C.; Cass, C.; Lai, R.; Mackey, J. R., The absence of human equilibrative nucleoside transporter 1 is associated with reduced survival in patients with gemcitabine-treated pancreas adenocarcinoma. *Clin. Cancer Res.* **2004,** *10*, 6956-6961.

47.   Fisher, P. H.; Pamukcu, R.; Bittner, G.; Willson, J. K. V., Enhancement of the sensitivity of human colon cancer cells to growth inhibition by acivicin acheived through inhibition of nucleic acid precursor salvage by dipyridamole. *Cancer Res.* **1984,** *44*, 3355-3359.

48.   Willson, J. K. V.; Fisher, P. H.; Tutsch, K.; Alberti, D.; Simon, K.; Hamiltion, R. D.; Bruggnik, J.; Koeller, J. M.; Tormey, D. C.; Earhart, R. H.; Ranhosky, A.; Trump, D. L., Phase I clinical trial of a combination of dipyridamole and acivicin based upon inhibition of nucleoside salvage. *Cancer Res.* **1988,** *48*, 5855-5590.

49.   Chan, T. C.; Markman, M.; Cleary, S.; Howell, S. B., Plasma uridine changes in cancer patient treated with combination of dipyridamole and N-phosphonacetyl-L-acetate. *Cancer Res.* **1986,** *46* (6), 3168-3172.

50.   Markman, M.; Chan, T. C.; Cleary, S.; Howell, S. B., Phase I trial of combination therapy of cancer with N-phosphonacetyl-L-aspartic acid and dipyridamole. *Cancer Chemother. Pharmacol.* **1987,** *19* (1), 80-83.

51.   Fleming, R. A.; Capizzi, R. L.; Muss, H. B.; Smith, S.; Fernandes, D. J.; Homesley, H.; Loggie, B. W.; Case, L. D.; Morris, R.; Russell, G. B.; Richards, F., Phase I study of N-(phosphonacetyl)-L-aspartate with fluorouracil and with or without dipyridamole in patients with advanced cancer. *Clin. Cancer Res.* **1996,** *2*, 1107-1114.

52.   Karle, J. M.; Anderson, L. W.; Dietrick, D. D.; R.L., C., Determination of serum and plasma uridine levels in mice, rats, and humans by high-pressure liquid chromatography. *Anal. Biochem.* **1980,** *109*, 41-46.

53.   Dorasamy, M. S.; Ab, A.; Nellore, K.; Wong, P. F., Synergistic inhibition of melanoma xenografts by brequinar sodium and doxorubicin. *Biomed. Pharmacother.* **2019,** *110*, 29-36.

54.   Tatani, K.; Hiratochi, M.; Kikuchi, N.; Kuramochi, Y.; Watanabe, S.; Yamauchi, Y.; Itoh, F.; Isaji, M.; Shuto, S., Identification of adenine and benzimidazole nucleosides as potent human concentrative nucleoside transporter 2 inhibitors: potential treatment for hyperuricemia and gout. *J. Med. Chem.* **2016,** *59* (8), 3719-3731.

55.   Madak, J. T.; Cuthbertson, C. R.; Miyata, Y.; Tamura, S.; Petrunak, E. M.; Stuckey, J. A.; Han, Y.; He, M.; Sun, D.; Showalter, H. D.; Neamati, N., Design, synthesis, and biological evaluation of 4-quinoline carboxylic acids as inhibitors of dihydroorotate dehydrogenase. *J. Med. Chem.* **2018,** *61* (12), 5162-5186.

56.   Chen, S.-F.; Papp, L. M.; Ardecky, R. J.; Rao, G. V.; Hesson, D. P.; Forbes, M.; Dexter, D. L., Structure-activity relationship of quinoline carboxylic acids. *Biochem. Pharmacol.* **1990,** *40* (4), 709-714.

57.   Greene, S.; Watanabe, K.; Braatz-Trulson, J.; Lou, L., Inhibition of dihydroorotate dehydrogenase by the immunosuppressive agent leflunomide. *Biochem. Pharmacol.* **1995,** *50* (6), 861-867.

58.   Chan, T. C. K.; Howell, S. B., Mechanism of synergy between N-phosponacetly-L-aspartate and dipyridamole in a human ovarian carcinoma cell line. *Cancer Res.* **1985,** *45*, 3598-3604.

59.   Chan, T. C.; Young, B.; King, M. E.; Taetle, R.; Howell, S. B., Modulation of the activity of PALA by dipyridamole. *Cancer Treat Rep.* **1985,** *69* (4), 425-430.

60.   Lomize, A. L.; Hage, J. M.; Schnitzer, K.; Golobokov, K.; LaFaive, M. B.; Forsyth, A. C.; Pogozheva, I. D., PerMM: A web tool and database for analysis of passive membrane permeability and translocation pathways of bioactive molecules. *J Chem Inf Model.* **2019,** *59* (7), 3094-3099.

61.   Lomize, A. L.; Pogozheva, I. D., Physics-based method for modeling passive membrane permeability and translocation pathways of bioactive molecules. *J Chem Inf Model.* **2019,** *59* (7), 3198-3213.

62.   Sainas, S.; Pippione, A. C.; Lupino, E.; Giorgis, M.; Circosta, P.; Gaidano, V.; Goyal, P.; Bonanni, D.; Rolando, B.; Cignetti, A.; Ducime, A.; Andersson, M.; Jarva, M.; Friemann, R.; Piccinini, M.; Ramondetti, C.; Buccinna, B.; Al-Karadaghi, S.; Boschi, D.; Saglio, G.; Lolli, M. L., Targeting myeloid differentiation using potent 2-hydroxypyrazolo[1,5- a]pyridine scaffold-based human dihydroorotate dehydrogenase inhibitors. *J Med Chem.* **2018,** *61* (14), 6034-6055.

63.   Di Veroli, G. Y.; Fornari, C.; Wang, D.; Mollard, S.; Bramhall, J. L.; Richards, F. M.; Jodrell, D. I., Combenefit: an interactive platform for the analysis and visualization of drug combinations. *Bioinformatics.* **2016,** *32* (18), 2866-2868.

64.   Bliss, C. I., The toxicity of poisons applied jointly. *Ann. Appl. Biol.* **1939,** *26* (3), 585-615.

65.   Andres, A.; Roses, M.; Rafols, C.; Bosch, E.; Espinosa, S.; Segarra, V.; Huerta, J. M., Setup and validation of shake-flask procedures for the determination of partition coefficients (logD) from low drug amounts. *Eur J Pharm Sci.* **2015,** *76*, 181-191.

66.   Davis, J. P.; Copeland, R. A., Histidine to alanine mutants of human dihydroorotate dehydrogenase. *Biochem. Pharmacol.* **1997,** *54* (4), 459-465.

67.   Papageorgiou, C.; Zurini, M.; Weber, H.-P.; Borer, X., Leflunomide's bioactive metabolite has the minimal structural requirements for the efficient inhibition of human dihydroorotate dehydrogenase. *Bioorg. Chem.* **1997,** *25* (4), 233-238.

68.   Pimple, S. R. Flavonoids and related compounds as nucleoside transporter inhibitors. University of Tennessee, Theses and Dissertations (ETD), 2008.

69.   Toan, S. V.; To, K. K.; Leung, G. P.; de Souza, M. O.; Ward, J. L.; Tse, C. M., Genomic organization and functional characterization of the human concentrative nucleoside transporter-3 isoform (hCNT3) expressed in mammalian cells. *Pflugers Arch.* **2003,** *447* (2), 195-204.

70.   Hummel, C. S.; Lu, C.; Loo, D. D.; Hirayama, B. A.; Voss, A. A.; Wright, E. M., Glucose transport by human renal Na+/D-glucose cotransporters SGLT1 and SGLT2. *Am. J. Physiol. Cell. Physiol.* **2011,** *300* (1), C14-21.

71.   Ward, J. L.; Sherali, A.; Mo, Z. P.; Tse, C. M., Kinetic and pharmacological properties of cloned human equilibrative nucleoside transporters, ENT1 and ENT2, stably expressed in nucleoside transporter-deficient PK15 cells. *J. Biol. Chem.* **2000,** *275* (12), 8375-8381.

72.   Wang, C.; Lin, W.; Playa, H.; Sun, S.; Cameron, K.; Buolamwini, J. K., Dipyridamole analogs as pharmacological inhibitors of equilibrative nucleoside transporters. Identification of novel potent and selective inhibitors of the adenosine transporter function of human equilibrative nucleoside transporter 4 (hENT4). *Biochem. Pharmacol.* **2013,** *86* (11), 1531-1540.

73.   Torphy, T. J.; Cieslinski, L. B., Characterization and selective inhibition of cyclic nucleotide phosphodiesterase isozymes in canine tracheal smooth muscle. *Mol. Pharmacol.* **1990,** *37*, 206-214.

74.   Thomas, M. K.; Francis, S. H.; Corbin, J. D., Characterization of a purified bovine lung cGMP-binding cGMP phosphodiesterase. *J. Biol. Chem.* **1990,** *265* (25), 14964-14970.

75.   Lin, W.; Buolamwini, J. K., Synthesis, flow cytometric evaluation, and identification of highly potent dipyridamole analogues as equilibrative nucleoside transporter 1 inhibitors. *J. Med. Chem.* **2007,** *50*, 3906-3920.

76.   Ehrenkranz, J. R.; Lewis, N. G.; Kahn, C. R.; Roth, J., Phlorizin: a review. *Diabetes Metab. Res. Rev.* **2005,** *21* (1), 31-38.

77.   Gresele, P.; Momi, S.; Falcinelli, E., Anti-platelet therapy: phosphodiesterase inhibitors. *Br. J. Clin. Pharmacol.* **2011,** *72* (4), 634-646.

CHAPTER IV   Pharmacophore-based Discovery of a Novel MTHFD2 Inhibitor

Introduction[4]

Methylenetetrahydrofolate dehydrogenase (MTHFD) is an enzyme that participates in the folate pathway of one-carbon metabolism. There are four human isoforms of MTHFD: MTHFD1, MTHFD1L, MTHFD2, and MTHFD2L. MTHFD1 is the only isoform that resides in the cytoplasm as all others are in the mitochondria and it possesses dehydrogenase (D), cyclohydrolase (C), and synthetase (S) activities. The three mitochondrial isoforms complement the trifunctional $NADP^+$-dependent cytoplasmic enzyme.[1] MTHFD2/2L both possess DC activity while MTHFD1L only performs the S function. The mitochondrial $NAD(P)^+$-dependent dehydrogenases convert 5,10-methylenetetrahydrofolate ($5,10-CH_2-THF$) to the 5,10-methenyltetrahydrofolate ($5,10-CH^+-THF$) intermediate.[1-2] The cyclohydrolase functionality then oxidizes the intermediate into 10-formyltetrahydrofolate (10-CHO-THF) through hydrolysis. The synthetase domain of MTHFD1L uses ATP to catalyze the formation of 10-CHO-THF from formate and THF. The seeming redundancy of MTHFD2/2L was discovered by examining expression of the enzymes in developmental and adult tissues and transformed cells.[3-5] MTHFD2 is exclusively expressed during embryonic development and in transformed cells, while MTHFD2L is expressed in differentiated adult tissues, making MTHFD2 an extremely attractive target for cancer treatment.[6]

Overexpression of MTHFD2 correlates with prognosis and clinicopathological parameters in breast, colorectal, kidney, liver, and pancreatic cancers with a complicated case in brain cancers.[6] Across a panel of metabolic enzymes and cell lines, MTHFD2 was one of the top enzymes whose expression significantly correlated with proliferation rate whereas the cytosolic isoform did not.[7] Silencing of MTHFD2 expression or inhibition of its enzymatic activity impairs cancer cell growth *in vitro* and *in vivo*.[5, 8-17] In some cases, knockdown of MTHFD2 did not affect cell proliferation but negatively impacted metastatic phenotypes such as migration.[18] Interestingly, MTHFD2 contributes to cancer cell proliferation independently of its enzymatic activity and this warrants in-depth investigation to better understand MTHFD2's role in cancer progression.[19-20]

Despite many reports on the significance of MTHFD2 in cancer, only a handful of inhibitors have been identified thus far (Figure IV-1). An *in silico* approach identified molecules that were predicted to bind in the THF and NAD binding sites, however this was not experimentally validated.[21] Unsurprisingly, a folate analog, LY345899, showed nanomolar activity against both MTHFD1 and MTHFD2, with ~7-fold selectivity towards MTHFD1.[22] The natural product carolacton was the first molecule that showed any selectivity towards the dehydrogenase activity of MTHFD2 (MTHFD1 IC_{50} = 38 nM; MTHFD2 IC_{50} = 6.5 nM), however towards the cyclohydrolase activity was MTHFD1 selective.[23] Finally, Kawai *et al*., disclosed DS44960156 as an MTHFD2 inhibitor, with an impressive 18-fold selectivity over MTHFD1.[24] Shortly thereafter an optimized inhibitor was revealed with nanomolar enzymatic inhibitory activity and *in vivo* efficacy.[8] Therefore, we sought to build on their work with the aim of identifying a novel scaffold. Herein we report a pharmacophore model that led to the discovery of a novel class of compounds as MTHFD2 inhibitors that have anti-cancer activity. Our hit compound **CBN-1** is the first covalent MTHFD2 inhibitor reported.
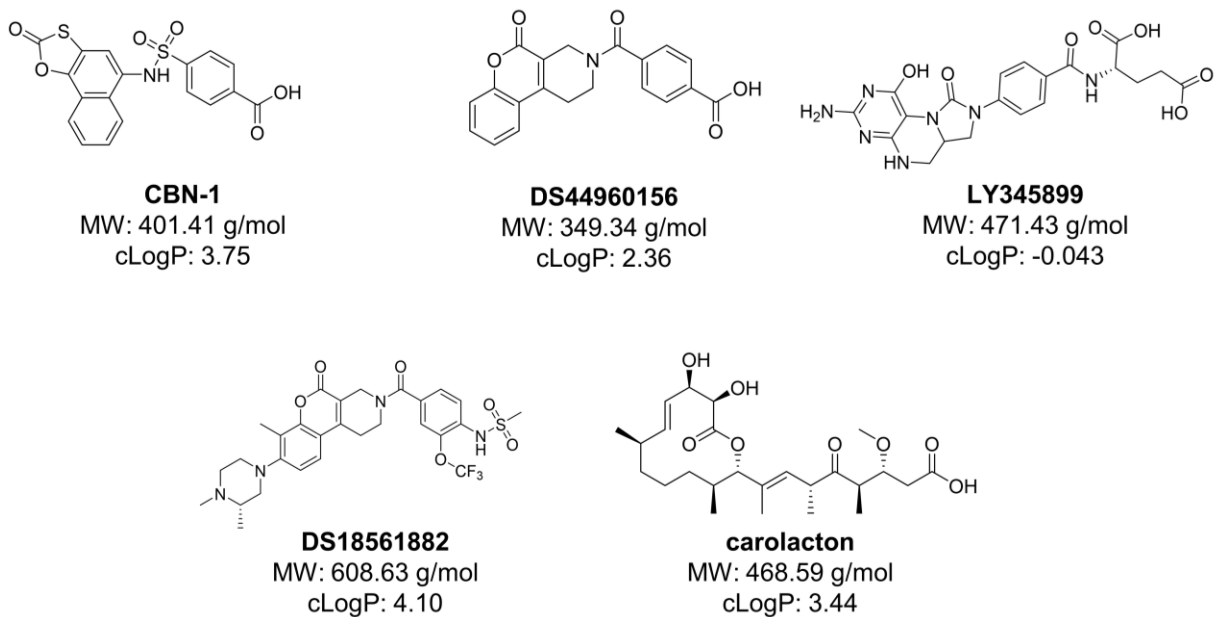
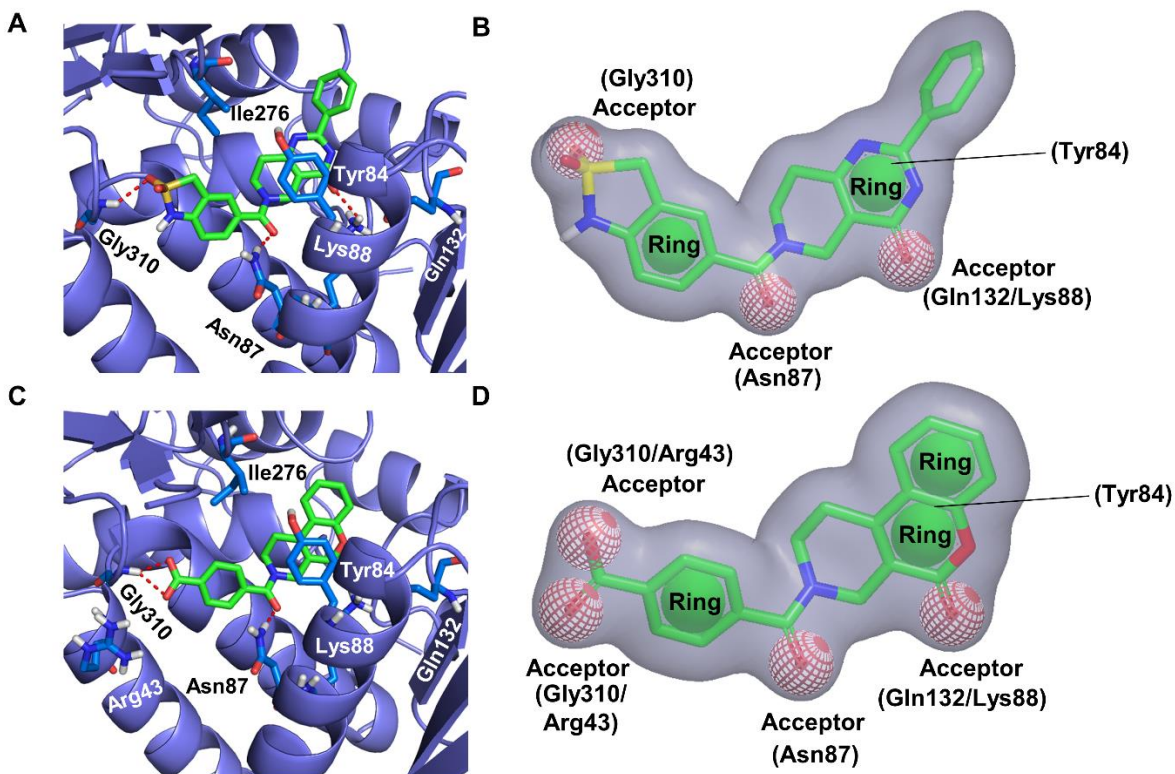Figure IV-1. Experimentally validated MTHFD2 inhibitors. **CBN-1**, this study.

Figure IV-2. ROCS pharmacophore model of MTHFD2 crystal structure PDB IDs (A, B) 6JID and (C, D) 6JIB.

Results and discussion

In silico screen identifies MTHFD2 inhibitors

The co-crystal structure of MTHFD2 with novel small-molecule inhibitor DS44960156 was recently disclosed by Daiichi-Sankyo. Residues that were hypothesized to be vital for binding include Gln132, Lys88, Asn87, Gly310, and Tyr84. In an effort to discover a more potent MTHFD2-selective inhibitor we built a pharmacophore model based on PDB IDs 6JIB and 6JID using ROCS (Figure IV-2).[25] Our in-house database of over 28,000 compounds was queried and 43 hits were identified (~0.15% hit rate). The hits were screened in the MTHFD2 enzymatic assay and only two showed activity at 625 μM (Figure IV-3A). Inspection of their structures revealed that **CBN-2** was likely a PAIN as it contained a 5-ene-rhodanine.[26] Therefore **CBN-2** and available in-house analogs were screened in an orthogonal assay. At 100 μM, **CBN-2** showed a 1.91 ± 0.5 °C shift in the thermal shift assay against MTHFD2, comparable to the positive control DS44960156 with a 1.81 ± 0.16 °C shift (Appendix Figure IV-1A). This carried over to the MTHFD2 assay as well, though the variability was high (Appendix Figure IV-1B). A total of 21 analogs by similarity (score ≥ 0.35) of **CBN-2** were screened against MTHFD2 in the thermal shift assay at 100 μM (Appendix Figure IV-1C). Only one was reported to shift the melting temperature of MTHFD2 by the analysis software (compound **CBN-2.8**), but closer examination showed that the "shift" was caused by a misshapenness of the melt curve – the derivative plots have the same melting temperatures (Appendix Figure IV-1D, vertical dotted line). The structure of **CBN-2.8** also contains the 5-ene-rhodanine core (Appendix Figure IV-1E). Additionally, LC-MS analysis of **CBN-2** showed < 70% purity, therefore this series was decided to not be pursued further due to unreliability of the results.

CBN-1 has not been reported in the literature and is completely novel. However, similar compounds have been reported as inhibitors of CXCR2, STAT3, NRF2-KEAP1, and acyl-homoserine lactone synthase.[27-32] Evaluation of the dose-response of **CBN-1** in the enzymatic

assay starting at 625 μM revealed a very steep curve, indicative of a solubility issue. Indeed, the solubility of both **CBN-1** and -**2** in DPBS decreases around 500 μM (Figure IV-3B). Therefore, all following assays were carried out at concentrations below 500 μM. The IC$_{50}$ of **CBN-1** against MTHFD2 is 19.6 ± 6.9 μM (Figure IV-3C). Docking of **CBN-1** into the active site of MTHFD2 predicted that many of the same interactions are upheld (Figure IV-3D). The kinetics of the reaction likely plays a factor in the lack of potency. Two previously published enzymatic assays are measured after only 2-5 min incubation with the substrate at 30 °C.[2, 23] From our QTOF experiments (see below) we find that after 35 min, two molecules of **CBN-1a** are bound to the enzyme. We were surprised to see that incubation of MTHFD2 and **CBN-1** for different periods of time before adding substrate (0, 15, or 30 min), produced no change in the IC$_{50}$ value (data not shown). Interestingly, the thiocarbonate of **CBN-1** is not predicted to occupy the same site as the ester of DS44960156 (Figure IV-3E). This could be due to the shape of the binding pocket.
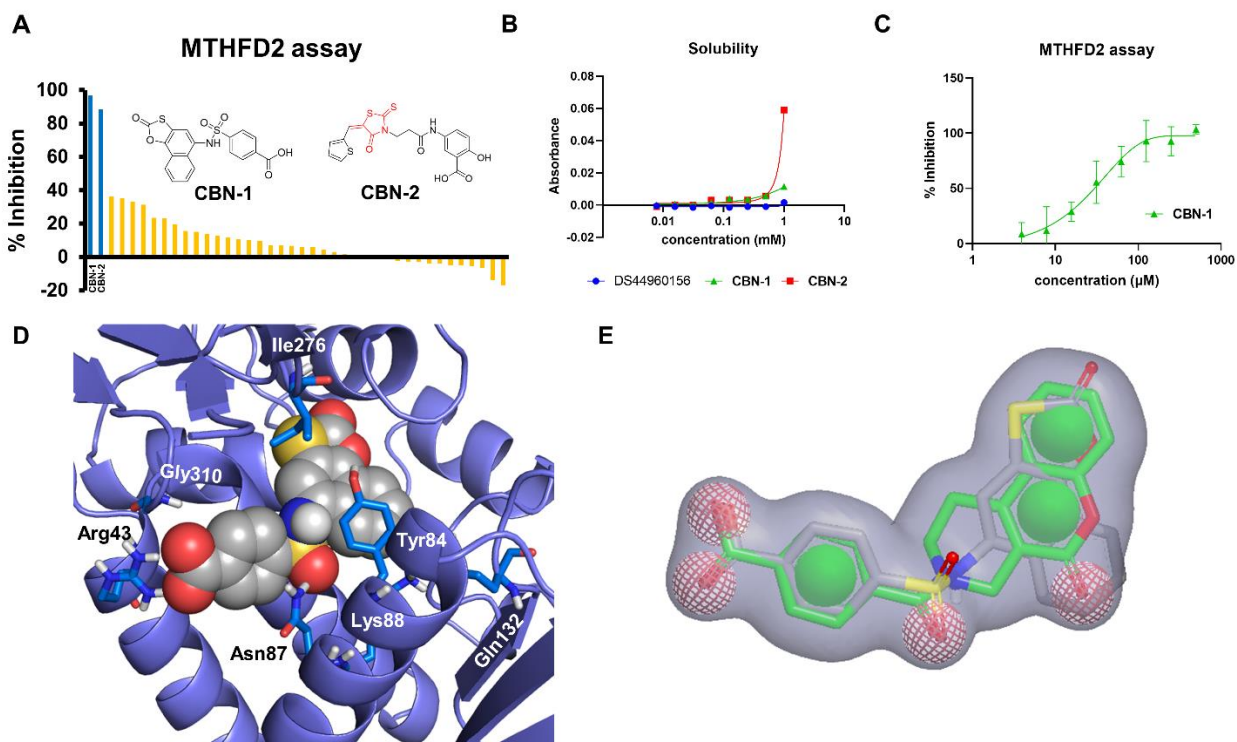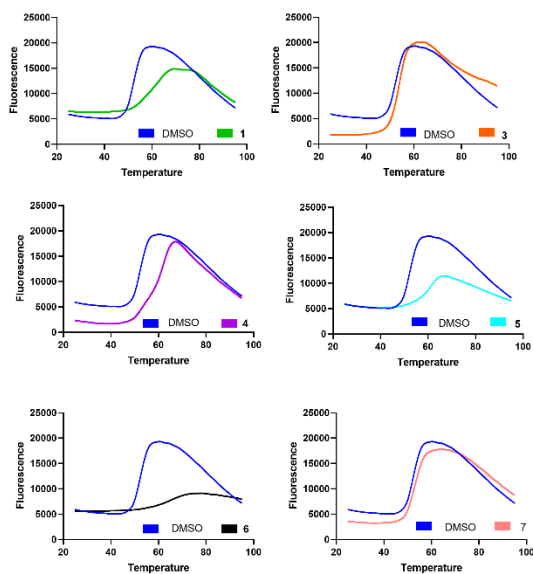

Figure IV-3. *In silico* screen identifies MTHFD2 inhibitor. (A) Hits from the virtual screen were evaluated for activity in the MTHFD2 enzymatic assay at 625 μM. (B) Solubility assay with DS44960156, **CBN-1**, and **CBN-2** in DPBS. (C) **CBN-1** inhibits

MTHFD2's enzymatic activity. (D) **CBN-1** docked into MTHFD2 crystal structure (6JIB). (E) ROCS pharmacophore with DS44960156 (green) superimposed with **CBN-1** (grey).

Validation was carried out in the thermal shift assay. A total of 27 analogs of **CBN-1** were screened in the thermal shift assay at 100 μM and six, including **CBN-1**, significantly increased the melting temperature of MTHFD2 (Figure IV-4A). To investigate structure-activity relationships (SAR), we performed docking with our thermal shift hits and MTHFD2 (Figure IV-4B/C). The protein-ligand interactions plot for different docking poses of inhibitors shows that they form 4-5 interactions out of the six co-crystal interactions (Figure IV-4B/C). Most poses seem to lack either a H-bond to Asn87 or Gly310. Asn87 is what is thought to be responsible for MTHDF2 selectivity because it is a Val in MTHFD1.[24] Additionally, interaction with this residue is critical for activity and is fulfilled by the carbonyl of the linker amide in DS44960156.[24] The sulfonamide of **CBN-1** and analogs superimpose nicely on this position (Figure IV-3E), so it is curious why they aren't forming interactions in the majority of the docking poses. The tenth pose of **CBN-1** is shown in Figure IV-3D, and the distance from the sulfonamide to Asn87 is 2.8 Å. Gly310 is the residue reported to interact with the carboxylic acid of the inhibitor.[24] However, Arg43 is in closer proximity (2.5 Å) to the carboxylic acid of **CBN-1** compared to Gly310 (3.6 Å) and likely plays a role in anchoring the molecule.
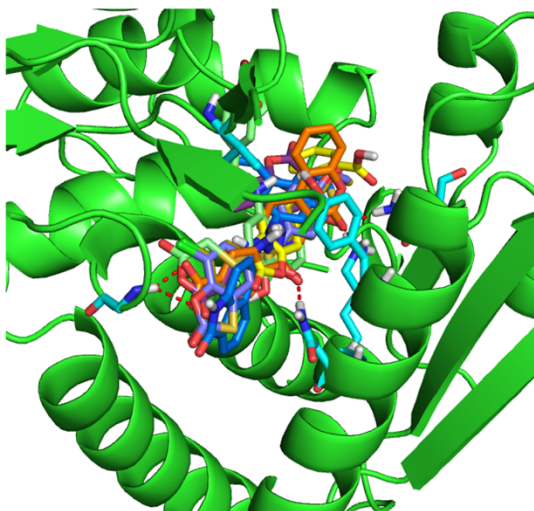
We then were interested in evaluating if **CBN-1** was capable of binding cellular MTHFD2 using the cellular thermal shift assay (CETSA). Interestingly, DS44960156 destabilized MTHFD2 in cell lysates (Figure IV-5A). We found that this compound is not cell permeable as we saw no shift in melting temperature using intact cells (Figure IV-5B). Evaluation of **CBN-1** revealed unprecedented stabilization in lysates and intact cells (Figure IV-5C/D).

A

CBN	Structure	MTHFD2 ΔTm (°C)	SHMT2 ΔTm (°C)
1		8.21 ± 1.2	NB
3		1.34 ± 0.3	NB
4		4.73 ± 1.3	NB
5		4.95 ± 1.4	NB
6		8.65 ± 1.4	2.55
7		0.81 ± 0.1	NB

B

Red = interactions
Blue = no interactions

C

Compound_D	TYR84 (pi-pi)	ASN87 (H-bond)	LYS88 (H-bond)	GLN132 (H-bond)	ILE276-Hy	GLY310 (H-bond)
DS44960156						
1						
3						
4						
5						
6						
7						

Figure IV-4. Analogs of **CBN-1** bind recombinant MTHFD2. (A) **CBN-1** and analogs stabilize MTHFD2 to thermal denaturation. Value for melting temperature of SHMT2 for **CBN-6** is only from one experiment due to compound availability. NB, no binding. (B) **CBN-1** analogs docking into the MTHFD2 active site (PDB ID 6JIB). (C) Protein-ligand interactions plot for docking poses of **CBN** analogs compared to DS44960156. Red and blue represent presence or absence of interactions, respectively.
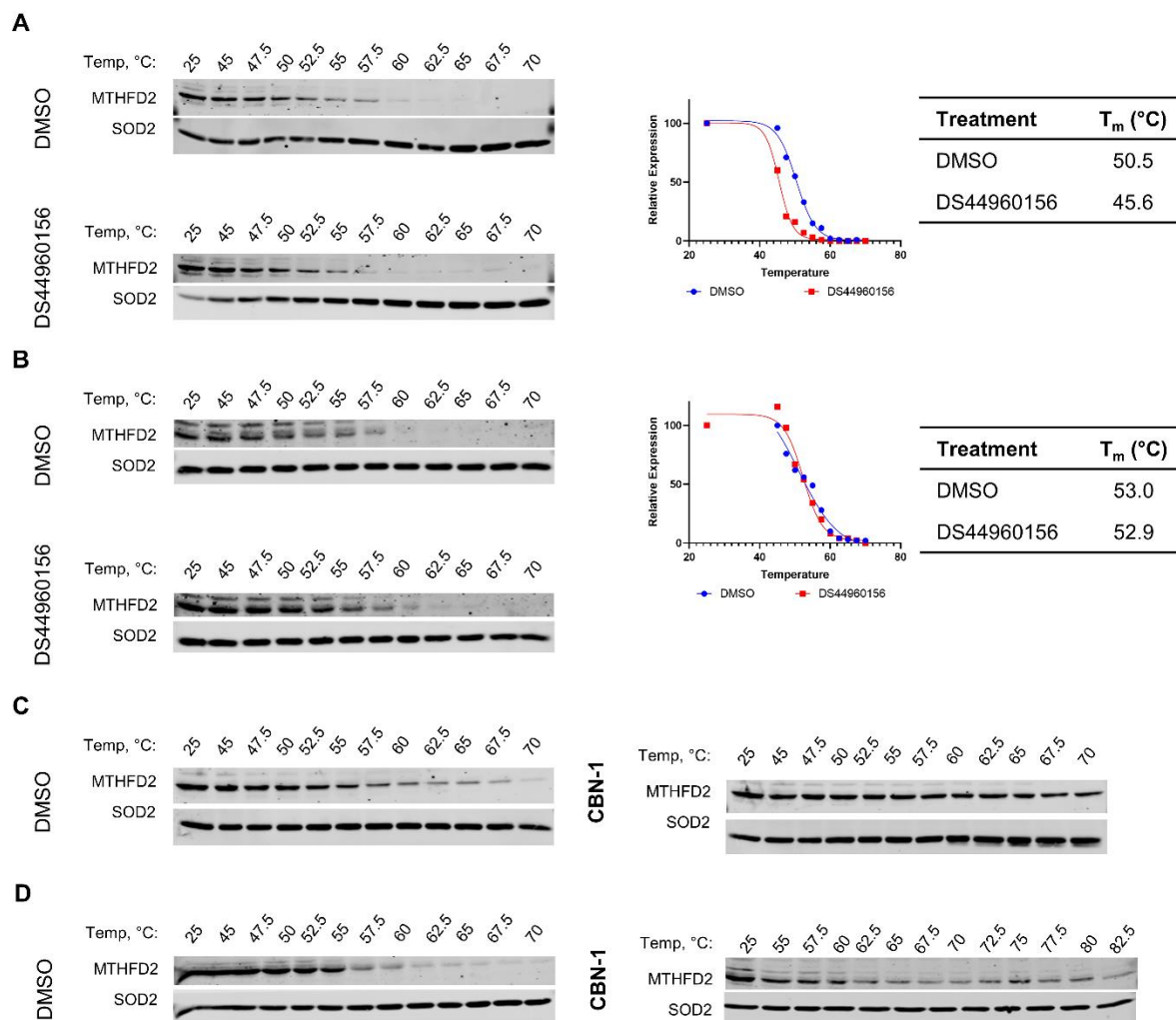
Figure IV-5. **CBN-1** binds cellular MTHFD2. (A) DS44960156 destabilizes cellular MTHFD2 in HAP1 lysates. (B) DS44960156 is not cell permeable. U2OS cells were incubated with 100 μM DS44960156 or DMSO for 1 h at 37 °C. (C) **CBN-1** stabilizes cellular MTHFD2 in U2OS lysates and (D) intact cells.

Thiol reactivity

CBN-6 is previously reported as an Mcl-1 inhibitor with anti-cancer activity and is thiol-reactive.[33-34] Screening of the hit compounds against another folate-dependent enzyme SHMT2 in the thermal shift assay revealed that all were selective for MTHFD2 except for **CBN-6**, thus this compound was not pursued further (Figure IV-4A). Under physiological conditions, it is possible that the thiocarbonate of **CBN-1** could hydrolyze and therefore would closely resemble **CBN-6** (Appendix Figure IV-2). Therefore, we sought to examine the possible thiol reactivity of the other analogs through several methods.

203

The five analogs (**CBN-1**, -**3**, -**4**, -**5**, and -**7**) along with DS44960156 were each incubated with N-acetylcysteine (NAC) in DMSO for 0 h, 4 h, and 24 h and the reaction was monitored via LC-MS. **CBN-3** was the only one that showed reaction with NAC (Appendix Figure IV-3A) and is the only analog with a halogen on the neighboring ring. A similar experiment was carried out with **CBN-1** ± glutathione (GSH) in a DMSO/H_2O mixture. Over time the retention time of the compound did not change – neither the addition of water nor glutathione (GSH) was detected under these conditions (Figure IV-6). Additionally, **CBN-1** did not compete with the covalent dye CMFDA for binding to the thioltransferase glutathione S-transferase omega-1 (Appendix Figure IV-3B).[35]

To investigate if there was any covalent modification of MTHFD2, adduct formation was monitored with quadrupole time-of-flight mass spectrometry (Q-TOF). We incubated 250 µM **CBN-1** with 25 µM MTHFD2 and injected the solution after the indicated incubation times. We found that over time two fragments corresponding to the mass of a hydrolyzed derivative of **CBN-1** (**CBN-1a**) bound to MTHFD2 (Figure IV-7). Therefore, we looked to see if there were nucleophilic residues that were in low abundance that could possibly account for these two additions (Appendix Figure IV-4A). Each monomer of MTHFD2 only has two cysteine residues, however, neither are proximate to the binding site of DS44960156 (Appendix Figure IV-4B, indicated in red) – one points towards the interior of the structure and the other is on the dimer interface. Inside the active site, Lys88 would be in a favorable position for nucleophilic attack in relation to the thiocarbonate assuming a similar binding mode as DS44960156 (Appendix Figure IV-4C). Indeed, acetylation at Lys88 inhibits MTHFD2's enzymatic activity.[36] Further studies are required to determine which residue is responsible for binding. Covalent modification of the

protein could account for the significant stabilization to thermal denaturation (Figure IV-4A and Figure IV-5C/D).
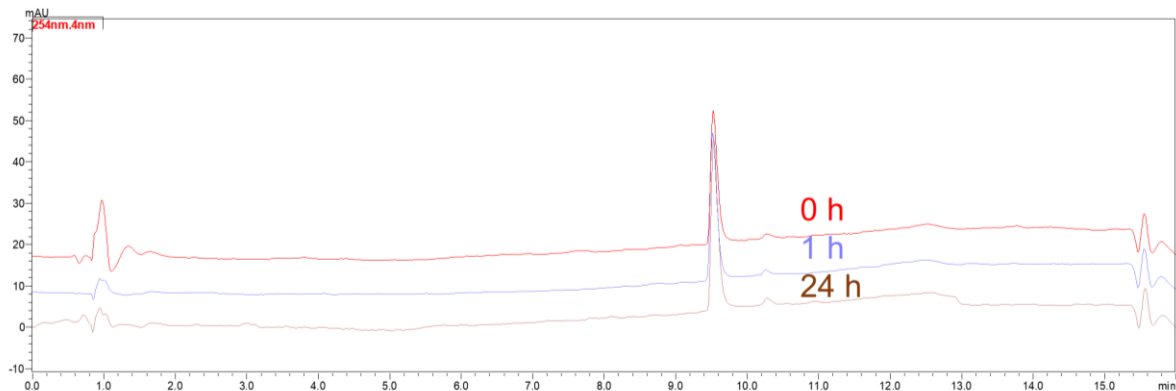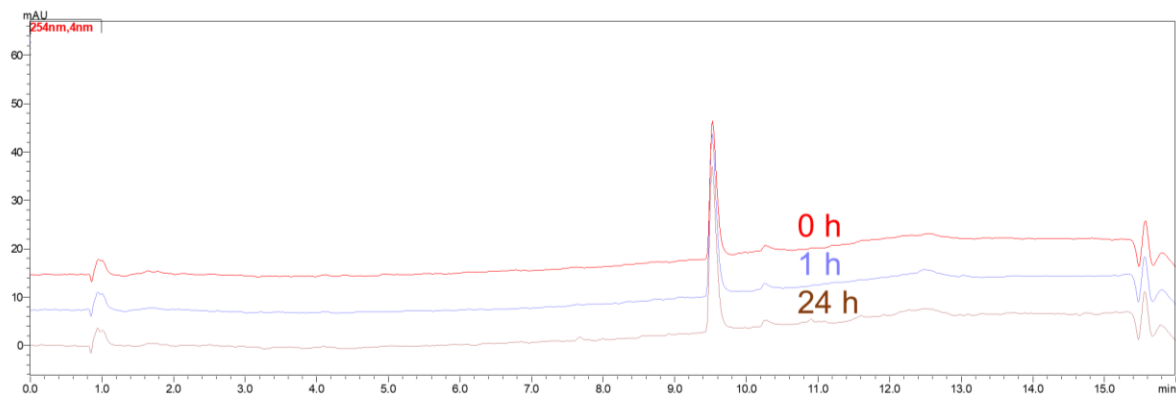

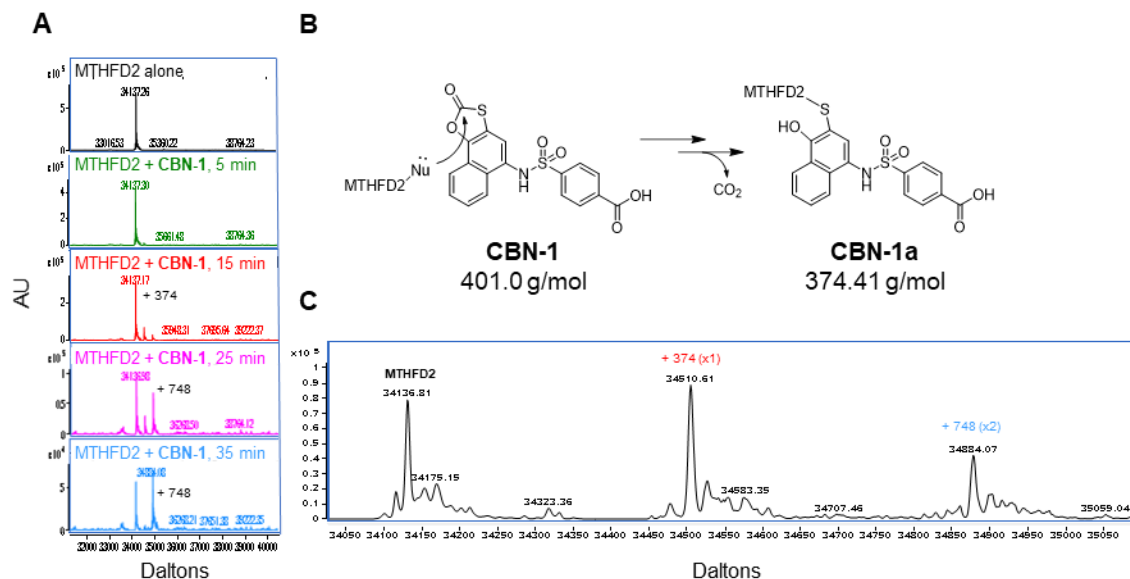Figure IV-6. **CBN-1** does not react with GSH.

Figure IV-7. **CBN-1** covalently binds MTHFD2. (A) Time-dependent binding of **CBN-1** to MTHFD2. (B) Proposed adduct and mechanism of inhibition. (C) Zoomed in view of mass spectra at 20 min incubation of MTHFD2 and **CBN-1**.

MTHFD2 inhibitors have anti-cancer activity

Encouraged by our CETSA results showing cell permeability of **CBN-1**, which DS44960156 lacks, we then turned to evaluation of the anti-cancer activity of our **CBN** compounds. **CBN-1** was the most potent of the analogs in the colony formation assay (CFA), but with only modest activity around 12 μM in WT and MTHFD2 KO cells (Figure IV-8A). This activity is on par with **CBN-1**'s enzymatic IC_{50}. Excitingly, **CBN-4** showed differential activity between the WT and MTHFD2 KO cells ($p = 0.016$) (Figure IV-8B). However, the other analogs had little to no anti-proliferative activity. Therefore, we investigated whether these **CBN** analogs were engaging cellular MTHFD2. The analogs were first screened with CETSA at 70 °C because **CBN-1** showed clear stabilization at this temperature (Figure IV-5C). **CBN-3**, **-4**, and **-5** all stabilized MTHFD2, but **CBN-7** did not (Figure IV-8C). This follows the trend seen with the recombinant protein in that **CBN-7** showed the smallest shift (Figure IV-4A). Since **CBN-4** showed the greatest stabilization (Figure IV-8D), we obtained a full melt curve. **CBN-4** stabilized cellular MTHFD2 to thermal denaturation by an impressive 9.0 °C (Figure IV-8E).

206

Although the compounds were not potent in inhibition of growth in the HAP1 cells, we sought to determine their anti-migratory activity as previous reports have noted that MTHFD2 plays a role in cancer cell migration.[9, 16, 18, 37] First the cell viability of U2OS in the presence of the **CBN** compounds was carried out to ensure the use of a subtoxic dose (Figure IV-8F). Unsurprisingly, DS44960156 displayed no anti-migratory activity (Figure IV-8G). All **CBN** analogs inhibited migration of U2OS cells except for **CBN-3** (Figure IV-8G). However, **CBN-3** did not engage cellular or recombinant MTHFD2 to the same degree as the other analogs.

MTHFD2 plays an important role in redox homeostasis due to its cofactor $NAD(P)^+$.[10, 15, 38] Knockdown of MTHFD2 reduced the NAD(P)H/NAD(P) ratio in colorectal cancer cell lines.[15] Additionally, knockdown of MTHFD2 suppressed glycolytic activity in renal cell carcinoma cell lines.[10] Testing a compound's activity in a cell line in the presence of glucose or galactose-enriched medium can be used to assess impact on mitochondrial function.[39] Oxidative phosphorylation (OXPHOS) occurs in the mitochondria and cells cultured in galactose must rely on OXPHOS for ATP generation rather than glycolysis. Therefore, cells cultured in galactose are very sensitive to mitochondrial inhibition.[39] **CBN-1** showed a 3.75-fold increase in potency in HCT 116 cells cultured in galactose versus glucose medium (Figure IV-8H). **CBN-3** and **-5** displayed roughly a 2-fold difference, while **CBN-4** and **-7** showed no difference. Hence, our **CBN** compounds negatively impact mitochondrial function.

Finally, we were interested in determining if the one-carbon metabolite formate was able to rescue growth inhibition induced by our compounds. Mitochondrial folate-dependent enzymes including MTHFD2 play a key role in the production of formate for *de novo* purine biosynthesis.[40] To our surprise, formate did not rescue **CBN-1** or **CBN-3**-induced growth inhibition, suggesting that they elicit their effects through additional unknown mechanisms (Figure IV-8I). We included

HK-16, a potent SHMT2 inhibitor,[41] as a positive control and observed clear rescue with 1 mM
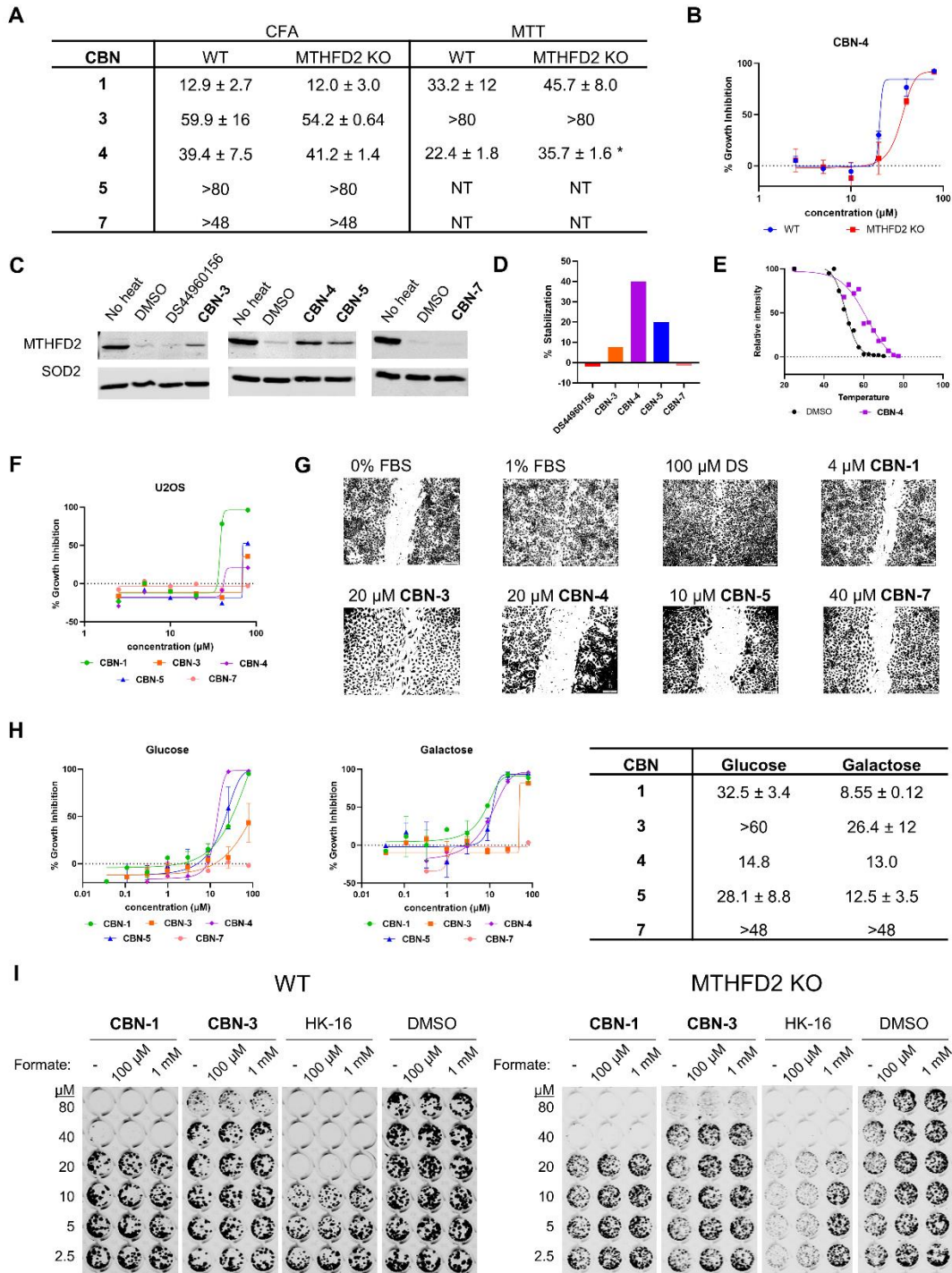
formate.

A

CBN	CFA		MTT	
	WT	MTHFD2 KO	WT	MTHFD2 KO
1	12.9 ± 2.7	12.0 ± 3.0	33.2 ± 12	45.7 ± 8.0
3	59.9 ± 16	54.2 ± 0.64	>80	>80
4	39.4 ± 7.5	41.2 ± 1.4	22.4 ± 1.8	35.7 ± 1.6 *
5	>80	>80	NT	NT
7	>48	>48	NT	NT

H

CBN	Glucose	Galactose
1	32.5 ± 3.4	8.55 ± 0.12
3	>60	26.4 ± 12
4	14.8	13.0
5	28.1 ± 8.8	12.5 ± 3.5
7	>48	>48

Figure IV-8. Anti-cancer activity of **CBN** compounds. (A) Table of IC$_{50}$ values in micromolar of the **CBN** compounds in colony formation (CFA) and MTT assays. (B) Differential activity of **CBN-4** in the MTT assay. (C) CETSA screen at 70 °C of **CBN** analogs at 100 μM in U2OS cell lysates. (D) Quantification of (C). (E) Melt curve of MTHFD2 in presence of DMSO or 100 μM **CBN-4** in U2OS lysates. (F) IC$_{50}$ curves of **CBN** analogs in the MTT assay in U2OS cells. (G) Wound-healing assay with U2OS

208

cells. (H) IC$_{50}$'s of **CBN** analogs in the OXPHOS MTT assay. (I) CFA of **CBN-1** and **-3** and HK-16 in presence and absence of sodium formate in HAP1 cells.

SAR

To expand the SAR, we explored commercially available compounds, our in-house database, as well as a few synthesized analogs. The majority of the compounds were derivatives of **CBN-1** (Table IV-1), but a few were derivatives of **CBN-7** with the sulfonamide in the opposite orientation (Table IV-2). Overall, **CBN-1** remained as the most active across all assays but there are some important modifications worth noting.

Removal of the benzene ring in the R$_2$ position from **CBN-1** (**CBN-8**) abolished enzymatic and cell activity (Table IV-1). This ring likely plays an important role in both orienting the hydrogen bond interactions while itself participating in π-π stacking with Tyr84. Likewise, elimination of the benzene ring from **CBN-4** resulted in a loss of activity (**CBN-14** and **CBN-15**). Interestingly, though **CBN-15** lacked enzymatic activity, it is the only compound shows differential activity between the HAP1 WT and MTHFD2 KO cell lines in the CFA. We were surprised to see activity with **CBN-10** which lacks a carboxylic acid in the position of interaction with Arg43 or Gly310. Consistent with what is mentioned above, removal of the R$_2$ benzene from **CBN-10** resulted in an inactive compound (**CBN-12**). Although a potentially important difference also exists in that the oxygen and sulfur are swapped in the thiocarbonate; if the covalent binding is part of the mechanism of inhibition this orientation could be important. There are exceptions to the R$_2$ trend, but these molecules have significantly different groups in the R$_3$ and R$_1$ positions, so it is difficult to make conclusions (**CBN-16**, **-17**, **-26**, **-28**, and **-29**).

Derivatives of **CBN-7** were largely inactive (Table IV-2). While it was inactive in the enzymatic assay, **CBN-45** was the solitary compound in this series with quantifiable anti-
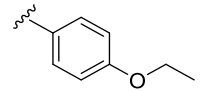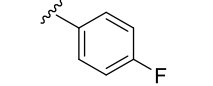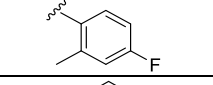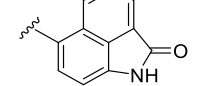
proliferative activity. **CBN-51** and **CBN-56** were the only other compounds with inhibitory
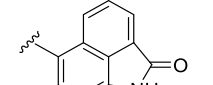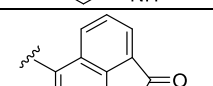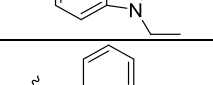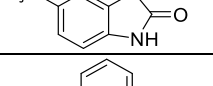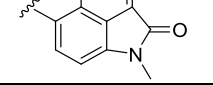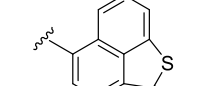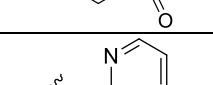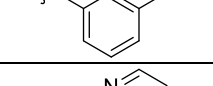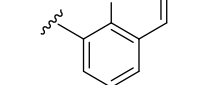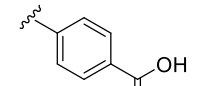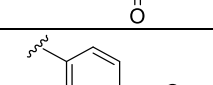
activity against MTHFD2 but were on par with **CBN-7**.

Most of the compounds were inactive in the thermal shift assay, so there is not enough data

to do a correlation analysis. The only compounds that have activity in the thermal shift assay are

shown in Figure IV-4. The compound from Daichi-Sankyo that was optimized from their first

publication that has nanomolar potency (IC_{50} = 6.3 nM) and *in vivo* activity (DS18561882) only

shifts MTHFD2's melting temperature by 2 °C at 100 μM (not shown). Therefore, if our

compounds are only in the micromolar range (our best compound **CBN-1** has an IC_{50} of 19 μM),

it is not surprising that they do not show stabilization in the thermal shift assay.

Table IV-1. SAR of **CBN-1**.
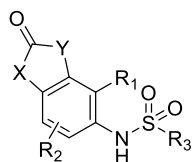
ID[a]	X	Y	R_1	R_2[b]	R_3	% Inhibition[c]	HAP1 WT IC_{50}[d]	MTHFD2 KO IC_{50}[d]
CBN-1 (2129)	O	S	H	benzene			12.9 ± 2.7	12.0 ± 3.0
CBN-4 (3370)	O	S	H	benzene		99.0	39.4 ± 7.5	41.2 ± 1.4
CBN-8 (CZ72)	O	S	H	*o,m*-H		29.6	>80	>80
CBN-5 (3411)	O	S	H	benzene		102.1	>80	>80
CBN-9 (CZ121)	O	S	H	*o,m*-H		57.1	41.5	54.4
CBN-10 (3478)	O	S	H	benzene		98.5	43.6 ± 23	45.6 ± 24
CBN-3 (2138)	S	O	Cl	*o,m*-H		-0.1	59.9 ± 16	54.2 ± 0.64

Compound					Structure			
CBN-11 (CZ18)	O	S	H	benzene	4-ethoxyphenyl	30.8	16.4	20.5
CBN-12 (2123)	S	O	H	*o,m*-H	4-fluorophenyl	12.6	53.9 ± 3.0	57.7 ± 16
CBN-13 (2127)	O	S	H	o,m-H	methyl-fluorophenyl	26.6	47.8 ± 11	59.4 ± 17
CBN-14 (2548)	O	S	H	*o*-Me, *m*-H	benzo[cd]indol-2(1H)-one	19.3	>80	>80
CBN-15 (2124)	O	S	H	*o,m*-H	benzo[cd]indol-2(1H)-one	5.9	45.2 ± 5.1	67.1 ± 9.2
CBN-16 (CZ101)	O	S	H	*o,m*-H	1-ethyl-benzo[cd]indol-2(1H)-one	70.7	69.1	>80
CBN-17 (1435)	C	C	OH	*o,m*-H	benzo[cd]indol-2(1H)-one	73.1	67.9 ± 14	56.2 ± 21
CBN-19 (CZ131)	CO₂H	C	H	*o,m*-H	1-methyl-benzo[cd]indol-2(1H)-one	59.3	>80	>80
CBN-20 (3371)	O-Me	C	H	*o,m*-H	naphtho-thiophenone	11.4	>80	>80
CBN-21 (4493)	O	S	H	*o*-Me, *m*-H	quinolin-8-yl	14.7	48.0 ± 0.42	59.7 ± 22
CBN-22 (2146)	O	S	H	*o,m*-H	quinolin-8-yl	15.4	>80	>80
CBN-23 (JRCH-4)	NH	NH	H	*o,m*-H	4-carboxyphenyl	57.1	>80	>80
CBN-24 (JRCH-3)	NH	NH	H	*o,m*-H	4-(methoxycarbonyl)phenyl	51.1	>80	>80
CBN-25 (JRCH-1)	NH	NH	H	*o,m*-H	4-methoxyphenyl	44.8	>80	>80
CBN-26 (JRCH-2)	NH	NH	H	*o,m*-H	4-bromophenyl	66.9	>80	>80

CBN-27 (CZ87)	N-Me	O	H	o,m-H	[m-acetamidophenyl structure]	15.6	>80	>80
CBN-28 (CZ89)	N-Me	O	H	o,m-H	[p-(2-oxopyrrolidin-1-yl)phenyl structure]	94.3	>80	>80
CBN-29 (CZ91)	N-Me	O	H	o,m-H	[3,4-dihydroquinolin-2(1H)-one structure]	67.1	>80	>80
CBN-30 (CZ95)	N-Me	N-Me	H	o,m-H	[3,4-dimethoxyphenyl structure]	44.8	66.6	>80
CBN-31 (CZ93)	N-Me	N-Me	H	o-N-Me$_2$, m-H	[phenyl structure]	28.8	>80	>80
CBN-32 (4104)	N-Me	N-Me	H	o,m-H	[benzo-1,4-dioxane structure]	22.0	32.2 ± 16	28.1 ± 11
CBN-33 (4117)	N-Me	N-Me	H	o,m-H	[3-fluoro-4-methoxyphenyl structure]	5.4	>80	>80
CBN-34 (5218)	C	C	H	o,m-H	[4-carboxyphenyl structure]	10.0	>80	>80
CBN-35 (5219)	C	C	F	o,m-H	[4-carboxyphenyl structure]	4.9	>80	>80
CBN-36 (5235)	F	C	H	o,m-H	[4-carboxyphenyl structure]	13.5	>80	>80
CBN-37 (CZ43)	[benzo-1,4-dioxane structure]				[4-carboxyphenyl structure]	2.8	>80	>80
CBN-38 (CZ73)	[pyrimidin-2-yl structure]				[4-carboxyphenyl structure]	NT[e]	NT	NT
CBN-39 (CZ99)	[benzothiazol-2-yl structure]				[4-carboxyphenyl structure]	65.2	>80	>80
CBN-40 (CZ100)	[4-methylbenzothiazol-2-yl structure]				[4-carboxyphenyl structure]	47.8	>80	>80
CBN-41 (6089/7001)	[quinolin-8-yl structure]				[4-carboxyphenyl structure]	5.2	>80	>80

CBN-42 (1530)			6.9	>80	>80

[a]Number in parentheses is the original compound code
[b]"o" or "m" indicate the ortho or meta position relative to the sulfonamide
[c]MTHFD2 assay at 500 µM, n=1
[d]IC$_{50}$ values are listed in µM in the CFA. Values for the CZ compounds are from one experiment.
[e]NT, not tested

Table IV-2. SAR of **CBN-7**.
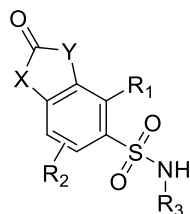
ID[a]	X	Y	R$_1$	R$_2$[b]	R$_3$	% Inhibition[c]	HAP1 WT IC$_{50}$[d]	MTHFD2 KO IC$_{50}$[d]
CBN-7 (25496)	NH	O	H	o,m-H		41.0	>48	>48
CBN-43 (CZ124)	NH	NH	H	o,m-H		NT[e]	>80	>80
CBN-44 (CZ80)	N-Me	O	H	o,m-H		3.5	>80	>80
CBN-45 (CZ81)	N-Me	O	H	o,m-H		2.2	22.0	24.5
CBN-46 (CZ79)	N-Me	O	H	o,m-H		2.3	>80	>80
CBN-47 (CZ82)	N-Me	O	H	o,m-H		12.9	>80	>80
CBN-48 (CZ88)	N-Me	O	H	o,m-H		16.0	>80	>80
CBN-49 (25010)	N-Me	O	H	o,m-H		17.9	>48	>48
CBN-50 (25030)	N-Me	O	H	o,m-H		38.5	>35	>35
CBN-51 (CZ90)	N-Me	O	H	o,m-H		52.1	>80	>80

213

Compound								
CBN-52 (4098)	N-Me	N-Me	H	*o,m*-H		26.8	>80	>80
CBN-53 (4381)	N-Me	N-Me	H	*o,m*-H		31.0	>80	>80
CBN-54 (24982)	N-Me	N-Me	H	*o,m*-H		16.6	>23	>23
CBN-55 (4365)	N-Me	N-Me	H	*o,m*-H		16.8	>80	>80
CBN-56 (CZ98)	N-Me	N-Me	H	*o,m*-H		49.8	77.7	>80
CBN-57 (24972)	N-Me	N-Me	H	*o,m*-H		21.9	>23	>23
CBN-58 (6964)	NH	C	H	*o,m*-H		NT	>80	>80
CBN-59 (3504)		C	H	*o,m*-H		1.0	>80	>80

[a]Number in parentheses is the original compound code

[b]"*o*" or "*m*" indicate the ortho or meta position relative to the sulfonamide

[c]MTHFD2 assay at 500 μM, n=1

[d]IC$_{50}$ values are listed in μM in the CFA. Values for the CZ compounds are from one experiment.

[e]NT, not tested

Conclusion

This study aimed to identify a novel chemotype for an MTHFD2 inhibitor based on a pharmacophore built from the co-crystal structures published by Kawai and colleagues.[24] *In silico* screening of our in-house database identified several candidates, but only two were active *in vitro*. Of these, **CBN-1** significantly stabilized MTHFD2 to thermal denaturation and inhibited its enzymatic activity. We also discovered analogs that bind and inhibit MTHFD2. Mechanistic studies revealed that **CBN-1** covalently binds MTHFD2 but does not react with antioxidants such as NAC or GSH. Therefore, future analysis is required to identify the residue(s) important for this interaction. Additionally, **CBN** analogs possess anti-proliferative and anti-migratory activity with

CBN-1 being the most potent in the series. Furthermore, **CBN-1** showed significant selectivity to cells cultured in galactose medium indicating impaired mitochondrial function. Structure-activity relationship studies with commercially available analogs did not produce a superior compound to **CBN-1**, thus further optimization is warranted to improve the potency of our hit compound. Moreover, evaluation of the selectivity over MTHFD1 will be important to investigate. Finally, though in select cell lines it seems MTHFD2L would play a limited role in a compensation mechanism for MTHFD2 inhibition,[42] we believe it is worth evaluating this selectivity as well.

Methods

Generation of shape-based pharmacophore. Shape-based pharmacophore of "1" and DS44960156 was generated using ROCS *v*3.2.0.4 (OpenEye Scientific).[25, 43] ROCS performs shape-based overlays of conformers from a candidate database to a query molecule with one or more conformations. Here, we have used combination of shape overlap and color overlap by aligning groups with similar properties in the color force field. The score, referred to as Tanimoto Combo was calculated as the sum of shape and color score.[25] The maximum value of the Combo score is 2 and the minimum value is 0.

Molecular docking. Compounds were docked against MTHFD2 protein (PDB: 6JIB) using GOLD (genetic optimization for ligand docking) software package, version 5.2.[44] Prior to docking, 10 different conformations were generated for each ligand using Omega (OpenEye Scientific, Santa Fe, NM), a systematic, knowledge-based conformer generator.[45] GOLD uses the genetic algorithm (GA) to explore the conformational space of a compound inside the active site of a protein.[46] Docking studies were performed using the standard default settings with 10 GA runs and 100,000 operations on each molecule. Default cutoff values of 3.0 Å (dH-X) for hydrogen bonds and 4.0 Å for van der Waals were employed.

Construction of MTHFD2 plasmid. A His$_6$-MTHFD2 expression plasmid (PV027058) was purchased from ABM (Richmond, British Columbia, Canada). Initial attempts at purification of the full length MTHFD2 were unsuccessful, so we sought to delete the mitochondrial targeting sequence (35 amino acids). Deletion of this sequence was accomplished with the QuikChange XL site-directed mutagenesis kit (Agilent) using the following primers: 5'- GCT ACA TCA CAA GTT TGT ACA AAA AAG CTG GCA ATG AAG CTG TTG TCA TTT CTG GAA -3' and 5'-CCT TCC AGA AAT GAC AAC AGC TTC ATT GCC AGC TTT TTT GTA CAA ACT TGT GAT GTA -3'.

MTHFD2 protein expression and purification. The expression and purification of human His$_6$-MTHFD2$^{36\text{-}350}$ were performed as described,[22] with some modifications. BL21 (DE3) cells harboring the His$_6$-MTHFD2$^{36\text{-}350}$ plasmid were cultured at 37 °C in LB medium containing 50 μg/mL kanamycin. When OD$_{600}$ reached ~0.8, the temperature was reduced to 20 °C, and expression was induced by the addition of IPTG (1 mM). MgCl$_2$ was added to a final concentration of 1 mM to ensure proper folding of the protein. After 4 h, cells were harvested by centrifugation at 8,326 g (7,000 rpm, F12-6×5000LEX rotor, Thermo Scientific, Rockford, IL) for 15 minutes and stored at -80 °C. Frozen cell pellets were thawed and resuspended in buffer A (Appendix Table IV-1) at room temperature. Cells were broken using ultra-sonication on ice. Cell debris was removed by centrifugation at 38,758 g (18,000 rpm, F21-8×50y rotor, Thermo Scientific, Rockford, IL) for 30 min at 4 °C. The clear supernatant was incubated with Ni-NTA resin, pre-equilibrated with buffer B (Appendix Table IV-1), for 1 h at 4 °C. The resin was loaded onto a column and was washed with buffer B containing 10 mM imidazole for three column volumes. His$_6$-MTHFD2 protein was eluted with buffer B with a gradient of imidazole of 50 mM, 100 mM, 250 mM and 500 mM. Fractions containing His$_6$-MTHFD2 as judged by SDS-PAGE were pooled.

The protein solution was concentrated using a Pierce concentrator (20K MWCO) at 4 °C and then the buffer was exchanged into buffer C (Appendix Table IV-1). MTHFD2 protein aliquots were frozen at -80 °C.

MTHFD2 assay. The enzymatic activity of MTHFD2 was evaluated as previously described with some modifications.[24] The assay buffer was composed of 50 mM KP_i, pH 7.4, 7.5 mM DTT, and 5 mM $MgCl_2$. A 1.5× solution of MTHFD2 (final concentration 8 μg/mL or 210 nM) was incubated with DMSO (6.25%) or test compound in a volume of 10 μL for 10 min in a 384-well plate (Corning, #3676, low volume/non-binding/round bottom black). Then 5 μL of a 3× substrate cocktail was added to final concentrations of 100 μM NAD^+, 0.5 mM THF, and 2.5 mM formaldehyde and the reaction was incubated at room temperature for 30 min. To measure the amount of NADH, 5 μL of the Amplite[TM] Fluorimetric NADPH detection reagent (#15262, AAT Bioquest, Sunnyvale, CA) was added and the fluorescence intensity (Ex: 540 nm; Em: 590 nm) was read by a CLARIOstar Plus microplate reader (BMG LabTech). Inhibition is presented as a percentage compared to DMSO-treated controls.

Thermal shift. All thermal shift assays were performed using the Protein Thermal Shift™ Dye Kit with the ViiA7 Real-Time PCR System (Applied Biosystems). For SHMT2, the buffer composition was 50 mM HEPES pH 8.0 and the final concentration of SHMT2 was 0.3 mg/mL. For MTHFD2, the assay was performed as previously described with 0.3 mg/mL MTHFD2.[22] Compounds were added to MicroAmp® optical 384-well reaction plates (ThermoFisher) to 100 μM final concentration in 20 μL reactions. The experiments were run according to the manufacturer's protocol (Applied Biosystems, cat. no. 4461146).

CETSA. CETSA was performed as previously described with some modifications.[22] Cells were grown in 15 cm dishes to 90% confluency before collection. For experiments using lysates, cells

were harvested via trypsinization and after inactivation with medium, were washed with DPBS twice by centrifugation. Cells were lysed by alternating temperatures between -80 °C and 37 °C for five minutes each, three times. Lysates were centrifuged at 13,000 rpm for 10 min at 4 °C. Cleared lysates were incubated with either DMSO or 100 μM compound for 30 min at room temperature. Aliquots (50 μL) were then heated to the indicated temperatures for 3 min, and insoluble proteins were removed via centrifugation for 20 min at 13,000 rpm at 4 °C. Samples were then prepared for western blot analysis by combining 20 μL of sample with 5 μL 5× SDS loading buffer.

For intact cells, cells were harvested via trypsinization and after inactivation with medium, were washed with DPBS twice by centrifugation. Cells were resuspended in DPBS and incubated with either DMSO or 100 μM compound for 1 hr at 37 °C with shaking. The compound was then removed by centrifugation at 1500 rpm for 5 min at room temperature. Cells were resuspended in DPBS and lysed by alternating temperatures between -80 °C and 37 °C for five minutes each, three times. Lysates were centrifuged at 13,000 rpm for 10 min at 4 °C. Aliquots were then heated to the indicated temperatures for 3 min, and insoluble proteins were removed via centrifugation for 20 min at 13,000 rpm at 4 °C. Samples were then prepared for western blot analysis by adding 5 μL 5× SDS loading buffer to 20 μL of sample.

Western blot. Cell lysates were incubated with loading buffer at 95 °C for 5 min. Proteins were separated via SDS-PAGE and transferred to low fluorescence PVDF membranes using the Trans-Blot® Turbo™ System (BioRad). Blots were blocked with StartingBlock™ (TBS) Blocking Buffer (ThermoFisher). Primary antibodies were incubated at 4 °C overnight or for 1 hr at room temperature. Membranes were washed three times with TBST for 5 min each. Secondary antibody incubation was carried out for 1 hr at room temperature. Following another three wash cycles with

TBST and one with TBS, protein expression was detected using the Odyssey CLx imager (Licor). Primary antibodies: 1:1000 MTHFD2 in 5% BSA (Abcam, ab56772), 1:100 SOD2 in 5% milk (Santa Cruz, sc-133134). Secondary antibodies: 1:7500 anti-rabbit (ThermoFisher, SA5-35571) or anti-mouse (ThermoFisher, SA5-35521) in 5% milk with 0.01% SDS.

NAC reactivity. Test compounds (5 mM) were incubated NAC at a one-to-one ratio in DMSO at room temperature. Aliquots (5 μL) were taken at the indicated time points and diluted in 500 μL MeOH. A Shimadzu LCMS 20-20 system was utilized for monitoring the reactions. The system is equipped with a PDA UV detector and Kinetex 2.6 μm, XB-C18 100 Å, 75 mm × 4.6 mm column, which was used at room temperature. HPLC gradient method utilized a 10% to 95% MeOH in H_2O with 0.01% formic acid over 15 min with a 0.50 mL/min flow rate.

GSH reactivity. CBN-1 (500 μM) was incubated with GSH at a 1:10 ratio in a 50% DMSO, 50% H_2O mixture at room temperature. Aliquots (25 μL) were taken at the indicated time points and diluted in 500 μL MeOH. A Shimadzu LCMS 20-20 system was utilized for analysis with the method detailed above.

GSTO1 assay. Competitive binding of compounds with CMFDA to GSTO1 was performed as previously described.[35] Briefly, 1 μM GSTO1 was incubated with compounds for 30 min at 37 °C and with 500 nM CMFDA for an additional 30 min. The reactions were quenched by boiling with 5X SDS loading dye for 5 min. The samples were resolved on a 10% polyacrylamide gel and scanned with the iBright imaging system (Thermo Fisher Scientific).

Q-TOF mass spectrometry. 250 μM **CBN-1** was incubated with 25 μM MTHFD2 at room temperature in buffer C (7.5% glycerol) for the indicated time points. The solution was injected into a G6535A Q-TOF LC/MS (Agilent Technologies). The system is equipped with a Waters Acquity BEH C4 300 Å, 1.7 μm, 2.1 mm × 50 mm column. The mobile phase was 5% B for 2

min, followed by a gradient of 5% to 100% B over 4 min, and 100% B for 2 min where A is 95% water, 5% acetonitrile with 0.1% formic acid and B is 95% acetonitrile, 5% water with 0.1% formic acid, with a 0.3 mL/min flow rate.

Cell culture. HAP1 WT, SHMT2 KO, and MTHFD2 KO were cultured in IMDM supplemented with 1% Pen-Strep (Gibco). U2OS was cultured in McCoy's 5A. HCT 116 was cultured in RPMI 1640 (+ glucose). For the OXPHOS assay, HCT 116 was seeded in RPMI 1640 with galactose at the time of the experiment. All media were supplemented with 10% FBS (Gibco). Cells were grown at 37 °C in a humidified atmosphere of 5% CO_2.

Colony formation assay. Cells were seeded in 96-well plates at 150 cells/well (HAP1 WT) or 300 cells/well (HAP1 MTHFD2 KO) and allowed to attach overnight. Compounds were added to the indicated concentrations and incubated with the cells for 7 days. At the end of treatment, media was removed, and cells were fixed and stained with crystal violet solution (0.05% crystal violet, 2% formaldehyde, 40% methanol). Wells were washed with water and allowed to dry overnight before imaging with the Odyssey CLx imager (Licor).

MTT assay. Cytotoxicity of compounds was evaluated with the MTT assay. Cells were seeded in 96-well plates at 2000-5000 cells/well. After overnight attachment, compounds were added to the wells at sequential dilutions. After 72 hr, the tetrazolium dye MTT was added to the media to a final concentration of 300 μg/mL and incubated for 3-4 hr at 37°C. The media was removed and the insoluble formazan was dissolved in 100 μL of DMSO. Absorbance at 570 nm was read by microplate reader (Molecular devices, Sunnyvale, CA). Cytotoxicity of compounds is presented as inhibition of cell proliferation against DMSO-treated controls.

Wound-healing assay. Cells were seeded in 12-well plates and allowed to attach overnight. After 24 h serum starvation with 1% FBS, a scratch was made with a 200 μL tip. Wells were washed

with DPBS to remove floating cells. The negative control was vehicle treatment in serum-free media. The positive control was vehicle treatment in media with 1% FBS. Test compounds were incubated with cells at the indicated concentrations in media containing 1% FBS. Once the wound had closed in the positive control well, media was removed, and cells were fixed and stained with crystal violet solution. Images were taken using an Olympus IX83 inverted microscope at 10X magnification.

Chemistry. The general scheme for synthesis can be found in Figure IV-9.
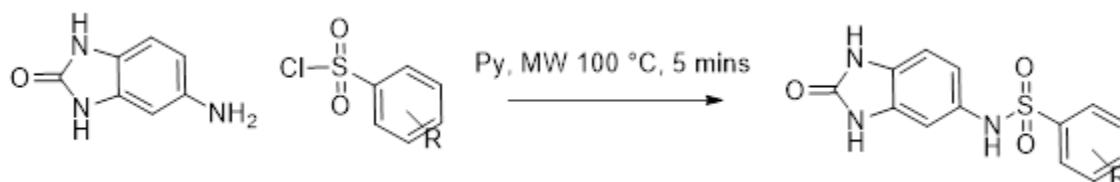

Figure IV-9. Scheme for synthesis of **CBN-23-26**. To a solution of 5-amino-1,3-dihydro-2H-benzo[d]imidazol-2-one (1 equiv.) in pyridine (2 mL), appropriate sulfonyl chloride (1.2 equiv.) was added in a microwave vial. The contents were heated at 100 °C for 5 min under microwave conditions. On completion of the reaction, the crude was concentrated and purified by HPLC analysis.

CBN-25 (JR-CH-1): *4-methoxy-N-(2-oxo-2,3-dihydro-1H-benzo[d]imidazol-5-yl)benzenesulfonamide.* White solid (Yield 78%). ^{1}H NMR (400 MHz, DMSO-d_6) δ 10.52 (s, 2H), 9.75 (s, 1H), 7.64 – 7.54 (m, 2H), 7.07 – 6.98 (m, 2H), 6.74 (d, $J = 8.2$ Hz, 1H), 6.70 (d, $J = 2.0$ Hz, 1H), 6.62 (dd, $J = 8.3, 2.1$ Hz, 1H), 3.78 (s, 3H). LCMS [M + H]$^+$ 320.34. NMR spectrum can be found in Appendix Figure IV-5.

CBN-26 (JR-CH-2): *4-bromo-N-(2-oxo-2,3-dihydro-1H-benzo[d]imidazol-5-yl)benzenesulfonamide.* White solid (Yield 82%). ^{1}H NMR (300 MHz, Methanol-d_4) δ 7.72 – 7.62 (m, 2H), 7.58 (d, $J = 8.7$ Hz, 2H), 6.93 – 6.81 (m, 2H), 6.67 (dd, $J = 8.3, 2.1$ Hz, 1H). LCMS [M + H]$^+$ 369.21. NMR spectrum can be found in Appendix Figure IV-6.
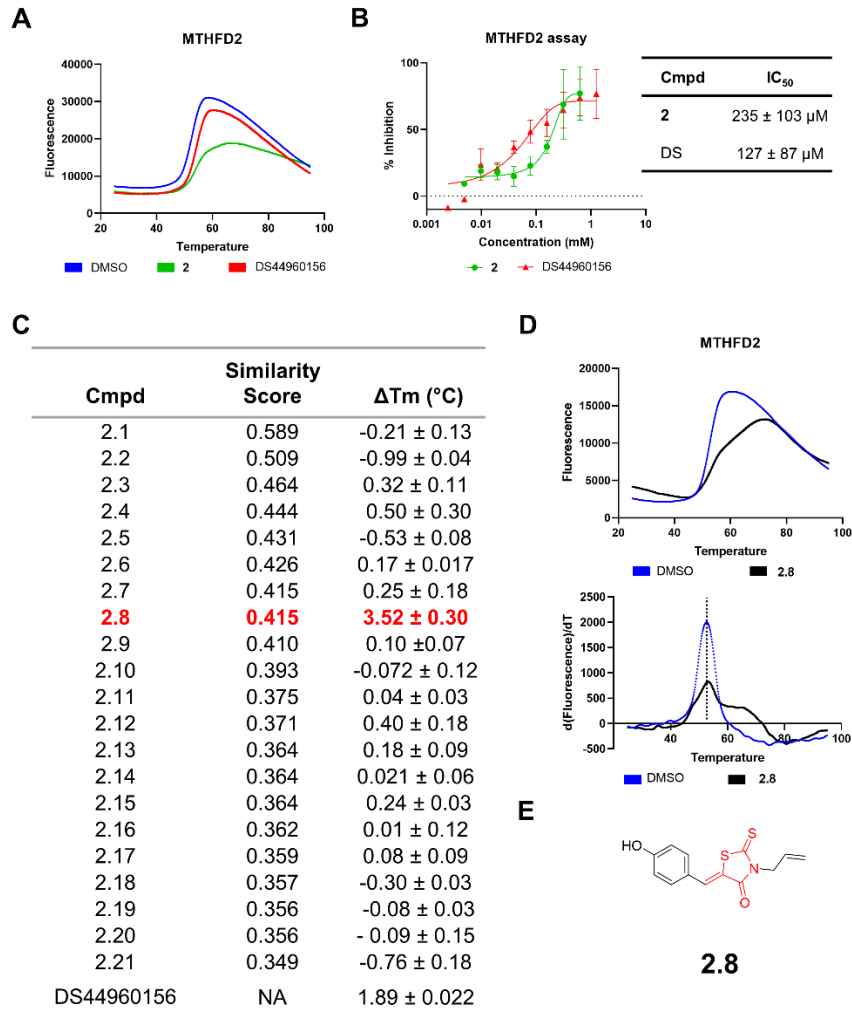
CBN-23 (JR-CH-4): *Methyl 4-(N-(2-oxo-2,3-dihydro-1H-benzo[d]imidazol-5-yl)sulfamoyl)benzoate.* White solid (Yield 75%). ^{1}H NMR (300 MHz, DMSO-d_6) δ 10.55 (d, $J = 8.8$ Hz, 2H), 10.07 (s, 1H), 8.14 – 7.99 (m, 2H), 7.85 – 7.70 (m, 2H), 6.75 (d, $J = 8.3$ Hz, 1H), 6.67

(d, J = 2.0 Hz, 1H), 6.60 (dd, J = 8.3, 2.1 Hz, 1H), 3.86 (s, 3H). LCMS [M + H]$^+$ 348.35. NMR

spectrum can be found in Appendix Figure IV-7.

CBN-24 (JR-CH-3): *4-(N-(2-oxo-2,3-dihydro-1H-benzo[d]imidazol-5-yl)sulfamoyl)benzoic acid.*

To a solution of **CBN-23** (1.0 eq) in THF and H_2O was added LiOH.H_2O (5.0 eq) at 0 °C and

stirred at room temperature for 5 h. The mixture was then diluted with H_2O, and the pH was

adjusted to 3 by 1N HCl solution. It was extracted with dichloromethane, and the organic layer

was washed with brine, dried over anhydrous Na_2SO_4, filtered and concentrated. The crude was

crystallized to give the carboxylic acid as a white solid (Yield 64%). ^{1}H NMR (300 MHz, DMSO-

d_6) δ 10.63 – 10.41 (m, 2H), 10.07 (s, 1H), 8.14 – 7.99 (m, 2H), 7.83 – 7.69 (m, 2H), 6.76 (d, J =

8.3 Hz, 1H), 6.68 (d, J = 2.0 Hz, 1H), 6.61 (dd, J = 8.3, 2.1 Hz, 1H). LCMS [M + H]$^+$ 334.33.

NMR spectrum can be found in Appendix Figure IV-8.

Appendix

A

MTHFD2

DMSO ■ 2 ■ DS44960156 ■

B

MTHFD2 assay

● 2   ▲ DS44960156

Cmpd	IC$_{50}$
2	235 ± 103 µM
DS	127 ± 87 µM

C

Cmpd	Similarity Score	ΔTm (°C)
2.1	0.589	-0.21 ± 0.13
2.2	0.509	-0.99 ± 0.04
2.3	0.464	0.32 ± 0.11
2.4	0.444	0.50 ± 0.30
2.5	0.431	-0.53 ± 0.08
2.6	0.426	0.17 ± 0.017
2.7	0.415	0.25 ± 0.18
2.8	**0.415**	**3.52 ± 0.30**
2.9	0.410	0.10 ±0.07
2.10	0.393	-0.072 ± 0.12
2.11	0.375	0.04 ± 0.03
2.12	0.371	0.40 ± 0.18
2.13	0.364	0.18 ± 0.09
2.14	0.364	0.021 ± 0.06
2.15	0.364	0.24 ± 0.03
2.16	0.362	0.01 ± 0.12
2.17	0.359	0.08 ± 0.09
2.18	0.357	-0.30 ± 0.03
2.19	0.356	-0.08 ± 0.03
2.20	0.356	- 0.09 ± 0.15
2.21	0.349	-0.76 ± 0.18
DS44960156	NA	1.89 ± 0.022

D

MTHFD2

DMSO ■   2.8 ■

DMSO ■   2.8 ■

E

2.8

Appendix Figure IV-1. In-house analogs of **CBN-2** do not inhibit MTHFD2. (A) **CBN-2** and DS44960156 in the thermal shift assay at 100 µM. (B) MTHFD2 enzymatic assay. (C) Analogs of **CBN-2** in the thermal shift assay at 100 µM, n=1. (D) Melt curve (top) and derivative (bottom) of **CBN-2.8**, n=1. (E) Structure of **CBN-2.8**, 5-ene-rhodanine core is highlighted in red.
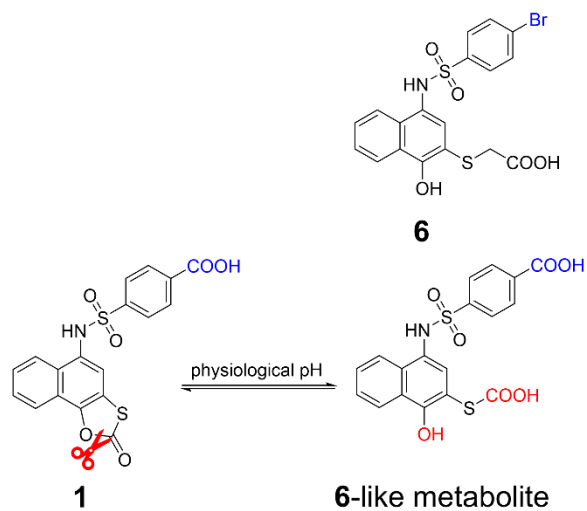
Appendix Figure IV-2. Hydrolysis of **CBN-1** affords a **CBN-6**-like metabolite.
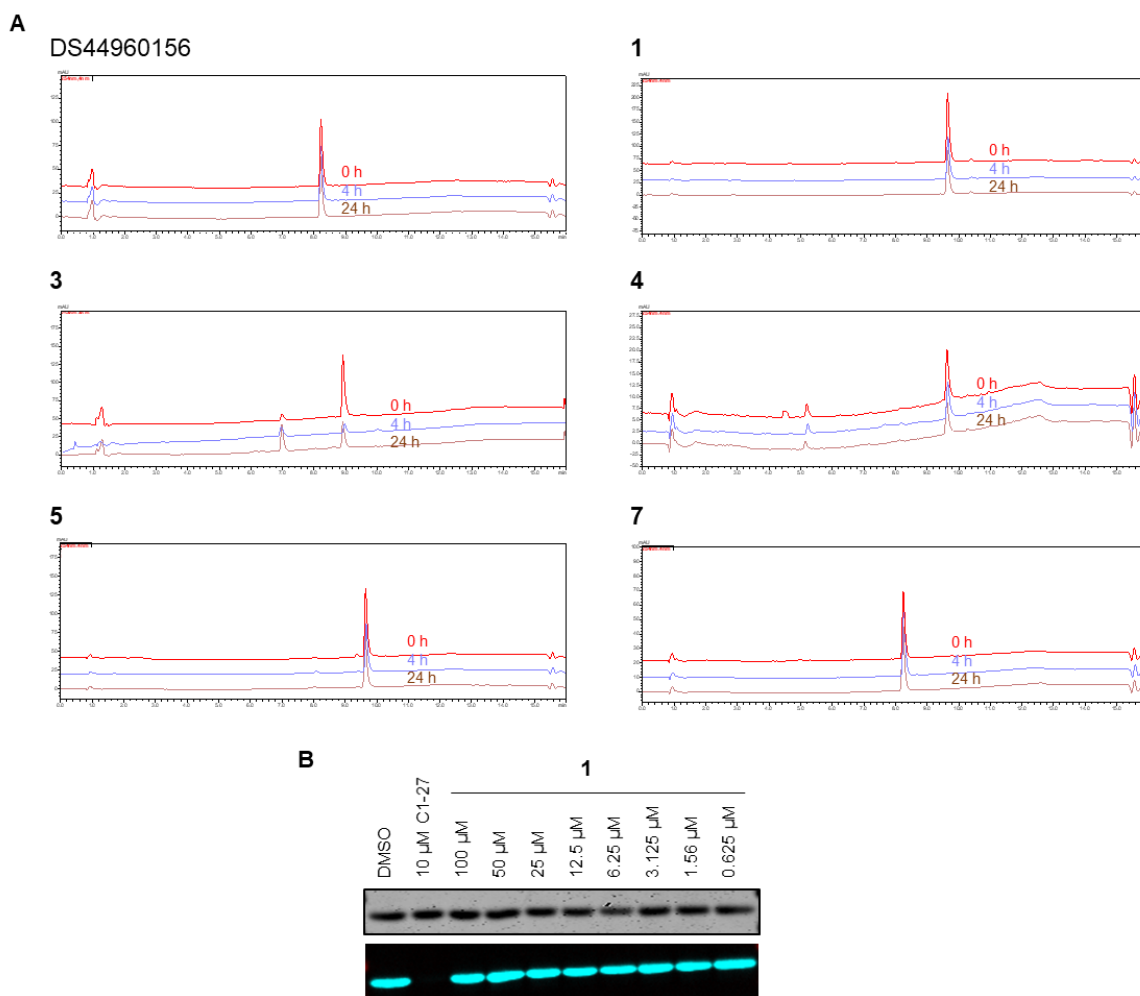
Appendix Figure IV-3. (A) HPLC traces of reactions at the indicated time points of **CBN-1** analogs with NAC. (B) In-gel fluorescence assay with recombinant GSTO-1.
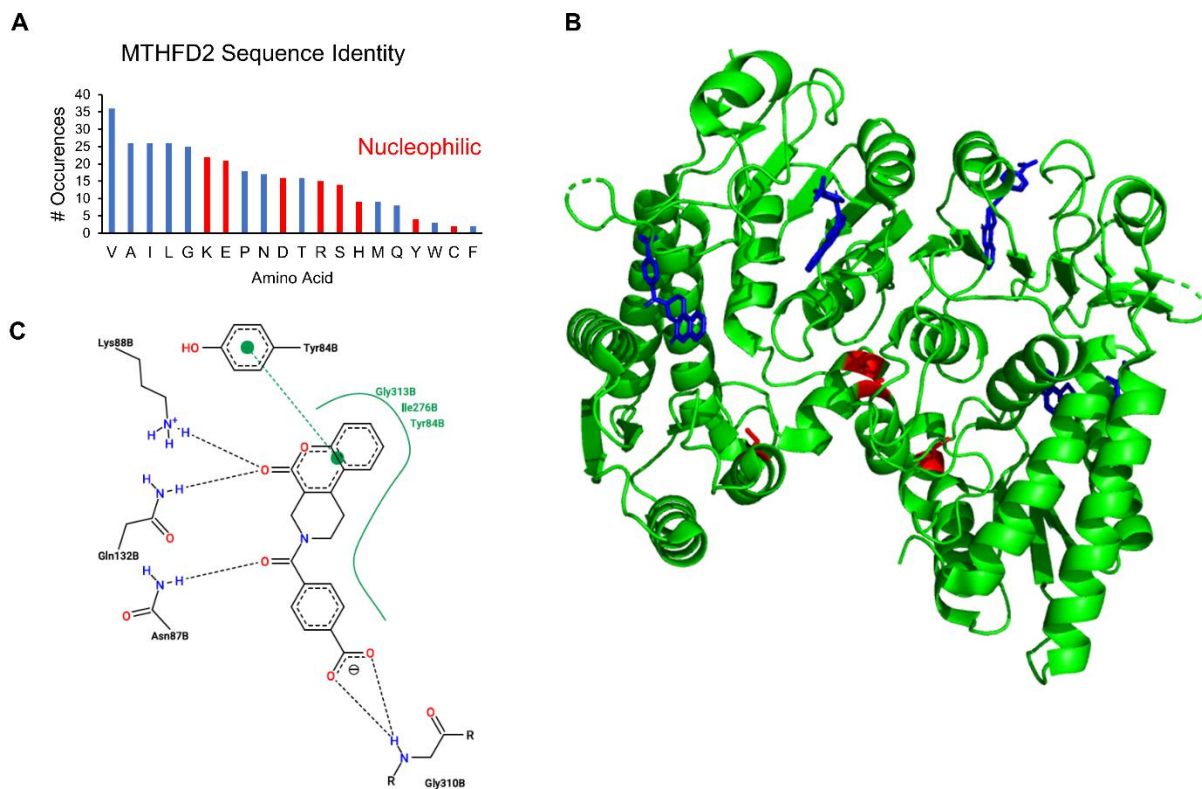
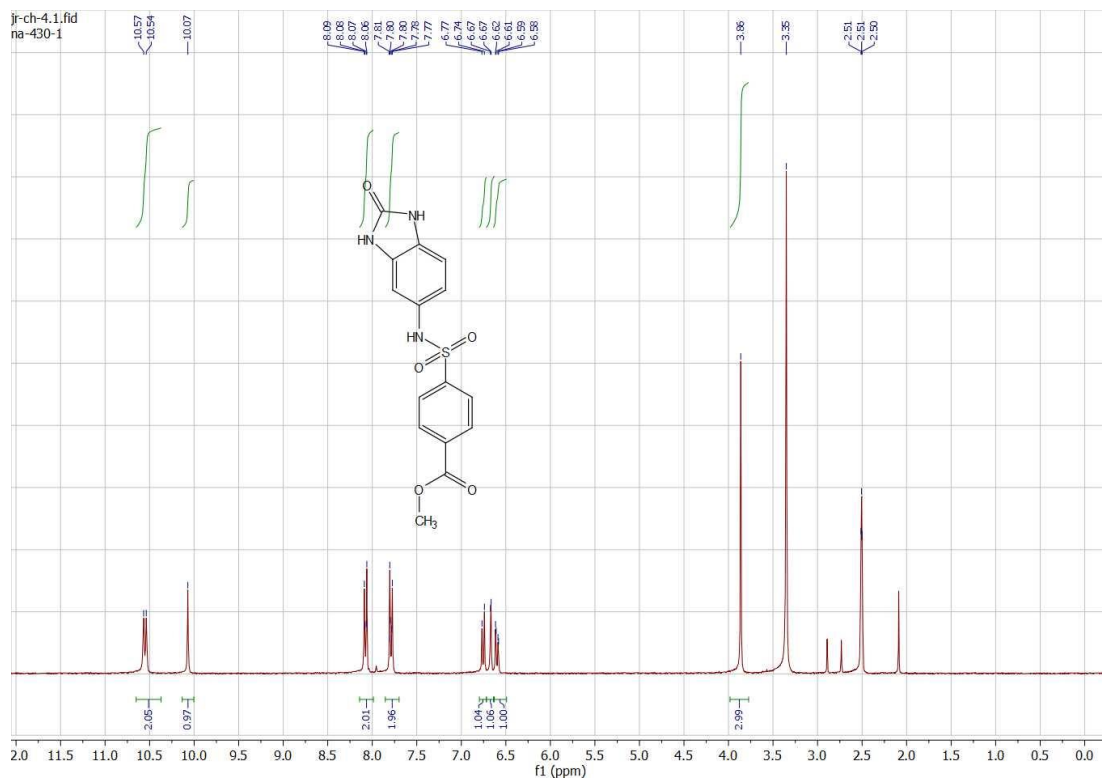Appendix Figure IV-4. (A) Prevalence of amino acids within the MTHFD2 sequence. (B) MTHFD2 structure (6JIB), DS44960156, blue; cysteine residues, red. (C) Two-dimensional ligand interaction plot between MTHFD2 and DS44960156.
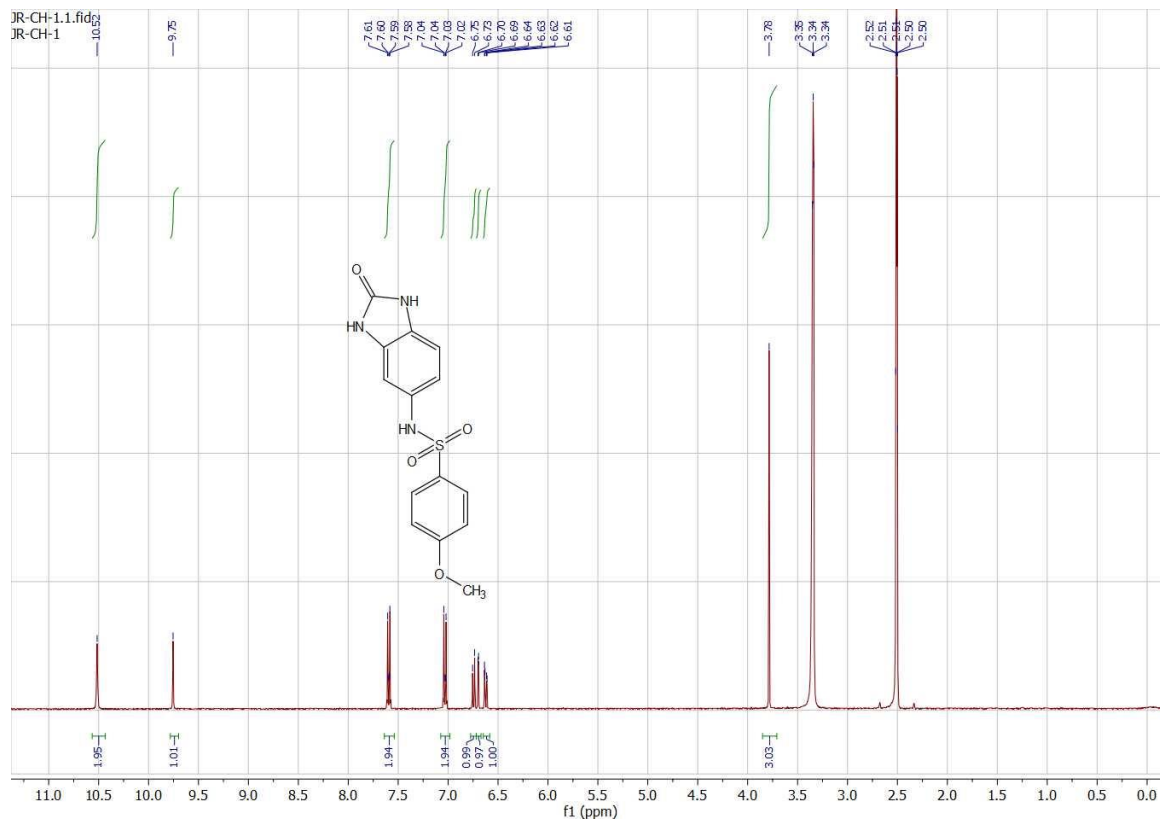
Appendix Figure IV-5. NMR spectrum of **CBN-25** (JRCH-1).
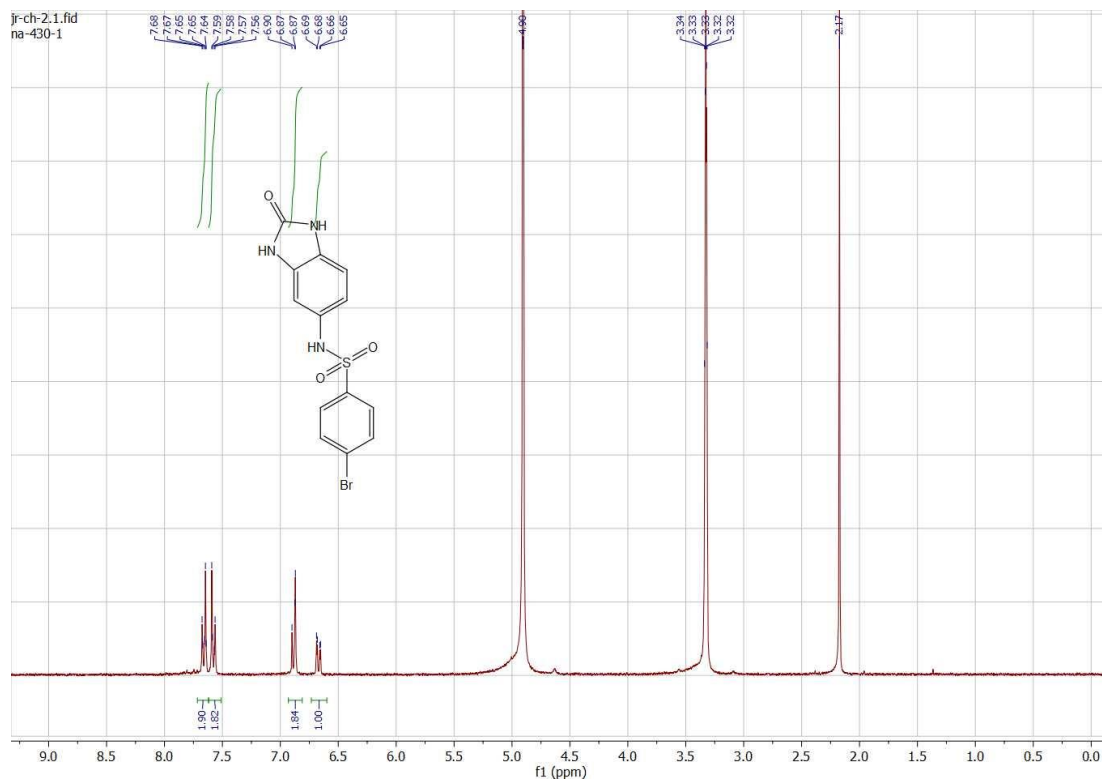
Appendix Figure IV-6. NMR spectrum of **CBN-26** (JRCH-2).

Appendix Figure IV-7. NMR spectrum of **CBN-23** (JRCH-4).
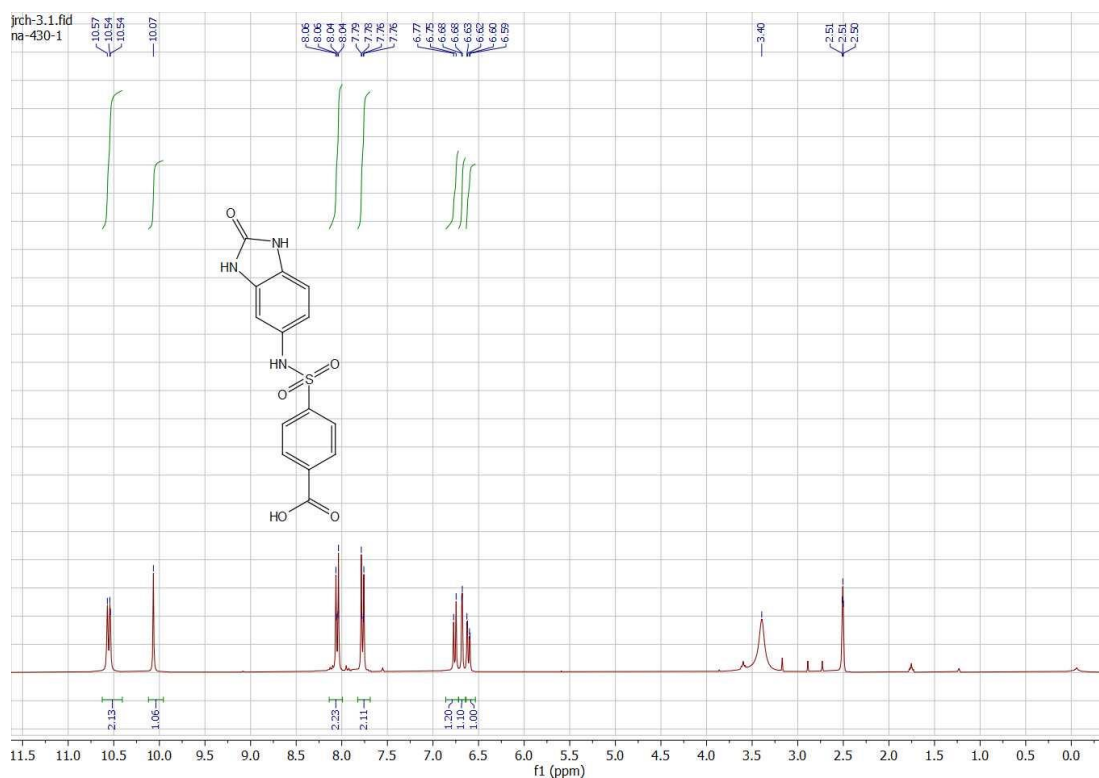
Appendix Figure IV-8. NMR spectrum of **CBN-24** (JRCH-3).

Appendix Table IV-1. Buffers used for protein purifications.

Buffer	Contents
A	B-PER (ThermoScientific, cat. no. 78243) supplemented with protease inhibitor cocktail, benzonase 2.5 U/mL (Sigma), and lysozyme 0.5 mg/mL (Sigma)
B	50 mM Tris-HCl pH 7.8, 250 mM NaCl, 5% glycerol
C	20 mM Tris-HCl pH 8.2, 250 mM NaCl, 15% glycerol, 1 mM TCEP

Notes

I would like to thank Dr. Daulat Khadka for pointing out the similarity between compounds **CBN-1** and **CBN-6**. I would also like to acknowledge Dr. Jenn Schmidt for her help and expertise with the Q-TOF experiments. I'd also like to thank Dr. Joyeeta Roy for synthesizing CBN analogs 23-26 as well as her effort in attempting other analogs but was unfortunately thwarted by hydrolysis issues. Finally, a thank you to Drs. Joe Madak and Qi Yan for synthesizing important positive controls HK-16 and DS44960156.

References

1.   Tedeschi, P. M.; Vazquez, A.; Kerrigan, J. E.; Bertino, J. R., Mitochondrial methylenetetrahydrofolate dehydrogenase (MTHFD2) overexpression is associated with tumor cell proliferation and is a novel target for drug development. *Mol Cancer Res.* **2015,** *13* (10), 1361-1366.

2.   Shin, M.; Momb, J.; Appling, D. R., Human mitochondrial MTHFD2 is a dual redox cofactor-specific methylenetetrahydrofolate dehydrogenase/methenyltetrahydrofolate cyclohydrolase. *Cancer Metab.* **2017,** *5*, 11.

3.   Bolusani, S.; Young, B. A.; Cole, N. A.; Tibbetts, A. S.; Momb, J.; Bryant, J. D.; Solmonson, A.; Appling, D. R., Mammalian MTHFD2L encodes a mitochondrial methylenetetrahydrofolate dehydrogenase isozyme expressed in adult tissues. *J Biol Chem.* **2011,** *286* (7), 5166-5174.

4.   Mejia, N. R.; Rios-Orlandi, E. M.; MacKenzie, R. E., NAD-dependent methylenetetrahydrofolate dehydrogenase-methenyltetrahydrofolate cyclohydrolase from ascites tumor cells. *J Biol Chem.* **1986,** *261*, 9509-9513.

5.   Nilsson, R.; Jain, M.; Madhusudhan, N.; Sheppard, N. G.; Strittmatter, L.; Kampf, C.; Huang, J.; Asplund, A.; Mootha, V. K., Metabolic enzyme expression highlights a key role for MTHFD2 and the mitochondrial folate pathway in cancer. *Nat Commun.* **2014,** *5*, 3128.

6.   Zhu, Z.; Leung, G. K. K., More than a metabolic enzyme: MTHFD2 as a novel target for anticancer therapy? *Front Oncol.* **2020,** *10*, 658.

7.   Jain, M. N., R.; Sharma, S.; Madhusuhan, N.; Kitami, T.; Souza, A.L.; Kafri, R.; Kirschner, M.W.; Clish, C.B. Mootha, V.K., Metabolite profiling identifies a key role for glycine in rapid cancer cell proliferation. *Science.* **2012,** *336*, 1040-1044.

8.   Kawai, J.; Toki, T.; Ota, M.; Inoue, H.; Takata, Y.; Asahi, T.; Suzuki, M.; Shimada, T.; Ono, K.; Suzuki, K.; Takaishi, S.; Ohki, H.; Matsui, S.; Tsutsumi, S.; Hirota, Y.; Nakayama, K., Discovery of a potent, selective, and orally available MTHFD2 inhibitor (DS18561882) with in vivo antitumor activity. *J Med Chem.* **2019,** *62* (22), 10204-10220.

9.   Cheung, C. H. Y.; Hsu, C. L.; Tsuei, C. Y.; Kuo, T. T.; Huang, C. T.; Hsu, W. M.; Chung, Y. H.; Wu, H. Y.; Hsu, C. C.; Huang, H. C.; Juan, H. F., Combinatorial targeting of MTHFD2 and PAICS in purine synthesis as a novel therapeutic strategy. *Cell Death Dis.* **2019,** *10* (11), 786.

10.   Green, N. H.; Galvan, D. L.; Badal, S. S.; Chang, B. H.; LeBleu, V. S.; Long, J.; Jonasch, E.; Danesh, F. R., MTHFD2 links RNA methylation to metabolic reprogramming in renal cell carcinoma. *Oncogene.* **2019,** *38* (34), 6211-6225.

11.   Koufaris, C.; Gallage, S.; Yang, T.; Lau, C. H.; Valbuena, G. N.; Keun, H. C., Suppression of MTHFD2 in MCF-7 breast cancer cells increases glycolysis, dependency on exogenous glycine, and sensitivity to folate depletion. *J Proteome Res.* **2016,** *15* (8), 2618-2625.

12.   Nishimura, T.; Nakata, A.; Chen, X.; Nishi, K.; Meguro-Horike, M.; Sasaki, S.; Kita, K.; Horike, S. I.; Saitoh, K.; Kato, K.; Igarashi, K.; Murayama, T.; Kohno, S.; Takahashi, C.; Mukaida, N.; Yano, S.; Soga, T.; Tojo, A.; Gotoh, N., Cancer stem-like properties and gefitinib resistance are dependent on purine synthetic metabolism mediated by the mitochondrial enzyme MTHFD2. *Oncogene.* **2019,** *38* (14), 2464-2481.

13.   Pikman, Y.; Puissant, A.; Alexe, G.; Furman, A.; Chen, L. M.; Frumm, S. M.; Ross, L.; Fenouille, N.; Bassil, C. F.; Lewis, C. A.; Ramos, A.; Gould, J.; Stone, R. M.; DeAngelo, D. J.; Galinsky, I.; Clish, C. B.; Kung, A. L.; Hemann, M. T.; Vander Heiden, M. G.; Banerji, V.; Stegmaier, K., Targeting MTHFD2 in acute myeloid leukemia. *J Exp Med.* **2016,** *213* (7), 1285-1306.

14.   Yu, C.; Yang, L.; Cai, M.; Zhou, F.; Xiao, S.; Li, Y.; Wan, T.; Cheng, D.; Wang, L.; Zhao, C.; Huang, X., Down-regulation of MTHFD2 inhibits NSCLC progression by suppressing cycle-related genes. *J Cell Mol Med.* **2020,** *24* (2), 1568-1577.

15.   Ju, H. Q.; Lu, Y. X.; Chen, D. L.; Zuo, Z. X.; Liu, Z. X.; Wu, Q. N.; Mo, H. Y.; Wang, Z. X.; Wang, D. S.; Pu, H. Y.; Zeng, Z. L.; Li, B.; Xie, D.; Huang, P.; Hung, M. C.; Chiao, P. J.; Xu, R. H., Modulation of redox homeostasis by inhibition of MTHFD2 in colorectal cancer: mechanisms and therapeutic implications. *J Natl Cancer Inst.* **2018,** *111*, 584-596.

16.   Wei, Y.; Liu, P.; Li, Q.; Du, J.; Chen, Y.; Wang, Y.; Shi, H.; Wang, Y.; Zhang, H.; Xue, W.; Gao, Y.; Li, D.; Feng, Y.; Yan, J.; Han, J.; Zhang, J., The effect of MTHFD2 on the proliferation and migration of colorectal cancer cell lines. *Onco Targets Ther.* **2019,** *12*, 6361-6370.

17.   Chan, C.-H.; Wu, C.-Y.; Dubey, N. K.; Wei, H.-J.; Lu, J.-H.; Mao, S.; Liang, J.; Liang, Y.-H.; Cheng, H.-C.; Deng, W.-P., Modulating redox homeostasis and cellular reprogramming through inhibited methylenetatrahydrofolate dehydrogenase 2 enzymatic activities in lung cancer. *Aging.* **2020,** *12*, 17930-17947.

18.   Lehtinen, L.; Ketola, K.; Makela, R.; Mpindi, J. P.; Viitala, M.; Kallioniemi, O.; Iljin, K., High-throughput RNAi screening for novel modulators of vimentin expression identifies MTHFD2 as a regulator of breast cancer cell migration and invasion. *Oncotarget.* **2013,** *4* (1), 48-63.

19.   Gustafsson Sheppard, N.; Jarl, L.; Mahadessian, D.; Strittmatter, L.; Schmidt, A.; Madhusudan, N.; Tegner, J.; Lundberg, E. K.; Asplund, A.; Jain, M.; Nilsson, R., The folate-coupled enzyme MTHFD2 is a nuclear protein and promotes cell proliferation. *Sci Rep.* **2015,** *5*, 15029.

20.   Koufaris, C.; Nilsson, R., Protein interaction and functional data indicate MTHFD2 involvement in RNA processing and translation. *Cancer Metab.* **2018,** *6*, 12.

21.   Asai, A.; Koseki, J.; Konno, M.; Nishimura, T.; Gotoh, N.; Satoh, T.; Doki, Y.; Mori, M.; Ishii, H., Drug discovery of anticancer drugs targeting methylenetetrahydrofolate dehydrogenase 2. *Heliyon.* **2018,** *4* (12), e01021.

22.   Gustafsson, R.; Jemth, A. S.; Gustafsson, N. M. S.; Farnegardh, K.; Loseva, O.; Wiita, E.; Bonagas, N.; Dahllund, L.; Llona-Minguez, S.; Haggblad, M.; Henriksson, M.; Andersson, Y.; Homan, E.; Helleday, T.; Stenmark, P., Crystal structure of the emerging cancer target MTHFD2 in complex with a substrate-based inhibitor. *Cancer Res.* **2017,** *77* (4), 937-948.

23.   Fu, C.; Sikandar, A.; Donner, J.; Zaburannyi, N.; Herrmann, J.; Reck, M.; Wagner-Dobler, I.; Koehnke, J.; Muller, R., The natural product carolacton inhibits folate-dependent C1 metabolism by targeting FolD/MTHFD. *Nat Commun.* **2017,** *8* (1), 1529.

24.   Kawai, J.; Ota, M.; Ohki, H.; Toki, T.; Suzuki, M.; Shimada, T.; Matsui, S.; Inoue, H.; Sugihara, C.; Matsuhashi, N.; Matsui, Y.; Takaishi, S.; Nakayama, K., Structure-based design and synthesis of an isozyme-selective MTHFD2 inhibitor with a tricyclic coumarin scaffold. *ACS Med Chem Lett.* **2019,** *10* (6), 893-898.

25.   Hawkins, P. C. D.; Skillman, A. G.; Nicholls, A., Comparison of shape-matching and docking as virtual screening tools. *J Med Chem.* **2007,** *50* (1), 74-82.

26.   Tomasic, T.; Peterlin Masic, L., Rhodanine as a scaffold in drug discovery: a critical review of its biological activities and mechanisms of target modulation. *Expert Opin Drug Discov.* **2012,** *7* (7), 549-560.

27.   Ha, H.; Debnath, B.; Odde, S.; Bensman, T.; Ho, H.; Beringer, P. M.; Neamati, N., Discovery of novel CXCR2 inhibitors using ligand-based pharmacophore models. *J Chem Inf Model.* **2015,** *55* (8), 1720-1738.

28.   Zhuang, C.; Narayanapillai, S.; Zhang, W.; Sham, Y. Y.; Xing, C., Rapid identification of Keap1-Nrf2 small-molecule inhibitors through structure-based virtual screening and hit-based substructure search. *J Med Chem.* **2014,** *57* (3), 1121-1126.

29.   Christensen, Q. H.; Grove, T. L.; Booker, S. J.; Greenberg, E. P., A high-throughput screen for quorum-sensing inhibitors that target acyl-homoserine lactone synthases. *Proc Natl Acad Sci U S A.* **2013,** *110* (34), 13815-13820.

30.   Tweardy, D. J.; Kasembeli, M. M.; Xu, M. X.; Eckols, T. K. Methods and compositions for treatment of muscle wasting, muscle weakness, and/or cachexia using inhibitors of STAT3. WO 2015010107, 2015.

31.   Tweardy, D. J.; Kasembeli, M. M.; Xu, M. X.; Milner, J. Methods and compositions for prevention of allergic reaction using inhibitors of STAT3. WO 2015010106, 2015.

32. Tweardy, D. J.; Kasembeli, M. M.; Xu, M. X.; Agarwal, S. K.; Pedroza, M. Methods and compositions for treatment of fibrosis using inhibitors of STAT3. WO 2015010102, 2015.

33. Dahlin, J. L.; Nissink, J. W.; Strasser, J. M.; Francis, S.; Higgins, L.; Zhou, H.; Zhang, Z.; Walters, M. A., PAINS in the assay: chemical mechanisms of assay interference and promiscuous enzymatic inhibition observed during a sulfhydryl-scavenging HTS. *J Med Chem.* **2015,** *58* (5), 2091-2113.

34. Abulwerdi, F.; Liao, C.; Liu, M.; Azmi, A. S.; Aboukameel, A.; Mady, A. S.; Gulappa, T.; Cierpicki, T.; Owens, S.; Zhang, T.; Sun, D.; Stuckey, J. A.; Mohammad, R. M.; Nikolovska-Coleska, Z., A novel small-molecule inhibitor of Mcl-1 blocks pancreatic cancer growth in vitro and in vivo. *Mol Cancer Ther.* **2014,** *13* (3), 565-575.

35. Ramkumar, K.; Samanta, S.; Kyani, A.; Yang, S.; Tamura, S.; Ziemke, E.; Stuckey, J. A.; Li, S.; Chinnaswamy, K.; Otake, H.; Debnath, B.; Yarovenko, V.; Sebolt-Leopold, J. S.; Ljungman, M.; Neamati, N., Mechanistic evaluation and transcriptional signature of a glutathione S-transferase omega 1 inhibitor. *Nat Commun.* **2016,** *7*, 13084.

36. Wan, X.; Wang, C.; Huang, Z.; Zhou, D.; Xiang, S.; Qi, Q.; Chen, X.; Arbely, E.; Liu, C. Y.; Du, P.; Yu, W., Cisplatin inhibits SIRT3-deacetylation MTHFD2 to disturb cellular redox balance in colorectal cancer cell. *Cell Death Dis.* **2020,** *11* (8), 649.

37. Lin, H.; Huang, B.; Wang, H.; Liu, X.; Hong, Y.; Qiu, S.; Zheng, J., MTHFD2 overexpression predicts poor prognosis in renal cell carcinoma and is associated with cell proliferation and vimentin-modulated migration and invasion. *Cell Physiol Biochem.* **2018,** *51* (2), 991-1000.

38. Ducker, G. S.; Chen, L.; Morscher, R. J.; Ghergurovich, J. M.; Esposito, M.; Teng, X.; Kang, Y.; Rabinowitz, J. D., Reversal of cytosolic one-carbon flux compensates for loss of the mitochondrial folate pathway. *Cell Metab.* **2016,** *23* (6), 1140-1153.

39. Xu, Y.; Xue, D.; Bankhead, A., 3rd; Neamati, N., Why all the fuss about oxidative phosphorylation (OXPHOS)? *J Med Chem.* **2020**.

40. Pietzke, M.; Meiser, J.; Vazquez, A., Formate metabolism in health and disease. *Mol Metab.* **2020,** *33*, 23-37.

41. Rabinowitz, J. D.; Kim, H.; Ducker, G. S.; Ghergurovich, J. M. SHMT inhibitors. WO 2016145252, 2016.

42. Nilsson, R.; Nicolaidou, V.; Koufaris, C., Mitochondrial MTHFD isozymes display distinct expression, regulation, and association with cancer. *Gene.* **2019,** *716*, 144032.

43. *ROCS*, 3.2.0.4; OpenEye Scientific Software: Santa Fe, NM.

44.   *GOLD*, 5.2; The Cambridge Crystallographic Data Centre (CCDC): Cambridge, UK.

45.   Hawkins, P. C. D.; Skillman, A. G.; Warren, G. L.; Ellingson, B. A.; Stahl, M. T., Conformer generation with OMEGA: algorithm and validation using high quality structures from the Protein Databank and Cambridge Structural Database. *J Chem Inf Model.* **2010,** *50*, 572-584.

46.   Jones, G.; Willett, P.; Glen, R. C.; Leach, A. R.; Taylor, R., Development and validation of a genetic algorithm for flexible docking. *J Mol Biol.* **1997,** *267*, 727-748.

CHAPTER V Significance and Future Directions

Significance of the study

This work details a successful investigation of inhibiting cell metabolism as a potential anti-cancer strategy. The approaches were varied in nature but overall highlight the importance of nucleotide and one-carbon metabolism in cancer progression. Transcriptomics is a powerful tool in generating hypotheses and by using this technique we identified several novel connections and signaling pathways that may prove to be important findings in better understanding SHMT2's and MTHFD2's roles in development and malignant diseases. A combination approach was evaluated to examine simultaneous inhibition of *de novo* pyrimidine biosynthesis and nucleotide salvage and remarkable synergy was observed. Finally, a traditional drug discovery method of pharmacophore screening resulted in the first ever covalent MTHFD2 inhibitor with anti-cancer activity. Collectively, this dissertation provides further evidence to pursue SHMT2, and MTHFD2 inhibitors for the treatment of cancer and a potential strategy to improve the efficacy of DHODH inhibitors in the clinic.

Future directions

Chapter II

Validation of transcriptomics-informed hypotheses

Many significant changes at the mRNA level were detected in response to knockout of MTHFD2 and SHMT2. However, before any solid conclusions can be drawn, validation of changes in gene (qPCR) and protein (Western blot) expression must be carried out.

Glycosylation

Prior literature reported that SHMT2 bears a GlcNAc glycosylation that is regulated by OGT.[1] Several glycosylation related proteins were differentially expressed in both the RNA-seq (e.g., *GALNT5*, *GALNT6*, and *GCNT2*) and Bru-seq (e.g., *COG8* and *PILRB*) experiments. In addition to validation of expression changes of these genes at the mRNA and protein levels, I think it would be interesting to evaluate global changes in the glycosylome upon knockout of SHMT2 (Figure V-1). This could be done using the Pro-Q™ Emerald 488 gel stain (ThermoFisher), or with *O*-GlcNAc or *O*-GalNAc antibodies. *O*-GlcNAcylation is an important regulator of metabolic reprogramming and therefore uncovering SHMT2's role in this process is important.[2]

ncRNA processing

SHMT2 has been reported to be under the control of several miRs and lncRNAs.[3-7] NcRNAs are also reported to regulate MTHFD2 expression including miR-9 (along with lncRNA *TUG1*), miR-92a, miR-940, miR-33a-5p, and *LIN28B* and miR-22.[8-14] MTHFD2 is a predicted target gene of miR-99a-3p, miR-186-5p, and miR-202.[15-17] While we did not observe changes in expression of the aforementioned ncRNAs, there were many others with significant changes in expression such as *HOXC-AS3*, *FZD10-AS1*, *LINC01551*, and *ESRG* which had |FC|'s greater than 10-fold for SHMT2 KO. Notably, *FZD10-AS1* and the *HOXC-AS1* transcripts have both been linked to metabolic processes and therefore their role in the context of 1CM warrants further investigation (Figure V-1).[18-19]

mTOR inhibitors

We observed significant differential activity of sensitivity to rapamycin between the WT and SHMT2 KO or MTHFD2 KO cells. Both KOs conferred resistance to cell growth inhibition by rapamycin. Activation of mTOR significantly upregulates the expression of MTHFD2, and the

addition of mTOR inhibitors prevents this effect.[20] Previous literature showed that rapamycin inhibited the expression of SHMT2 and MTHFD2 in activated T-cells.[21] Furthermore in a liver regeneration model, knockdown of SHMT2 inhibited the phosphorylation of mTOR, but not total levels of mTOR; likewise, overexpression of SHMT2 increased phosphorylation of mTOR.[22] However, there is no existing evidence that inhibition of SHMT2 and MTHFD2 provides resistance to cell growth inhibition via mTOR inhibition by rapamycin. Rapamycin is an allosteric inhibitor of the mTOR complex 1 (mTORC1) and only inhibits mTORC2 with long-term exposure.[23] WYE-354, the compound identified by our CMAP analysis, potently inhibits both mTORC1 and mTORC2.[24] Therefore, it would be interesting to know if SHMT2 KO or MTHFD2 KO conferred resistance to simultaneous inhibition of mTORC1/2. mTORC2 responds to different stimuli than mTORC1 and effects different downstream consequences (Figure V-1); mTORC2 is involved with cytoskeleton organization and cell survival pathways whereas mTORC1 promotes anabolic processes and cell growth in the presence of sufficient nutrients.

Bru-Seq

The Bru-seq experiments were done without biological replicates and therefore should be interpreted lightly. I also think traditional RNA-seq of the doxycycline-inducible cell lines would be more appropriate for overexpression and knockdown of SHMT2. Though I do think Bru-seq would be useful to monitor changes in the RNA expression after the doxycycline is removed, but possibly at a shorter time point than 7 days. The H1299 engineered lines showed the best overexpression and knockdown of SHMT2 coupled with significant differences in proliferation rates and thus was chosen for analysis. Although the A549 set did not show as significant of a knockdown of SHMT2, this cell line was the only one in which overexpression of SHMT2 provided a proliferative advantage. Therefore, I think it would be interesting to investigate this cell

line in comparison to H1299's overexpression of SHMT2 to tease out possible causative mechanisms. It should be noted that doubling time has not been determined for the H226 set of cell lines.
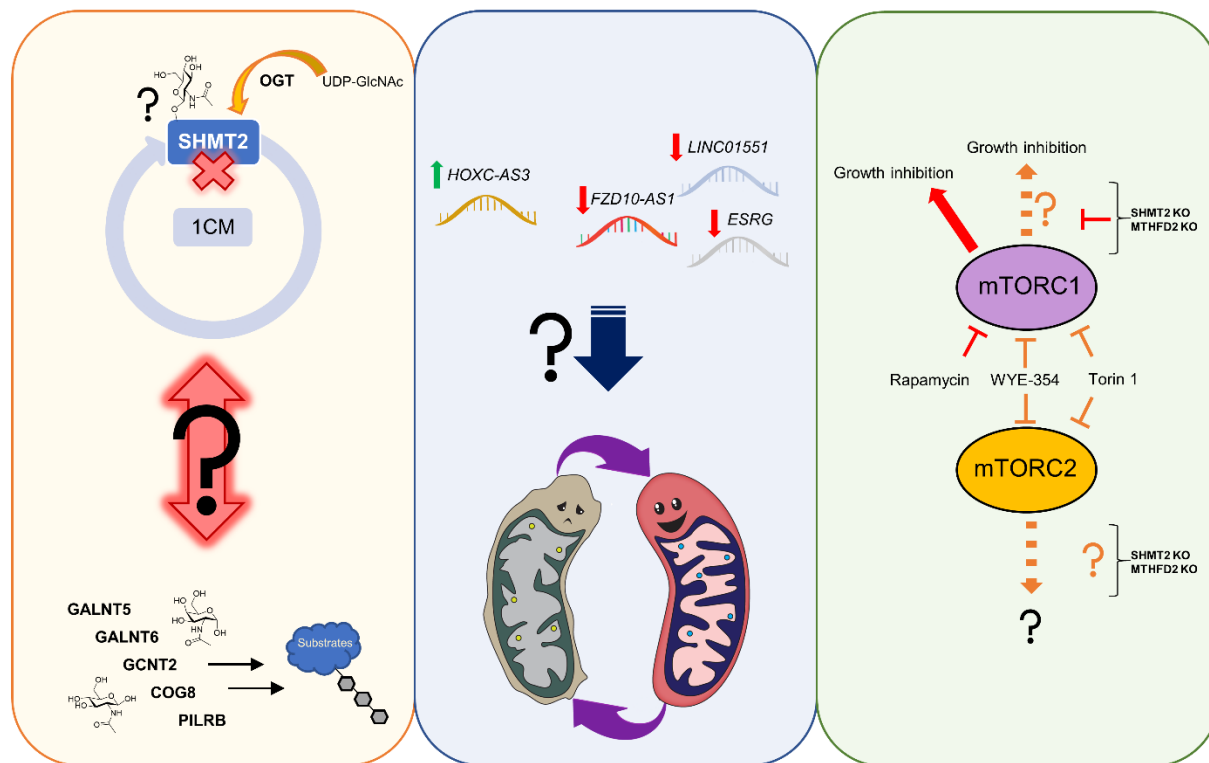

Figure V-1. Future directions for Chapter 2. Credit to ya-webdesign.com for image of mitochondria.

Chapter III

Mechanistic studies elucidating details of DHODH/ENT synergy

The synergy we observed between DHODH inhibitors and ENT inhibitors was very significant. We observed that the combination of brequinar and the CNT inhibitor phlorizin produced no effect, but this does not necessarily rule out that the DHODH/CNT inhibition combination would not be synergistic. Experiments using more potent inhibitors of CNTs or siRNA targeting these proteins combined with brequinar are necessary to further validate this result. We identified that the ENT1 and ENT2 isoforms together are responsible for salvage using potent ENT1/2 inhibitors 8MDP and NBMPR. It would be interesting to evaluate if one transporter

over the other was more responsible for the synergy through siRNA. These experiments should be carried out over a panel of cell lines as it is likely that not every case will be the same. Additionally, it would be important to see if knockdown of one transporter upregulated the other and if this affected the observed synergy.

In vivo efficacy

BREQ + DPM

The major disappointment to this study was the lack of translation of synergy to our *in vivo* model. Unfortunately, there was no additive effect with the combination of BREQ and DPM either, leaving much room for optimization. We know from previous murine xenograft models that both BREQ and DPM are able to reach tumors to elicit their effects.[25-27] Studies with DPM and an inhibitor of the aspartate transcarbamoylase function of CAD (an upstream enzyme of DHODH) found that the combination was able to significantly reduce concentrations of nucleotides in the tumors more than either agent alone and that addition of DPM reduced PALA's LD_{50} in mice by 50%.[26-27] The dose of DPM in the study that saw a significant reduction in tumoral nucleotide levels was 10-fold higher than what we used in ours (100 mg/kg vs 10 mg/kg).[27] Their ratio of PALA:DPM was the same as ours for BREQ:DPM (2:1). High doses of BREQ are well-tolerated humans,[28] but the maximum tolerated dose in mice is 50 mg/kg.[29-30] In our study we used a dose of 20 mg/kg BREQ. Therefore, for the next *in vivo* study I would recommend increasing the dose of BREQ to 50 mg/kg with groups of DPM at 10 mg/kg, 25 mg/kg, and 50 mg/kg. Another angle that could be optimized is the scheduling of the doses. In order to best inform this, pharmacokinetics and pharmacodynamics of the administrations should be evaluated. Pharmacokinetic studies have been carried out for both brequinar and dipyridamole in mice previously, but we don't know how they would interact with each other.[31] Unfortunately, nearly

all the pre-clinical work with dipyridamole was published in German, underscoring the importance of carrying out PK/PD for these drugs.

Compound 41

Compound **41**, despite having a similar pharmacokinetic profile and DHODH IC$_{50}$ as BREQ,[32] showed no antitumor efficacy. We found through computational prediction and logD calculations that **41** is disfavored for cell permeability. With this knowledge in conjunction with the fact that **41**'s cellular IC$_{50}$ is ~6-fold higher than BREQ's in HCT 116, it comes as no surprise that a two-fold lower dose than BREQ would be inactive. A maximum tolerated dose (MTD) study was not performed with **41**, therefore if this compound is to be pursued further, then identifying the highest dose for treatment would be the next step. Additionally, while **41**'s pharmacokinetic (PK) profile is similar to BREQ's, the half-life is roughly 2-fold lower. Thus, increasing the dosing frequency to every 12 hours rather than daily administration could also prove to be beneficial. Alternatively, compound **52** in addition to a DHODH IC$_{50}$ on par with BREQ, had a 2-fold lower cellular IC$_{50}$ than BREQ in HCT 116.[32] Hence, **52** may be a better candidate to pursue if a favorable PK profile was obtained (Figure V-2).
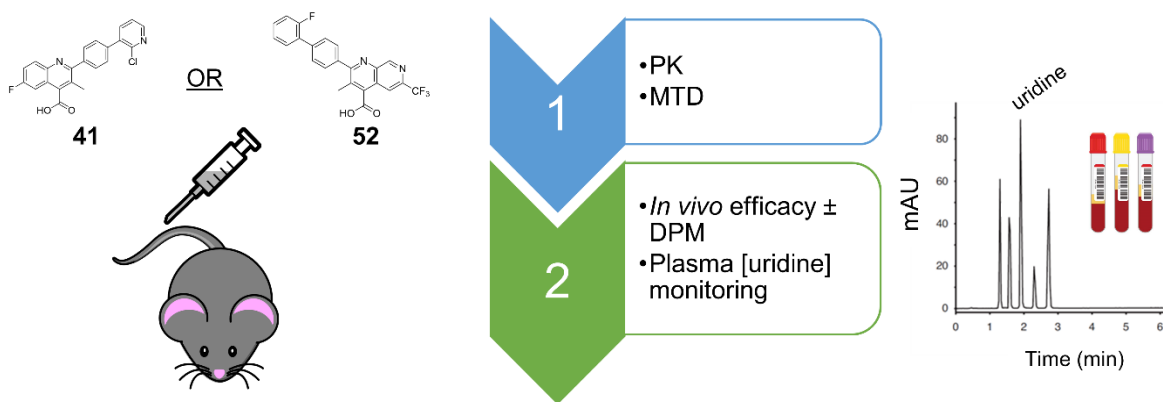

Figure V-2. *In vivo* optimization of **41** or **52**.

In vivo monitoring

We showed that *in vitro*, 5 μM uridine was not enough to rescue toxicity caused by the combination of BREQ and DPM. This is the estimated concentration of uridine in mouse plasma.[33] A previous study found that treatment with a subtoxic dose of BREQ resulted in an increase in plasma uridine concentrations by 3-fold.[30] At high concentrations of uridine (50 μM) the inhibition is abrogated,[29] therefore it is possible that a rebound is causing the lack of synergy. I recommend monitoring the plasma levels of uridine as well as assessing tumoral nucleotide levels as previously described (Figure V-2).[27]

Chapter IV

Virtual screening

Though **CBN-1** has a novel mechanism of action, the potency of the molecule is only in the micromolar range. Our current approach used a ligand-based pharmacophore model which could restrict the hits. Instead, a virtual screen using the protein structure itself could be employed and there are several software programs available.[34]

Mechanism of binding

From the Q-TOF experiments we learned that **CBN-1** covalently binds MTHFD2. What remains to be elucidated is where and how. This can be approached in several ways. The best way is to acquire a co-crystal structure to confirm the proposed binding mode and mechanism of inhibition. A complementary approach would be to mutate nucleophilic residues within the active site and evaluate binding. I propose Lys88 as the residue responsible for this interaction due to its proximity to the thiocarbonate and also that recent literature shows that acetylation of this residue inhibits MTHFD2's activity.[35]

MTHFD selectivity

MTHFD2 is selectively expressed in transformed cells or during embryonic development whereas MTHFD1 is broadly expressed.[36-38] Therefore, it is important to achieve selectivity in order to avoid systemic toxicity. Both MTHFD1 and MTHFD2L possess the same function as MTHFD2 in normal adult tissues and are ubiquitously expressed. MTHFD2 shares ~60-65% sequence similarity with MTHFD2L and 40% with MTHFD1.[39-40] The active site residues are highly conserved; an important difference between MTHFD2 and MTHFD1 is an Asn to Val, respectively. Current inhibitors show selectivity in some capacity.[41-43] **CBN-1** maintains a H-bond acceptor in the same position as the carbonyl of DS44960156 that affords selectivity over MTHFD1.[42] Consequently, I hypothesize that **CBN-1** would be selective for MTHFD2. This could be evaluated through CETSA and with recombinant protein in the enzymatic and thermal shift assays for MTHFD1. Additionally, though in select cell lines it seems the complementary mitochondrial isoform MTHFD2L would play a limited role in a compensation mechanism for MTHFD2 inhibition,[44] I recommend evaluating this selectivity as well.

Optimization of CBN-1

In order to best facilitate optimization of our hit compound, a co-crystal structure should be acquired. It should also be determined if a covalent inhibitor is ultimately desired. Anti-metabolite suicide substrates have been met with great success in the clinic (e.g. 5FU),[45] however, noncovalent MTHFD2 inhibitors have already shown efficacy *in vivo*.[43] If the noncovalent route is pursued, a carbamate or urea would be potential substitutions for the thiocarbonate, but the binding mode will be important to understand if H-bond donors would be accepted at these positions. Though **CBN-1** was the most potent in our series, its IC_{50} is only in the micromolar range and should be optimized for potency. Kawai and colleagues found that substitution of the carboxylic acid of DS44960156 for a sulfonamide improved cell penetration and was well-

tolerated for inhibitory activity.[43] Additionally, they identified that more bulk was tolerated in the position in what would be the naphthalene ring of **CBN-1**, and that positively charged groups were favorable as they formed a salt bridge with the NAD^+ cofactor.[43]

There are only a handful of CBN analogs that have activity in the HAP1 cell line. In HCT 116, **CBN-5** is active with similar activity as **CBN-1** (28 μM vs 34 μM respectively). Therefore, I don't think the issue is permeability, but rather cell line sensitivity. Although, the original compound DS44960156 was not cell permeable, so screening the molecules with a computational permeability predictor (i.e. PerMM)[46-47] along with experimental calculations of $logD^{7.4}$ could provide valuable information as to why some compounds are inactive in the cells. However, I think the top compounds should be screened in a panel of cell lines to find one which is sensitive.
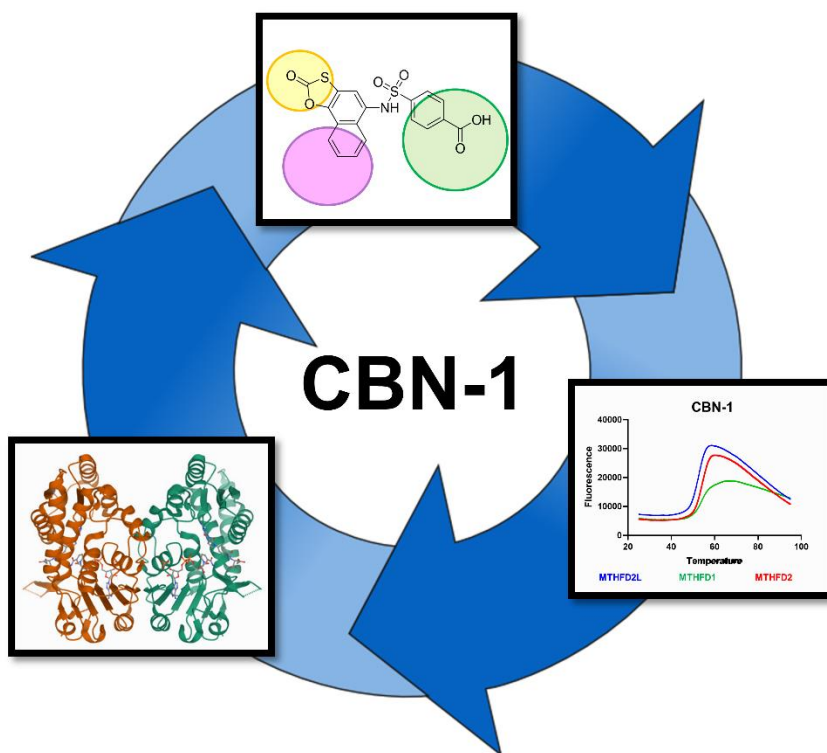

Figure V-3. Future directions of Chapter 4.

References

1.   Chaiyawat, P.; Chokchaichamnankit, D.; Lirdprapamongkol, K.; Srisomsap, C.; Svasti, J.; Champattanachai, V., Alteration of O-GlcNAcylation affects serine phosphorylation and regulates gene expression and activity of pyruvate kinase M2 in colorectal cancer cells. *Oncol Rep.* **2015,** *34* (4), 1933-1942.

2.   Jozwiak, P.; Forma, E.; Brys, M.; Krzeslak, A., O-GlcNAcylation and metabolic reprograming in cancer. *Front Endocrinol (Lausanne).* **2014,** *5*, 145.

3.   Lin, C.; Zhang, Y.; Chen, Y.; Bai, Y.; Zhang, Y., Long noncoding RNA LINC01234 promotes serine hydroxymethyltransferase 2 expression and proliferation by competitively binding miR-642a-5p in colon cancer. *Cell Death Dis.* **2019,** *10* (2), 137.

4.   Wu, X.; Deng, L.; Tang, D.; Ying, G.; Yao, X.; Liu, F.; Liang, G., miR-615-5p prevents proliferation and migration through negatively regulating serine hydromethyltransferase 2 (SHMT2) in hepatocellular carcinoma. *Tumour Biol.* **2016,** *37* (5), 6813-6821.

5.   Pinweha, P.; Rattanapornsompong, K.; Charoensawan, V.; Jitrapakdee, S., MicroRNAs and oncogenic transcriptional regulatory networks controlling metabolic reprogramming in cancers. *Comput Struct Biotechnol J.* **2016,** *14*, 223-233.

6.   Leivonen, S. K.; Rokka, A.; Ostling, P.; Kohonen, P.; Corthals, G. L.; Kallioniemi, O.; Perala, M., Identification of miR-193b targets in breast cancer cells and systems biological analysis of their functional impact. *Mol Cell Proteomics.* **2011,** *10* (7), M110.005322.

7.   Qi, C.; Qin, X.; Zhou, Z.; Wang, Y.; Yang, Q.; Liao, T., Circ_0072995 promotes cell carcinogenesis via up-regulating miR-149-5p-mediated SHMT2 in breast cancer. *Cancer Manag Res.* **2020,** *12*, 11169-11181.

8.   Selcuklu, S. D.; Donoghue, M. T.; Rehmet, K.; de Souza Gomes, M.; Fort, A.; Kovvuru, P.; Muniyappa, M. K.; Kerin, M. J.; Enright, A. J.; Spillane, C., MicroRNA-9 inhibition of cell proliferation and identification of novel miR-9 targets by transcriptome profiling in breast cancer cells. *J Biol Chem.* **2012,** *287* (35), 29516-29528.

9.   Gu, Y.; Si, J.; Xiao, X.; Tian, Y.; Yang, S., miR-92a inhibits proliferation and induces apoptosis by regulating methylenetetrahydrofolate dehydrogenase 2 (MTHFD2) expression in acute myeloid leukemia. *Oncol Res.* **2017,** *25* (7), 1069-1079.

10.   Xu, T.; Zhang, K.; Shi, J.; Huang, B.; Wang, X.; Qian, K.; Ma, T.; Qian, T.; Song, Z.; Li, L., MicroRNA-940 inhibits glioma progression by blocking mitochondrial folate metabolism through targeting of MTHFD2. *Am J Cancer Res.* **2019,** *9* (2), 250-269.

11.   Yan, Y.; Zhang, D.; Lei, T.; Zhao, C.; Han, J.; Cui, J.; Wang, Y., MicroRNA-33a-5p suppresses colorectal cancer cell growth by inhibiting MTHFD2. *Clin Exp Pharmacol Physiol.* **2019,** *46* (10), 928-936.

12.   Zhou, J.; Bi, C.; Ching, Y. Q.; Chooi, J. Y.; Lu, X.; Quah, J. Y.; Toh, S. H.; Chan, Z. L.; Tan, T. Z.; Chong, P. S.; Chng, W. J., Inhibition of LIN28B impairs leukemia cell growth and metabolism in acute myeloid leukemia. *J Hematol Oncol.* **2017,** *10* (1), 138.

13.   Zhao, X. B.; Ren, G. S., LncRNA taurine-upregulated gene 1 promotes cell proliferation by inhibiting microRNA-9 in MCF-7 cells. *J Breast Cancer.* **2016,** *19* (4), 349-357.

14.   Tong, D.; Zhang, J.; Wang, X.; Li, Q.; Liu, L.; Lu, A.; Guo, B.; Yang, J.; Ni, L.; Qin, H.; Zhao, L.; Huang, C., MiR-22, regulated by MeCP2, suppresses gastric cancer cell proliferation by inducing a deficiency in endogenous S-adenosylmethionine. *Oncogenesis.* **2020,** *9* (11), 99.

15.   Wei, G. G.; Guo, W. P.; Tang, Z. Y.; Li, S. H.; Wu, H. Y.; Zhang, L. C., Expression level and prospective mechanism of miRNA-99a-3p in head and neck squamous cell carcinoma based on miRNA-chip and miRNA-sequencing data in 1, 167 cases. *Pathol Res Pract.* **2019,** *215* (5), 963-976.

16.   Jones, D. Z.; Schmidt, M. L.; Suman, S.; Hobbing, K. R.; Barve, S. S.; Gobejishvili, L.; Brock, G.; Klinge, C. M.; Rai, S. N.; Park, J.; Clark, G. J.; Agarwal, R.; Kidd, L. R., Micro-RNA-186-5p inhibition attenuates proliferation, anchorage independent growth and invasion in metastatic prostate cancer cells. *BMC Cancer.* **2018,** *18* (1), 421.

17.   Gamazon, E. R.; Trendowski, M. R.; Wen, Y.; Wing, C.; Delaney, S. M.; Huh, W.; Wong, S.; Cox, N. J.; Dolan, M. E., Gene and microRNA perturbations of cellular response to pemetrexed implicate biological networks and enable imputation of response in lung adenocarcinoma. *Sci Rep.* **2018,** *8* (1), 733.

18.   Dong, Y.; Li, X.; Lin, Z.; Zou, W.; Liu, Y.; Qian, H.; Jia, J., HOXC-AS1-MYC regulatory loop contributes to the growth and metastasis in gastric cancer. *J Exp Clin Cancer Res.* **2019,** *38* (1), 502.

19.   Zheng, X.; Zhou, Y.; Chen, W.; Chen, L.; Lu, J.; He, F.; Li, X.; Zhao, L., Ginsenoside 20(S)-Rg3 prevents PKM2-targeting miR-324-5p from H19 sponging to antagonize the Warburg effect in ovarian cancer cells. *Cell Physiol Biochem.* **2018,** *51* (3), 1340-1353.

20.   Ben-Sahra, I.; Hoxhaj, G.; Ricoult, S. J. H.; Asara, J. M.; Manning, B. D., mTORC1 induces purine synthesis through control of the mitochondrial tetrahydrofolate cycle. *Science.* **2016,** *351* (6274), 728-733.

21.   Tan, H.; Yang, K.; Li, Y.; Shaw, T. I.; Wang, Y.; Blanco, D. B.; Wang, X.; Cho, J. H.; Wang, H.; Rankin, S.; Guy, C.; Peng, J.; Chi, H., Integrative proteomics and phosphoproteomics profiling reveals dynamic signaling networks and bioenergetics pathways underlying T cell activation. *Immunity.* **2017,** *46* (3), 488-503.

22.   Wang, M.; Yuan, F.; Bai, H.; Zhang, J.; Wu, H.; Zheng, K.; Zhang, W.; Miao, M.; Gong, J., SHMT2 promotes liver regeneration through glycine-activated Akt/mTOR pathway. *Transplantation.* **2019,** *103* (7), e188-e197.

23.   Li, J.; Kim, S. G.; Blenis, J., Rapamycin: one drug, many effects. *Cell Metab.* **2014,** *19* (3), 373-379.

24.   Yu, K.; Toral-Barza, L.; Shi, C.; Zhang, W. G.; Lucas, J.; Shor, B.; Kim, J.; Verheijen, J.; Curran, K.; Malwitz, D. J.; Cole, D. C.; Ellingboe, J.; Ayral-Kaloustian, S.; Mansour, T. S.; Gibbons, J. J.; Abraham, R. T.; Nowak, P.; Zask, A., Biochemical, cellular, and in vivo activity of novel ATP-competitive and selective inhibitors of the mammalian target of rapamycin. *Cancer Res.* **2009,** *69* (15), 6232-6240.

25.   Dexter, D. L.; Hesson, D. P.; Ardecky, R. J.; Rao, G. V.; Tippett, D. L.; Dusak, B. A.; Paull, K. D.; Plowman, J.; DeLarco, B. M.; Narayanan, V. L.; Forbes, M., Activity of a novel 4-quinolinecarboxylic acid, NSC 368390 [6-Fluoro-2-(2'-fluoro-1,1'-biphenyl-4-yl)-3-methyl-4-quinolinecarboxylic acid sodium salt], against experimental tumors. *Cancer Res.* **1985,** *45*, 5563-5568.

26.   Chan, T. C.; Young, B.; King, M. E.; Taetle, R.; Howell, S. B., Modulation of the activity of PALA by dipyridamole. *Cancer Treat Rep.* **1985,** *69* (4), 425-430.

27.   Chan, T. C. K.; Howell, S. B., Mechanism of synergy between N-phosponacetly-L-aspartate and dipyridamole in a human ovarian carcinoma cell line. *Cancer Res.* **1985,** *45*, 3598-3604.

28.   Madak, J. T.; Bankhead, A., 3rd; Cuthbertson, C. R.; Showalter, H. D.; Neamati, N., Revisiting the role of dihydroorotate dehydrogenase as a therapeutic target for cancer. *Pharmacol. Ther.* **2019,** *195*, 111-131.

29.   Peters, G. J.; Kraal, I.; Pinedo, H. M., In vitro and in vivo studies on the combination of brequinar sodium (DUP-785; NSC 368390) with 5-fluorouracil; effects of uridine. *Br. J. Cancer.* **1992,** *65*, 229-233.

30.   Peters, G. J.; Schwartsmann, G.; Nadal, J. C.; Laurensse, E. J.; van Groeningen, C. J.; van der Vijgh, W. J. F.; Pinedo, H. M., In vivo inhibition of the pyrimidine de novo enzyme dihydroorotic acid dehydrogenase by brequinar sodium (DUP-785; NSC 368390) in mice and patients. *Cancer Res.* **1990,** *50*, 4644-4649.

31.   Schwartsmann, G.; Van der Vijgh, W. J. F.; Van Hennick, M. B.; Klein, I.; Vermorken, J. B.; Dodoin, P.; ten Bokkel Huinink, W. W.; Joggi, G.; Gall, H.; Crespeigne, N.; Simonetti, G.; Winograd, B.; Pinedo, H. M., Pharmacokinetics of brequinar sodium (NSC 368390) in patients with solid tumors during a Phase I study. *Eur J Cancer Clin Oncol.* **1989,** *25* (12), 1675-1681.

32.   Madak, J. T.; Cuthbertson, C. R.; Miyata, Y.; Tamura, S.; Petrunak, E. M.; Stuckey, J. A.; Han, Y.; He, M.; Sun, D.; Showalter, H. D.; Neamati, N., Design, synthesis, and biological evaluation of 4-quinoline carboxylic acids as inhibitors of dihydroorotate dehydrogenase. *J. Med. Chem.* **2018,** *61* (12), 5162-5186.

33.   Karle, J. M.; Anderson, L. W.; Dietrick, D. D.; R.L., C., Determination of serum and plasma uridine levels in mice, rats, and humans by high-pressure liquid chromatography. *Anal. Biochem.* **1980,** *109*, 41-46.

34.   Maia, E. H. B.; Assis, L. C.; de Oliveira, T. A.; da Silva, A. M.; Taranto, A. G., Structure-based virtual screening: from classical to artificial intelligence. *Front Chem.* **2020,** *8*, 343.

35.   Wan, X.; Wang, C.; Huang, Z.; Zhou, D.; Xiang, S.; Qi, Q.; Chen, X.; Arbely, E.; Liu, C. Y.; Du, P.; Yu, W., Cisplatin inhibits SIRT3-deacetylation MTHFD2 to disturb cellular redox balance in colorectal cancer cell. *Cell Death Dis.* **2020,** *11* (8), 649.

36.   Uhlen, M.; Fagerberg, L.; Hallstrom, B. M.; Lindskog, C.; Oksvold, P.; Mardinoglu, A.; Sivertsson, A.; Kampf, C.; Sjostedt, E.; Asplund, A.; Olsson, I.; Edlund, K.; Lundberg, E.; Navani, S.; Szigyarto, C. A.; Odeberg, J.; Djureinovic, D.; Takanen, J. O.; Hober, S.; Alm, T.; Edqvist, P. H.; Berling, H.; Tegel, H.; Mulder, J.; Rockberg, J.; Nilsson, P.; Schwenk, J. M.; Hamsten, M.; von Feilitzen, K.; Forsberg, M.; Persson, L.; Johansson, F.; Zwahlen, M.; von Heijne, G.; Nielsen, J.; Ponten, F., Tissue-based map of the human proteome. *Science.* **2015,** *347* (6220), 1260419.

37.   Zhu, Z.; Leung, G. K. K., More than a metabolic enzyme: MTHFD2 as a novel target for anticancer therapy? *Front Oncol.* **2020,** *10*, 658.

38.   The Human Protein Atlas - Summary - MTHFD1. https://www.proteinatlas.org/ENSG00000100714-MTHFD1 (accessed November 19, 2020).

39.   Shin, M.; Momb, J.; Appling, D. R., Human mitochondrial MTHFD2 is a dual redox cofactor-specific methylenetetrahydrofolate dehydrogenase/methenyltetrahydrofolate cyclohydrolase. *Cancer Metab.* **2017,** *5*, 11.

40.   Dekhne, A. S.; Hou, Z.; Gangjee, A.; Matherly, L. H., Therapeutic targeting of mitochondrial one-carbon metabolism in cancer. *Mol Cancer Ther.* **2020**.

41.   Fu, C.; Sikandar, A.; Donner, J.; Zaburannyi, N.; Herrmann, J.; Reck, M.; Wagner-Dobler, I.; Koehnke, J.; Muller, R., The natural product carolacton inhibits folate-dependent C1 metabolism by targeting FolD/MTHFD. *Nat Commun.* **2017,** *8* (1), 1529.

42.   Kawai, J.; Ota, M.; Ohki, H.; Toki, T.; Suzuki, M.; Shimada, T.; Matsui, S.; Inoue, H.; Sugihara, C.; Matsuhashi, N.; Matsui, Y.; Takaishi, S.; Nakayama, K., Structure-based design and synthesis of an isozyme-selective MTHFD2 inhibitor with a tricyclic coumarin scaffold. *ACS Med Chem Lett.* **2019,** *10* (6), 893-898.

43.   Kawai, J.; Toki, T.; Ota, M.; Inoue, H.; Takata, Y.; Asahi, T.; Suzuki, M.; Shimada, T.; Ono, K.; Suzuki, K.; Takaishi, S.; Ohki, H.; Matsui, S.; Tsutsumi, S.; Hirota, Y.; Nakayama, K., Discovery of a potent, selective, and orally available MTHFD2 inhibitor (DS18561882) with in vivo antitumor activity. *J Med Chem.* **2019,** *62* (22), 10204-10220.

44.   Nilsson, R.; Nicolaidou, V.; Koufaris, C., Mitochondrial MTHFD isozymes display distinct expression, regulation, and association with cancer. *Gene.* **2019,** *716*, 144032.

45.   Vodenkova, S.; Buchler, T.; Cervena, K.; Veskrnova, V.; Vodicka, P.; Vymetalkova, V., 5-fluorouracil and other fluoropyrimidines in colorectal cancer: Past, present and future. *Pharmacol Ther.* **2020,** *206*, 107447.

46.   Lomize, A. L.; Hage, J. M.; Schnitzer, K.; Golobokov, K.; LaFaive, M. B.; Forsyth, A. C.; Pogozheva, I. D., PerMM: A web tool and database for analysis of passive membrane permeability and translocation pathways of bioactive molecules. *J Chem Inf Model.* **2019,** *59* (7), 3094-3099.

47.   Lomize, A. L.; Pogozheva, I. D., Physics-based method for modeling passive membrane permeability and translocation pathways of bioactive molecules. *J Chem Inf Model.* **2019,** *59* (7), 3198-3213.